DE GRUYTER

Tharwat F. Tadros

FORMULATION SCIENCE AND TECHNOLOGY

VOLUME 4: AGROCHEMICALS, PAINTS AND COATINGS AND FOOD COLLOIDS

Tharwat F. Tadros

Formulation Science and Technology

Also of Interest

Handbook of Colloid and Interface Science.
Volumes 1–4
Tadros, 2018
ISBN 978-3-11-054050-5

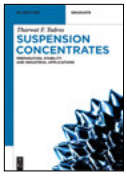

Suspension Concentrates.
Preparation, Stability and Industrial Applications
Tadros, 2017
ISBN 978-3-11-048678-0, e-ISBN 978-3-11-048687-2

Polymeric Surfactants.
Dispersion Stability and Industrial Applications
Tadros, 2017
ISBN 978-3-11-048722-0, e-ISBN 978-3-11-048728-2

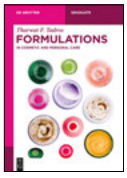

Formulations.
In Cosmetic and Personal Care
Tadros, 2016
ISBN 978-3-11-045236-5, e-ISBN 978-3-11-045238-9

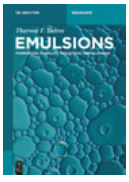

Emulsions.
Formation, Stability, Industrial Applications
Tadros, 2016
ISBN 978-3-11-045217-4, e-ISBN 978-3-11-045224-2

Tharwat F. Tadros

Formulation Science and Technology

Volume 4:
Agrochemicals, Paints and Coatings and Food Colloids

DE GRUYTER

Author
Prof. Tharwat F. Tadros
89 Nash Grove Lane
Workingham RG40 4HE
Berkshire, UK
tharwattadros3@gmail.com

ISBN 978-3-11-058755-5
e-ISBN (PDF) 978-3-11-058800-2
e-ISBN (EPUB) 978-3-11-058756-2

Library of Congress Control Number: 2018935454

Bibliographic information published by the Deutsche Nationalbibliothek
The Deutsche Nationalbibliothek lists this publication in the Deutsche Nationalbibliografie; detailed bibliographic data are available on the Internet at http://dnb.dnb.de.

Cover image: Nik_Merkulov / iStock / Getty Images
Typesetting: PTP-Berlin, Protago-TEX-Production GmbH, Berlin
Printing and binding: CPI books GmbH, Leck

www.degruyter.com

Preface

This volume describes industrial applications in agrochemicals (Part I), paints and coatings (Part II) and food colloids (Part III). The discussion of agrochemical formulations begins with a general introduction (Chapter 1) describing the requirements of the various types of systems. This is followed by Chapter 2, which focuses on emulsifiable concentrates (ECs), in which the active ingredient is mixed (or dissolved) in an oil and two surfactants. When this oil is added to an aqueous solution in the spray tank, it spontaneously emulsifies forming an oil/water (O/W) emulsion. The mechanism of self-emulsification is described. These ECs are now mostly replaced with a concentrated O/W emulsion (Chapter 3), which provides a number of advantages, such as using less oil and surfactant and the possibility of incorporating an adjuvant (which enhances the biological efficacy) in the continuous phase. Chapter 4 deals with the formulation of suspension concentrates (SCs), which are commonly used to replace wettable powders (which can be dusty and hazardous to the operator). The main factors involved in SC formulation and its long-term physical stability are described with particular reference to the rheological methods that can be applied for their assessment. Chapter 5 describes the formulation of oil-based suspensions, whereby the oil can be polar or nonpolar. The requirements for both types to achieve colloid stability are described and this is followed by a description of the use of anti-settling systems in nonaqueous suspensions. Finally, the emulsification of the oil-based suspension in aqueous and electrolyte solution media is described. Chapter 6 describes the formulation of suspoemulsions (mixtures of suspensions and emulsions) highlighting the possible interactions between the suspension particles and the emulsion droplets. This can lead to various instability problems such as homoflocculation, heteroflocculation, coalescence of emulsion droplets and recrystallization. The methods that can be used to reduce or eliminate such instabilities are described with particular reference to polymeric surfactants. Chapter 7 deals with the formulation of controlled-release systems with particular reference to the microencapsulation of liquid and solid AIs, controlled release from matrix-based microparticles and granules. Chapter 8 describes the formulation of adjuvants that are required to enhance the bioefficacy of the AI Several factors must be considered when selecting an adjuvant for a given AI These include interactions at the air/water interface and their effect on spray droplet formation, spray impaction and adhesion, wetting and spreading, evaporation of spray droplets and formation of deposits, solubilisation of the AI by surfactant micelles and its effect on transport and interaction between agrochemical, surfactants and target species.

Part II deals with the formulation of paints and coatings. Chapter 9 describes the nature of the dispersed particle, the dispersion medium and film formers, the deposition of particles and their adhesion on substrates and the flow characteristics (rheology) of the paint formulation. Chapter 10 describes the formulation of film formers

https://doi.org/10.1515/9783110588002-001

using emulsion and dispersion polymerization. Chapter 11 deals with the formulation of pigments for paint application. Topics such as the wetting of powders, breaking of aggregates and agglomerates, wet milling and colloid stabilization of the paint dispersion must be considered. Chapter 12 describes the process of enhancing particle deposition and its final adhesion. This is governed by long-range forces such as double layer repulsion (or attraction) and short-range (surface forces). Chapter 13 illustrates the rheological techniques that can be applied during paint formulation, whereas Chapter 14 shows how these rheological methods can be applied during paint formulation. Chapter 15 gives examples of the flow properties of some commercial paints.

Part III describes the formulation of food colloids. It starts with a general introduction (Chapter 16) highlighting the complexity of food systems. Chapter 17 starts with a description of the interaction between food grade surfactants and the structure of the liquid crystalline phases. This is followed by a description of binary and tertiary phase diagrams, monolayer formation and the relationship between the liquid crystalline structure and emulsion stability. Chapter 18 deals with the formulation of food emulsions using proteins, protein/polysaccharide and surfactant/polysaccharide interactions. The structure of portents and their interaction and conformation at the liquid/liquid interface are described. Chapter 19 describes the process of surfactant association structures, microemulsions and emulsions in food. Chapter 20 deals with the rheology of food emulsions with particular reference to interfacial and bulk rheology. The correlation between interfacial rheology and emulsion stability is highlighted using two examples, namely mixed surfactant and protein films. The bulk rheology of emulsions is described with particular reference to microgel dispersions and the fractal nature of the aggregated network. Chapter 21 deals with foam formulations in food of which whipping cream and bread dough are the most common. In the first case, the air bubbles are stabilized by fat crystals that adhere to air bubbles during the whipping process forming a protective layer and preventing bubble coalescence. In the latter case, the bread quality is determined by a high bread volume and a fine crumb structure. Several theories have been proposed to explain foam stability, namely: surface viscosity and elasticity theory, where the adsorbed surfactant film is assumed to control the mechanical-dynamical properties of the surface layers by virtue of its surface viscosity and elasticity; the Gibbs–Marangoni effect theory; surface forces theory (disjoining pressure π), which operates under static (equilibrium) conditions in relatively dilute surfactant solutions ($h < 100$ nm); stabilisation by micelles (high surfactant concentrations > cmc); stabilization by lamellar liquid crystalline phases, which is particularly the case with nonionic surfactants that produce lamellar liquid crystalline structure in the film between the bubbles; stabilisation of foam films by mixed surfactants whereby a combination of surfactants give slower drainage and improved foam stability; and stabilization by solid particles, which involves particles adsorbing at the air/liquid interface. Chapter 22 looks at the relationship between rheology and mouth feel. After describing the main rheological measurements that need to be applied to obtain such a correlation, some emphasis is given to the break-up of Newtonian and

non-Newtonian liquids. The complexity of flow in the oral cavity is described and subsequently a description is given of the relationship between texture and rheology. Finally, some examples of practical food colloids are given.

This book (Volume 4) gives a number of formulation examples in the areas of agrochemicals, paints and coating and food colloids. It is a valuable text for formulation scientists involved in the formulation of these systems. It may also be useful for academics involved in a research area related to any of these formulations.

Tharwat Tadros
May 2018

Contents

Part I: **The formulation of agrochemicals**

1 Introduction to the formulation of agrochemicals

Agrochemical formulations include a wide range of systems suited to specific applications [1, 2]. Agrochemicals are usually effective at several grams to hundreds of grams of active ingredient per 1,000 m^2. It is, however, difficult to apply such a small amount uniformly to the crop. The active ingredient is always first formulated in a suitable diluent such as water or an organic solvent and when the formulation is applied it is further diluted in the spray tank to ensure uniform deposition upon spraying. In some cases, an agrochemical is a water-soluble compound of which paraquat and glyphosate (both are herbicides) are probably the most familiar. Paraquat is a 2,2 bypyridium salt and the counter ions are normally chloride. It is formulated as a 20 % aqueous solution which is simply diluted into water at various ratios (1 : 50 up to 1 : 200 depending on the application) upon application. To such an aqueous solution, surface active agents (sometimes referred to as wetters) are added which are essential for a number of reasons. The most obvious reason for adding surfactants is to enable the spray solution to adhere to the target surface and spread over it to cover a large area. However, this picture is an oversimplification since the surface-active agent plays a more subtle role in the optimization of the biological efficacy. Thus, the choice of the surfactant system in an agrochemical formulation is crucial since it must perform a number of functions. To date, this choice is made by a trial and error procedure, due to the complex nature of application and the lack of understanding of the mode of action of the chemical. It is the objective of this book to apply the basic principle of colloid and interface science to agrochemical formulations, their subsequent application, and the optimization of their biological efficacy.

The main purpose of any agrochemical formulation is to make handling and application of the active ingredient as easy as possible. An important function of the formulation is to optimize its biological efficacy. In most cases, this is achieved by controlling the physical characteristics of the formulation and use of adjuvants. An important criterion for any agrochemical is its safety both to the crop and the agrochemical worker. This requires adequate control of the spray droplet spectrum, reduction of any drift and removal of any toxic effect on contact with the individual. These stringent requirements can be achieved through careful analysis of all the interfacial phenomena that are involved in application. The concept of "Pesticide Delivery System" (PDS) must be applied, whereby the active ingredients are made available to a specified target at a concentration and duration designed to accomplish an intended effect, i.e., obtain the fullest biological efficacy while minimizing various harmful effects.

Most agrochemicals are water-insoluble compounds with various physical properties, which have first to be determined in order to decide on the type of formulation. One of the earliest types of formulations are wettable powders (WP), which are suitable for formulating solid water-insoluble compounds that can be produced in a pow-

https://doi.org/10.1515/9783110588002-002

der form. The chemical (which may be micronized) is mixed with a filler such as china clay and a solid surfactant such as sodium alkyl or alkyl aryl sulphate or sulphonate is added. When the powder is added to water, the particles are spontaneously wetted by the medium and, upon agitation, dispersion of the particles takes place. It is clear that the particles should remain suspended in the continuous medium for a period of time depending on the application. Some physical testing methods are available to evaluate the suspensibility of the WP. Clearly, the surfactant system plays a crucial role in wettable powders. In the first place, it enables spontaneous wetting and dispersion of the particles. Second, by adsorption on the particle surface, it provides a repulsive force that prevents aggregation of the particles. This process of aggregation increases the settling of the particles and may also cause problems upon application, such as nozzle blockage.

The second and most familiar type of agrochemical formulation is emulsifiable concentrates (ECs), as described in Chapter 2. This is produced by mixing one agrochemical oil with another one, such as xylene or trimethylbenzene, or a mixture of various hydrocarbon solvents [1]. Alternatively, a solid pesticide could be dissolved in a specific oil to produce a concentrated solution. In some cases, pesticide oil may be used without the addition of any extra oils. A surfactant system (usually a mixture of two or three components) is always added for a number of purposes. First, the surfactant enables self emulsification of the oil on addition to water. This occurs by a complex mechanism that involves a number of physical changes, such as lowering interfacial tension at the oil/water interface, enhancement of turbulence at that interface with the result of spontaneous production of droplets. Second, the surfactant film that adsorbs at the oil/water interface, stabilizes the produced emulsion against flocculation and/or coalescence. As we will see in later sections, emulsion breakdown must be prevented, otherwise excessive creaming or sedimentation or oil separation may take place during application. This results in an inhomogeneous application of the agrochemical on the one hand, and possible losses on the other. The third role of the surfactant system in agrochemicals is to enhance biological efficacy. As we will look at later, it is essential to arrive at optimum conditions for effective use of agrochemicals. In this case, the surfactant system will help spreading the pesticide at the target surface and may enhance its penetration.

In recent years, there has been great demand to replace ECs with concentrated aqueous oil-in-water (O/W) emulsions [1–3] as will be described in Chapter 3. This replacement provides several potential advantages. In the first place, the added oil can be replaced with water, which is of course much cheaper and environmentally acceptable. Secondly, removing the oil could help to reduce undesirable effects such as phytotoxicity, skin irritation, etc. Third, by formulating the pesticide as an O/W emulsion, it is possible to control the droplet size to an optimum value, which may be crucial for biological efficacy. Fourth, water-soluble surfactants, which may be desirable for biological optimization, can be added to the aqueous continuous phase. As we will see in the subsequent chapters, the choice of a surfactant, or a mixed sur-

factant system is crucial for preparation of a stable O/W emulsion. In recent years, macromolecular surfactants have been designed to produce very stable O/W emulsions which could be easily diluted into water and applied without any detrimental effects to the emulsion droplets.

More recently, microemulsions are being considered as potential systems for formulating agrochemicals. Microemulsions are isotropic, thermodynamically stable systems consisting of oil, water and surfactant(s) where the free energy of formation of the system is zero or negative [4]. It is obvious why such systems, when they can be formulated, are very attractive, since they have an indefinite shelf life (within a certain temperature range). Since the droplet size of microemulsions is very small (usually less than 50 nm), they appear transparent. The microemulsion droplets may be considered as swollen micelles and hence they will solubilize the agrochemical. This may result in considerable enhancement of the biological efficacy. Thus, microemulsions may offer several advantages over the commonly used macroemulsions. Unfortunately, formulating the agrochemical as microemulsion is not straightforward since one usually uses two or more surfactants, an oil and the agrochemical. These tertiary systems produce various complex phases and it is essential to investigate the phase diagram before arriving at the optimum composition of microemulsion formation. A high concentration of surfactant (10–20 %) is needed to produce such a formulation. This makes such systems relatively more expensive to produce when compared to macroemulsions. However, the extra cost incurred could be offset by an enhancement of biological efficacy which means that a lower agrochemical application rate could be achieved.

A similar concept has been applied to replace wettable powders, namely with aqueous suspension concentrates (SCs) that will be described in Chapter 4. These systems are more familiar than ECs and they were introduced several decades ago [2, 5]. Indeed, SCs are probably the most widely used systems in agrochemical formulations. Again, SCs are much more convenient to apply than WPs. Dust hazards are absent, and the formulation can be simply diluted in the spray tanks, without any vigorous agitation. As we will see in Chapter 20, SCs are produced by a two or three stage process. The pesticide powder is first dispersed in an aqueous solution of a surfactant or a macromolecule (usually referred to as the dispersing agent) using a high-speed mixer. The resulting suspension is then subjected to a wet milling process (usually bead milling) to break any remaining aggregates or agglomerates and reduce the particle size to smaller values. One usually aims at a particle size distribution ranging from 0.1 to 5 μm., with an average of 1–2 μm. The surface or polymer added adsorbs on the particle surfaces, resulting in their colloidal stability. The particles must be stably maintained over a long period of time, since any strong aggregation in the system may cause various problems. First, as the aggregates are larger than the primary particles, they tend to settle faster. Second, any gross aggregation may result in lack of dispersion on dilution. The large aggregates can block the spray nozzles and may reduce biological efficacy as a result of the inhomogeneous distribution of the particles

on the target surface. Apart from their role in ensuring the colloidal stability of the suspension, surfactants are added to many SCs to enhance their biological efficacy. This is usually produced by solubilization of the insoluble compared in the surfactant micelles. This will be discussed in later sections. Another role a surfactant may play in SCs is to reduce crystal growth (Ostwald ripening). The latter process may occur when the solubility of the agrochemical is appreciable (say greater than 100 ppm) and when the SC is polydisperse. The smaller particles will have a higher solubility than the larger ones. With time, the small particles dissolve and become deposited on the larger ones. Surfactants may reduce this Ostwald ripening by adsorption on the crystal surfaces, thus preventing deposition of the molecules at the surface. This will be described in detail in Chapter 5.

Chapter 6 describes the formulation of oil-based suspensions, which are currently used for the formulation of many agrochemicals, in particular those which are chemically unstable in aqueous media [2]. These suspensions permit the use of oils (such as methyl oleate) which may enhance the biological efficacy of the active ingredient. In addition, one may incorporate water-insoluble adjuvants into the formulation. The most important criterion for the oil used is to have the minimum solubility of the active ingredient otherwise Ostwald ripening or crystal growth will occur upon storage. The oil-based suspension has to be diluted in water to produce an oil-in-water emulsion. A self-emulsifiable system must be produced and this requires the presence of the appropriate surfactants for self emulsification. The surfactants used for self emulsification should not interfere with the dispersing agent that is used to stabilize the suspension particles in the nonaqueous media. Displacement of the dispersing agent with the emulsifiers can lead to flocculation of the suspension. To prevent sedimentation of the particles (sine the density of the active ingredient is higher than that of the oil in which it is dispersed), an appropriate rheology modifier (anti-settling agent) that is effective in the nonaqueous medium must be incorporated into the suspension. This rheology modifier should not interfere with the self emulsification process of the oil based suspension. Two main types of nonaqueous suspensions may be distinguished:

(i) Suspensions in polar media such as alcohol, glycols, glycerol, esters. These media have a relative permittivity $\varepsilon_r > 10$; in this case, double layer repulsion plays an important role, in particular when using ionic dispersing agents.
(ii) Suspensions in nonpolar media, $\varepsilon_r < 10$, such as hydrocarbons (paraffinic or aromatic oils), which can have a relative permittivity as low as 2. In this case, charge separation and double layer repulsion are not effective and hence one has to depend on the use of dispersants that produce steric stabilization.

Chapter 7 describes the formulation of suspoemulsions [2], which are mixtures of suspensions and emulsions where two active ingredients are formulated with one as an aqueous suspension and the other as an oil/water emulsion. This offers convenience to the farmer and may also result in synergism in biological efficacy. A wider spectrum of disease control may be achieved, particularly with many fungicides and her-

bicides. With many suspoemulsions, an adjuvant that enhances the biological efficacy is added. The formulation of suspoemulsions is not an easy task; one may produce a stable suspension and emulsion separately but when these mix they become unstable due to the following interactions:

(i) Homoflocculation of the suspension particles. This can happen if the dispersing agent used for preparation of the suspension is not strongly adsorbed and hence it becomes displaced by the emulsifier, which is more strongly adsorbed but not a good stabilizer for the suspension particles.
(ii) Emulsion coalescence. This can happen if the emulsifier is not strongly adsorbed at the O/W or W/O interface, resulting in its partial or complete displacement by the suspension dispersant, which is not a good emulsion stabilizer, and this results in coalescence of the emulsion droplets with ultimate separation of oil (for O/W) or water (for W/O).
(iii) Heteroflocculation between the oil droplets and suspension particles. The latter may be partially wetted by the oil and reside at the O/W interface (this is particularly the case if the oil droplets are much larger than the suspension particles). Heteroflocculation can also occur with suspension particles dispersed in a W/O emulsion.
(iv) Phase transfer and crystallization. This happens when the suspension particles have some solubility in the oil phase. The small suspension particles which have higher solubility than the larger ones (due to curvature effects) may become dissolved in the oil phase and they become recrystallized onto the larger suspension particles (a form of an Ostwald ripening process). Large and sometimes needle shaped crystals may be produced as a result of crystal habit modification (that sometimes occurs with Ostwald ripening).

An important application in agrochemicals is that of controlled release formulations, as described in Chapter 8. Several methods are used for controlled release, of which microcapsules (CS) are probably the most widely used [2]. These are small particles with size range 1–1,000 μm consisting of a core material and an outer wall. The latter isolates the core material from the environment and protects it from degradation and interaction with other materials. The core active ingredient is designed to be released in a controlled manner as required. Microencapsulation of agrochemicals is usually carried out by interfacial condensation, in situ polymerization or coacervation. Interfacial condensation, whereby two monomers, one oil-soluble (placed say in an emulsion droplet) and one water-soluble, placed in the continuous medium undergo interfacial polycondensation producing a capsule wall of polyurea or polyurethane. The polymer wall must have appropriate molecular weight, glass transition temperature, and thickness to achieve the desirable controlled release. The polymer wall should not interact with the agrochemical. This polymer wall must not cause any environmental damage on degradation after application and hence a biodegradable polymer is preferred. The polymer wall must be easily manufactured and should also be stable on

storage and usage. The main advantages of micrcapsule formulatios are: controlled or slow release of the core active ingredients thus improving residual activity; reduction of application dosage; stabilization of the core active ingredient against environmental degradation; reduction of mammalian and fish toxicity; reduction of phytotxicity; reduction of environmental pollution.

It can be seen from the above short discussion that agrochemical formulations are complex multi-phase systems and their preparation, stabilization and subsequent application require the application of the basic principles of colloid and interface science, as is described in several textbooks [6–8].

2 Formulation of emulsifiable concentrates

Many agrochemicals are formulated as emulsifiable concentrates (ECs), which, when added to water, produce oil-in-water (O/W) emulsions either spontaneously or by gentle agitation [1]. Such formulations are produced by the addition of surfactants to the agrochemical if the latter is an oil with reasonably low viscosity or to an oil solution of the agrochemical if the latter is a solid or an oil with high viscosity. As discussed below, spontaneous emulsification requires a number of criteria that must be met to control the properties of the interfacial region, in particular producing a low interfacial tension. The latter is generally produced by using a mixed emulsifier system, e.g. a mixture of calcium dodecyl benzene sulphonate and an ethoxylated nonionic surfactant, as will be described below. With such an emulsifier mixture, 5 % concentration may be sufficient to produce spontaneous emulsification. In some agrochemicals, specific emulsifier systems have to be used to ensure the spontaneity of emulsification. One of the main problems with ECs is the batch-to-batch variation of the agrochemical and emulsifier systems which may result in lack of spontaneity of emulsification. Thus, to successfully formulate an EC, one must have rigorous quality assurance and use several tests such as effect of water hardness, temperature, agitation in the spray tank, etc. Quantitative evaluation of the formulation is required using interfacial tension measurements, droplet size analysis of the resulting O/W emulsion, subjecting the EC to stress tests, e.g. temperature variation, etc.

In most cases, ECs are formulated by a simple trial and error approach, by screening a number of emulsifier systems for a specific agrochemical formulation. Unfortunately, the hydrophilic–lipophilic balance (HLB) method that is commonly used for selection of emulsifiers (Chapter 3) is inadequate for selecting emulsifiers for ECs [9]. Other indices such as the cohesive energy ratio concept (CER), described by Beerbower and Hill [10], may provide a better option. Essentially, the method involves selecting suitable emulsifiers by balancing the interactions of their hydrophobic parts with the oil phase and the hydrophilic parts with the aqueous phase. This requires knowledge of the solubility, polar and hydrogen bonding parameters of the various components. Unfortunately, these interaction parameters are only available for a small number of emulsifiers and hence their application to the wide variety of emulsifiers used in ECs is limited. This discussion clearly shows that selecting emulsifiers for ECs still requires a large number of experimental screening to produce a product that satisfies the spontaneity of emulsification and stability under practical conditions. In addition, with many ECs, other components such as crystal growth inhibitors (for solution of solids in oil), defoamers and other stabilizers are added and this requires investigation of their presence on the final formulation properties.

The most common procedure for testing ECs is based on the recommendation of the World Health Organization (WHO), which states that “any creaming of the emulsion at the top, or separation of the emulsion at the bottom, in a 100 ml cylinder shall

https://doi.org/10.1515/9783110588002-003

not exceed 2 ml when the emulsion is tested as follows". Into a 250 ml beaker having an internal diameter of 6–6.5 cm and 100 ml calibration mark and containing 75–80 ml of standard hard water (containing 342 ppm, calculated as calcium carbonate, prepared using 0.304 of anhydrous $CaCl_2$ and 0.39 g $MgCl_2 \cdot 6H_2O$ to make 1 l using distilled water), 5 ml of EC is added, using a Mohr-type pipette, during stirring with a glass rod (4–6 mm in diameter), at about 4 revolutions per second (rps). The EC should be added at a rate of 25–30 ml/min, with the point of the pipette 2 cm inside the beaker; the flow of the concentrate should be directed toward the centre, and not against the side, of the beaker. The final emulsion is made to 100 ml with standard hard water, stirring continuously, and then immediately poured into a clean, dry 100 ml graduated cylinder. The emulsion is kept at 29–30 °C for 1 h and examined for any creaming or separation. Both temperature and water hardness have a major effect on the performance of the EC. This is illustrated in Fig. 2.1 and Fig. 2.2, which show the effect of water hardness on the amount of cream that separates from a typical formulation.

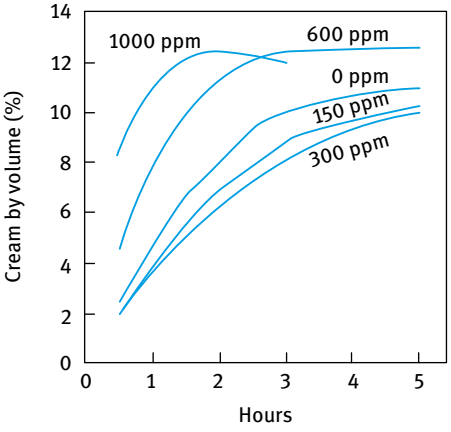

Fig. 2.1: Effect of water hardness on the amount of cream separated as a function of time for a typical EC.

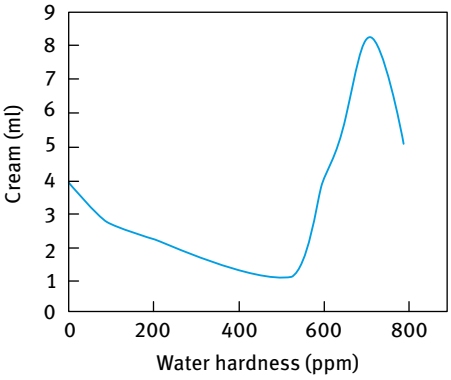

Fig. 2.2: Amount of cream separated as a function of water hardness.

Fig. 2.1 shows that the rate at which the amount of cream reaches equilibrium is fairly independent from the water hardness. This means that measuring the separated cream at an arbitrary time of 1 h is adequate for relative comparison of the various formulations. The best performance for this particular EC appears to be observed at a water hardness of 300 ppm, but this may not be generalizable for all other ECs. Fig. 2.2 shows that the stability of the produced emulsion improves as water hardness increases, reaching a maximum at ≈ 500 ppm, above which the stability of the emulsion decreases with further increase in water hardness.

Fig. 2.3 shows the effect of temperature on the stability of the emulsion produced from an EC.

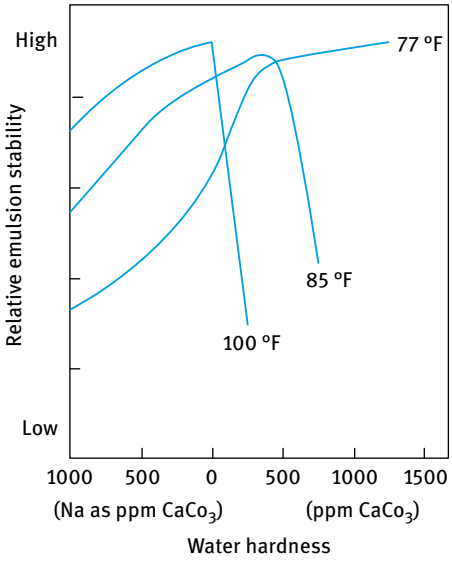

Fig. 2.3: Effect of temperature on the stability of an emulsion produced from an EC.

It can be seen from Fig. 2.3 that temperature variations encountered in practice have a significant effect on emulsion stability. Generally speaking, increasing temperature shifts the optimum performance to softer water and lowering it has the opposite effect. This reflects the effect of temperature on the solution properties of the emulsifiers, in particular those of the nonionic ethoxylate type. The latter becomes less water soluble as the temperature or electrolyte concentration increases, as a result of the dehydration of the ethoxylate chain (breaking of hydrogen bonds between ethylene oxide and water). This amounts to a decrease of the HLB number of the emulsifier with increase of temperature and electrolyte concentration resulting in reduction of the emulsion stability.

Several mechanisms have been proposed to explain the spontaneity of emulsification of ECs. The first mechanism is due to interfacial turbulence that may occur as a result of mass transfer, schematically represented [1, 2] in Fig. 2.4

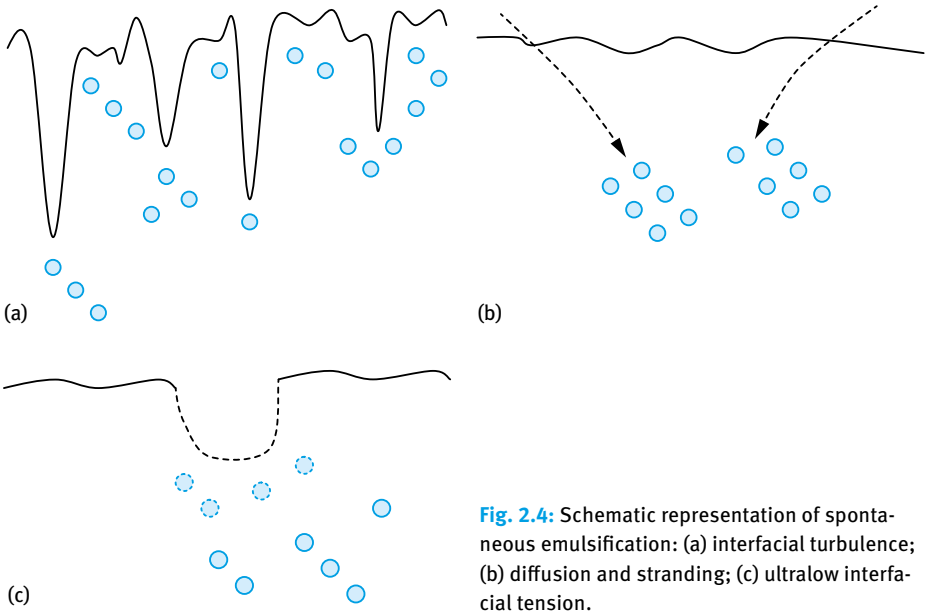

Fig. 2.4: Schematic representation of spontaneous emulsification: (a) interfacial turbulence; (b) diffusion and stranding; (c) ultralow interfacial tension.

In many cases, the interface exhibits unsteady movement; streams of one phase are ejected and penetrate into the second phase as is illustrated in Fig. 2.4 (a), which shows localized reduction in interfacial tension caused by the non-uniform adsorption of the surfactant molecules at the O/W interface [11] or by the mass transfer of the surfactant molecules at the O/W interface [12, 13]. With two phases that are not in chemical equilibrium, convection currents may be formed, conveying liquid rich in surfactants towards areas of liquid deficient of surfactant [14, 15]. These convection currents may give rise to local fluctuations in interfacial tension, causing oscillations of the interface. Such disturbances may amplify themselves leading to violent interfacial perturbations or eventual disintegration of the interface; when liquid droplets are "thrown" into the other [16].

The second mechanism that may account for spontaneous emulsification is based on diffusion and stranding as illustrated in Fig. 2.4 (b). This is best illustrated by carefully placing an ethanol-toluene mixture (containing say 10 % alcohol) onto water. The aqueous layer eventually become turbid as a result of the presence of toluene droplets [17]. In this case, interfacial turbulence does not occur, although spontaneous emulsification apparently takes place. It has been suggested [18, 19] that the alcohol molecules diffuse into the aqueous phase, carrying some toluene in a saturated three-component subphase. At some distance from the interface, the alcohol becomes sufficiently diluted in water to cause the toluene to precipitate in the aqueous phase. This phase transition might be expected to occur when the third component increases the mutual solubility of the two previously immiscible phases.

The third mechanism of spontaneous emulsification may be due to the production of an ultralow (or transiently negative) interfacial tension [20], as illustrated in Fig. 2.4 (c). This mechanism is thought to be the cause of formation of microemulsions.

3 Formulation of emulsion concentrates

Many agrochemicals have been formulated as oil-in-water (O/W) emulsion concentrates (EWs). These systems offer many advantages over the more traditionally used emulsifiable concentrates (ECs). By using an O/W system, one can reduce the amount of oil in the formulation since in most cases a small proportion of oil is added to the agrochemical oil (if this has a high viscosity) before emulsification. In some cases, if the agrochemical oil has a low to medium viscosity one can emulsify the active ingredient directly into water. With many agrochemicals with low melting points, which are not suitable for the preparation of a suspension concentrate, one can dissolve the active ingredient in a suitable oil and the oil solution is then emulsified into water. EWs which are aqueous-based produce less hazard to the operator, reducing skin irritation. In addition, in most cases EWs are less phytotoxic to plants when compared to ECs. The O/W emulsion is convenient for the incorporation of water-soluble adjuvants (mostly surfactants). EWs can also be less expensive compared to ECs since a lower surfactant concentration is used to produce the emulsion and also one replaces a great proportion of oil by water. The only drawback of EWs compared to ECs is the need to use high speed stirrers and/or homogenizers to obtain the required droplet size distribution. In addition, EWs require control and maintenance of its physical stability. As will be discussed later, EWs are only kinetically stable and one has to control the breakdown process that occur on storage such as creaming or sedimentation, flocculation, Ostwald ripening, coalescence, and phase inversion.

In this section, we will start with the principles of formation of emulsions and the role of the surfactants [3]. This is followed by a section on the procedures that can be applied to select the emulsifiers. The third section will deal with the breakdown processes that may occur on storage and methods of their prevention. The last section will deal with the assessment and prediction of the long-term physical stability of EWs.

3.1 Formation of emulsions

Consider a system in which an oil is represented by a large drop 2 of area A_1 immersed in a liquid 2, which is now subdivided into a large number of smaller droplets (1) with total area A_2 ($A_2 \gg A_1$) as shown in Fig. 3.1 The interfacial tension γ_{12} is the same for the larger and smaller droplets since the latter are generally in the region of 0.1 to few μm.

The change in free energy from state I to state II is made from two contributions [3]: A surface energy term (that is positive) that is equal to $\Delta A \gamma_{12}$ (where $\Delta A = A_2 - A_1$). An entropy of dispersions term which is also positive (since producing a large number of droplets is accompanied by an increase in configurational entropy) which is equal to $T\Delta S^{\text{conf}}$.

https://doi.org/10.1515/9783110588002-004

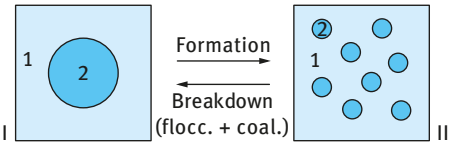

Fig. 3.1: Schematic representation of emulsion formation and breakdown.

From the second law of thermodynamics,

$$\Delta G_{\text{form}} = \Delta A \gamma_{12} - T\Delta S^{\text{conf}}. \tag{3.1}$$

In most cases, $\Delta A \gamma_{12} \gg T\Delta S^{\text{conf}}$, which means that ΔG_{form} is positive, i.e. the formation of emulsions is non-spontaneous and the system is thermodynamically unstable. In the absence of any stabilization mechanism, the emulsion will break by flocculation, coalescence, Ostwald ripening, or a combination of all these processes. In the presence of a stabilizer (surfactant and/or polymer), an energy barrier is created between the droplets and therefore the reversal from state II to state I becomes non-continuous as a result of the presence of these energy barriers. This is illustrated in Fig. 3.2. In the presence of the above energy barriers, the system becomes kinetically stable [3]. As discussed in Chapters 7 and 8 of Vol. 1, the energy barrier can be created by electrostatic and/or steric repulsion which overcomes the everlasting van der Waals attraction.

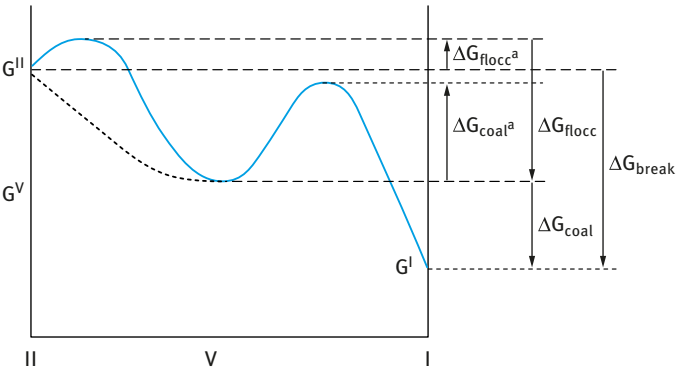

Fig. 3.2: Schematic representation of free energy path for breakdown (flocculation and coalescence) for systems containing an energy barrier.

3.2 Mechanisms and methods of emulsification

To prepare an emulsions oil, water, surfactant and energy are needed [3]. This can be considered by looking at the energy required to expand the interface, $\Delta A\gamma$ (where ΔA is the increase in interfacial area when the bulk oil with area A_1 produces a large number

of droplets with area A_2; $A_2 \gg A_1$, γ is the interfacial tension). Since γ is positive, the energy to expand the interface is large and positive. This energy term cannot be compensated by the small entropy of dispersion $T\Delta S$ (which is also positive) and as discussed before, the total free energy of formation of an emulsion, ΔG is positive.

Thus, emulsion formation is non-spontaneous and energy is required to produce the droplets. The formation of large droplets (few μm) as in the case of macroemulsions is fairly easy and hence high-speed stirrers such as the Ultra-Turrax or Silverson mixer are sufficient to produce the emulsion. In contrast, the formation of small drops (submicron as is the case with nanoemulsions) is difficult and this requires a large amount of surfactant and/or energy. The high energy required for the formation of nanoemulsions can be understood from a consideration of the Laplace pressure p (the difference in pressure between inside and outside the droplet) [3],

$$\Delta p = \gamma\left(\frac{1}{R_1} + \frac{1}{R_2}\right), \tag{3.2}$$

where R_1 and R_2 are the principal radii of curvature of the drop.

For a spherical drop, $R_1 = R_2 = R$ and,

$$\Delta p = \frac{\gamma}{2R}. \tag{3.3}$$

To break up a drop into smaller ones, it must be strongly deformed and this deformation increases p [3]. Surfactants play major roles in the formation of emulsions: By lowering the interfacial tension, p is reduced and hence the stress needed to break up a drop is reduced [21]. Surfactants prevent the coalescence of newly formed drops.

To assess emulsion formation, one usually measures the droplet size distribution using, for example, laser diffraction techniques. A useful average diameter d is,

$$d_{nm} = \left(\frac{S_m}{S_n}\right)^{1/(n-m)}. \tag{3.4}$$

In most cases, d_{32} (the volume/surface average or Sauter mean) is used. The width of the size distribution can be given as the variation coefficient c_m, which is the standard deviation of the distribution weighted with dm divided by the corresponding average d. Generally, C_2 will be used, which corresponds to d_{32}.

An alternative way to describe the emulsion quality is to use the specific surface area A (surface area of all emulsion droplets per unit volume of emulsion),

$$A = \pi s^2 = \frac{6\phi}{d_{32}}, \tag{3.5}$$

where ϕ is the volume fraction of the emulsion.

Several procedures [3] may be applied for emulsion preparation, these include

- simple pipe flow (low agitation energy, L);
- static mixers and general stirrers (low to medium energy, L–M);
- high speed mixers such as the Ultra-Turrax (M);

- colloid mills and high pressure homogenizers (high energy, H);
- ultrasound generators (M–H).

The method of preparation can be continuous (C) or batch-wise (B):
- pipe flow and static mixers – C;
- stirrers and Ultra-Turrax – B, C;
- colloid mill and high pressure homogenizers – C;
- ultrasound – B, C.

In all methods, there is liquid flow [3]: unbounded and strongly confined flow. In the unbounded flow, every droplet is surrounded by a large amount of flowing liquid (the confining walls of the apparatus are far away from most of the droplets). The forces can be frictional (mostly viscous) or inertial. Viscous forces cause shear stresses to act on the interface between the droplets and the continuous phase (primarily in the direction of the interface). The shear stresses can be generated by laminar flow (LV) or turbulent flow (TV).

Within each regime, an essential variable is the intensity of the forces acting:

$$\text{viscous stress during laminar flow} = \eta G, \tag{3.6}$$

where G is the velocity gradient.

The intensity of the turbulent flow [3] is expressed by the power density ε (the amount of energy dissipated per unit volume per unit time,

$$\varepsilon = \eta G^2. \tag{3.7}$$

The viscosity of the oil plays an important role in the break-up of droplets; the higher the viscosity, the longer it will take to deform a drop. The deformation time τ_{def} is given by the ratio of oil viscosity to the external stress acting on the drop,

$$\tau_{\text{def}} = \frac{\eta_{\text{D}}}{\sigma_{\text{ext}}}. \tag{3.8}$$

The viscosity of the continuous phase η_{C} plays an important role in some regimes. For turbulent viscous regime, larger η_{C} leads to smaller droplets. For laminar viscous regimes, the effect is even stronger.

3.3 Role of surfactants in emulsion formation

Surfactants lower the interfacial tension γ and this causes a reduction in droplet size. The latter decrease with decrease in γ. For turbulent regimes, the droplet diameter is proportional to $\gamma^{3/5}$. The amount of surfactant required to produce the smallest drop size will depend on its activity a (concentration) in the bulk which determines the

reduction in γ, as given by the Gibbs adsorption equation,

$$-\mathrm{d}\gamma = RT\Gamma\,\mathrm{d}\ln a, \tag{3.9}$$

where R is the gas constant, T is the absolute temperature and Γ is the surface excess (number of moles adsorbed per unit area of the interface). Γ increases with increase in surfactant concentration and eventually it reaches a plateau value (saturation adsorption).

The value of γ obtained depends on the nature of the oil and surfactant used. Small molecules such as nonionic surfactants lower γ more than polymeric surfactants such as PVA. Another important role of the surfactant is its effect on the interfacial dilational modulus ε [3],

$$\varepsilon = \frac{\mathrm{d}\gamma}{\mathrm{d}\ln A}. \tag{3.10}$$

During emulsification, an increase in the interfacial area A takes place and this causes a reduction in Γ. The equilibrium is restored by adsorption of surfactant from the bulk, but this takes time (shorter times occur at higher surfactant activity). Thus ε is small at small a and also at large a. Because of the lack or slowness of equilibrium with polymeric surfactants, ε will not be the same for expansion and compression of the interface.

In practice, surfactant mixtures are used and these have pronounced effects on γ and ε. Some specific surfactant mixtures give lower γ values than either of the two individual components [3]. The presence of more than one surfactant molecule at the interface tends to increase ε at high surfactant concentrations. The various components vary in surface activity. Those with the lowest γ tend to predominate at the interface, but if present at low concentrations, it may take a long time to reach the lowest value. Polymer–surfactant mixtures may experience some synergetic surface activity.

Apart from their effect on reducing γ, surfactants play major roles in the deformation and break-up of droplets [3]. This is summarized as follows. Surfactants allow the existence of interfacial tension gradients, which is crucial for the formation of stable droplets. In the absence of surfactants (clean interface), the interface cannot withstand a tangential stress; the liquid motion will be continuous. If a liquid flows along the interface with surfactants, the latter will be swept downstream causing an interfacial tension gradient. The interface will then drag some of the bordering liquid with it (the Marangoni effect).

Interfacial tension gradients [3] are very important in stabilizing the thin liquid film between the droplets which is very important during the beginning of emulsification (films of the continuous phase may be drawn through the disperse phase and collision is very large). The magnitude of the γ-gradients and of the Marangoni effect depends on the surface dilational modulus ε.

Another important role of the emulsifier is to prevent coalescence during emulsification. This is certainly not due to the strong repulsion between the droplets, since the

pressure at which two drops are pressed together is much greater than the repulsive stresses. The counteracting stress must be due to the formation of γ-gradients.

Closely related to the above mechanism, is the Gibbs–Marangoni effect. The depletion of surfactant in the thin film between approaching drops results in a γ-gradient without liquid flow. This results in an inward flow of liquid that tends to drive the drops apart [3].

The Gibbs–Marangoni effect also explains the Bancroft rule, which states that the phase in which the surfactant is most soluble forms the continuous phase. If the surfactant is in the droplets, a γ-gradient cannot develop and the drops would be prone to coalescence. Thus, surfactants with HLB > 7 tend to form O/W emulsions and HLB < 7 tend to form W/O emulsions. The Gibbs–Marangoni effect also explains the difference between surfactants and polymers for emulsification. Polymers give larger drops compared with surfactants. Polymers give a smaller value of ε at small concentrations when compared to surfactants.

Various other factors should also be considered for emulsification: The disperse phase volume fraction ϕ. Increase in ϕ leads to increase in droplet collision and hence coalescence during emulsification. With increase in ϕ, the viscosity of the emulsion increases and could change the flow from turbulent to laminar.

The presence of many particles results in a local increase in velocity gradients. This means that G increases. In turbulent flow, an increase in ϕ will induce turbulence depression. This will result in larger droplets. Turbulence depression by added polymers tends to remove the small eddies, resulting in the formation of larger droplets.

If the mass ratio of surfactant to continuous phase is kept constant, increase in ϕ results in a decrease in surfactant concentration and hence an increase in γ_{eq}. This results in larger droplets. If the mass ratio of surfactant to disperse phase is kept constant, the above changes are reversed.

3.4 Selection of emulsifiers

3.4.1 Hydrophilic–lipophilic balance concept

The selection of different surfactants in the preparation of either O/W or W/O emulsions is often made on an empirical basis. A semi-empirical scale for selecting surfactants is the hydrophilic–lipophilic balance (HLB number) developed by Griffin [21, 22]. This scale is based on the relative percentage of hydrophilic to lipophilic (hydrophobic) groups in the surfactant molecule(s). For an O/W emulsion droplet, the hydrophobic chain resides in the oil phase whereas the hydrophilic head group resides in the aqueous phase. For a W/O emulsion droplet, the hydrophilic group(s) reside in the water droplet, whereas the lipophilic groups reside in the hydrocarbon phase. A summary of HLB ranges and their application is given in Tab. 3.1.

Tab. 3.1: Summary of HLB ranges and their applications.

HLB range	Application
3–6	W/O emulsifier
7–9	Wetting agent
8–18	O/W emulsifier
13–15	Detergent
15–18	Solubilizer

Tab. 3.1 gives a guide to the selection of surfactants for a particular application. The HLB number depends on the nature of the oil [21, 22]. As an illustration, Tab. 3.2 gives the required HLB numbers to emulsify various oils.

Tab. 3.2: Required HLB numbers to emulsify various oils.

Oil	W/O emulsion	O/W emulsion
Paraffin oil	4	10
Beeswax	5	9
Linolin, anhydrous	8	12
Cyclohexane	—	15
Toluene	—	15

The relative importance of the hydrophilic and lipophilic groups was first recognized when using mixtures of surfactants containing varying proportions of a low and high HLB number [21, 22]. The efficiency of any combination (as judged by phase separation) was found to pass a maximum when the blend contained a particular proportion of the surfactant with the higher HLB number. This is illustrated in Fig. 3.3, which shows the variation of emulsion stability, droplet size and interfacial tension as a function of % surfactant with high HLB number.

The average HLB number may be calculated from additivity,

$$\mathrm{HLB} = x_1\mathrm{HLB}_1 + x_2\mathrm{HLB}_2, \tag{3.11}$$

where x_1 and x_2 are the weight fractions of the two surfactants with HLB_1 and HLB_2.

Griffin [21, 22] developed simple equations for calculating the HLB number of relatively simple nonionic surfactants. For a polyhydroxy fatty acid ester,

$$\mathrm{HLB} = 20\left(1 - \frac{S}{A}\right), \tag{3.12}$$

where S is the saponification number of the ester and A is the acid number.

For a glyceryl monostearate, $S = 161$ and $A = 198$. The HLB is 3.8 (suitable for W/O emulsion).

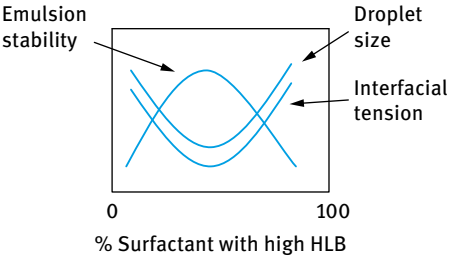

Fig. 3.3: Variation of emulsion stability, droplet size and interfacial tension with % surfactant with high HLB number.

For a simple alcohol ethoxylate, the HLB number can be calculated from the weight percent of ethylene oxide (E) and polyhydric alcohol (P),

$$\text{HLB} = \frac{E + P}{5} \tag{3.13}$$

If the surfactant contains PEO as the only hydrophilic group contribution from one OH group neglected,

$$\text{HLB} = \frac{E}{5} \tag{3.14}$$

For a nonionic surfactant $C_{12}H_{25}–O–(CH_2–CH_2–O)_6$, the HLB is 12 (suitable for O/W emulsion).

The above simple equations cannot be used for surfactants containing propylene oxide or butylene oxide. They also cannot be applied for ionic surfactants. Davies [23] devised a method for calculating the HLB number for surfactants from their chemical formulae, using empirically determined group numbers. A group number is assigned to various component groups. A summary of the group numbers for some surfactants is given in Tab. 3.3.

The HLB is given by the following empirical equation,

$$\text{HLB} = 7 + \sum(\text{hydrophilic group numbers}) - \sum(\text{lipohilic group numbers}). \tag{3.15}$$

Davies [23] has shown that the agreement between HLB numbers calculated from the above equation and those determined experimentally is quite satisfactory.

Various other procedures have been developed to obtain a rough estimate of the HLB number. Griffin found good correlation between the cloud point of 5 % solution of various ethoxylated surfactants and their HLB number.

Davies [23] attempted to relate HLB values to the selective coalescence rates of emulsions. This correlation was not found since it was found that the emulsion stability and even its type depends to a large extent on the method of dispersing the oil into the water and vice versa. At best, the HLB number can only be used as a guide for selecting optimum compositions of emulsifying agents.

One may take any pair of emulsifying agents, which fall at opposite ends of the HLB scale, e.g. Tween 80 (sorbitan monooleate with 20 mol EO, HLB = 15) and Span 80 (sorbitan monooleate, HLB = 5), using them in various proportions to cover a wide

Tab. 3.3: HLB group numbers.

	HLB group number
Hydrophilic	
$-SO_4Na^+$	38.7
–COO–	21.2
–COONa	19.1
N (tertiary amine)	9.4
Ester (sorbitan ring)	6.8
–O–	1.3
CH–(sorbitan ring)	0.5
Lipophilic	
(–CH–), ($-CH_2-$), CH_3	0.475
Derived	
$-CH_2-CH_2-O$	0.33
$-CH_2-CH_2-CH_2-O-$	–0.15

range of HLB numbers. The emulsions should be prepared in the same way, with a few percent of the emulsifying blend. The stability of the emulsions is then assessed at each HLB number from the rate of coalescence or qualitatively by measuring the rate of oil separation. In this way one may be able to find the optimum HLB number for a given oil. Having found the most effective HLB value, various other surfactant pairs are compared at this HLB value, to find the most effective pair.

3.4.2 Phase inversion temperature concept

This concept, which was developed by Shinoda [24, 25], is closely rated to the HLB balance concept described above. Shinoda and coworkers found that many O/W emulsions stabilized with nonionic surfactants undergo a process of inversion at a critical temperature (PIT). The PIT can be determined by following the emulsion conductivity (small amount of electrolyte is added to increase the sensitivity) as a function of temperature. The conductivity of the O/W emulsion increases with increase of temperature till the PIT is reached, above which there will be a rapid reduction in conductivity (W/O emulsion is formed).

Shinoda and coworkers [24, 25] found that the PIT is influenced by the HLB number of the surfactant. The size of the emulsion droplets was found to depend on the temperature and HLB number of the emulsifiers. The droplets are less stable towards coalescence close to the PIT. However, by rapid cooling of the emulsion, a stable system may be produced. Relatively stable O/W emulsions were obtained when the PIT of the system was 20–65 °C higher than the storage temperature. Emulsions prepared at a temperature just below the PIT followed by rapid cooling generally have smaller

droplet sizes. This can be understood if one considers the change of interfacial tension with temperature. The interfacial tension decreases with increase of temperature reaching a minimum close to the PIT, after which it increases. Thus, the droplets prepared close to the PIT are smaller than those prepared at lower temperatures. These droplets are relatively unstable towards coalescence near the PIT, but by rapid cooling of the emulsion one can retain their smaller size. The above procedure may be applied to prepare mini (nano) emulsions.

The optimum stability of the emulsion was found to be relatively insensitive to changes in the HLB value or the PIT of the emulsifier, but instability was very sensitive to the PIT of the system. It is essential, therefore, to measure the PIT of the emulsion as a whole (with all other ingredients). At a given HLB value, the stability of the emulsions against coalescence increases markedly as the molar mass of both the hydrophilic and lipophilic components increases. The enhanced stability using high molecular weight surfactants (polymeric surfactants) can be understood from a consideration of the steric repulsion, which produces more stable films. Films produced using macromolecular surfactants resist thinning and disruption thus reducing the possibility of coalescence.

The emulsions showed maximum stability when the distribution of the PEO chains was broad. The cloud point is lower but the PIT is higher than in the corresponding case for narrow size distributions. The PIT and HLB number are directly related parameters.

Addition of electrolytes reduces the PIT and hence an emulsifier with a higher PIT value is required when preparing emulsions in the presence of electrolytes. Electrolytes cause dehydration of the PEO chains and in effect this reduces the cloud point of the nonionic surfactant. One needs to compensate for this effect by using a surfactant with higher HLB. The optimum PIT of the emulsifier is fixed if the storage temperature is fixed. In view of the above correlation between PIT and HLB and the possible dependence of the kinetics of droplet coalescence on the HLB number, Sherman [26, 27] suggested the use of PIT measurements as a rapid method for assessing emulsion stability. However, one should be careful in using such methods for assessment of the long-term stability since the correlations were based on a very limited number of surfactants and oils. Measurement of the PIT can at best be used as a guide for preparation of stable emulsions. Assessment of the stability should be evaluated by following the droplet size distribution as a function of time using a Coulter counter or light diffraction techniques. The rheology of the emulsion as a function of time and temperature may also be used for assessment of the stability against coalescence. Care should be taken in analysing the rheological results. Coalescence results in an increase in the droplet size and this is usually followed by a reduction in the viscosity of the emulsion. This trend is only observed if the coalescence is not accompanied by flocculation of the emulsion droplets (which results in an increase in the viscosity). Ostwald ripening can also complicate the analysis of the rheological data.

3.5 Emulsion stability

Several breakdown processes may occur on storage depending on [3]:

(i) particle size distribution and density difference between the droplets and the medium;
(ii) magnitude of the attractive versus repulsive forces which determine flocculation;
(iii) solubility of the disperse droplets and the particle size distribution, which determines Ostwald ripening;
(iv) stability of the liquid film between the droplets that determines coalescence;
(v) phase inversion.

The various breakdown processes are illustrated in Fig. 3.4.
A description of each of the breakdown processes and methods that can be applied to prevent this instability is given below.

Creaming or sedimentation of emulsions is the result of gravity, when the density of the droplets and the medium are not equal. Fig. 3.5 provides a schematic picture for creaming for three cases [3].

Case (a) represents the situation for small droplets (< 0.1 μm, i.e. nanoemulsions) whereby the Brownian diffusion kT (where k is the Boltzmann constant and T is the absolute temperature) exceeds the force of gravity (mass × acceleration due to gravity g),

$$kT \ll \frac{4}{3}\pi R^3 \Delta\rho g L, \tag{3.16}$$

where R is the droplet radius, $\Delta\rho$ is the density difference between the droplets and the medium and L is the height of the container.

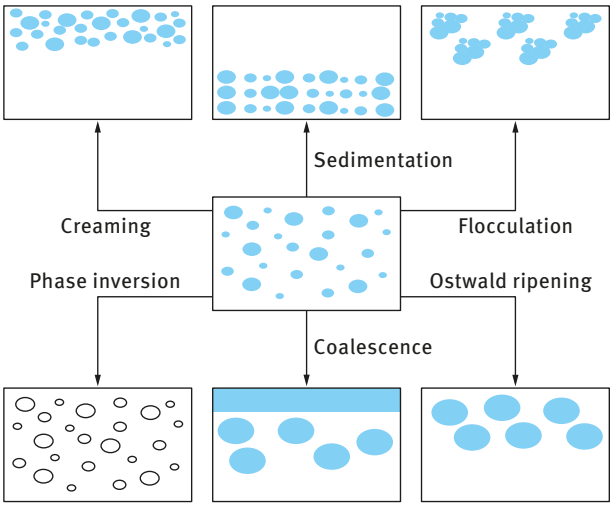

Fig. 3.4: Schematic representation of the various breakdown processes in emulsions.

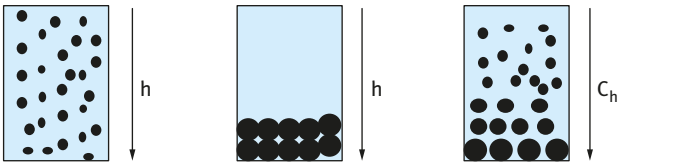

Fig. 3.5: Schematic representation of emulsion creaming.

Case (b) represents emulsions consisting of "monodisperse" droplets with radius >1 µm. In this case, the emulsion separates into two distinct layers with the droplets forming a cream leaving the clear supernatant liquid. This situation is seldom observed in practice.

Case (c) is that for polydisperse (practical) emulsions, in which case the droplets will cream at various rates. In the last case, a concentration gradient builds up with the larger droplets staying at the top of the cream layer,

$$C(h) = C_0 \exp\left(-\frac{mgh}{kT}\right), \tag{3.17}$$

$$m = \frac{4}{3}\pi R^3 \Delta\rho g, \tag{3.18}$$

where $C(h)$ is the concentration (or volume fraction ϕ) of droplets at height h, whereas C_0 is the concentration at the top of the container.

For very dilute emulsions ($\phi < 0.01$), the rate of creaming could be calculated using Stokes' law, which balances the hydrodynamic force with gravity force,

$$\text{hydrodynamic force} = 6\pi\eta R\upsilon_0, \tag{3.19}$$

$$\text{gravity force} = \frac{4}{3}\pi R^3 \Delta\rho g, \tag{3.20}$$

$$\upsilon_0 = \frac{2}{9}\frac{\Delta\rho g R^2}{\eta_0}, \tag{3.21}$$

where υ_0 is the Stokes velocity and η_0 is the viscosity of the medium.

For an O/W emulsion with $\Delta\rho = 0.2$ in water ($\eta_0 \approx 10^{-3}$ Pa s), the rate of creaming or sedimentation is $\approx 4.4 \times 10^{-5}$ m s^{-1} for 10 µm droplets and $\approx 4.4 \times 10^{-7}$ m s^{-1} for 1 µm droplets. This means that in a 0.1 m container creaming or sedimentation of the 10 µm droplets is complete in ≈ 0.6 h and for the 1 µm droplets this takes ≈ 60 h.

For moderately concentrated emulsions ($0.2 < \phi < 0.1$) one has to take into account the hydrodynamic interaction between the droplets, which reduces the Stokes velocity to a value υ, given by the following expression,

$$\upsilon = \upsilon_0(1 - k\phi), \tag{3.22}$$

where k is a constant that accounts for hydrodynamic interaction. k is of the order of 6.5, which means that the rate of creaming or sedimentation is reduced by about 65 %.

For concentrated emulsions ($\phi > 0.2$), the rate of creaming becomes a complex function of ϕ as is illustrated in Fig. 3.6, which also shows the change of relative viscosity η_r with ϕ. As can be seen from Fig. 3.8, v decreases with increase in ϕ and ultimately it approaches zero when ϕ exceeds a critical value, ϕ_p, which is the so-called "maximum packing fraction". The value of ϕ_p for monodisperse "hard-spheres" ranges from 0.64 (for random packing) to 0.74 for hexagonal packing. The value of ϕ_p exceeds 0.74 for polydisperse systems. For emulsions which are deformable, ϕ_p can also be much larger than 0.74.

The above figure also shows that when ϕ approaches ϕ_p, η_r approaches ∞. In practice most emulsions are prepared at ϕ values well below ϕ_p, usually in the range 0.2–0.5, and under these conditions creaming or sedimentation is the rule rather than the exception.

Several procedures may be applied to reduce or eliminate creaming or sedimentation.

(i) Matching density of oil and aqueous phases. Clearly, if $\Delta\rho = 0$, $v = 0$. However, this method is seldom practical. Density matching, if possible, only occurs at one temperature.

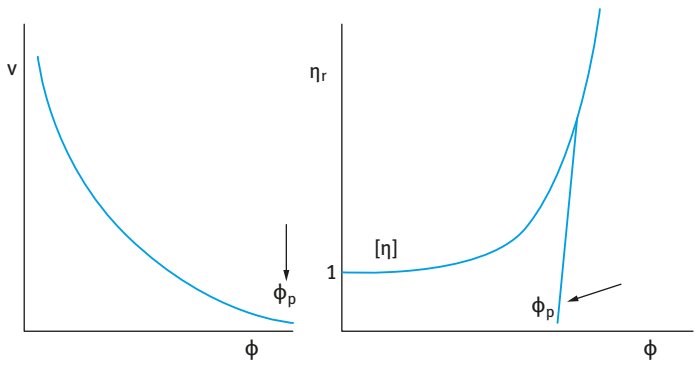

Fig. 3.6: Variation of v and η_r with ϕ

(ii) Reduction of droplet size. Since the gravity force is proportional to R^3, then if R is reduced by a factor of 10, the gravity force is reduced by 1,000. Below a certain droplet size (which also depends on the density difference between oil and water), the Brownian diffusion may exceed gravity and creaming or sedimentation is prevented. This is the principle of formulation of nanoemulsions (with size range 50–200 nm), which may show very little or no creaming or sedimentation. The same applies for microemulsions (size range 5–50 nm).

(iii) Use of "thickeners". These are high molecular weight polymers, natural or synthetic such as Xanthan gum, hydroxyethyl cellulose, alginates, carragenans, etc. To understand the role of these "thickeners", let us consider the gravitational stresses exerted during creaming or sedimentation,

$$\text{stress} = \text{mass of drop} \times \text{acceleration of gravity} = \frac{4}{3}\pi R^3 \Delta\rho g. \tag{3.23}$$

To overcome such stress one needs a restoring force,

$$\text{restoring force} = \text{area of drop} \times \text{stress of drop} = 4\pi R^2 \sigma_p. \tag{3.24}$$

Thus, the stress exerted by the droplet σ_p is given by,

$$\sigma_p = \frac{\Delta\rho R g}{3}. \tag{3.25}$$

Simple calculation shows that σ_p is in the range 10^{-3}–10^{-1} Pa, which implies that for prediction of creaming or sedimentation one needs to measure the viscosity at such low stresses. This can be obtained by using constant stress or creep measurements.

The above described "thickeners" satisfy the criteria for obtaining very high viscosities at low stresses or shear rates. This can be illustrated from plots of shear stress τ and viscosity η versus shear rate (or shear stress) as shown in Fig. 3.7

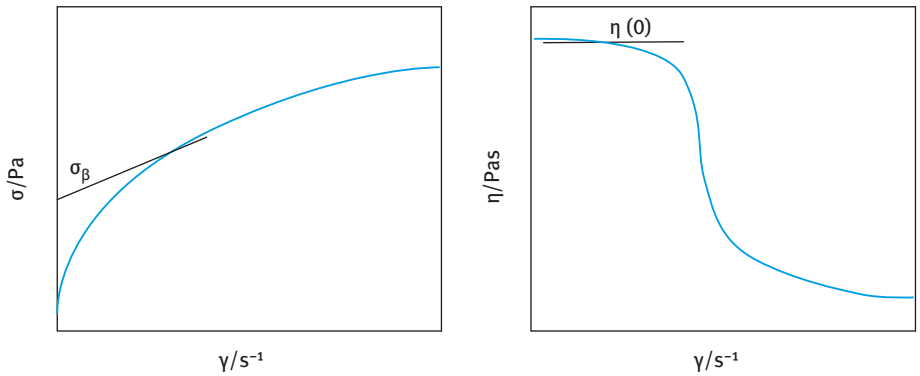

Fig. 3.7: Variation of (stress) σ and viscosity η with shear rate γ.

These systems are described as "pseudoplastic" or shear thinning. The low shear (residual or zero shear rate) viscosity $\eta(0)$ can reach several hundred Pa s and such high values prevent creaming or sedimentation. This above behaviour is obtained above a critical polymer concentration (C^*) which can be located from plots of log η versus log C. Below C^* the log η–log C curve has a slope in the region of 1, whereas above C^* the slope of the line exceeds 3.

(iv) Controlled flocculation. As described in Chapter 7 of Vol. 1, the total energy–distance of separation curve for electrostatically stabilized emulsions shows a shallow minimum (secondary minimum) at relatively long distances of separation between the droplets. With the addition of small amounts of electrolyte, this minimum can be made sufficiently deep for weak flocculation to occur. The same applies for sterically stabilized emulsions, which have only one minimum whose depth can be controlled by reducing the thickness of the adsorbed layer (Chapter 8 of Vol. 1). This can be obtained by reducing the molecular weight of the stabilizer and/or addition of a nonsolvent for the chains (e.g. electrolyte). This phenomenon of weak flocculation may be applied to reduce creaming or sedimentation, although in practice this is not easy since one also has to control the droplet size.

(v) Depletion flocculation. This is obtained by the addition of a "free" (nonadsorbing) polymer in the continuous phase [28]. At a critical concentration, or at a volume fraction of free polymer, ϕ_p^+, weak flocculation occurs, since the free polymer coils become "squeezed out" from between the droplets. This is illustrated in Fig. 3.8, which shows the situation when the polymer volume fraction exceeds the critical concentration. The osmotic pressure outside the droplets is higher than in between the droplets and this results in attraction whose magnitude depends on the concentration of the free polymer and its molecular weight, as well as the droplet size and ϕ. The value of ϕ_p^+ decreases with increase of the molecular weight of the free polymer. It also decreases as the volume fraction of the emulsion increases.

The above weak flocculation can be applied to reduce creaming or sedimentation although it suffers from the following drawbacks: Temperature dependence; as the temperature increases, the hydrodynamic radius of the free polymer decreases (due

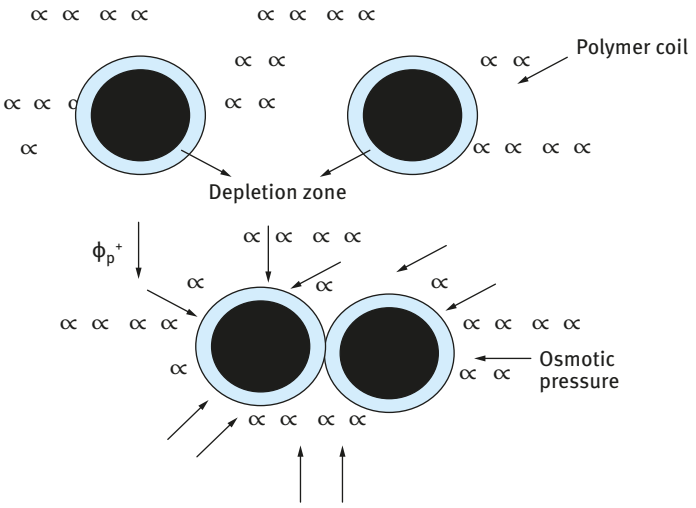

Fig. 3.8: Schematic representation of depletion flocculation.

to dehydration) and hence more polymer will be required to achieve the same effect at lower temperatures. If the free polymer concentration is increased above a certain limit, phase separation may occur and the flocculated emulsion droplets may cream or sediment faster than in the absence of the free polymer.

Flocculation of emulsions is the result of van der Waals attraction, which is universal for all disperse systems. The van der Waals attraction G_A was described in detail in Chapter 7 of Vol. 1. It showed that G_A is inversely proportional to the droplet-droplet distance of separation h and it depends on the effective Hamaker constant A of the emulsion system. One way to overcome the van der Waals attraction is by electrostatic stabilization using ionic surfactants, resulting in the formation of electrical double layers that introduce a repulsive energy that ovecomes the attractive energy. Emulsions stabilized by electrostatic repulsion become flocculated at intermediate electrolyte concentrations. The second and most effective method of overcoming flocculation is by "steric stabilization" using nonionic surfactants or polymers. Stability may be maintained in electrolyte solutions (as high as 1 mol dm^{-3} depending on the nature of the electrolyte) and up to high temperatures (in excess of 50 °C) provided the stabilizing chains (e.g. PEO) are still in better than θ-conditions ($\chi < 0.5$).

For charge-stabilized emulsions, e.g. using ionic surfactants, the most important criterion to reduce or eliminate flocculation is to make G_{max} as high as possible; this can be achieved given three main conditions, namely high surface or zeta potential, low electrolyte concentration and low valency of ions. For sterically stabilized emulsions, four main criteria are necessary:

(i) Complete coverage of the droplets by the stabilizing chains.
(ii) Firm attachment (strong anchoring) of the chains to the droplets. This requires the chains to be insoluble in the medium and soluble in the oil. However, this is incompatible with stabilization, which requires a chain that is soluble in the medium and strongly solvated by its molecules. These conflicting requirements are solved by the use of A–B, A–B–A block or BA_n graft copolymers (B is the "anchor" chain and A is the stabilizing chain(s)). Examples for the B chains for O/W emulsions are polystyrene, polymethylmethacrylate, polypropylene oxide and alkyl polypropylene oxide. For the A chain(s), polyethylene oxide (PEO) or polyvinyl alcohol are good examples.
(iii) Thick adsorbed layers. The adsorbed layer thickness should be in the region of 5–10 nm. This means that the molecular weight of the stabilizing chains could be in the region of 1,000–5,000.
(iv) The stabilizing chain should be maintained in good solvent conditions ($\chi < 0.5$) under all conditions of temperature changes on storage.

The driving force for Ostwald ripening is the difference in solubility between the small and large droplets (the smaller droplets have higher Laplace pressure and higher solubility than the larger ones). The radius r_1 of the smaller droplets decreases and that of the larger droplets r_2 increases as a result of diffusion of molecules from the smaller

to the larger droplets. The difference in chemical potential between different sized droplets was given by Lord Kelvin [29],

$$S(r) = S(\infty)\exp\left(\frac{2\gamma V_m}{rRT}\right), \tag{3.26}$$

where $S(r)$ is the solubility surrounding a particle of radius r, $S(\infty)$ is the bulk solubility, V_m is the molar volume of the dispersed phase, R is the gas constant and T is the absolute temperature. The quantity ($2\gamma V_m$/ RT) is termed the characteristic length. It has an order of ≈ 1 nm or less, indicating that the difference in solubility of a 1 μm droplet is of the order of 0.1 % or less. Theoretically, Ostwals ripening should lead to condensation of all droplets into a single drop [3]. This does not occur in practice since the rate of growth decreases with increase of droplet size.

For two droplets with radii r_1 and r_2 ($r_1 < r_2$),

$$\frac{RT}{V_m}\ln\left[\frac{S(r_1)}{S(r_2)}\right] = 2\gamma\left[\frac{1}{r_1} - \frac{1}{r_2}\right]. \tag{3.27}$$

Equation (3.27) shows that the larger the difference between r_1 and r_2, the higher the rate of Ostwald ripening.

Ostwald ripening can be quantitatively assessed from plots of the cube of the radius versus time t [30, 31],

$$r^3 = \frac{8}{9}\left[\frac{S(\infty)\gamma V_m D}{\rho RT}\right]t, \tag{3.28}$$

where D is the diffusion coefficient of the disperse phase in the continuous phase.

Several methods may be applied to reduce Ostwald ripening:

(i) Addition of a second disperse phase component which is insoluble in the continuous medium (e.g. squalane) [32]. In this case, partitioning between different droplet sizes occurs, and the component with low solubility is expected to be concentrated in the smaller droplets. During Ostwald ripening in a two component system, equilibrium is established when the difference in chemical potential between different size droplets (which results from curvature effects) is balanced by the difference in chemical potential resulting from partitioning of the two components. This effect reduces the droplets' further growth.

(ii) Modification of the interfacial film at the O/W Interface. According to equation (3.28), reduction in γ results in reduction of the Ostwald ripening rate. By using surfactants that are strongly adsorbed at the O/W interface (i.e. polymeric surfactants) and which do not desorb during ripening (by choosing a molecule that is insoluble in the continuous phase) the rate could be significantly reduced [33]. An increase in the surface dilational modulus ε (= $\mathrm{d}\gamma/\mathrm{d}\ln A$) and decrease in γ would be observed for the shrinking drop and this tends to reduce further growth. A–B–A block copolymers such as PHS–PEO–PHS (which is soluble in the oil droplets but insoluble in water) can be used to achieve this effect. This polymeric emulsifier enhances the Gibbs elasticity and causes reduction of γ to very low values.

Coalescence of emulsions may occur when two emulsion droplets come in close contact in a floc or creamed layer. During Brownian diffusion, thinning and disruption of the liquid film may also occur, resulting in eventual rupture. On close approach of the droplets, film thickness fluctuations may occur. Alternatively, the liquid surfaces undergo some fluctuations forming surface waves. The latter may grow in amplitude and the apices may join as a result of the strong van der Waals attraction (at the apex, the film thickness is the smallest). The same applies if the film thins to a small value (critical thickness for coalescence). A very useful concept was introduced by Deryaguin [34] who suggested that a "disjoining pressure" $\pi(h)$ is produced in the film, balancing the excess normal pressure,

$$\pi(h) = P(h) - P_0, \tag{3.29}$$

where $P(h)$ is the pressure of a film with thickness h and P_0 is the pressure of a sufficiently thick film such that the net interaction free energy is zero.

$\pi(h)$ may be equated to the net force (or energy) per unit area acting across the film,

$$\pi(h) = -\frac{\mathrm{d}G_\mathrm{T}}{\mathrm{d}h}, \tag{3.30}$$

where G_T is the total interaction energy in the film.

$\pi(h)$ is made of three contributions due to electrostatic repulsion (π_E), steric repulsion (π_S) and van der Waals attraction (π_A),

$$\pi(h) = \pi_\mathrm{E} + \pi_\mathrm{S} + \pi_\mathrm{A}. \tag{3.31}$$

To produce a stable film $\pi_\mathrm{E} + \pi_\mathrm{S} > \pi_\mathrm{A}$ and this is the driving force for prevention of coalescence, which can be achieved by two mechanisms and their combination:

(i) increased repulsion both electrostatic and steric;
(ii) dampening of the fluctuation by enhancing the Gibbs elasticity.

In general, smaller droplets are less susceptible to surface fluctuations and hence coalescence is reduced. This explains the high stability of nanoemulsions. Several methods may be applied to achieve these effects:

(i) Use of mixed surfactant films; using mixtures of say anionic and nonionic or long chain alcohols which reduce coalescence as a result of the high Gibbs elasticity, high surface viscosity and hindered diffusion of surfactant molecules from the film.
(ii) Formation of lamellar liquid crystalline phases at the O/W interface suggested by Friberg and coworkers [35], who showed that surfactant or mixed surfactant film can produce several bilayers that "wrap" the droplets. As a result of these multilayer structures, the potential drop is shifted to longer distances thus reducing the van der Waals attraction. For coalescence to occur, these multilayers have to be removed "two-by-two" and this forms an energy barrier preventing coalescence.

Since film drainage and rupture is a kinetic process, coalescence is also a kinetic process. If one measures the number of particles n (flocculated or not) at time t,

$$n = n_t + n_v m, \tag{3.32}$$

where n_t is the number of primary particles remaining, n is the number of aggregates consisting of m separate particles.

For studding emulsion coalescence, one should consider the rate constant of flocculation and coalescence. If coalescence is the dominant factor, then the rate K follows a first-order kinetics,

$$n = \frac{n_0}{Kt}[1 + \exp -(Kt)] \tag{3.33}$$

which shows that a plot of log n versus t should give a straight line from which K can be calculated.

Phase inversion of emulsions can be one of two types: Transitional inversion induced by changing facers which affect the HLB of the system, e.g. temperature and/or electrolyte concentration. Catastrophic inversion, which is induced by increasing the volume fraction of the disperse phase [3]. Earlier theories of phase inversion were based on packing parameters. When ϕ exceeds the maximum packing (≈ 0.64 for random packing and ≈ 0.74 for hexagonal packing of monodisperse spheres; for polydisperse systems, the maximum packing exceeds 0.74) inversion occurs. However, these theories are not adequate, since many emulsions invert at ϕ values well below the maximum packing as a result of the change in surfactant characteristics with variation of conditions. For example, when using a nonionic surfactant based on PEO, the latter chain changes its solvation by increase of temperature and/or addition of electrolyte. Many emulsions experience phase inversion at a critical temperature (the phase inversion temperature) that depends on the HLB number of the surfactant as well as the presence of electrolytes. By increasing temperature and/or addition of electrolyte, the PEO chains become dehydrated and finally they become more soluble in the oil phase. Under these conditions, the O/W emulsion will invert to a W/O emulsion. This dehydration effect amounts to a decrease in the HLB number and when the latter reaches a value that is more suitable for W/O emulsion inversion will occur. At present, there is no quantitative theory that accounts for phase inversion of emulsions.

Several methods may be applied to assess the stability of the emulsion on storage. The rate of creaming or sedimentation of emulsion can be qualitatively assessed by direct observation of emulsion separation using graduated cylinders that are placed at constant temperature. This method allows one to obtain the rate as well as the equilibrium cream or sediment volume. Quantitatively one can measure the turbidity measurements as a function of height at various times, using for example the Turboscan (which measures turbidity from the back scattering of near IR light). Alternatively one can measure the ultrasonic velocity and absorption at various heights in the cream or sedimentation tubes [3].

The rate of flocculation of the emulsion can be assessed for a dilute system (which may be obtained by carefully diluting the concentrate in the supernatant liquid), by measuring turbidity, τ, as a function of time,

$$\tau = An_0V_1^2(1 + n_0kt), \tag{3.34}$$

where A is an optical constant, n_0 is the number of droplets at time $t = 0$, V_1 is the volume of the droplets and k is the rate constant of flocculation.

Thus, a plot of τ versus t gives a straight line, in the initial time of flocculation, and k can be calculated from the slope of the line. Flocculation of emulsions can also be assessed by direct droplet counting using optical microscopy (with image analysis), using the Coulter counter and light diffraction techniques (e.g. using the Mastersizer, Malvern, UK).

The flocculation of emulsion concentrate can be followed using rheological methods. In the absence of any Ostwald ripening and/or coalescence, flocculation of the emulsion concentrates is accompanied by an increase in its viscosity, yield value or elastic modulus. These rheological parameters can be easily measured using rotational viscometers. Clearly, if Ostwald ripening and/or coalescence occurs at the same time as emulsion flocculation, the parameters of viscosity, yield value or elastic modulus depend complexly on time and this makes analysis of the rheological results very difficult.

The best procedure to follow Ostwald ripening is to plot r^3 versus time, following equation (3.28). This gives a straight line from which the rate of Ostwald ripening can be calculated. In this way, one can assess the effect of the various additives that may reduce Ostwald ripening, e.g. addition of highly insoluble oil and/or an oil soluble polymeric surfactant.

The rate of coalescence is measured by following the droplet number n or average droplet size d (diameter) as a function of time. Plots of log droplet number or average diameter versus time give straight lines (at least in the initial stages of coalescence) from which the rate of coalescence K can be estimated using equation (3.33). In this way, one can compare the different stabilizers, e.g. mixed surfactant films, liquid crystalline phase and macromolecular surfactants.

The most common procedure to assess phase inversion is to measure the conductivity or the viscosity of the emulsion as a function of ϕ, increase of temperature and/or addition of electrolyte. For example, for an O/W emulsion, phase inversion to W/O is accompanied by a rapid decrease in conductivity and viscosity.

4 Formulation of suspension concentrates

4.1 Introduction

The formulation of agrochemicals as dispersions of solids in aqueous solution (referred to here as suspension concentrates or SCs) has many advantages when compared with wettable powders. First, one can control the particle size by controlling the milling conditions and proper choice of the dispersing agent. Second, it is possible to incorporate high concentrations of surfactants into the formulation, which is sometimes essential for enhancing wetting, spreading and penetration. Stickers may also be added to enhance adhesion and in some cases to provide slow release. There has been considerable research into the factors that govern the stability of suspension concentrates [36–38]. The theories of colloid stability could be applied to predict the physical states of these systems on storage. In addition, analysis has been undertaken of the problem of sedimentation on SCs at a fundamental level [37]. Since the density of the particles is usually larger than that of the medium (water), SCs tend to separate as a result of sedimentation. The sedimented particles tend to form a compact layer at the bottom of the container (sometimes referred to as clay or cake), which is very difficult to redisperse. It is, therefore, essential to reduce sedimentation and formation of clays by incorporating an anti-settling agent.

In this section, I will attempt to address the above-mentioned phenomena at a fundamental level. The section will start with a section on the preparation of suspension concentrates and the role of surfactants (dispersing agents). This is followed by a section on the control of the physical stability of suspensions. The problem of Ostwald ripening (crystal growth) will also be briefly described and particular attention will be paid to the role of surfactants. The next section will deal with the problem of sedimentation and prevention of claying. The various methods that may be applied to reduce sedimentation and prevention of the formation of hard clays will be summarized. The last part in this section will deal with the methods that may be applied for the assessment of the physical stability of SCs. For the assessment of flocculation and crystal growth, particle size analysis techniques are commonly applied. The bulk properties of the suspension, such as sedimentation, separation and redispersion on dilution may be assessed using rheological techniques. The latter will be summarized with particular emphasis on their application in the prediction of the long-term physical stability of suspension concentrates.

https://doi.org/10.1515/9783110588002-005

4.2 Preparation of suspension concentrates and the role of surfactants/dispersing agents

Suspension concentrates are usually formulated using a wet milling process which requires the addition of a surfactant/dispersing agent. The latter should satisfy the following criteria:

(i) A good wetting agent for the agrochemical powder (both external and internal surfaces of the powder aggregates or agglomerates must be spontaneously wetted).

(ii) A good dispersing agent to break such aggregates or agglomerates into smaller units and subsequently help in the milling process (one usually aims at a dispersion with a volume mean diameter of 1–2 μm).

(iii) It should provide good stability in the colloid sense (this is essential for maintaining the particles as individual units once formed). Powerful dispersing agents are particularly important for the preparation of highly concentrated suspensions (sometimes require for seed dressing). Any flocculation will cause a rapid increase in the viscosity of the suspension and this makes the wet milling of the agrochemical a difficult process

Dry powders of organic compounds usually consist of particles of various degrees of complexity, depending on the isolation stages and the drying process. Generally, the particles in a dry powder form aggregates (in which the particles are joined together with their crystal faces) or agglomerates (in which the particles touch at edges or corners) forming a looser, more open structure. It is essential in the dispersion process to wet the external as well as the internal surfaces and displace the air entrapped between the particles. This is usually achieved by the use of surface active agents of the ionic or nonionic type. In some cases, macromolecules or polyelectrolytes may be efficient in this wetting process. This may be the case since these polymers contain a very wide distribution of molecular weights and the low molecular weight fractions may act as efficient wetting agents. For efficient wetting, the molecules should lower the surface tension of water (see below) and they should diffuse quickly in solution and quickly become adsorbed at the solid/solution interface.

Wetting of a solid is usually described in terms of the equilibrium contact angle θ and the appropriate interfacial tensions, as described in Chapter 5 of Vol. 1. The contact angle θ is related to the solid/vapour, solid liquid and liquid/vapour interfacial tensions γ_{SV}, γ_{SL} and γ_{LV} respectively by Young's equation,

$$\gamma_{SV} - \gamma_{SL} = \gamma_{LV} \cos\theta \tag{4.1}$$

or

$$\cos\theta = \frac{(\gamma_{SV} - \gamma_{SL})}{\gamma_{LV}}. \tag{4.2}$$

It is clear from equation (4.2) that if $\theta < 90°$, a reduction in γ_{SL} and γ_{LV} improves wetting. Hence the use of surfactants which reduce both γ_{SL} and γ_{LV} to aid wetting is clear. However, the process of wetting particulate solids is more complex and it involves at least three distinct types of wetting [5], namely adhesional wetting, spreading wetting and immersional wetting. All these processes are determined by the liquid surface tension and the contact angle. The difference between γ_{SV} and γ_{SL} or $\gamma_{LV} \cos\theta$ is referred to as adhesion or wetting tension.

Let us consider an agrochemical powder with surface area A. Before the powder is dispersed in the liquid, it has a surface tension γ_{SV} and after immersion in the liquid it has a surface tension γ_{SL}. The work of dispersion W_d is simply given by the difference in adhesion or wetting tension of the SL and SV,

$$W_d = A(\gamma_{SL} - \gamma_{SV}) = -A\gamma_{LV} \cos\theta. \tag{4.3}$$

It is clear from equation (4.3) that if $\theta < 90°$, $\cos\theta$ is positive and W_d is negative, i.e. wetting of the powder is spontaneous. Since surfactants are added in sufficient amounts ($\gamma_{dynamic}$ is lowered sufficiently) spontaneous dispersion is the rule rather than the exception.

Wetting of the internal surface requires penetration of the liquid into channels between and inside the agglomerates. This process is similar to forcing a liquid through fine capillaries. To force a liquid through a capillary with radius r, a pressure p is required that is given by,

$$p = -\frac{2\gamma_{LV} \cos\theta}{r} = \left[\frac{-2(\gamma_{SV} - \gamma_{SL})}{r\gamma_{LV}}\right]. \tag{4.4}$$

γ_{SL} has to be made as small as possible; rapid surfactant adsorption to the solid surface, low θ. When $\theta = 0$, $p \propto \gamma_{LV}$. Thus a high γ_{LV} is required for penetration into pores. Thus, wetting of the external surface requires a low contact angle θ and low surface tension γ_{LV}. Wetting of the internal surface (i.e. penetration through pores) requires a low θ but high γ_{LV}. These two conditions are incompatible and a compromise must be made: $\gamma_{SV} - \gamma_{SL}$ must be kept at a maximum; γ_{LV} should be kept as low as possible but not too low.

The above conclusions illustrate the problem of choosing the best dispersing agent for a particular powder. This requires measurement of the above parameters as well as testing the efficiency of the dispersion process.

The next stage to be considered is the wetting of the internal surface, which implies penetration of the liquid into channels between and inside the agglomerates. This is more difficult to define precisely. However, one may make use of the equation derived for capillary phenomena as discussed by Rideal and Washburn [39, 40], who considered the penetration of liquids in capillaries.

For horizontal capillaries (gravity neglected), the depth of penetration l in time t is given by the Rideal–Washburn equation [39, 40],

$$l = \left[\frac{rt\gamma_{LV} \cos\theta}{2\eta}\right]^{1/2}. \tag{4.5}$$

To enhance the rate of penetration, γ_{LV} must be as high as possible, θ as low as possible and η as low as possible.

For dispersion of powders into liquids one should use surfactants that lower θ while not reducing γ_{LV} too much. The viscosity of the liquid should also be kept at a minimum. Thickening agents (such as polymers) should not be added during the dispersion process. It is also necessary to avoid foam formation during the dispersion process.

For a packed bed of particles, r may be replaced by k, which contains the effective radius of the bed and a tortuosity factor, which takes into account the complex path formed by the channels between the particles, i.e.,

$$l^2 = \frac{kt\gamma_{LV}\cos\theta}{2\eta}. \tag{4.6}$$

Thus a plot of l^2 versus t gives a straight line and from the slope of the line one can obtain θ.

The Rideal–Washburn equation [39, 40] can be applied to obtain the contact angle of liquids (and surfactant solutions) in powder beds. k should first be obtained using a liquid that produces a zero contact angle. A packed bed of powder is prepared, for example, in a tube fitted with a sintered glass at the end (to retain the powder particles). It is essential to pack the powder uniformly in the tube (a plunger may be used in this case). The tube containing the bed is immersed in a liquid that gives spontaneous wetting (e.g. a lower alkane), i.e. the liquid gives a zero contact angle and $\cos\theta = 1$. By measuring the rate of penetration of the liquid (this can be carried out gravimetrically using for example a microbalance or a Kruss instrument) one can obtain k. The tube is then removed from the lower alkane liquid and left to stand for evaporation of the liquid. It is then immersed in the liquid in question and the rate of penetration is measured again as a function of time. Using equation (4.6), one can calculate $\cos\theta$ and hence θ.

Thus, in summary, the dispersion of a powder in a liquid depends on three main factors, namely the energy of wetting of the external surface, the pressure involved in the liquid penetrating inside and between the agglomerates and the rate of penetration of the liquid into the powder. All these factors are related to two main parameters, namely γ_{LV} and θ. In general, the process is likely to be more spontaneous the lower the θ and the higher γ_{LV}. Since these two factors tend to operate in opposite senses, the choice of the proper surfactant (dispersing agent) can be a difficult task.

The dispersion of aggregates and agglomerates into smaller units requires high speed mixing, e.g. an Ultra-Turrax or Silverson mixer. In some cases, the dispersion process is easy and the capillary pressure may be sufficient to break up the aggregates and agglomerates into primary units. The process is aided by the surfactant, which becomes adsorbed on the particle surface. However, one should be careful during the mixing process not to entrap air (foam) which causes an increase in the viscosity of the suspension and prevents easy dispersion and subsequent grinding. If foam formation

becomes a problem, one should add antifoaming agents such as polysiloxane antifoaming agents.

After completing the dispersion process, the suspension is transferred to a ball or bead mill for size reduction. Milling or comminution (the generic term for size reduction) is a complex process and there is little fundamental information on its mechanism. For the breakdown of single crystals into smaller units, mechanical energy is required. This energy in a bead mill, for example, is supplied by impaction of the glass beads with the particles. As a result, permanent deformation of the crystals and crack initiation result. This will eventually lead to the fracture of the crystals into smaller units. However, since the milling conditions are random, it is inevitable that some particles receive impacts that are far in excess of those required for fracture, whereas others receive impacts that are insufficient to fracture them. This makes the milling operation grossly inefficient and only a small fraction of the applied energy is actually used in comminution. The rest of the energy is dissipated as heat, vibration, sound, interparticulate friction, friction between the particles and beads, and elastic deformation of unfractured particles. For these reasons, milling conditions are usually established by a trial and error procedure. Of particular importance is the effect of various surface active agents and macromolecules on the grinding efficiency. The role played by these agents in the comminution process is far from being understood, although Rehbinder and collaborators [41] have given this problem particular consideration. As a result of adsorption of surfactants at the solid/liquid interface, the surface energy at the boundary is reduced, which facilitates the process of deformation or destruction. The adsorption of the surfactant at the solid/solution interface in cracks facilitates their propagation. This is usually referred to as the "Rehbinder effect" [41]. The surface energy manifests itself in destructive processes on solids, since the generation and growth of cracks and separation of one part of a body from another is directly connected with the development of new free surface. Thus, as a result of adsorption of surface active agents at structural defects in the surface of the crystals, fine grinding is facilitated. In the extreme case where there is a very great reduction in surface energy at the sold/liquid boundary, spontaneous dispersion may take place with the result that colloidal particles (< 1 μm) are formed. Rehbinder [41] has developed a theory to explain this spontaneous dispersion.

Surfactants lower the surface tension of water, γ, and they adsorb at the solid/liquid interface. A plot of γ_{LV} versus log C (where C is the surfactant concentration) results in a gradual reduction in γ_{LV} followed by a linear decrease of γ_{LV} with log C (just below the critical micelle concentration, cmc). When the cmc is reached γ_{LV} remains virtually constant. This was discussed in detail in Chapter 4 of Vol. 1. From the slope of the linear portion of the γ–log C curve (just below the cmc), one can obtain the surface excess (number of moles of surfactant per unit area at the L/A interface). Using the Gibbs adsorption isotherm,

$$\frac{d\gamma}{d \log C} = -2.303 RT \Gamma, \tag{4.7}$$

where Γ is the surface excess (mol m^{-2}), R is the gas constant and T is the absolute temperature.

From Γ one can obtain the area per molecule,

$$\text{area per molecule} = \frac{1}{\Gamma N_{av}}\ [\text{m}^2] = \frac{10^{18}}{\Gamma N_{av}}\ [\text{nm}^2]. \tag{4.8}$$

Most surfactants produce a vertically oriented monolayer just below the cmc. The area/molecule is usually determined by the cross-sectional area of the head group. For ionic surfactants containing, for example, a $-OSO_3-$ or $-SO_3-$ head group, the area per molecule is in the region of 0.4 nm^2. For nonionic surfactants containing several moles of ethylene oxide (12–14), the area per molecule can be much larger (1–2 nm^2). Surfactants will also adsorb at the solid/liquid interface. For hydrophobic surfaces, the main driving force for adsorption is by hydrophobic bonding. This results in lowering of the contact angle of water on the solid surface. For hydrophilic surfaces, adsorption occurs via the hydrophilic group, e.g. cationic surfactants on silica. Initially, the surface becomes more hydrophobic and the contact angle θ increases with increase in surfactant concentration. However, at higher cationic surfactant concentration, a bilayer is formed by hydrophobic interaction between the alkyl groups and the surface becomes more and more hydrophilic and eventually the contact angle reaches zero at high surfactant concentrations.

Smolders [42] suggested the following relationship for change of θ with C,

$$\frac{d\gamma_{LV}\cos\theta}{d\ln C} = \frac{d\gamma_{SV}}{d\ln C} - \frac{d\gamma_{SL}}{d\ln C}. \tag{4.9}$$

Using the Gibbs equation,

$$\sin\theta\left(\frac{dd\gamma}{d\ln C}\right) = RT(\Gamma_{SV} - \Gamma_{SL} - \gamma_{LV}\cos\theta). \tag{4.10}$$

Since $\gamma_{LV}\sin\theta$ is always positive, $(d\theta/d\ln C)$ will always have the same sign as the RHS of equation (4.10). Three cases may be distinguished:

- $(d\theta/d\ln C) < 0$; $\Gamma_{SV} < \Gamma_{SL} + \Gamma_{LV}\cos\theta$; addition of surfactant improves wetting.
- $(d\theta/d\ln C) = 0$; $\Gamma_{SV} = \Gamma_{SL} + \Gamma_{LV}\cos\theta$; surfactant has no effect on wetting.
- $(d\theta/d\ln C) > 0$; $\Gamma_{SV} > \Gamma_{SL} + \Gamma_{LV}\cos\theta$; surfactant causes dewetting.

4.3 Control of the physical stability of suspension concentrates

When considering the stability of suspension concentrates one must distinguish between the colloid stability and the overall physical stability. Colloid stability implies an absence of any aggregation between the particles which requires the presence of an energy barrier that is produced by electrostatic, steric repulsion or combination of the two (electrosteric). Physical stability implies the absence of any sedimentation

and/or separation, ease of dispersion on shaking and/or dilution in the spray tanks. As will be discussed later, to achieve overall physical stability one may apply control and reversible flocculation methods and/or use a rheology modifier.

The colloid stability can be described in terms of three different energy–distance curves:

(i) electrostatic, produced for example by the presence of ionogenic groups on the surface of the particles, or adsorption of ionic surfactants;
(ii) steric, produced for example by adsorption of nonionic surfactants or polymers;
(iii) electrosatic + steric (electrosteric) as for example produced by polyelectrolytes.

These are illustrated below in Fig. 4.1.

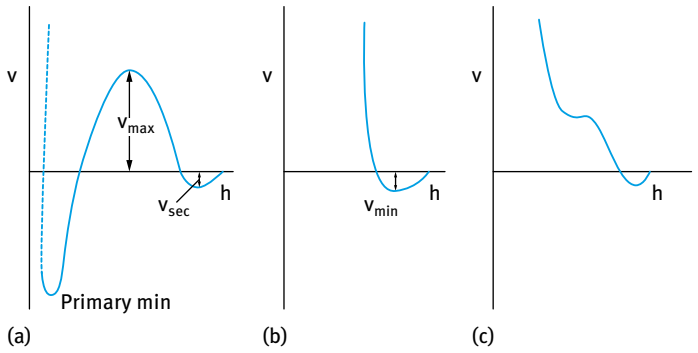

Fig. 4.1: Energy–distance curves for three stabilization mechanisms.

The control of stability against irreversible flocculation (where the particles are held together into aggregates that cannot be redispersed by shaking or on dilution) is achieved by the use of powerful dispersing agents, e.g. surfactants of the ionic or nonionic type, nonionic polymers or polyelectrolytes. These dispersing agents must be strongly adsorbed onto the particle surfaces and fully cover them. With ionic surfactants, irreversible flocculation is prevented by the repulsive force generated from the presence of an electrical double layer at the particle solution interface. Depending on the conditions, this repulsive force can be made sufficiently large to overcome the ubiquitous van der Waals attraction between the particles at intermediate distances of separation.

With nonionic surfactants and macromolecules, repulsion between the particles is ensured by the steric interaction of the adsorbed layers on the particle surfaces (Chapter 8 of Vol. 1). With polyelectrolytes, both electrostatic and steric repulsion exist.

Ionic surfactants such as sodium dodecyl benzene sulphonate (NaDBS) or cetyl trimethyl ammonium chloride (CTACl) adsorb on hydrophobic particles of agrochem-

icals as a result of the hydrophobic interaction between the alkyl group of the surfactant and the particle surface. As a result, the particle surface will acquire a charge that is compensated by counter ions (Na^+ in the case of NaDBS and Cl^- in the case of CTACl), forming an electrical double layer.

The adsorption of ionic surfactants at the solid/solution interface is of vital importance in determining the stability of suspension concentrates. As discussed in Chapter 5 of Vol. 1, the adsorption of ionic surfactants on solid surfaces can be directly measured by equilibrating a known amount of solid (with known surface area) with surfactant solutions of various concentrations. After reaching equilibrium, the solid particles are removed (for example by centrifugation) and the concentration of surfactant in the supernatant liquid is determined analytically. From the difference between the initial and final surfactant concentrations (C_1 and C_2, respectively), the number of moles of surfactant adsorbed, Γ, per unit area of solid is determined and the results may be fitted to a Langmuir isotherm,

$$\Gamma = \frac{\Delta C}{mA} = \frac{abC_2}{1 + bC_2} \tag{4.11}$$

where $\Delta C = C_1 - C_2$, m is the mass of the solid with surface area A, a is the saturation adsorption and b is a constant that is related to the free energy of adsorption, ΔG ($b \propto \exp \Delta G/RT$). From a, the area per surfactant ion on the surface can be calculated (area per surfactant ion = $1/aN_{av}$).

The above discussion shows that ionic surfactants can be used to stabilize agrochemical suspensions by producing sufficient electrostatic repulsion. When two particles with adsorbed surfactant layers approach each other to a distance where the electrical double layers begin to overlap, strong repulsion occurs preventing any particle aggregation (Chapter 7 of Vol. 1). The energy–distance curve for such electrostatically stabilized dispersions is schematically shown in Fig. 4.1 (a). This has an energy maximum, which if high enough ($> 25kT$) prevents particle aggregation into the primary minimum. However, ionic surfactants are the least attractive dispersing agents for the following reasons. Adsorption of ionic surfactants is seldom strong enough to prevent some desorption with the result of production of "bare" patches which may induce particle aggregation. The system is also sensitive to ionic impurities which are present in the water used for suspension preparation. In particular, the system will be sensitive to bivalent ions (Ca^{2+} or Mg^{2+}) which produce flocculation at relatively low concentrations.

Nonionic surfactants of the ethoxylate type, e.g. $R(CH_2CH_2O)_nOH$ or $RC_6H_5(CH_2CH_2O)_nOH$, provide a better alternative provided the molecule contains sufficient hydrophobic groups to ensure their adsorption and enough ethylene oxide units to provide an adequate energy barrier. As discussed in Chapter 8 of Vol. 1, the origin of steric repulsion arises from two main effects. The first effect arises from the unfavourable mixing of the poly(ethylene oxide) chains which are in good solvent conditions (water as the medium). This effect is referred to as the mixing or osmotic

repulsion. The second effect arises from the loss in configurational entropy of the chains when these are forced to overlap on approach of the particles. This is referred to as the elastic or volume restriction effect. The energy–distance curve for such systems (Fig. 4.1 (b)) clearly demonstrates the attraction of steric stabilization. Apart from a small attractive energy minimum (which can be reasonably shallow with sufficiently long poly(ethylene oxide) chains), strong repulsion occurs and there is no barrier to overcome. A better option is to use block and graft copolymers (polymeric surfactants) consisting of A and B units combined together in A–B, A–B–A or BA_n fashion. B represents units with high affinity for the particle surface that are basically insoluble in the continuous medium, thus providing strong adsorption ("anchoring units"). A, on the other hand, represents units with high affinity to the medium (high chain-solvent interaction) and little or no affinity to the particle surface. An example of such a powerful dispersant is a graft copolymer of polymethyl methacrylate-methacrylic acid (the anchoring portion) and methoxy polyethylene oxide (the stabilizing chain) methacrylate [5]. Adsorption measurements of such a polymer on a pesticide, namely ethirimol (a fungicide), showed a high affinity isotherm with no desorption. By using such a macromolecular surfactant, a suspension of high volume fractions could be prepared.

The third class of dispersing agents which is commonly used in SC formulations is that of polyelectrolytes. Of these, sulphonated naphthalene-formaldehyde condensates and lignosulphonates are the most commonly used in agrochemical formulations. These systems have a combined electrostatic and steric repulsion and the energy–distance curve is schematically illustrated in Fig. 4.1 (c). It has a shallow minimum and maximum at intermediate distances (characteristic of electrostatic repulsion) and exhibits strong repulsion at relatively short distances (characteristic of steric repulsion). The stabilization mechanism of polyelectrolytes is sometimes referred to as electrosteric. These polyelectrolytes offer some versatility in SC formulations. Since the interaction is fairly long-range in nature (due to the double layer effect), one does not obtain "hard sphere" type behaviour which may lead to the formation of hard sediments. The steric repulsion ensures the colloid stability and prevents any aggregation on storage.

There are several ways in which crystals can grow in an aqueous suspension. One of the most familiar is the phenomenon of "Ostwald ripening", which occurs as a result of the difference in solubility between the small and large crystals [43],

$$\frac{RT}{M}\ln\frac{S_1}{S_2} = \frac{2\sigma}{\rho}\left(\frac{1}{r_1} - \frac{1}{r_2}\right), \tag{4.12}$$

where S_1 and S_2 are the solubilities of crystals of radii r_1 and r_2 respectively, σ is the specific surface energy, ρ is the density, M is the molecular weight of the solute molecules, R is the gas constant and T is the absolute temperature. Since r_1 is smaller than r_2, S_1 is larger than S_2. Another mechanism for crystal growth is related to polymorphic changes in solutions, and again the driving force is the difference in solubility

between the two polymorphs. In other words, the less soluble form grows at the expense of the more soluble phase. This is sometimes also accompanied by changes in the crystal habit. Different faces of the crystal may have different surface energies and deposition may preferentially take place on one of the crystal faces, modifying its shape. Other important factors are the presence of crystal dislocations, kinks, surface impurities, etc. The growth of crystals in suspension concentrates may create undesirable changes. As a result of the drastic change in particle size distribution, the settling of the particles may be accelerated, leading to caking and cementing together of some particles in the sediment. Moreover, increase in particle size may lead to a reduction in biological efficiency. Thus, prevention of crystal growth or at least reducing it to an acceptable level is essential in most suspension concentrates. Surfactants affect crystal growth in a number of ways. The surfactant may affect the rate of dissolution by affecting the rate of transport away from the boundary layer at the crystal solution interface. On the other hand, if the surfactant forms micelles that can solubilize the solute, crystal growth may be enhanced as a result of increasing the concentration gradient. Thus, with the proper choice of dispersing agent one may reduce crystal growth in suspension concentrates. This has been demonstrated for terbacil suspensions [1, 2]. When using Pluronic P75 (polyethylene oxide–polypropylene oxide block copolymer), crystal growth was significant. By replacing the Pluronic surfactant with polyvinyl alcohol, the rate of crystal growth was greatly reduced and the suspension concentrate was acceptable.

It should be mentioned that many surfactants and polymers may act as crystal growth inhibitors if they adsorb strongly on the crystal faces, thus preventing solute deposition. However, the choice of an inhibitor is still an art and there are not many rules that can be used to select crystal growth inhibitors.

Once a dispersion that is stable in the colloid sense has been prepared, the next task is to eliminate claying or caking. This is the consequence of the colloidally stable suspension particles settling. The repulsive forces necessary to ensure this colloid stability allow the particles to move past each other, forming a dense sediment which is very difficult to redisperse. Such sediments are dilatant (shear thickening, see section on rheology) and hence the SC becomes unusable.

The sedimentation velocity v_0 of a very dilute suspension of rigid non-interacting particles with radius a can be determined by equating the gravitational force with the opposing hydrodynamic force, as given by Stokes' law, as described in Chapter 3,

$$v_0 = \frac{2}{9}\frac{\Delta\rho g R^2}{\eta_0}, \tag{4.13}$$

where $\Delta\rho$ is the density difference between the particles and the medium, η_0 is the viscosity of the medium and g is the acceleration due to gravity. Equation (4.13) predicts a sedimentation rate for particles with radius 1 μm in a medium with a density difference of 0.2 g cm^{-3} and a viscosity of 1 mPa s (i.e. water at 20 °C) of 4.4×10^{-7} m s^{-1}. Such particles will sediment to the bottom of a 0.1 m container in about 60 h. For 10 μm

particles, the sedimentation velocity is 4.4×10^{-5} m s^{-1} and such particles will sediment to the bottom of 0.1 m container in about 40 minutes.

The above treatment using Stokes' law applied only to very dilute suspensions (volume fraction $\phi < 0.01$). For more concentrated suspensions, the particles no longer sediment independently from each other and one has to take into account both the hydrodynamic interaction between the particles (which applies for moderately concentrated suspensions) and other higher order interactions at relatively high volume fractions. A theoretical relationship between the sedimentation velocity v of non-flocculated suspensions and particle volume fraction has been derived by Batchelor [44]. Such theories apply to relatively low volume fractions (< 0.1) and they show that the sedimentation velocity v at a volume fraction ϕ is related to that at infinite dilution v_0 (the Stokes velocity) by an equation of the form,

$$v = v_0(1 - k\phi), \tag{4.14}$$

where k is a constant that is equal to 6.55. This theory applies up to a volume fraction of 0.1. At higher volume fractions, the sedimentation velocity becomes a complex function of ϕ and only empirical equations are available to describe the variation of v with ϕ. However, there is a correlation between the reduction in sedimentation rate and the increase in relative viscosity of the suspension as the volume fraction of the suspension is increased. This is schematically shown in Fig. 4.2, which shows that $v \to 0$ and $\eta_r \to \infty$ as $\phi \to \phi_p$. The latter is referred to as the maximum packing fraction (equal to 0.74 for hexagonally arranged equal size spheres and 0.64 for random packing of these spheres). This implies that suspension concentrates with volume fractions approaching the maximum packing do not show any appreciable settling.

However, such dense suspensions have extremely high viscosities and are not a practical solution for reducing settling. In most cases, one prepares a suspension concentrate at practical volume fractions (0.2–0.4) and then uses an anti-settling agent to reduce settling. Most of the anti-settling agents used in practice are high molecular

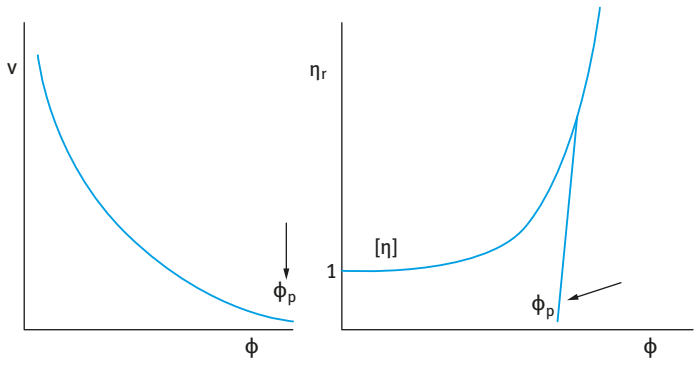

Fig. 4.2: Variation of v and η_r with ϕ.

weight polymers. These materials show an increase in the viscosity of the medium with increase in their concentration. However, at a critical polymer concentration (which depends on the nature of the polymer and its molecular weight), they show a very rapid increase in viscosity with further increase in their concentration. This critical concentration (sometimes denoted by C^*) represents the situation where the polymer coils or rods begin to overlap. Under these conditions, the solutions become significantly non-Newtonian (viscoelastic, see section on rheology) and they produce stresses that are sufficient to overcome the stress exerted by the particles. The settling of suspensions in these non-Newtonian fluids is not simple since one has to consider the non-Newtonian behaviour of these polymer solutions. This problem has been addressed by Buscall et al. [45], who studied the setting of polystyrene particles with radius 1.55 μm in ethyl hydroxyethyl cellulose (EHEC) at various concentrations. In order to adequately describe the settling of particles in non-Newtonian fluids one need to know how the viscosity of the medium changes with shear rate or shear stress. Most of these viscoelastic fluids show a gradual increase in viscosity with decrease of shear rate or shear stress, but below a critical stress or shear rate they show a Newtonian region with a limiting high viscosity that is denoted as the residual (or zero shear) viscosity. This is illustrated in Fig. 4.3, which shows the variation of the viscosity with shear stress for a number of solutions of EHEC at various concentrations. It can be seen that the viscosity increases with decrease of stress and the limiting value, i.e. the residual viscosity $\eta(0)$, and increases rapidly with increase in polymer concentration. The shear thinning behaviour of these polymer solutions is shown clearly, since above

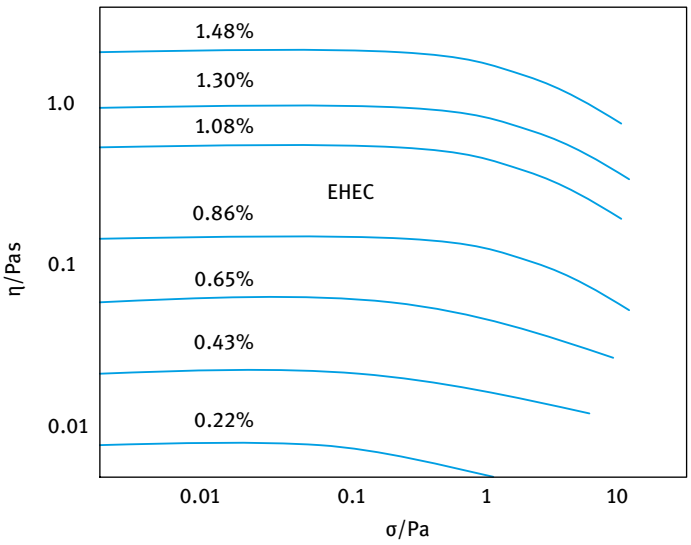

Fig. 4.3: Constant stress (creep) measurements for PS latex dispersions as a function of EHEC concentration.

a critical stress value the viscosity decreases rapidly with increase in shear stress. The limiting value of the viscosity is reached at low stresses (< 0.2 Pa).

It is now important to calculate the stress exerted by the particles. This stress is equal to $R\Delta\rho g/3$. For polystyrene latex particles with radius 1.55 µm and density 1.05 g cm^{-3}, this stress is equal to 1.6×10^{-4} Pa. This stress is lower than the critical stress for most EHEC solutions. In this case, one would expect a correlation between the settling velocity and the zero shear viscosity. This is illustrated in Fig. 4.4 whereby v/a^2 is plotted versus $\eta(0)$. As is clear, a linear relationship between $\log(v/R^2)$ and $\log \eta(0)$ is obtained, with a slope of –1 over three decades of viscosity. This indicates that the settling rate is proportional to $[\eta(0)]^{-1}$. Thus, the settling rate of isolated spheres in non-Newtonian (pseudoplastic) polymer solutions is determined by the zero shear viscosity in which the particles are suspended. As we will see in the section on rheological measurements, determination of the zero shear viscosity is not straightforward and requires the use of constant stress rheometers.

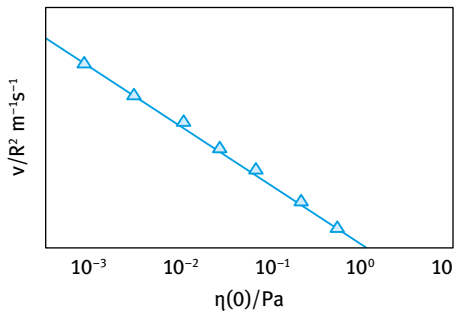

Fig. 4.4: Sedimentation rate versus $\eta(0)$.

The above correlation applies to the simple case of relatively dilute suspensions. For more concentrated suspensions, other parameters should be taken into consideration, such as the bulk (elastic) modulus. It is also clear that the stress exerted by the particles depends not only on the particle size but the density difference between the particle and the medium.

Many suspension concentrates have particles with radii up to 10 µm and density differences of more than 1 g cm^{-3}. However, the stress exerted by such particles will seldom exceed 10^{-2} Pa and most polymer solutions will reach their limiting viscosity value at higher stresses than this value. Thus, in most cases the correlation between settling velocity and zero shear viscosity is justified, at least for relatively dilute systems. For more concentrated suspensions, an elastic network is produced in the system which encompasses the suspension particles as well as the polymer chains. In this case, settling of individual particles may be prevented. However, in this case, the elastic network may collapse under its own weight and some liquid may be squeezed out from between the particles. This is manifested in a clear liquid layer at the top of the suspension, a phenomenon usually referred to as syneresis. If this

separation is not significant, it may not cause any application problems since by shaking the container the whole system redisperses. However, significant separation is not acceptable since it becomes difficult to homogenize the system. In addition, such extensive separation is cosmetically unacceptable and the formulation rheology should be controlled to reduce such separation to a minimum.

Several methods are applied in practice to control the settling and prevent the formation of dilatant clays.

(i) Balance of the density of disperse phase and medium. This is obviously the simplest method for retarding settling, since, as is clear from equation (4.13), if $\Delta\rho = 0$, then $v_0 = 0$. However, this method is of limited application and can only be applied to systems where the difference in density between the particle and the medium is not too large. For example, for many organic solids with densities between 1.1 and 1.3 g cm^{-3} suspended in water, some soluble substances such as sugar or electrolytes may be added to the continuous phase to increase the density of the medium to a level that is equal to that of the particles. However, one should be careful that the added substance does not cause any flocculation for the particles. This is particularly the case when using electrolytes, whereby one should avoid any "salting out" materials which cause the medium to be a poor solvent for the stabilizing chains. It should also be mentioned that density matching can only be achieved at one temperature. Liquids usually have larger thermal expansion coefficients than solids and if, for example, the density is matched at room temperature, settling may occur at higher temperatures. Thus, one has to be careful when applying the density matching method, particularly if the formulation is subjected to large temperature changes.

(ii) Use of high molecular weight polymers ("thickeners") such as natural gums, hydroxyethyl cellulose, xanthan gum or synthetic polymers such as poly(ethylene oxide). The most commonly used material in agrochemical formulations is xanthan gum, which is effective at relatively low concentrations (of the order of 0.1–0.2 % depending on the formulation). As mentioned above, these high molecular weight materials produce viscoselastic solutions above a critical concentration. This viscoselasticity produces sufficient residual viscosity to stop the settling of individual particles. The solutions also give enough elasticity to overcome separation of the suspension. However, one cannot rule out the interaction of these polymers with the suspension particles, which may result in "bridging" and hence the role by which such molecules reduce settling and prevent the formation of clays may be complex. To arrive at the optimum concentration and molecular weight of the polymer necessary for prevention of settling and claying, one should study the rheological characteristics of the formulation as a function of the variables of the system such as its volume fraction, the concentration and molecular weight of the polymer and temperature.

(iii) Use of "inert" fine particles such as swellable clays (bentonite) and finely divided oxides (silica or alumina). These fine inorganic materials form a "three-dimensional" network in the continuous medium which, by virtue of its elasticity, prevents sedimentation and claying. With swellable clays such as sodium montmo-

rillonite, the gel arises from the interaction between the plate-like particles in the medium. The plate-like particles of sodium montmorillonite consist of an octahedral alumina sheet sandwiched between two tetrahedral silica sheets [46]. The charge on the surface of the plate is produced by isomorphic substitution [46], i.e. an atom of higher valency is replaced by one of lower valency. This results in a deficit of positive charges or an excess of negative charges. Thus, the faces of the clay platelets become negatively charged and these negative charges are compensated by counter ions such as Na^+ or Ca^{2+}. As a result, a double layer is produced with a constant charge (that is independent of the pH of the solution). However, at the edges of the platelets, some disruption of the bonds occurs, resulting in the formation of an oxide-like layer, e.g. –Al–OH, which undergoes dissociation, giving a negative (–Al–O–) or positive ($–Al–OH_2^+$) depending on the pH of the solution. An isoelectric point may be identified for the edges (usually between pH 7–9). This means that the double layer at the edges is different from that at the faces and the surface charges can be positive or negative depending on the pH of the solution. For that reason, van Olphen [46] has suggested an edge-to-face association of clay platelets (which he termed the "house of cards" structure), which is assumed to be the driving force for the gelation of swellable clays. However, Norrish [47] has suggested that clay gelation is caused simply by the interaction of the expanded double layers. This is particularly the case in dilute electrolyte solutions whereby the double layer thickness can be several orders of magnitude higher than the particle dimensions. With oxides, such as finely divided silica, gel formation is caused by the formation of chain aggregates, which interact, forming a three-dimensional network that is elastic in nature. Clearly, the formation of such networks depends on the nature and particle size of the silica particles. For effective gelation, one should choose silicas with very small particles and highly hydrated surfaces.

(iv) Use of mixtures of polymers and finely divided solids, e.g. hydroxyethyl cellulose or xanthan gum with sodium montmorillonite or silica. By optimizing the ratio of the polymer to the solid particles, one can arrive at the right viscosity and elasticity to reduce settling and separation. Such systems are more shear thinning than polymer solutions and hence they are more easily dispersed in water on application. Bridging or depletion flocculation is probably the most likely mechanism by which these mixtures produce a viscoelastic network. The polymer-particulate mixtures also show less temperature dependence for viscosity and elasticity than the polymer solutions and hence they ensure long term physical stability at high temperatures.

(v) Controlled flocculation. For systems where the stabilizing mechanism is electrostatic in nature, for example those stabilized by surfactants or polyelectrolytes, the energy–distance curve (Fig. 4.1 (a)) shows a secondary minimum at larger particle separations. Such a minimum can be quite deep (a few tens of kT units), particularly for large (> 1 μm) and asymmetric particles. The depth of the minimum also depends on the electrolyte concentration. Thus, by adding small amounts of electrolyte, weak flocculation may be obtained. The weakly flocculated systems may produce a

gel network (self-structured systems) which has sufficient elasticity to reduce settling and eliminate claying. This has been demonstrated by Tadros [1] for ethirimol suspensions stabilized with phenol formaldehyde sulphonated condensate (a polyelectrolyte with modest molecular weight). By increasing NaCl concentration, the depth of the secondary minimum increases, reaching $\approx 50kT$ at the highest electrolyte concentration. By using electrolytes of higher valency such as $CaCl_2$ or $AlCl_3$, such deep minima are produced at much lower electrolyte concentrations. Thus, by controlling electrolyte concentration and valency, one can reach a sufficiently deep secondary minimum to produce a gel with enough elasticity to reduce settling and eliminate claying. For systems stabilized by nonionic surfactants or macromolecules, the energy–distance curve also shows a minimum (Fig. 4.1 (b)) whose depth depends on particle size, Hamaker constant and the thickness of the adsorbed layer, which in turn depends on the molecular weight of the polymer. As the molecular weight of the polymer is reduced below a certain value, the depth of the minimum becomes sufficiently high for weak flocculation to occur. The gel network structure of these weakly flocculated suspensions prevents sedimentation.

(vi) Depletion flocculation produced by the addition of "free" (non-adsorbing) polymer, when the concentration or volume fraction of the free polymer (ϕ_p) exceeds a critical value that is denoted by ϕ_p^+ [28]. When two particles approach a distance of separation that is smaller than the diameter of the free coil, exclusion of the polymer molecules from the interstices between the particles takes place, leading to the formation of a polymer free zone (depletion zone). This was illustrated in Fig. 3.8, which shows the situation below and above ϕ_p^+. As a result of this process, an attractive force, associated with the lower osmotic pressure in the region between the particles, is produced. This weak flocculation process can be applied to prevent the sedimentation and formation of clays. This has been illustrated by using ethirimol suspensions stabilized by a graft copolymer containing poly(ethylene oxide) (PEO) side chains (with $M = 750$) to which free HEC with various molecular weights was added. Above a critical volume fraction of the free polymer (which decreased with increase of molecular weight), weak flocculation occurred which increased with further increase in free polymer concentration. This structure may have a sufficient yield value or modulus, G^*, preventing particle sedimentation.

4.4 Characterizing suspension concentrates and assessing of their long-term physical stability

For the full assessment of the properties of suspension concentrates, three main types of investigation are needed:

(i) fundamental investigation of the system at a molecular level;
(ii) investigation into the state of the suspension on standing;
(iii) Investigation into the bulk properties of the suspension.

All theses investigations require a number of sophisticated techniques such as zeta potential measurements, surfactant and polymer adsorption and their conformation at the solid/liquid interface, measurement of the rate of flocculation and crystal growth, and several rheological measurements In all the above methods, care should be taken in sampling the suspension, which should cause as little disturbance as possible to the "structure" to be investigated. For example, when one investiagtes the flocculation of a concentrated suspension, dilution of the system for microscopic invesigation may lead to break down of the flocs, resulting in a false assessment. The same applies when one investiagates the rhology of a concentrated suspension, since transfer of the system from its container to the rheometer may lead to the break down of the structure. For these above reasons, one must establish well-defined procedures for every technique, which requires a great deal of skill and experience. It is advisable in all cases to develop standard operation procedures for the above investigations.

The main procedure that may be applied to investigate the charge at the solid/liquid interface (e.g. when using ionic surfactants or polyelectrolytes), which is important in the assessment of electrostatic stabilization is to measure the zeta potential. The zeta potential is obtained from the measured electrophoretic mobility provided information is available on particle size and electrolyte concentration. In case the above information is not available (as is the case with many practical systems) one should use the electrophoretic mobility for relative comparison between various systems; the assumption can be made that the higher the mobility, the higher the surface charge and the more likely the system is stable against flocculation, if the charge is the main stabilizing factor. Clearly, for systems stabilized by nonionic surfactants and polymers, electrophoretic mobility measurements are less informative. However, zeta potential measurements can be qualitatively used to obtain information on the adsorbed layer thickness for nonionic surfactants and polymers. When a nonionic surfactant or polymer adsorbs at the solid/liquid interface, a shift in the shear plane occurs and this results in a reduction in the zeta potential. If the zeta potential of the particles is measured in the presence and absence of nonionic surfactant or polymer, then the adsorbed layer thickness can be roughly estimated from the reduction in zeta potential.

Measurement of surfactant and polymer adsorption is obtained by equilibrating a representative sample of the solid with known mass m and surface area A per gram with a surfactant or polymer concentration with concentration C_1. After equilibrium is reached (at a given constant temperature), the solid is removed by centrifugation and the equilibrium concentration C_2 is determined analytically. The amount of adsorption Γ in mol m^{-2} is given by,

$$\Gamma = \frac{(C_1 - C_2)}{mA} = \frac{\Delta C}{mA}. \tag{4.15}$$

In most cases (particularly with surfactants), a plot of Γ versus C_2 gives a Langmuir type isotherm. The data can be fitted using the Langmuir equation,

$$\Gamma = \frac{\Gamma_\infty b C_2}{(1 + bC_2)}, \tag{4.16}$$

where b is a constant that is related to the free energy of adsorption,

$$b \propto \left(-\frac{\Delta G_{\text{ads}}}{RT}\right). \tag{4.17}$$

Most polymers (particularly those with high molecular weight) give a high affinity isotherm.

Two general techniques may be applied for measuring the rate of flocculation of suspensions, both of which can only be applied for dilute systems. The first method is based on measuring the scattering of light by the particles. For monodisperse particles with a radius that is less than $\lambda/20$ (where λ is the wave length of light) one can apply the Rayleigh equation, whereby the turbidity τ_0 is given by,

$$\tau_0 = A' n_0 V_1^2, \tag{4.18}$$

where A' is an optical constant (which is related to the refractive index of the particle and medium and the wave length of light) and n_0 is the number of particles, each with a volume V_1.

By combining the Rayleigh theory with the Smoluchowski–Fuchs theory of flocculation kinetics [5], one can obtain the following expression for the variation of turbidity with time,

$$\tau = A' n_0 V_1^2 (1 + 2 n_0 k t), \tag{4.19}$$

where k is the rate constant of flocculation.

The second method for obtaining the rate constant of flocculation is by direct particle counting as a function of time. For this purpose, optical microscopy or image analysis may be used, provided the particle size is within the resolution limit of the microscope. Alternatively, the particle number may be determined using electronic devices such as a Coulter counter or a flow ultramicroscope.

The rate constant of flocculation is determined by plotting $1/n$ versus t, where n is the number of particles after time t, i.e.,

$$\left(\frac{1}{n}\right) = \left(\frac{1}{n_0}\right) + kt. \tag{4.20}$$

The rate constant k of slow flocculation is usually related to the rapid rate constant k_0 (the Smoluchowski rate) by the stability ratio W,

$$W = \left(\frac{k}{k_0}\right). \tag{4.21}$$

One usually plots log W versus log C (where C is the electrolyte concentration) to obtain the critical coagulation concentration (CCC), which is the point at which log $W = 0$.

Measurement of the incipient flocculation of sterically stabilized suspensions, when the medium for the chains becomes a θ-solvent, e.g. on heating an aqueous suspension stabilized with poly(ethylene oxide) (PEO) or pol(vinyl alcohol) chains is followed by measuring the turbidity of the suspension as a function of temperature. Above the critical flocculation temperature (CFT), the turbidity of the suspension rises very sharply.

To obtain a measure of the rate of crystal growth, the particle size distribution of the suspension is followed as a function of time, using either a Coulter counter, a Mastersizer or an optical disc centrifuge. One usually plots the cube of the average radius versus time which gives a straight line from which the rate of crystal growth can be determined (the slope of the linear curve).

Two methods are used for measuring the bulk properties of suspension concentrates:

(i) Measurement of equilibrium sediment volume (or height) and redpispersion. For a "structured" suspension, obtained by "controlled" flocculation or addition of "thickeners" (such polysaccarides, clays or oxides), the "flocs" sediment at a rate depending on their size and the porosity of the aggregated mass. After this initial sedimentation, compaction and rearrangement of the floc structure occurs, a phenomenon referred to as consolidation. Normally in sediment volume measurements, one compares the initial volume V_0 (or height H_0) with the ultimately reached value V (or H). A colloidally stable suspension gives a "closely packed" structure with relatively small sediment volume (dilatant sediment referred to as clay). A weakly "flocculated" or "structured" suspension gives a more open sediment and hence a higher sediment volume. Thus, by comparing the relative sediment volume V/V_0 or height H/H_0, one can distinguish between a clayed and flocculated suspension.

(ii) Rheological measurements. Three different rheological measurements may be applied [48]:
   (a) steady state shear stress–shear rate measurements (using a controlled shear rate instrument);
   (b) constant stress (creep) measurements (carried out using a constant stress instrument);
   (c) dynamic (oscillatory) measurements (preferably carried out using a constant strain instrument).

These techniques were described in detail in Chapter 14 of Vol. 1. The rheological techniques can be used to assess sedimentation and flocculation of suspensions.

As mentioned before, to predict sedimentation, one has to measure viscosity at very low stresses (or shear rates). These measurements can be carried out using a constant stress rheometer (Carrimed, Bohlin, Rheometrics or Physica). A constant stress σ (using for example a drag cup motor that can apply very small torques and using an air bearing system to reduce the frictional torque) is applied on the system (which

may be placed in the gap between two concentric cylinders or a cone-plate geometry) and the deformation (strain γ or compliance $J = \gamma/\sigma = \mathrm{Pa}^{-1}$) is followed as a function of time [48]. For a viscoelastic system, the compliance shows a rapid elastic response J_0 at $t \to 0$ (instantaneous compliance $J_0 = 1/G_0$, where G_0 is the instantaneous modulus that is a measure of the elastic (i.e. "solid-like") component). At $t > 0$, J increases slowly with time and this corresponds to the retarded response ("bonds" are broken and reformed but not at the same rate). Above a certain time period (that depends on the system), the compliance shows a linear increase with time (i.e. the system reaches a steady state with constant shear rate). If after the steady state is reached the stress is removed, elastic recovery occurs and the strain changes sign. This is referred to as creep curve. The slope of the linear part of the creep curve gives the value of the viscosity at the applied stress, η_σ. One measures creep curves as a function of the applied stress (starting from a very small stress of the order of 0.01 Pa). The viscosity η_σ (which is equal to the reciprocal of the slope of the straight portion of the creep curve) is plotted as a function of the applied stress. Below a critical stress, σ_{cr}, the viscosity reaches a limiting value, $\eta(0)$ namely the residual (or zero shear) viscosity. σ_{cr} may be denoted as the "true yield stress" of the suspension, i.e. the stress above which the "structure" of the system is broken down. Above σ_{cr}, η_σ decreases rapidly with further increase of the shear stress (the shear thinning regime). It reaches another Newtonian value η_∞, which is the high shear limiting viscosity. $\eta(0)$ could be several orders of magnitudes (10^3–10^5) higher than η_∞. Usually one obtains good correlation between the rate of sedimentation υ and the residual viscosity $\eta(0)$ [48], as illustrated in Fig. 4.4. Above a certain value of $\eta(0)$, υ becomes equal to 0. Clearly, to minimize sedimentation one has to increase $\eta(0)$; an acceptable level for the high shear viscosity η_∞ must be achieved, depending on the application. In some cases, a high $\eta(0)$ may be accompanied by a high η_∞ (which may not be acceptable for application, for example if spontaneous dispersion on dilution is required). If this is the case, the formulation chemist should look for an alternative thickener.

Another problem encountered with many suspensions is that of "syneresis", i.e. the appearance of a clear liquid film at the top of the suspension. "Syneresis" occurs with most "flocculated" and/or "structured" (i.e. those containing a thickener in the continuous phase) suspensions. "Syneresis" may be predicted from measurement of the yield value (using steady state measurements of shear stress as a function of shear rate) as a function of time or using oscillatory techniques (whereby the storage and loss modulus are measured as a function of strain amplitude and frequency of oscillation. When a network of the suspension particles (either alone or combined with the thickener) is produced, the gravity force will cause some contraction of the network (which behaves as a porous plug) thus causing some separation of the continuous phase which is entrapped between the droplets in the network.

Rheological techniques are most convenient to assess suspension flocculation without the need for any dilution (which in most cases results in break-down of the floc structure). In steady state measurements, the suspension is carefully placed in

the gap between concentric cylinder or cone-and-plate platens. For the concentric cylinder geometry, the gap width should be at least 10× larger than the largest particle size (a gap width that is greater than 1 mm is usually used). For the cone-and-plate geometry, a cone angle of 4° or smaller is usually used. A controlled rate instrument is usually used for the above measurements; the inner (or outer) cylinder, the cone (or the plate) is rotated at various angular velocities (which allows one to obtain the shear rate γ) and the torque is measured on the other element (this allows one to obtain the stress σ).

For most practical suspensions (with $\phi > 0.1$ and containing thickeners to reduce sedimentation), a plot of σ versus γ is not linear (i.e. the viscosity depends on the applied shear rate). The most common flow is a pseudoplastic or shear thinning system where the viscosity decreases with increase in shear rate, reaching a Newtonian value above a critical shear rate. The flow curve is used to obtain the yield value σ_β (obtained by extrapolation of the shear stress–shear rate curve to $\gamma = 0$) and the plastic viscosity η_{pl}, which is the slope of the linear portion of the σ–γ curve.

Both σ_β and η_{pl} may be related to the flocculation of the suspension. At any given volume fraction of the emulsion and at a given particle size distribution, the higher the value of σ_β and η_{pl} the more the flocculated the suspension is. Thus, if one stores a suspension at any given temperature and makes sure that the particle size distribution remains constant (i.e. no Ostwald ripening occurs), an increase in the above parameters indicate flocculation of the suspension on storage. Clearly, if Ostwald ripening occurs simultaneously, σ_β and η_{pl} may change in a complex manner with storage time. Ostwald ripening results in a shift of the particle size distribution to higher diameters; this has the effect of reducing σ_β and η_{pl}. If flocculation occurs simultaneously (with the effect that these rheological parameters are increased), the net effect may be an increase or decrease of the rheological parameters. These trends depend on the extent of flocculation relative to Ostwald ripening. Therefore, following σ_β and η_{pl} with storage time requires knowledge of Ostwald ripening and/or coalescence. Only in the absence of this latter breakdown process can one use rheological measurements as a guideline for assessing flocculation.

Many suspensions (particularly those that are weakly flocculated or "structured" to reduce sedimentation) show time effects during flow. At any given shear rate, the viscosity of the suspension continues to decrease when the time of shear is increased; if the shear is stopped, the viscosity recovers to its initial value. This reversible decrease of viscosity is referred to as thixotropy. The most common procedure for studying thixotropy is to apply a sequence of shear stress=shear rate regimes within controlled periods. If the flow curve is carried out within a very short time (for example, increasing the rate from 0 to 500 s^{-1} in 30 s and then reducing it again from 500 to 0 s^{-1} within the same period), one finds that the descending curve is below the ascending one. The ascending and descending flow curves show hysteresis that is usually referred to as "thixotropic loop". If the same experiment is now repeated within a longer time experiment (for example, 120 s for the ascending and 120 s for the descending

curves), the hysteresis decreases, i.e. the "thixotropic loop" becomes smaller. This behaviour can be explained by considering the structure of the system. If, for example, the suspension is weakly flocculated, then when a shear force is applied to the system, this flocculated structure is broken down (this is the cause of the shear thinning behaviour). When the shear rate is reduced back to zero, the structure builds up only in part within the duration of the experiment (30 s). This study may be used to investigate the state of flocculation of a suspension. Weakly flocculated suspensions usually show thixotropy and the change of thixotropy with applied time may be used as an indication of the strength of this weak flocculation. Strongly flocculated suspensions usually show much less thixotropy than weakly flocculated systems. Again, one must be careful about drawing definite conclusions without other independent techniques (e.g. microscopy).

Constant stress (creep) experiments, described above, can also be applied to study the flocculation of the suspension. The values of $\eta(0)$ and σ_{cr} may be used to assess the flocculation of the suspension on storage. If flocculation occurs on storage (without any Ostwald ripening), the values of $\eta(0)$ and σ_{cr} may show a gradual increase with increase in storage time. As discussed above regarding steady state measurements, the trend becomes complicated if Ostwald ripening occurs simultaneously (both have the effect of reducing $\eta(0)$ and σ_{cr}. Thus the measurements should be supplemented by the particle size distribution measurements of the diluted suspension (making sure that no flocs are present after dilution) to assess the extent of Ostwald ripening. Further complication may arise from the nature of the flocculation. If the latter occurs in an irregular way (producing strong and tight flocs), $\eta(0)$ may increase, while σ_{cr} may decrease slightly, which complicates the analysis of the results. The above experiments are carried out at various storage times (for example, every two weeks) and temperatures. From the change of $\eta(0)$ and σ_{cr} with storage time and temperature, one can obtain information on the degree and the rate of flocculation of the system.

Dynamic (oscillatory) measurements are by far the most commonly used method to obtain information on the flocculation of a suspension. These measurements were described in detail in Chapter 14 of Vol. 1. Basically, a strain is applied in a sinusoidal manner, with an amplitude γ_0 and a frequency ν (cycles/s or Hz) or ω (rad s^{-1}). In a viscoelastic system (as is the case with a flocculated suspension), the stress oscillates with the same frequency, but out of phase from the strain. From measurement of the time shift between strain and stress amplitudes (Δt), one can obtain the phase angle shift δ ($= \Delta t\, \omega$).

From the amplitudes of stress and strain and the phase angle shift, one can obtain the various viscoelastic parameters (Chapter 14 of Vol. 1): The complex modulus G^*, the storage modulus (the elastic component of the complex modulus) G', the loss modulus (the viscous component of the complex modulus) G'', $\tan\delta$ and the dynamic viscosity η'. G' is a measure of the energy stored in a cycle of oscillation. G'' is a measure of the energy dissipated as viscous flow in a cycle of oscillation. $\tan\delta$ is a

measure of the relative magnitudes of the viscous and elastic components. Clearly, the smaller the value of tan δ, the more elastic the system is and vice versa.

In oscillatory measurements, one carries out two sets of experiments [48].

(a) Strain sweep measurements. In this case, the oscillation is fixed (for example at 0.1 or 1 Hz) and the viscoelastic parameters are measured as a function of strain amplitude. G^*, G' and G'' remain virtually constant up to a critical strain value, γ_{cr}. This region is the linear viscoelastic region. Above γ_{cr}, G^* and G' start to fall, whereas G'' starts to increase. This is the nonlinear region. The value of γ_{cr} may be identified with the minimum strain above which the "structure" of the suspension starts to break down (for example breakdown of flocs into smaller units and/or breakdown of a "structuring" agent).

From γ_{cr} and G', one can obtain the cohesive energy E_c (J m^{-3}) of the flocculated structure,

$$E_c = \int_0^{\gamma_{cr}} \sigma \, d\gamma = \int_0^{\gamma_{cr}} G'\gamma \, d\gamma = \frac{1}{2} G'\gamma_{cr}^2 \tag{4.22}$$

E_c may be used in a quantitative manner as a measure of the extent and strength of the flocculated structure in a suspension. The higher the value of E_c the more flocculated the structure is. Clearly, E_c depends on the volume fraction of the suspension as well as the particle size distribution (which determines the number of contact points in a floc). Therefore, for quantitative comparison between various systems, one has to make sure that the volume fraction of the dispersed particles is the same and the suspensions have very similar particle size distributions. E_c also depends on the strength of the flocculated structure, i.e. the energy of attraction between the particles. This depends on whether the flocculation is in the primary or secondary minimum. Flocculation in the primary minimum is associated with a large attractive energy and this leads to higher values of E_c when compared with the values obtained for secondary minimum flocculation. For a weakly flocculated suspension, as is the case with secondary minimum flocculation of an electrostatically stabilized suspension, the deeper the secondary minimum, the higher the value of E_c (at any given volume fraction and particle size distribution of the suspension). With a sterically stabilized suspension, weak flocculation can also occur when the thickness of the adsorbed layer decreases. Again, the value of E_c can be used as a measure of the flocculation; the higher the value of E_c, the stronger the flocculation. If incipient flocculation occurs (on reducing the solvency of the medium for the change to worse than the θ-condition) a much deeper minimum is observed and this is accompanied by a much larger increase in E_c. Providing the system does not undergo any Ostwald ripening, the change of the moduli with time and in particular the change of the linear viscoelastic region may be used as an indication of flocculation. Strong flocculation is usually accompanied by a rapid increase in G' and this may be accompanied by a decrease in the critical strain above which the "structure" breaks down. This may be used as an indication of the formation of "irregular" flocs which become sensitive to the applied strain. The floc structure will

entrap a large amount of the continuous phase and this leads to an apparent increase in the volume fraction of the suspension and hence an increase in G'.

(b) Oscillatory sweep. In this case, the strain amplitude is kept constant in the linear viscoelastic region (one usually takes a point far from γ_{cr} but not too low, i.e. in the mid point of the linear viscoelastic region) and measurements are carried out as a function of frequency. Both G^* and G' increase with increase in frequency and ultimately, above a certain frequency, they reach a limiting value and show little dependence on frequency. G'' is higher than G' in the low frequency regime; it also increases with increase in frequency and at a certain characteristic frequency ω^* (which depends on the system) it becomes equal to G' (usually referred to as the crossover point), after which it reaches a maximum and then shows a reduction with further increase in frequency. In the low frequency regime, i.e. below ω^*, $G'' > G'$; this regime corresponds to longer times (remember that the time is reciprocal to frequency) and under these conditions the response is more viscous than elastic. In the high frequency regime, i.e. above ω^*, $G' > G''$; this regime corresponds to short times and under these conditions the response is more elastic than viscous. At sufficiently high frequency, G'' approaches zero and G' becomes nearly equal to G^*; this corresponds to very short time scales whereby the system behaves as a near elastic solid. Very little energy dissipation occurs at such high frequencies. The characteristic frequency ω^* can be used to calculate the relaxation time of the system t^* ($= 1/\omega^*$). The relaxation time may be used as a guide for the state of the suspension. For a colloidally stable suspension (at a given particle size distribution), t^* increases with increase of the volume fraction of the oil phase, ϕ. In other words, the crossover point shifts to lower frequency with increase in ϕ. For a given suspension, t^* increases with increase in flocculation providing the particle size distribution remains the same (i.e. no Ostwald ripening).

The value of G' also increases with increase in flocculation, since aggregation of particles usually results in liquid entrapment and the effective volume fraction of the suspension shows an apparent increase. With flocculation, the net attraction between the droplets also increases and this results in an increase in G'. G' is determined by the number of contacts between the particles and the strength of each contact (which is determined by the attractive energy.

5 Oil-based suspension concentrates

5.1 Introduction

Oil-based suspensions are currently used for the formulation of many agrochemicals, in particular those which are chemically unstable in aqueous media. These suspensions allow one to use oils (such as methyl oleate) which may enhance the biological efficacy of the active ingredient. In addition, one may incorporate water-insoluble adjuvants into the formulation. The most important criterion for the oil used is to have the minimum solubility of the active ingredient otherwise Ostwald ripening or crystal growth will occur on storage. The oil-based suspension has to be diluted in water to produce an oil-in-water emulsion. A self-emulsifiable system has to be produced and this requires the presence of the appropriate surfactants for self emulsification. The surfactants used for self emulsification should not interfere with the dispersing agent that is used to stabilize the suspension particles in the nonaqueous media. Displacement of the dispersing agent with the emulsifiers can lead to flocculation of the suspension. To prevent sedimentation of the particles (sine the density of the active ingredient is higher than that of the oil in which it is dispersed), an appropriate rheology modifier (anti-settling agent) that is effective in the nonaqueous medium must be incorporated into the suspension. This rheology modifier should not interfere with the self-emulsification process of the oil-based suspension.

We may distinguish between two main types of nonaqueous suspensions:

(i) Suspensions in polar media such as alcohol, glycols, glycerol, esters. These media have a relative permittivity $\varepsilon_r > 10$ In this case, double layer repulsion plays an important role, in particular when using ionic dispersing agents.

(ii) Suspensions in nonpolar media, $\varepsilon_r < 10$, such as hydrocarbons (paraffinic or aromatic oils) which can have a relative permittivity as low as 2. In this case, charge separation and double layer repulsion are not effective and hence one has to depend on the use of dispersants that produce steric stabilization.

5.2 Stability of nonaqueous suspensions

The stability of suspensions in polar media follows the same principles as aqueous suspensions, but one must take the "incomplete" dissociation of the ionic species into account when $\varepsilon_r < 40$. This could result in a low surface charge and hence a low zeta potential. However, the latter may be sufficient to produce an effective energy barrier, preventing any flocculation as explained by the Deryaguin–Landau–Verwey–Overbeek (DLVO) theory [49, 50]. Due to the lack of complete dissociation, one cannot use the electrolyte concentration to calculate the thickness of the double layer. In this case, one has to obtain the effective electrolyte concentration, which must take into

https://doi.org/10.1515/9783110588002-006

account the incomplete dissociation. The effective ionic concentration C can be determined from conductivity measurements and this allows one to calculate the double layer thickness $(1/\kappa)$.

$$\frac{1}{\kappa} = \left(\frac{\varepsilon_r \varepsilon_0 kT}{2e^2 N_A C 10^3} \right)^{1/2}, \tag{5.1}$$

where ε_0 is the permittivity of free space, k is the Boltzmann constant, T is the absolute temperature and N_A is the Avogadro constant.

Since the effective ionic concentration in a polar medium is less than that in water, the double layer will be more extended [50]. For polar agrochemicals in polar media, the double layer charge may be sufficient for effective repulsion to occur and in this case a stable dispersion may be produced. For hydrophobic particles, which exist in most agrochemicals stabilized with ionic surfactants or polyelectrolytes, the double layer charge is also effective for stabilization of the suspension. In this above case, one may describe stability using the classical theory of colloid stability due to Deyaguin, Landau, Verwey and Overbeek (DLVO theory) [49, 50]. As described in detail in Chapter 7 of Vol. 1, for systems where $\kappa a > 1$ (where a is the particle radius) and there is weak interaction, the electrostatic repulsion, G_{elec}, is given by the following expression,

$$G_{elec} = 4\pi\varepsilon_r \varepsilon_0 a \psi_0^2 \ln[1 + \exp(-\kappa h)], \tag{5.2}$$

where h is the surface-to-surface separation and ψ_0 is the surface potential which can be replaced by the measured zeta potential. G_{elec} decreases exponentially with increase of h and the rate of decay increases with increase in electrolyte concentration.

The van der Waals attraction is simply given by the expression [51],

$$G_A = -\frac{Aa}{12h}, \tag{5.3}$$

where A is the effective Hamaker constant,

$$A = (A_{11}^{1/2} - A_{22}^{1/2})^2, \tag{5.4}$$

where A_{11} is the Hamaker constant of the particles and A_{22} is the Hamaker constant of the medium. G_A increases with decrease of h and at very short distances it reaches very high values.

The basis of the DLVO theory is to sum G_{el} and G_A at all distances,

$$G_T = G_{el} + G_A. \tag{5.5}$$

The general form of the G_T–h curve is schematically shown in Fig. 5.1, which shows the case of low electrolyte concentrations. The manner in which G_T varies with interparticle distance is determined by the way in which G_{el} and G_A vary with h. G_{el} decays exponentially with h and approaches 0 at large separation distances. G_A decays with h as an inverse power law and a residual attraction remains at large values of h. The G_T–h curve shows two minima (at long and short distances of separation) and one

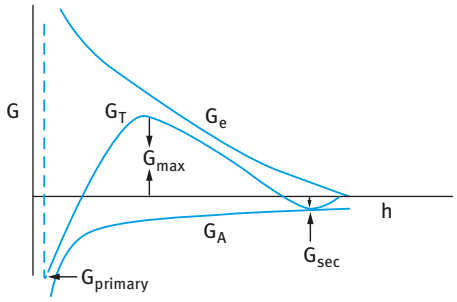

Fig. 5.1: Energy–distance curves according to the DLVO theory.

maximum (at an intermediate distance) as is illustrated in Fig. 5.1. At large h, $G_A > G_{el}$, resulting in a shallow secondary minimum. At small h, $G_A \gg G_{el}$, resulting in a deep primary minimum. At intermediate h, $G_{el} > G_A$, resulting in an energy maximum G_{max}. Three cases can be distinguished:

(i) large G_{max} ($> 25kT$), resulting in a colloidally stable suspension;
(ii) small or absent G_{max}, resulting in an unstable suspension (coagulated);
(iii) intermediate G_{max} and deep G_{sec} ($1–10kT$), resulting in weak (reversible) flocculation.

It should be mentioned that for hydrophobic particles in polar solvents, stabilized by ionic surfactants, the surface charge may be very low and hence electrostatic stabilization cannot be achieved. For this case, it is essential to use a dispersant that strongly adsorbs on the particle surface (with an anchor B chain). This dispersant should contain stabilizing chains (A chains) that are strongly solvated by the medium. The use of block and graft copolymers for stabilization of particles in polar media follows the same principles that are applied for stabilization in nonpolar media. This stabilizing mechanism is referred to as steric stabilization and will be discussed below.

The choice of dispersants for stabilization of suspensions in polar media is not an easy task. The "anchor" chain B needs to be insoluble in the polar medium and to have a high affinity to the surface. Since most polymer chains have some solubility in nonaqueous polar media, it is very difficult to achieve strong adsorption to the particle surface. The stabilizing chains A must be highly soluble in the polar solvent and strongly solvated by its molecules. This is not as difficult as the choice of the B chains. For these reasons, it is difficult to find commercially available dispersant for stabilization of hydrophobic particles in polar media .

For nonpolar media such as hydrocarbon oils (e.g. paraffinic oils) or some modified vegetable oils such as methyl oleate that are commonly used for formulation of oil based suspensions, the relative permittivity is lower than 10 and can reach values as low as 2. In this case, the double layer is very extended, since the effective ionic concentration is very small ($\approx 10^{-10}$ mol dm^{-3}) and ($1/\kappa$) can be as high as 10 µm. In this case, the double layer repulsion plays a very minor role. Effective stabilization requires the presence of an adsorbed layer of an effective dispersant with particular

properties (sometimes referred to as "protective colloid"). The most effective dispersants are polymeric surfactants which may be classified into two main categories [52]:
(i) homopolymers;
(ii) block and graft copolymers.

The hompolymers adsorb as random coils with tail–train–loop configurations. In most cases, there is no specific interaction between the homopolymer and the particle surface and it can seldom provide effective stabilization. The block and graft copolymers can provide effective stabilization if they satisfy the following criteria:
(i) Strong adsorption of the dispersant to the particle surface. This can be provided by a block B that is chosen to be insoluble in the nonaqueous medium and has some affinity to the particle surface. In case the affinity to the surface is not strong one can rely on "rejection anchoring" whereby the insoluble B chain is rejected towards the surface as a result of its insolubility in the nonaqueous medium.
(ii) Strongly solvated A blocks that provide effective steric stabilization as a result of their unfavourable mixing and loss of entropy when the particles approach each other in the suspension.
(iii) A reasonably thick adsorbed layer to prevent any strong flocculation.

Based on the above principles, various dispersants have been designed for suspensions in nonaqueous media. One of the most effective stabilizing chains in nonaqueous media is poly (12-hydroxystearic acid) (PHS), which has a molar mass in the region of 1,000–2,000 Da. This chain is strongly solvated in most hydrocarbon oils (paraffinic or aromatic oils). It is also strongly solvated in many esters such as methyl oleate, which is commonly used for oil-based suspensions. For the B chain, one can choose a polar chain such as polethylene imine or poyvinylpyrrolidone, which is insoluble in most oils. The B chain could also be polystyrene or polymethylmethacrylate, which is insoluble in aliphatic hydrocarbons and may have some affinity to hydrophobic agrochemical particles.

For a full characterization of the adsorbed polymer layer one needs to determine the following parameters [52]:
(i) Amount of polymer adsorbed per unit area, Γ. This requires determining the adsorption isotherms at various temperatures. The influence of solvency on the stabilizing chain should be studied.
(ii) Number of segments in direct contact with the surface, p (in trains). This can be obtained using pulse gradient NMR [52].
(iii) The adsorption energy per segment χ^s. For polymer adsorption to occur, a minimum value for χ^s is required to overcome the entropy loss when the polymer adsorbs at the surface. The adsorption energy can be determined using microcalorimetry.
(iv) Extension of the layer from the surface, i.e. segment density distribution $\rho(z)$ or the adsorbed layer thickness δ.

The most convenient method for determining δ is to use dynamic light scattering, usually referred to as photon correlation spectroscopy (PCS) [52]. For this purpose, small spherical particles such as polymethylmethacrylate can be used.

The theory of steric stabilization was described in detail in Chapter 8 of Vol. 1 and only a brief summary will be given in this section. When two particles with adsorbed polymer layers each with thickness δ approach a distance of separation, h, that is smaller than twice the adsorbed layer thickness 2δ, the layers will either overlap with each other or become compressed [52]. There will be an increase in the local segment density of the polymer chains in the interaction region. Provided the dangling chains (the A chains in A–B, A–B–A block or BA_n graft copolymers) are in a good solvent, this local increase in segment density in the interaction zone will result in strong repulsion as a result of two main effects:

(i) Increase in the osmotic pressure in the overlap region as a result of the unfavourable mixing of the polymer chains, when these are in good solvent conditions [52]. This is referred to as osmotic repulsion or mixing interaction and it is described by a free energy of interaction G_{mix}.
(ii) Reduction of the configurational entropy of the chains in the interaction zone. This entropy reduction results from the decrease in the volume available for the chains when these either overlap or are compressed. This is referred to as volume restriction interaction, entropic interaction or elastic interaction and it is described by a free energy of interaction G_{el}.

The combination of G_{mix} and G_{el} is usually referred to as the steric interaction free energy, G_s. The sign of G_{mix} depends on the solvency of the medium for the chains. If in a good solvent, i.e. the Flory–Huggins interaction parameter χ is less than 0.5, then G_{mix} is positive and the mixing interaction leads to repulsion. In contrast, if $\chi > 0.5$ (i.e. the chains are in a poor solvent condition), G_{mix} is negative and the mixing interaction becomes attractive. G_{el} is always positive and hence in some cases one can produce stable dispersions in a relatively poor solvent (enhanced steric stabilization).

Combination of G_{mix} and G_{el} with G_A gives the total energy of interaction G_T (assuming there is no contribution from any residual electrostatic interaction). A schematic representation of the variation of G_{mix}, G_{el}, G_A and G_T with surface–surface separation distance h is shown in Fig. 5.2.

G_{mix} increases very sharply with decrease of h, when $h < 2\delta$. G_{el} increases very sharply with decrease of h when $h < \delta$. G_T versus h shows a minimum, G_{min}, at separation distances comparable to 2δ. When $h < 2\delta$, G_T shows a rapid increase with decrease in h. Unlike the G_T–h curve predicted by the DLVO theory (which shows two minima and one energy maximum), the G_T–h for systems that are sterically stabilized shows only one minimum, G_{min}, followed by sharp increase in G_T with decrease of h (when $h < 2\delta$). The depth of the minimum depends on the Hamaker constant A, the particle radius R and the adsorbed layer thickness δ. G_{min} increases with increase of A and R. At a given A and R, G_{min} increases with decrease in δ (i.e. with decrease of

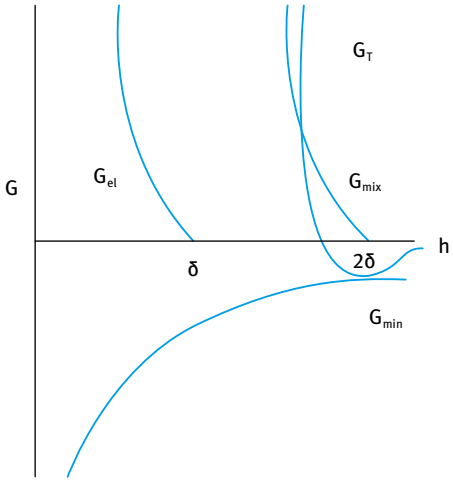

Fig. 5.2: Energy–distance curves for sterically stabilized systems.

the molecular weight, M_w, of the stabilizer). The larger the value of δ/R, the smaller the value of G_{min}. In this case the system approaches thermodynamic stability, as is the case with nano-dispersions, several criteria must be satisfied for effective steric stabilization [52]:

(i) Full coverage of the particles by the polymer. The amount of polymer added should correspond to the plateau of the adsorption isotherm. Any bare patches may lead to flocculation as a result of van der Waals attraction and/or bridging.
(ii) Strong adsorption of the polymer to the particle surface, i.e. strong B "anchor" chain. This requires the chain be insoluble in the medium and have some affinity to the surface. Lack of a strong "anchor" may lead to chain displacement upon approach of the particles in a suspension. This is particularly important for concentrated suspensions.
(iii) The stabilizing chain(s) A should be in good solvent conditions. The Flory–Huggins interaction parameter χ should be less than 0.5 under all storage conditions, e.g. temperature changes.
(iv) An optimum layer thickness δ to ensure that G_{min} is not deep. This is particularly the case with concentrated suspensions whereby weak flocculation may occur at relatively small G_{min}. In most cases, an adsorbed layer thickness in the region 5–10 nm is sufficient. This is particularly the case with graft copolymers whereby the A chains are stretched ("comb-like" or "brush" structure).

The oil-based suspension should not exhibit any sedimentation and formation of dilatant sediments. This follows the same principles as described for aqueous suspension concentrates described in Chapter 4. Settling (or sedimentation) results from gravity forces [5]. When $\rho_{particles} > \rho_{medium}$, the gravity force $(4/3)\pi R^3 \Delta\rho g L$ (where g is the acceleration due to gravity and L is the height of the container) will overcome the thermal (Brownian) motion, leading to particle sedimentation. Only when $kT >$

$(4/3)\pi R^3 \Delta\rho g L$, sedimentation becomes insignificant. This condition is only satisfied with very small particles (< 0.1 μm) and $\Delta\rho < 0.1$. Thus, with most colloidally stable suspensions, sedimentation is the rule rather than the exception. The particles may sediment individually to the bottom of the container and the repulsive forces necessary to maintain stability allow them to move past each other with the result of the formation of a very compact sediment. The compact sediment, technically referred to as "clay" or "cake", is very difficult to redisperse by shaking. Such clays are dilatant (shear thickening) and must be avoided.

Several suspending agents can be applied to prevent settling in nonaqueous suspensions. The main criteria for an effective suspending agent are as follows.

(i) It should produce a "three-dimensional" gel network in the continuous phase with optimum rheological characteristics.
(ii) It should have a very high viscosity at low shear rates. A residual (zero shear) viscosity in excess of 100 Pa s is desirable. The residual viscosity can be measured using constant stress (creep) measurements.
(iii) It should have a sufficient "bulk" modulus to prevent separation of the suspension and syneresis. The bulk modulus is related to the shear modulus, which can be measured using dynamic (oscillatory) techniques.
(iv) The suspending agent should produce a shear thinning system such that on application of the suspension, the high shear viscosity is not too high.

Several suspending systems can be used:

(i) Hydrophobically modified clays (Bentones). Clays such as sodium montmorillonite can be made hydrophobic through the addition of long chain alkyl ammonium surfactants (e.g. dodecyl or cetyl trimethyl ammonium chloride). The alkyl ammonium cation exchanges with the Na+ ions, producing a hydrophobic surface and the Bentone particles can be dispersed in the nonaqueous medium. The exchange is carried out in an optimum manner such that some hydrophilic sites remain on the Bentone particles. On addition of a polar solvent such as propylene carbonate or alcohol, a gel is produced. The most likely mechanism of gel formation in this case is hydrogen bonding by the polar molecules between the polar sites on the Bentone particles.
(ii) Fumed silica. These are commercially available under the trade name "Aerosil" or "Cabosil". They are produced by the reaction of silicon teterachloride with steam. Fine particles (primary particle size < 0.02 μm) are produced with a surface containing silanol groups that are separated by siloxane bonds. When dispersing the fumed silica powder in nonaqueous media, a gel is produced by hydrogen bonding between the silanol groups. Chain aggregates are produced and, by controlling the dispersion procedure, adequate rheological characteristics are produced.
(iii) Trihydroxystearin (thixin). This product is derived from castor oil and it needs both shear and heat for full activation to produce a gel.

(iv) Aluminium magnesium hydroxide stearate. This has been used to gel a number of oils and it has some suspending properties. However, one should be careful in applying this system since in many cases the gel strength is too high for adequate dispersion on application.
(v) Use of high molecular weight polymers. Polyethylenes and copolymers of polyethylene can be used to gel mineral oils and several aliphatic solvents. Some of these materials need high incorporation temperatures and one must keep in mind that the cooling procedures affect the final appearance and rheological characteristics of the gel.

The above systems are the most commonly used rheology modifiers in most nonaqueous suspensions. However, two other methods may be applied for reduction of settling of nonaqueous suspensions:

(i) Controlled flocculation (self-structured systems). By reducing the adsorbed layer thickness, one can increase the depth of the minimum, G_{min}, to such an extent that weak flocculation may produce a "three-dimensional" gel structure that is sufficient to reduce sedimentation and formation of dilatant clays. The adsorbed layer thickness may be reduced by reducing the molecular weight of the stabilizer of by the addition of a small amount of a nonsolvent. This procedure is particularly useful with large and asymmetric particles.
(ii) Depletion flocculation [28]. This is obtained by the addition of "free" (nonadsorbing) polymer to a sterically stabilized suspension. As discussed in Chapter 4, above a critical volume fraction, ϕ_p^+ of the free polymer, weak flocculation occurs. Above ϕ_p^+, the polymer chains are "squeezed out" from between the particles, leaving a polymer-free zone in the interstices. The higher osmotic pressure outside the particle surfaces causes weak flocculation. This was schematically shown in Fig. 3.8. The critical polymer volume fraction above which flocculation occurs decreases with increase of the molecular weight of the free polymer. Thus, high molecular weight oil soluble polymers should be used in order to reduce the amount required for flocculation. The amount of free polymer required for flocculation also decreases with increase of the volume fraction of the suspension. Therefore, depletion flocculation is more applicable for concentrated suspensions.

5.3 Emulsification of oil-based suspensions

The nonaqueous suspension concentrate containing the active ingredient particles and any anti-settling system is emulsified into the spray tank before application. Here, the same principles applied for self-emulsification of emulsifiable concentrates (ECs), described in Chapter 2, are applied. Alternatively, the nonaqueous suspension concentrate is emulsified into an aqueous solution containing another water soluble active

ingredient (normally an electrolyte such as glyphosate) to produce a combined mixture for two active ingredients. In the first case, spontaneous emulsification is necessary since only gentle agitation in the spray tank is possible. In the second case, one may apply a normal emulsification procedure if a combined formulation is required. In some cases, spontaneous emulsification into an aqueous electrolyte solution may also be required.

The above oil-based suspension concentrates require careful formulation to achieve the required properties:

(i) A stable nonaqueous suspension with adequate weak flocculation (to produce a shear thinning system) and no settling.
(ii) The anti-settling agent used in the formulation should be water dispersible (e.g. fumed silica, Aerosil).
(iii) The emulsifying system used should not interfere with the stabilizing polymeric surfactant used for preparation of the nonaqueous suspension.
(iv) The viscosity of the formulation at intermediate shear rates should be low enough to ensure spontaneity of emulsification.

As discussed in Chapter 2, three mechanisms were established to explain the process of spontaneous emulsification:

(i) Interfacial turbulence (Fig. 2.4 (a)) that occurs as a result of mass transfer from one phase to the other. When the two phases are not in equilibrium, convection currents may be formed, transferring liquid rich in surfactant towards areas of liquid deficient in surfactant. These convection currents lead to local fluctuations in the interfacial tension causing oscillation of the interface (turbulence). Such disturbances may amplify themselves leading to violent interfacial perturbations and eventual disintegration of the interface when liquid droplets of one phase are "thrown" into the other phase. This mechanism requires the presence of two surfactant molecules or a surfactant plus alcohol. This facilitates the mass transfer and induces interfacial tension gradients. Several "phases" may be produced at the O/W interface.
(ii) Diffusion and stranding (Fig. 2.4 (b)). This is best illustrated by placing an ethanol–toluene mixture (e.g. containing 10 % alcohol) onto water. The aqueous layer eventually becomes turbid as a result of the presence of toluene droplets. In this case, interfacial turbulence does not occur although spontaneous emulsification takes place. The alcohol molecules diffuse into the aqueous phase carrying some toluene molecules in a saturated three-component subphase. At some distance from the interface, the alcohol becomes sufficiently diluted in the water and the toluene droplets precipitate as droplets in the aqueous phase. This mechanism requires the presence of a third component (sometimes referred to as the cosurfactant) that increases the miscibility of the two previously immiscible phases (toluene and water). Many emulsifiable concentrates contain a high proportion of a polar solvent such as alcohol or ketone, which facilitates spontaneous emulsifi-

cation. Its application for emulsification of nonaqueous suspension concentrates needs to be tested (the addition of a polar solvent may enhance crystal growth).

(iii) Production of ultralow (or transiently negative) interfacial tension (Fig. 2.4 (c)). This is the same mechanism for the production of microemulsions. The ultralow interfacial tension is produced by a combination of a surfactant and a cosurfactant.

Several other mechanisms have been proposed to explain the dynamics of spontaneous emulsification. Direct observation using phase contrast and polarizing microscopy showed that, in some cases, vesicles (closed bilayers) are produced in the oil phase near the interface with the water. These vesicles tend to "explode", thereby pulverizing oil droplets into the aqueous phase. The above structures can be produced for example by using a mixture of nonionic surfactant such as $C_{12}E_5$ and a long chain alcohol such as $C_{12}H_{25}OH$ and an oil such as hexadecane. The oil/surfactant mixture is transparent, but upon addition of a small amount of water it becomes turbid and vesicles can be observed under the microscope. The interfacial tension of the oil/surfactant mixture/water is also very low.

5.4 Polymeric surfactants for oil-based suspensions and the choice of emulsifiers

When formulating a nonaqueous suspension concentrate that can be spontaneously emulsified into aqueous solutions one should consider the following criteria: The polymeric emulsifiers should be chosen from the A–B, A–B–A block or BA_n graft copolymer, as discussed above. The B chain should be chosen to be insoluble in the oil and should become strongly adsorbed on the particle surface (either by specific interaction or by rejection "anchoring". As discussed before, for nonpolar oils (hydrocarbons), the B chain could be a polar molecule such as polyethylene imine, which adsorbs on the particle by rejection anchoring. The A chain should be soluble in the oil and highly solvated by its molecules – poly(hydroxystearic acid) or polyisobutylene are ideal.

The emulsifier system should be soluble in the oil phase and it should not cause desorption of the polymeric surfactant. A two component emulsifier system is normally used, one predominantly water-soluble (such as an ethoxylated surfactant) and one oil-soluble, such as a medium or long-chain alcohol. In many cases, calcium dodecyl benzene sulphonate may be used. The emulsifier system should lower the interfacial tension of O/W to very low values ($< 0.1\,mN\,m^{-1}$).

5.5 Emulsification into aqueous electrolyte solutions

To prepare a combined formulation with one active ingredient suspended in the oil phase and another active ingredient soluble in water (salt), one can emulsify the nonaqueous suspension into the aqueous electrolyte solution using a polymeric surfactant with a high HLB number, e.g. Pluronic PF127 (which contains ≈ 55 units polypropylene oxide, PPO, and two polyethylene oxide (PEO) chains with ≈ 100 units each). The PEO–PPO–PEO block copolymer is insoluble in the oil phase and hence it does not interfere with the polymeric surfactant used for preparation of the nonaqueous suspension. Depending on the density of the active ingredient in the oil phase and the amount suspended, the density of the oil drops produced could be smaller or larger than that of the aqueous electrolyte. Thus the combined formulation could undergo creaming or settling on storage. It is, therefore, essential to include an anti-settling system in the aqueous electrolyte phase, e.g. xanthan gum. In formulations where spontaneous emulsification into the aqueous electrolyte solution is required, one should apply the same principles discussed above, except in this case the emulsifier system should be more hydrophilic (higher HLB number) to prevent "salting-out" of the emulsifier by the electrolyte. The nature and HLB number of the emulsifier system depends on the electrolyte concentration and nature and this could be checked independently using cloud point measurements. The resulting interfacial tension should be low.

5.6 Proper choice of anti-settling system

The anti-settling system used for nonaqueous suspensions should be dispersible into water. Fumed silica (Aerosil 200) or microcrystalline cellulose are ideal systems for structuring nonaqueous suspensions. These systems produce a "three-dimensional" gel network in the oil phase by hydrogen bonding between the particles, forming chains and cross-chains. These gels produce enough "yield stress" to prevent sedimentation of the coarse active ingredient particles. They also produce a very high viscosity at low shear rates thus preventing sedimentation. One of the main advantages to these hydrophilic particles is that they can partition into the aqueous phase and this produces two main effects. During partition into the aqueous phase and crossing the interface, they can enhance the interfacial tension gradients and hence promote the turbulence effect described above. This will facilitate self emulsification. When these particles leave the oil phase, the yield value and viscosity of the suspension is lowered and this helps the self emulsification process.

Hydrophilic polymers such as hydroxypropyl cellulose may also be used either alone or in combination with silica or microcrystalline cellulose. The combined particulate–polymer system may help to reduce sedimentation and enhance the self emulsification of the oil. The optimum ratio between particles and polymer depends on the nature of the active ingredient suspended in the oil phase.

5.7 Rheological characteristics of oil-based suspensions

The rheological characteristics of the nonaqueous suspension (its yield value, zero shear viscosity and elastic modulus) need to be carefully adjusted to achieve the following criteria:

(i) no settling or separation of the nonaqueous suspension on storage under all storage conditions;
(ii) ease of spontaneous emulsification with minimum agitation.

These two criteria are not compatible and hence one must control the rheology very carefully. For prevention of settling and separation, one needs a high "yield stress", high zero shear viscosity and a high modulus. High rheological parameters reduce the ease of spontaneous emulsification. For these reasons, it is necessary to prepare a highly shear thinning system. The suspension concentrate should have a high viscosity at low shear rates, but once the shear rate exceeds a certain value (say 10–100 s^{-1}), depending on application, the viscosity drops significantly. One can achieve this effect by properly choosing the anti-settling system. By using an anti-settling system that diffuses rapidly into the water phase, one can reduce the yield value, zero shear viscosity and modulus during the process of emulsification. Measurement of the rheological parameters is essential when formulating a nonaqueous suspension concentrate and this requires low shear rheometers (constant stress and oscillatory techniques). Details on these techniques are given in Chapter 14 of Vol. 1.

6 Formulation of suspoemulsions

6.1 Introduction

Suspoemulsions are mixtures of suspensions and emulsions that are applied in many agrochemical formulations whereby two active ingredients are formulated with one as an aqueous suspension and the other as an oil/water emulsion [1]. A schematic representation of suspoemulsions is given in Fig. 6.1. We can distinguish between two main types of suspoemulsions:

(i) a system whereby the solid particles and emulsion droplets remain as separate entities;
(ii) a system whereby the solid particles are dispersed in the oil droplets.

The first system is commonly applied in agrochemical formulations. With suspoemulsions, two active ingredients are formulated together which offers convenience to the farmer and may also result in synergism in biological efficacy. A wider spectrum of disease control may be achieved particularly with many fungicides and herbicides. With many suspoemulsions, an adjuvant that enhances the biological efficacy is added.

The formulation of suspoemulsions is not an easy task; one may produce a stable suspension and emulsion separately but when these are mixed they become unstable due to the following interactions:

(i) Homoflocculation of the suspension particles. This can happen if the dispersing agent used to prepare the suspension is not strongly adsorbed and hence it becomes displaced by the emulsifier which is more strongly adsorbed but not a good stabilizer for the suspension particles.
(ii) Emulsion coalescence. This can happen if the emulsifier is not strongly adsorbed at the O/W or W/O interface, resulting in its partial or complete displacement by the suspension dispersant which is not a good emulsion stabilizer and this results in coalescence of the emulsion droplets with ultimate separation of oil (for O/W) or water (for W/O).

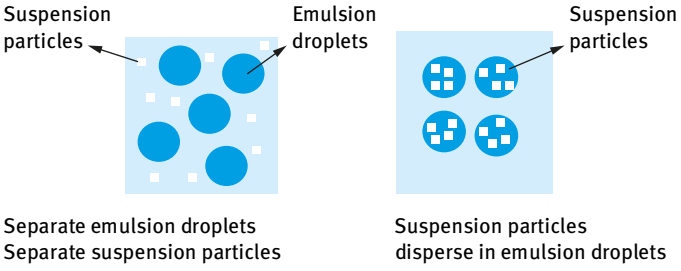

Fig. 6.1: Schematic representation of suspoemulsions.

https://doi.org/10.1515/9783110588002-007

(iii) Heteroflocculation between the oil droplets and suspension particles. The latter may be partially wetted by the oil and reside at the O/W interface (this occurs particularly when the oil droplets are much larger than the suspension particles). Heteroflocculation can also occur with suspension particles dispersed in a W/O emulsion.
(iv) Phase transfer and crystallization. This happens when the suspension particles have some solubility in the oil phase. The small suspension particles, which have higher solubility than the larger ones (due to curvature effects) may become dissolved in the oil phase and become recrystallized onto the larger suspension particles (a form of an Ostwald ripening process). Large and sometimes needle-shaped crystals may be produced as a result of crystal habit modification (that sometimes occurs with Ostwald ripening).

One of the most useful methods for studying interaction in suspoemulsions is rheology, in particular viscoelastic measurements [48].

6.2 Suspoemulsions investigated

Two agrochemical systems were investigated, namely chlorothalonil (density ρ = 1.85 g cm^{-3}) or dichlobutrazol (ρ = 1.25 g cm^{-3}) suspensions prepared by bead milling (prepared using Synperonic NP1800, nonyl phenol with 13 mol propylene oxide (PPO) and 27 mol ethylene oxide (PEO) and tridemorph (ρ = 0.87 g cm^{-3}) emulsions prepared using the same surfactants (emulsification was carried out using a Silverson mixer. The particle size was determined using light diffraction using a Malvern Mastersizer) The equilibrium sediment and cream volumes were obtained using measuring cylinders at room temperature. Viscoelastic measurements were carried out using a Bohlin VOR.

Assuming that a stable suspoemulsion (in the colloid sense) could be prepared, e.g. by the use of a polymeric dispersant and emulsifier, the creaming and/or sedimentation behaviour of the suspoemulsion shows different patterns depending on the density difference between the oil droplets and suspension particles as well as the total volume fraction ϕ of the whole system. This behaviour could be illustrated by using agrochemical suspoemulsions consisting of an oil, namely tridemorph, and two different suspensions, namely dichlobutrazol and chlorothalonil. To ensure colloid stability and absence of heteroflocculation, both the emulsion and suspension were prepared using an A–B–C block copolymer (Synperonic NPE 1800) consisting of an anchor chain (B–C) of propylene oxide (13 mol) and nonyl phenol and a stabilizing chain of polyethylene oxide (23 mol). Synperonic NPE 1800 is an excellent emulsifier for tridemorph and it is also an excellent dispersant for both dichlobutrazol and chlorothalonil. The colloid stability of both emulsion and suspensions was confirmed by optical microscopy, which showed no coalescence of the emulsion or

flocculation of the suspensions In addition, when mixing the emulsion and suspension, no heteroflocculation occurred. The suspoemulsions were prepared by simple mixing of the emulsion and suspension, keeping the total volume fraction ϕ constant while varying the ratio of suspension to emulsion. Two ϕ values were investigated < 0.2 and > 0.2 and a comparison was made between systems with small density differences (dichlobutrazol/tridemorph) and large density differences (chloroithalonil/tridemorph). The results are illustrated in Fig. 6.2–6.4.

When the density difference between the suspension particles and emulsion droplets is not large and $\phi < 0.2$, the emulsion creams and the suspension sediments separately (Fig. 6.2). When the density difference between the suspension particles and emulsion droplets is small but $\phi > 0.2$, the system forms a cream layer when the suspension: emulsion ratio is 2 : 8 and it forms a sediment layer when the ratio is 8 : 2 (Fig. 6.3). When the density difference between the suspension particles and emulsion droplets is large, the average density of the suspension particle/emulsion droplet is > 1 and in this case sedimentation is observed when the ratio is 2 : 8 but some creaming occurs when the ratio is 8 : 2 (Fig. 6.4). This creaming/sedimentation behaviour indicates some interaction between the emulsion droplets and the suspension particles.

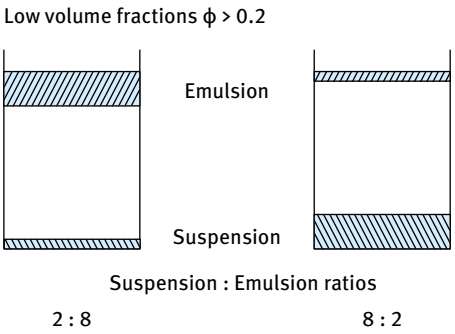

Fig. 6.2: Chlobutrazol/tridemorph ($\phi < 0.2$).

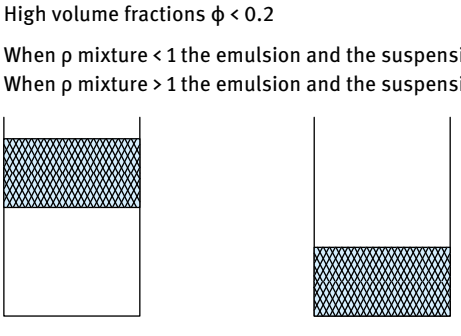

Fig. 6.3: Chlobutrazol/tridemorph ($\phi > 0.2$).

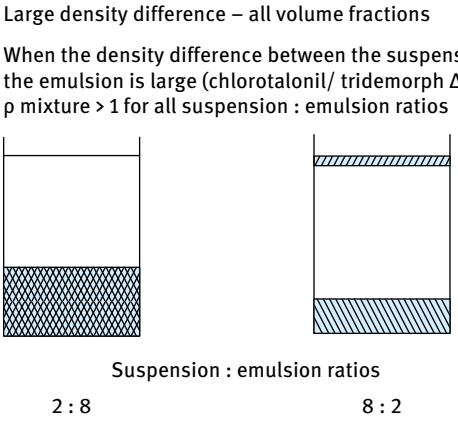

Fig. 6.4: Chlorothalonil/tridemorph (all volume fractions).

A particularly useful method for illustrating the interactions in suspoemulsions is to compare the total observed sediment plus cream height with that based on simple additivity. This is illustrated in Fig. 6.5 for chlorothalonil/tridemorph suspoemulsions.

It can be seen from Fig. 6.5 that the observed sediment + cream heights are smaller than would be expected from simple additivity. It is possible that the small suspension particles become trapped between the larger oil droplets in the cream layer and the small suspension particles become entrapped between the larger suspension particles. Some deformation of the oil droplets may also occur in the sedimented layer.

Optical microscopic investigation of some other suspoemulsions showed heteroflocculation and this could be reduced or eliminated by using Atlox 4913 (an acrylic graft copolymer of polymethylmethacrylate backbone and PEO Chains) [52] as discussed below.

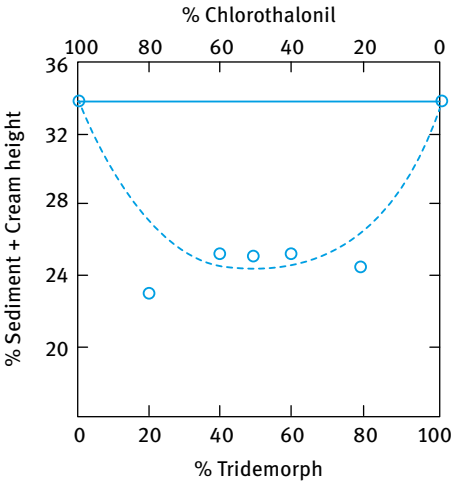

Fig. 6.5: Comparison of experimental (---) and predicted, based on additivity (—) sediment + cream heights for chlorothalonil/ tridemorph suspoemulsions.

The use of strongly "anchored" dispersants and emulsifiers is crucial for reduction of the interaction between the particles and droplets. The interaction can also be significantly reduced by the addition of rheology modifiers such hydroxyethyl cellulose (HEC) or xanthan gum. These thickeners produce a "three-dimensional" gel network by the overlap of the polymer coils of HEC or the double helices of xanthan gum. Apart from their effect in reducing creaming and sedimentation by producing a high residual viscosity (at low shear rates) these polymers will also prevent the oil droplets from becoming trapped in the suspension and the suspension particles from becoming trapped in the emulsion.

Heteroflocculation results from the competitive adsorption between the dispersant and emulsifier, particularly when these are not strongly anchored to the surfaces. Displacement of some or all of the dispersant by the emulsifier and vice versa may result in attraction between the particles and droplets. The repulsive barrier is weakened in both cases. If the particles are partially wetted by the oil they may reside at the O/W interface if the oil droplets are sufficiently large. This processes of attraction may continue for long periods of time and ultimately the suspoemulsion may become physically unstable. Any flocculation will result in entrapment of the liquid between the particles in the floc structure and this causes a significant increase in the viscosity of the system. Competitive adsorption may be reduced by using the same surfactant for dispersing the solid and emulsifying the oil. This was demonstrated above when using Synperonic NPE 1800. However, since this molecule shows some reversible adsorption, interaction between the particles and droplets is not completely prevented. A better method for reducing competitive adsorption is to use a polymeric surfactant that is strongly and irreversibly adsorbed on the suspension particles and emulsion droplets, such as the graft copolymer of polymethylmethacrylate backbone with several polyethylene oxide chains grafted on the backbone [52]. This graft copolymer (Atlox 4913) has a weight average molecular weight of ≈ 20,000 and it adsorbs strongly and irreversibly on hydrophobic particles, e.g. polystyrene latex and most agrochemical suspensions. By using this graft copolymer as a dispersant and an A–B–A block copolymer of PEO (A) and polypropylene oxide (PPO, B) as emulsifier, one can obtain very stable suspoemulsions. A good polymeric stabilizer is INUTEC® SP1 (ORAFTI, Belgium), which consists of an inulin (linear polyfrucose with degree of polymerization > 23) chain on which several alkyl chains are grafted [52]. This polymeric surfactant adsorbs on hydrophobic particles and emulsion droplets by multi-point attachment with several alky groups leaving strongly hydrated loops and tails of polyfructose that provide an effective steric barrier.

Coalescence of the emulsion droplets on storage accelerates the instability of the suspoemulsion. Large oil droplets can induce heteroflocculation with the suspension particles residing at the O/W interface. Emulsion coalescence can be reduced by one or more of the following methods:

(i) Reduction of droplet size by using a high pressure homogenizer.
(ii) Use of an effective emulsion stabilizer such as INUTEC® SP1.

(iii) Incorporation of an oil soluble polymeric surfactant such as Atlox 4912, that is an A–B–A block copolymer of polyhydroxy stearic acid (PHS, A) and PEO (B).

A summary of the criteria for preparation of a stable suspoemulsion is:

(i) Use of a strongly adsorbed ("anchored") dispersant by multi-point attachment of a block or graft copolymer.
(ii) Use of a polymeric stabilizer for the emulsion (also with multi-point attachment), e.g. INUTEC® SP1.
(iii) Preparation of the suspension and emulsion separately and allowing enough time for complete adsorption (equilibrium).
(iv) Using low shear when mixing the suspension and emulsion.
(v) When dissolving an active ingredient in an oil (e.g. with many agrochemicals) one should choose an oil in which the suspension particles are insoluble and also the oil should not wet the particles.
(vi) Increasing dispersant and emulsifier concentrations to ensure that the life time of any bare patches produced during collision is very short.
(vii) Reducing emulsion droplet size by using a high-pressure homogenizer; the smaller droplets are less deformable and coalescence is prevented. In addition, accumulation of the suspension particles at the O/W interface is prevented.
(viii) Use of a rheology modifier such as HEC or xanthan gum that produces a viscoelastic solution that prevents creaming or sedimentation and prevent entrapment of the oil droplets in between the suspension particles or the suspension particles in between the emulsion droplets.
(ix) If possible, it is preferable to use a higher volume fraction of the oil when compared with the suspension. In many cases, flocculation is more rapid at higher solid volume fractions. The emulsion oil phase volume can be increased by incorporating an inert oil.

When one must prepare a suspoemulsion with a high volume fraction ϕ of suspension and emulsion (e.g. $\phi > 0.4$), it is preferable to emulsify the oil directly into a prepared suspension. In this case, one prepares the suspension first (e.g. by bead milling) using the polymeric dispersant. The suspension is left to equilibrate for a sufficient period of time (preferably overnight) to endure complete adsorption of the polymer. The polymeric emulsifier is then added and the oil is emulsified into the SC, using for example a Silverson or Ultra Turrax. Overmixing, which may result in orthokinetic (or shear) flocculation and dilatancy, must be avoided and the whole system should be cooled as much as possible during emulsification.

Prevention of crystallization is by far the most serious instability problem with suspoemulsions (particularly with many agrochemicals). It arises from the partial solubility of the suspension particles into the oil droplets. The process is accelerated at higher temperatures and also on temperature cycling.

As mentioned in Chapter 2, smaller particles will have higher solubility than larger ones. This is due to the fact that the higher the curvature the higher the solubility, as described by the Kelvin equation [43],

$$S(r) = S(\infty)\exp\left(\frac{2\gamma V_m}{rRT}\right), \tag{6.1}$$

where $S(r)$ is the solubility of a particle with radius r and $S(\infty)$ is the solubility of a particle with infinite radius (the bulk solubility), γ is the S/L interfacial tension, R is the gas constant and T is the absolute temperature.

During storage, the smaller particles will dissolve in the oil and they recrystallize on the larger particles, which may be in the vicinity of the O/W interface. Some crystal habit modification may be produced and large plates or needles are formed which can reach several μm. Several methods may be applied to inhibit recrystallization:

(i) Diluting the oil phase with another inert oil in which the particles are insoluble.
(ii) Use of a strongly adsorbed polymeric surfactant such as Atlox 4913 or INUTEC® SP1 that prevents entry of the suspension particles into the oil droplets.
(iii) Addition of electrolytes in the continuous phase. This has the effect of enhancing the polymeric surfactant adsorption thus preventing particle entry into the oil droplets.
(iv) Use of crystal growth inhibitors: e.g. flat dye molecules, which are insoluble in the oil and adsorb strongly on the particles surface. This prevents particle entry into the oil droplets.
(v) Use of analogues of the solid active ingredient (having the same basic structure) that are insoluble in the oil and become incorporated into the surface of the solid particles.
(vi) Use of thickeners such as HEC and xanthan gum. This will increase the low shear rate viscosity of the medium and hence slow down the diffusion of the small particles thereby preventing their entry into the oil droplets. These thickeners can produce gels in the continuous phase that are viscoelastic and this can prevent particle diffusion.

7 Formulation of controlled-release systems

7.1 Introduction

Controlled release formulation of agrochemicals offer a number of advantages of which the following is worth mentioning [1, 53]:

(i) Improvement of residual activity.
(ii) Reduction of application dosage.
(iii) Stabilization of the core active ingredient (AI) against environmental degradation.
(iv) Reduction of mammalian toxicity by reducing worker exposure.
(v) Reduction of phytotoxicity.
(vi) Reduction of fish toxicity.
(vii) Reduction of environmental pollution.

One of the main advantages of using controlled release formulations, in particular microcapsules, is that this reduces physical incompatibility when mixtures are used in the spray tank. Then mixtures are applied in the field , their use can also reduce biological antagonism.

There are several types of controlled-release systems:

(i) Microcapsules with particles in the size range 1–100 µm that consist of a distinct capsule wall (mostly a polymer) surrounding the agrochemical core.
(ii) Microparticles (size range 1–100 µm) consisting of a matrix in which the agrochemical is uniformly dissolved or dispersed.
(iii) Granules with matrix particles of 0.2–2.0 mm with the agrochemical uniformly dissolved or dispersed within the matrix.

In this section, I will give a brief account for the different types of slow release systems. For more detail, the reader can refer to the text edited by Scher [53].

7.2 Microencapsulation

Microencapsulation of agrochemicals is mainly carried out by interfacial condensation, in situ polymerization and coacervation. Interfacial condensation [54] is perhaps the most widely used method for encapsulation in industry. The active ingredient (AI), which may be oil-soluble, oil-dispersible or an oil itself is first emulsified in water using a convenient surfactant or polymer. A hydrophobic monomer A is placed in the oil phase (oil droplets of the emulsion) and a hydrophilic monomer B is placed in the aqueous phase. The two monomers interact at the interface between the oil and the aqueous phase, forming a capsule wall around the oil droplet. There are two main types of systems. For example, if the material to be encapsulated is oil soluble,

https://doi.org/10.1515/9783110588002-008

oil-dispersible or an oil itself, an oil-in-water (O/W) emulsion is first prepared. In this case, the hydrophobic monomer is dissolved in the oil phase which forms the dispersed phase. The role of surfactant in this process is crucial since an oil–water emulsifier (with high hydrophilic–lipophilic balance, HLB) is required. Alternatively, a polymeric surfactant such as partially hydrolyzed polyvinyl acetate (referred to as polyvinyl alcohol, PVA) or an ethylene oxide-propylene oxide-ethylene oxide, PEO–PPO–PEO (Pluronic) block copolymer can be used. The emulsifier controls the droplet size distribution and hence the size of capsules formed. On the other hand, if the material to be encapsulated is water soluble, a water-in-oil (W/O) emulsion is prepared using a surfactant with a low HLB number or an A–B–A block copolymer of polyhydroxystearic acid–polyethylene oxide–polyhydroxystearic acid (PHS–PEO–PHS). In this case, the hydrophilic monomer is dissolved in the aqueous internal phase droplets.

In interfacial polymerization, the monomers A and B are polyfunctional monomers capable of causing polycondensation or polyaddition reaction at the interface [54]. Examples of oil-soluble monomers are polybasic acid chloride, bis-haloformate and polyisocyantates, whereas water soluble monomers can be polyamine or polyols. Thus, a capsule wall of polyamide, polyurethane or polyurea may be formed. Some trifunctional monomers are present, allowing cross linking reactions. If water is the second reactant with polyisocyanates in the organic phase, polyurea walls are formed. The latter modification has been termed in situ interfacial polymerization [55].

One of the most useful microencapsulation processes involves reactions that produce formation of urea-formaldehyde (UF) resins. Urea along with other ingredients such as amines, maleic anhydride copolymers or phenols are added to the aqueous phase that contains oily droplets of the active ingredient that is to be encapsulated. Formaldehyde or formaldehyde oligomers are added and the reaction conditions are adjusted to form UF condensates, sometimes referred to as aminoplasts, which should preferentially wet the disperse phase [53]. The reaction is continued until completion over several hours. Fairly high activity products can be obtained. A modification of this technique is the use of etherified UF resins. The UF prepolymers are dissolved in the organic phase, along with the active ingredient, through the use of protective colloids (such as PVA), and the reaction is initiated through temperature and acid catalyst. This promotes the formation of the shell in the organic phase adjacent to the interface between the bulk-oil phase droplets and the aqueous phase solution [53]. The role of surfactants in the encapsulation process is very important. Apart from their direct role in the preparation of microcapsules dispersions, surfactants can be used to control the release of the active ingredient (AI) from the microcapsule dispersion. For example, Wade et al. [53] have shown that the efficacy of an edifenphos suspension can be improved by the addition of a surfactant either to the aqueous medium or to the core. This was attributed to the possible solubilization of the AI by the surfactant micelles, thus increasing the release rate.

There are generally two mechanisms for release of the active ingredient (AI) from a capsule:

(i) diffusion of the AI through the microcapsule wall;
(ii) destruction of the microcapsule wall either by physical means, e.g. mechanical power, or by chemical means, e.g. hydrolysis, biodegradation, thermal degradation, etc.

The release behaviour is controlled by several factors such as particle size, wall thickness, type of wall material, wall structure (porosity, degree of polymerization, crosslink density, additives, etc.), type of core material (chemical structure, physical state, presence or absence of solvents) and amount or concentration of the core material. The release behaviour is determined by the interaction of these factors and optimization is essential for achieving the desirable release rate. In order to achieve better performance of the microcapsule for biological efficacy, time-dependent or site-specific release is desirable. It is essential in this case to develop various functional microcapsules that are specific to the target organism (e.g. for insecticides). Temperature, pH, light, and enzyme-responsive microcapsules are desirable.

The simplest release kinetics of microcapsules is diffusion controlled, as predicted by Fick's first law. The amount of AI that diffuses through the wall of a microcapsule, $\mathrm{d}m/\mathrm{d}t$ (mol s^{-1}) is proportional to the diffusion coefficient D, the surface area A and the concentration gradient $\mathrm{d}c/\mathrm{d}x$ (where $\mathrm{d}c$ is the difference in concentration between the inside and outside wall and $\mathrm{d}x$ is the thickness of the capsule wall),

$$\frac{\mathrm{d}m}{\mathrm{d}t} = -DA\frac{\mathrm{d}c}{\mathrm{d}x}. \tag{7.1}$$

Equation (7.1) clearly shows that the release rate increases with increase of A (i.e. when using small capsules) and decrease of $\mathrm{d}x$ (thinner capsule wall). To decrease the rate of diffusion one has to use larger capsules with a thicker capsule wall.

7.3 Encapsulation by phase separation from aqueous solution

There are four types of encapsulation utilizing the system of phase separation from aqueous solution [54, 55]:

(i) complex coacervation or phase separation resulting from two oppositely charged colloids neutralizing one another;
(ii) simple coacervation where a non-electrolyte such as alcohol causes the formation of a separate polymer-rich phase;
(iii) salt coacervation where a polymer separates as a result of salting-out process;
(iv) precipitation and insolubilization of a polymer by changing the pH of the aqueous solution system.

An example of complex coacervation is [56], the interaction between gelatin and gum arabic. In this case a dispersion of oil in a dilute solution of gelatin-gum arabic mixture is prepared. Gelatin usually has an iso-electric point (i.e.p.) at about pH = 4.8, whereas gum arabic, which contains only carboxylic groups, is usually negative over a wide range of pH values. Thus, by lowering the pH to value below the i.e.p. of gelatin, say to pH = 4.0, the gelatin acquires a positive charge and becomes coacervated with gum arabic forming capsules around the oil droplets. Various other anionic polyelectrolytes may be used, such as sodium alginate, agar, polyvinylbenzene sulphonic acid, etc. In general, effective materials include polymers, surface active agents and organic compounds which have acid groups in the molecule [56].

Encapsulation by phase separation can also be applied in nonaqueous media. This is particularly suitable for encapsulation of water soluble materials. A W/O emulsion of the active ingredient that is dissolved in the water droplets using an oil soluble polymer. Phase separation of the oil soluble polymer may be induced by the addition of another polymer, nonsolvent or by changing the temperature.

Salt coacervation is best exemplified by the formation of calcium alginate capsules. In this process, a drop of a solution, an emulsion or suspension containing the AI and sodium alginate is dropped into a solution of calcium chloride. When the drop touches the calcium chloride solution, a membrane of calcium alginate forms instantaneously, maintaining the drop shape in this aqueous/aqueous system. Calcium ions diffuse, gelling the entire drop. This drop is then placed in a solution of a polycation which displaces the calcium ions from the outer surface, forming a permanent membrane. This capsule is then placed in sodium citrate, which slowly solubilizes the calcium through the formation of a soluble citrate complex, ungelling the internal portion of the drop. By controlling the molecular weight of the reactants and the times of reaction, the thickness and size selectivity of the permanent wall can be controlled over a wide range.

7.4 Microencapsulation of solid particles

This is by far the most challenging process of encapsulation since one has to coat the particles individually without any aggregation. These particles range from 0.1–5 µm with an average of 1–2 µm. Clearly, when encapsulating these particles one has to make sure that the smallest size fraction is retained without any aggregation. This is vital for biological efficacy since the smaller particles are more effective for disease control (due to their higher solubility when compared with larger particles). Beestan [57] suggests an injection treatment coating method for encapsulation of solid particles. This method utilizes air at a sonic velocity to atomize the coating material and accelerate the particles in such a manner that they become coated on all surfaces. The liquid coating material may be melted wax or resins, solutions of polymers or coating materials or suspensions of film-forming solids such as polymer latexes. Coating is

accomplished by metering the solid particles in the shear zone concurrently with metering the liquid coating material into the air stream. The latter is accelerated to the speed of sound through a restriction zone to create a shear zone of sufficient intensity to affect coating. The mixing action within the shear zone coats the solid particles individually with the coating material. On-line particle size measurement of the encapsulated solid particles showed that the particle size range of the solid particles remained virtually unchanged by this injection treatment coating process, indicating that individual particles of all sizes are discretely coated.

Another method that can be applied to encapsulate solid particles is a modification of the coacervation process described above. In this method, a technique of solvent evaporation is used to precipitate the polymers as intact coatings. The solid particles are suspended in a solvent solution of the polymer and emulsified into a liquid. The emulsion is then heated to evaporate the solvent, causing the polymer to insolubilize as a coating around the suspended particles. Alternatively, a nonsolvent for the polymer is added to the suspension of particles in polymer solution, causing the solvent to phase separate and the polymers to insolubilize to coatings

7.5 Controlled release of agrochemicals from matrix-based microparticles

Matrix-based microparticles are of three main types [58]:

(i) Matrix powders where the active ingredient (AI) is dispersed throughout the matrix and the mixture is ground (if necessary to form a powder that can be applied as wettable powder. Surface active agents are incorporated to aid wetting and dispersion of the microparticles. The matrices used include polymers such as lignin, starch or proteins, high molecular weight natural polymers such as waxes or cyclodextrin, and synthetic polymers such as urea formaldehyde resins or acrylic acid polymers. Inorganic materials such as glass, silica or diatomaceous earth can also be used. These inorganic materials can also act as carriers.

(ii) Carriers plus matrix whereby the particles are based on a porous powder that is used as a carrier. Two types can be distinguished, namely co-loaded (where the AI/matrix mixture is loaded into the carrier) and postcoated (where the AI is loaded into the carrier and the matrix is then loaded separately).

(iii) Matrix emulsions whereby the microparticles are made by emulsifying a hot solution of the AI plus matrix, typically in water. On cooling, the emulsion droplets solidify, producing an aqueous suspension of the microparticles.

One component of the formulation, the “matrix”, will be responsible for the controlled release of the formulation. It is convenient to consider the controlled release as result of the interaction among the AI, the matrix and the environment. Matrix systems where the AI is uniformly dispersed through a matrix material are the basis of com-

mercial formulations [59]. Three models may be used to describe the behaviour of such systems. The first two mechanisms apply where the AI is uniformly dispersed throughout the matrix and is essentially impermeable to water or the external environment. Leaching of the AI occurs at the edge of the particle, setting up a concentration gradient within the particle that provides the driving force for diffusion of the AI to the edge of the particle and into the external environment. In such a system, the rate of release is governed by the solubility of the AI in the matrix, the diffusion coefficient for the transport of the AI through the matrix and the geometry of the particle. Matrix particles usually contain pores and cracks thus increasing the effective surface area between the particle and the external environment and hence the release rate. The second mechanism is applied to rigid, often glassy matrices where diffusion of the AI within the matrix of the active is negligible. Leaching is controlled by surface exposure of the AI through biological or chemical degradation of the matrix. The third mechanism applies to systems where the matrix material is permeable to the external environment, e.g. water. This corresponds to a system where the AI is dispersed in a latex. In this case, water permeates the matrix through a combination of capillary and osmotic effects. The AI dissolves and diffuses to the edge of the particle into the surrounding medium. The process is diffusion controlled and is governed by the solubility and diffusion coefficient of the AI in water.

The release of AI from conventional formulations generally follows an exponential decay, i.e. the release rate is proportional to the concentration of the AI remaining in the formulation. This decay follows first-order kinetics, which means that the initial concentration in the environment is initially very high (often resulting in an undesirable toxic effect) and decreases rapidly to a low (ineffective) level. In contrast, a controlled release formulation generally exhibits lower initial concentrations and a longer time before the concentration decreases to an ineffective level. This is schematically illustrated in Fig. 7.1, which clearly shows that when using a conventional formulation several treatments are required for biological control. During these treatments the AI concentration may reach an undesirably high concentration which is above the toxic limit. In contrast, a controlled release formulation maintains an effective concentration that is sufficient for bioefficacy without reaching the toxic limit. Thus, with a conventional treatment a higher dose of AI is required to maintain the bioefficacy. This dose is significantly reduced when using a controlled release formulation. The high AI concentrations reached with conventional formulations can also have adverse effects on toxicity for humans, birds, fish, etc.

Most controlled-release systems rely on diffusion of AI through a rate controlling membrane or polymer matrix. Transport through a polymer membrane or matrix occurs by a solution-diffusion process, whereby the AI first dissolves in the polymer and then diffuses across the polymer to the external surface, where the concentration is lower. As discussed before the process follows Fick's first law of diffusion (equation (7.1)).

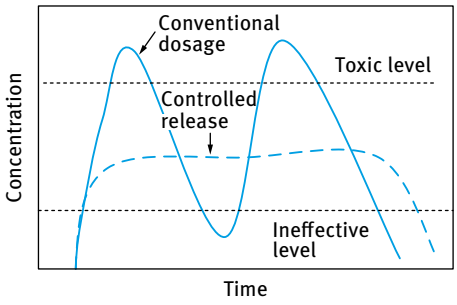

Fig. 7.1: Release of active ingredient from conventional and controlled release formulations.

The rate of AI release from controlled-release systems can follow a variety of patterns, ranging from first-order (exponential) decay (as with conventional systems) to zero-order kinetics in which the release rate is constant over most of the life-time of the device. In the latter case, the release rate decreases proportionally to the square root of time. A comparison of the release kinetics is shown in Fig. 7.2. As can be clearly seen, the zero-order kinetics (membrane coated reservoir) results in lower peak concentration and more extended release when compared with the case of first-order kinetics.

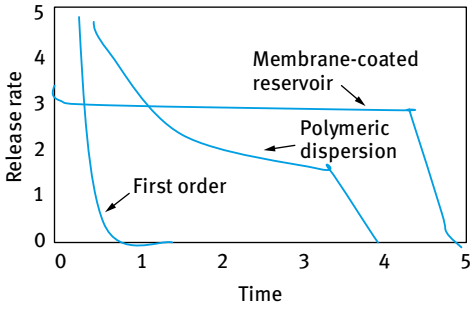

Fig. 7.2: Comparison of release kinetics observed from controlled release formulations.

As mentioned above, the most common types of controlled release microparticles are membrane-coated reservoirs and polymeric matrices. A reservoir system consists of a core of pure or saturated AI surrounded by a rate-controlling membrane (polymer shells). The AI is released from the reservoir system by diffusion through the rate-controlling membrane at a constant rate (zero-order kinetics) and this follows Fick's law. For a spherical capsule with outer and inner radii r_2 and r_1 and hence a membrane thickness of $(r_2 - r_1)$ the release rate at time t, $\mathrm{d}M_t/\mathrm{d}t$, is given by the following equation,

$$\frac{\mathrm{d}M_t}{\mathrm{d}t} = 4\pi D \frac{\mathrm{d}c}{\mathrm{d}x} \frac{r_2 r_1}{(r_2 - r_1)}, \tag{7.2}$$

where D is the diffusion coefficient of the AI and $\mathrm{d}c/\mathrm{d}x$ is the concentration gradient within the membrane.

The release rate remains constant as long as D and dc/dx remain constant. However, the latter values are temperature dependent and hence the release rate will increase with increase of temperature. In many cases, the release rate is doubled for every 10 °C increase of temperature. In addition, dc/dx remains constant as long as the activity of the AI remains constant within the reservoir. If the activity of the AI decreases as a result of release of the chemical, the release rate will decrease.

Another important factor that affects the release rate of membrane-coated reservoir type microparticles is the polydispersity of the system. The release rate from each microparticle may be constant and hence initially the release rate may also be constant. However, with time the release rate may change as a result of polydispersity. The quantity of the AI in the microparticle is a function of its volume, i.e. the cube of the radius, but the release rate is a function of the radius. Thus, the duration which is approximately equal to the mass of the AI divided by the release rate is a function of the square of the radius. Thus, the smaller microparticles become depleted before the larger ones and this results in a decrease in the overall release rate from a collection of microparticles with different sizes. To maintain a constant release rate, the membrane must remain intact. In general, large microparticles and those with a high loading of AI are more susceptible to rupture, resulting in rapid release.

With matrix-type microparticles whereby the AI is dispersed or dissolved in a polymeric matrix, the release of the AI occurs by diffusion through the matrix to the surface and hence the process follows Fick's law (equation (7.1)). However, the release kinetics can depend on the quantity of the AI and whether this is dispersed or dissolved in the matrix.

7.6 Controlled release from granules

Many agrochemicals are formulated as water-dispersible granules (WG) which disperse quickly and completely when added to water. The main advantage of WGs is that they don't require the use of solvents and thus reduce the risks during manufacture and to farm workers during application and they can be applied with slow release. Several processes can be applied to produce WGs of insoluble AI:

(i) those in which the starting materials are essentially dry, and are subsequently made wet and then redried;
(ii) those in which the starting materials are wet and are granulated and dried.

A typical composition of a WG is one or two AIs, dispersing agent, suspending agent, wetting agent, binder (such as lignosulphonate or a gum) and a filler (mineral filler or water soluble salt). Granulation is carried out using a dry or wet route process. Several dry route processes are possible such as pan granulation, fluid-bed granulation, Schugi granulator, extrusion and peg or pin granulator [60]. The wet route process can be carried out by spray drying or spray granulation [60].

Approaches to achieve controlled release in granules fall into two main categories:
(i) the matrix (monolith) with the AI dispersed throughout the structure;
(ii) the reservoir in which a polymeric coating entraps the AI with or without a support [61].

Particle size and uniformity are very important especially in applications where the duration of release is critical. Three types of granule dimensions can be distinguished, namely fine granules 0.3–2.5 mm in diameter, microgranules 0.1–0.6 mm and macrogranules 2–6 mm. A formulation containing a range of particle sizes (from dusts to macrogranules) will have an extended period of effectiveness. A controlled-release system based on a monolithic polymer granule made from extruding the AI with a release-rate-modifying inert material ("porisogen") in a thermoplastic matrix can play an important role for pest management for periods of up to 2–3 years (following a single treatment of a nonpersistent agrochemical).

Although the above approach based on synthetic polymers is the most successful of the controlled-release granules, natural polymers showed great success in matrix formulations for AI delivery. Examples of natural polymers are crosslinked starch, polysaccharides, crosslinked alginates and cellulose derivatives. To provide effective delay of release, alginate gels crosslinked with calcium require the incorporation of absorbents such as silica, alumina, clays or charcoal. Further control of the release rate could be achieved by combining kaolin clay with linseed oil in the granule. Other gel-forming polymers include carboxymethylcellulose stabilized with gelatin and crosslinked with cupric or aluminum ions. Coating of granules with rate-controlling polymer film can also be applied. Controlled delivery of agrochemicals has also been achieved with superabsorbent acrylamide and acrylate polymers.

The biodegradability of the formulating material is an important aspect of controlled release for environmental applications. Several synthetic and natural polymers used for formulating granules are biodegradable. The delivery of bioactives from controlled-release granules can be enhanced by the inclusion of biosurfactants.

Several lignin-based granules have been introduced for controlled release of several AIs. Lignin is a polyphenolic material that occurs in the cell wall of most terrestrial plants, where it is strongly associated with carbohydrates. It is a polymer produced by random dehydrogenation of a number of phenolic precursors linked to the polysaccharide component of the plant cell. This produces a complex structure without any regular repeating monomer. Lignin is separated from lignocellulosic plants by physical or chemical means.

Several agrochemicals are formulated as granules using lignin, in particular for oil application. The AI is characterized by some physicochemical properties such as moderate sorption on soil components, low volatility, moderate to high melting points, crystallinity and low to moderate water solubility. Such properties make them compatible with alkali lignins for preparing matrices by melting the components together. This produces a glassy matrix upon cooling.

The compatibility of a lignin and an agrochemical can be assessed by observing a film of the melt mixture under the microscope for presence of unsolvated lignin particles. Where solvation occurs, the melting point of the agrochemical is depressed and this can be determined using differential scanning calorimetry (DSC). The density of the glassy adhesive matrix is usually lower than that of the lignin and often less than that of the AI This can be explained by the presence of voids or pores that cannot be observed by microscopy.

The effect of water on the matrix formulation varies according to the agrochemical compatibility with lignin and the ratio of AI to lignin. With highly compatible AI such as diuron the surface of the matrix changes from dark brown to dull light brown on exposure to water. With further exposure, some swelling occurs and the outer region is very porous. Diffusion of diuron is enhanced compared to that in the unswollen glassy interior. The swelling and water uptake depends to a large extent on the lignin type used.

The mechanism of release from lignin matrix granules intended for use in soil and aqueous media is studied by immersing the granule in water under static, stirred or flowing conditions. Granules prepared from various lignin types always have release rates that decrease with time. This is illustrated in Fig. 7.3, which also shows the dependence on lignin type.

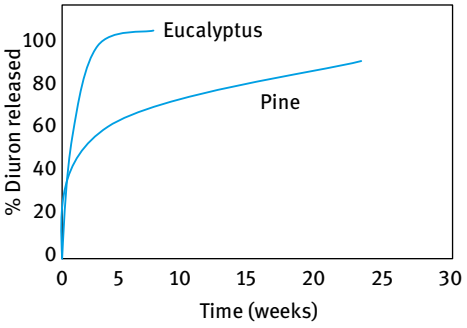

Fig. 7.3: % release of diuron (50 %) from granules based on two different lignin types.

The release kinetics fit with the generalized model [61],

$$\frac{M_t}{M_z} = kt^n + c, \tag{7.3}$$

where M_t/M_z is the proportion of AI released at time t, the constant k incorporates the polymer properties, the exponent n characterizes the transport mechanism and c is a constant.

The results of Fig. 7.3 could be fitted to equation (7.3) giving an exponent n ranging from 0.35 to 0.53, indicating that the release is mainly diffusion-controlled.

8 Formulation of adjuvants

8.1 Introduction

The development of effective agrochemicals that can be used with maximum efficiency and minimum risk to the user requires the optimization of their transfer to the target during application [1, 2]. Optimization of the transfer of the agrochemical to the target requires careful analysis of the steps involved during application. Most agrochemicals are applied as liquid sprays, particularly for foliar application. The spray volume applied ranges from high values of the order of 1,000 l per hectare (when the agrochemical concentrate is diluted with water) to ultra-low volumes of the order of 1 l per hectare (when the agrochemical formulation is applied without dilution). Various spray application techniques are used, of which spraying using hydraulic nozzles is probably the most common. In this case, the agrochemical is applied as spray droplets with a wide spectrum of droplet sizes (usually in the range 100–400 µm in diameter). On application, parameters such as droplet size spectrum, their impaction and adhesion, sliding and retention, wetting and spreading are of central importance to ensuring maximum capture by the target surface as well as adequate coverage of the target surface. In addition to these "surface chemical" factors, i.e. the interaction with various interfaces, other parameters that affect biological efficacy are deposit formation, penetration and interaction with the site of action. Deposit formation, i.e. the residue left after evaporation of the spray droplets, has a direct effect on the efficacy of the pesticide, since such residues act as "reservoirs" of the agrochemical and hence they control the efficacy of the chemical after application. The penetration of the agrochemical and its interaction with the site of action is very important for systemic compounds. Enhancement of penetration is sometimes crucial to avoid removal of the agrochemical by environmental conditions such as rain and or/wind. All these factors are influenced by surfactants and polymers. In addition, some adjuvants that are used in combination with the formulation consist of oils and/or surfactant mixtures. The role of these adjuvants in enhancing biological efficacy is far from being understood and in most cases they are arrived at by a trial and error procedure. A great deal of research is required in this area in order to understand the surface chemical processes both static and dynamic, e.g. static and dynamic surface tension and contact angles, as well as their effects on penetration and uptake of the chemical. The role of these complex mixtures of oils and/or surfactants in controlling agrochemical efficiency is important from a number of points of view. In the first place, there is greater demand to reduce the application rate of chemicals and to make better use of the present agrochemicals, for example in greater selectivity. In addition, in order to minimize hazards for the operator and the long-term effects of such residues and wastage, it is necessary to better understand the role of adjuvants in the application

https://doi.org/10.1515/9783110588002-009

of agrochemicals. This should lead to the optimization of the efficacy of the chemical as well as a reduction of the hazards to operators, crops and the environment.

The most important adjuvants are surfactants (anionic, cationic, zwitterionic and nonionic) and polymers (nonionic or ionic) that are sometimes used as stickers or anti-drift agents. In some cases, these are used in combination with crop oils (e.g. methyl oleate). Basically, a surfactant molecule consists of a hydrophobic chain (usually a hydrogenated or fluorinated alkyl or alkyl aryl chain with 8 to 18 carbon atoms) and a hydrophilic group or chain (ionic or polar nonionic such as polyethylene oxide). At the air/water interface (as for spray droplets) and the solid/liquid interface (such as the leaf surface), the hydrophobic group points towards the hydrophobic surface (air or leaf), leaving the hydrophilic group in bulk solution. This results in a reduction of the the air/liquid surface tension, γ_{LV}, and the solid/liquid interfacial tension, γ_{SL}. As the surfactant concentration is gradually increased, both γ_{LV} and γ_{SL} decrease until the critical micelle concentration (cmc) is reached, after which both values remain virtually constant. This situation represents the conditions under equilibrium whereby the rate of adsorption and desorption are the same. The situation under dynamic conditions, such as during spraying, may be more complicated since the rate of adsorption is not equal to the rate of formation of droplets. Above the cmc, micelles are produced, which at low C values are essentially spherical (with an aggregation number in the region of 50–100 monomers). Depending on the conditions (e.g. temperature, salt concentration, structure of the surfactant molecules) other shapes may be produced, e.g. rod-shaped and lamellar micelles. Micelle formation is a dynamic process, i.e. a dynamic equilibrium is set up whereby surface active agent molecules are constantly leaving the micelles while others enter the micelles (same applies to the counterions). The dynamic process of micellization is described by two relaxation processes:

(i) a short relaxation time τ_1 (of the order of 10^{-8}–10^{-3} s) which is the lifetime for a surfactant molecule in a micelle;
(ii) a longer relaxation time τ_2 (of the order of 10^{-3}–1 s) which is a measure of the micellization-dissolution process.

τ_1 and τ_2 depend on the surfactant structure and its chain length, and these relaxation times determine some of the important factors in selecting adjuvants, such as the dynamic surface tension.

The cmc of nonionic surfactants is usually two orders of magnitude lower than the corresponding anionic of the same alkyl chain length. This explains why nonionics are generally preferred when selecting adjuvants. For a given series of nonionics, with the same alkyl chain length, the cmc decreases with decrease in the number of ethylene oxide (EO) units in the chain. Under equilibrium, the γ–log C curves shift to lower values as the EO chain length decreases. However, under dynamic conditions, the situation may be reversed, i.e. the dynamic surface tensions could become lower for the surfactant with the longer EO chain. This trend is understandable if one consid-

ers the dynamics of micelle formation. The surfactant with the longer EO chain has a higher cmc and it forms smaller micelles when compared with the surfactant containing shorter EO chain. This means that the lifetime of a micelle with longer EO chain is shorter than one with a longer EO chain. This explains why the dynamic surface tension of a solution of a surfactant containing a longer EO chain can be lower than that of a solution of an analogous surfactant (at the same concentration) with a shorter EO chain.

For a series of anionic surfactants with the same ionic head group, the life time of a micelle decreases with decrease in the alkyl chain length of the hydrophobic component. Branching of the alkyl chain could also play an important role in the life time of a micelle. It is, therefore, important to carry out dynamic surface tension measurements when selecting a surfactant as an adjuvant as this may play an important role in spray retention.

However, the above measurements should not be taken in isolation as other factors may also play an important role, e.g solubilization which may require larger micelles. The selection of a surfactant as an adjuvant requires knowledge of the factors involved, which will be discussed in some detail below.

At high surfactant concentrations (usually above 10 %) several liquid crystalline phases are produced. Three main types of liquid crystals may be distinguished:

(i) hexagonal (middle) phases that consists of cylindrical anisotropic units with high viscosity;
(ii) cubic, body-centered isotropic phases with a viscosity that is higher than the hexagonal phase;
(iii) lamellar (neat) phases consisting of sheetlike units that are anisotropic, but with a viscosity that is lower than the hexagonal phase.

These phases may form during evaporation of a spray drop. In some cases, a middle phase is first produced when further evaporation may produce a cubic phase which may entrap the agrochemical given its very high viscosity. This could be advantageous for some of the systemic fungicides which require "deposits" that act as reservoirs for the chemical. The viscous cubic phases may also enhance the tenacity of the agrochemical particles (particularly with SCs) and hence enhance rain fastness. In some other applications, a lamellar phase is preferred as this provides some mobility (due to its lower viscosity).

There are generally two main approaches to selecting adjuvants:

(i) An interfacial (surface) physicochemical approach which is designed to increase the dose of the agrochemical received by the target plant or insect, i.e. enhancement of spray deposition, wetting, spreading, adhesion and retention.
(ii) Uptake activation that is enhanced by the addition of surfactant, which is the result of specific interactions between the surfactant, the agrochemical and the target species. These interactions may not be related to the intrinsic surface active properties of the surfactant/adjuvant.

Adjuvants are applied in two different ways:
(i) being incorporated in the formulation – mostly the case with flowables (SCs and EWs);
(ii) used in tank mixtures during application – such adjuvants can be complex mixtures of several surfactants, oils, polymers, etc.

The choice of an adjuvant depends on:
(i) the nature of the agrochemical, water soluble or insoluble (lipophilic) whereby its solubility and log *P* values are important;
(ii) the mode of action of the agrochemical, i.e. systemic or non-systemic, selective or non-selective;
(iii) the type of formulation that is used, i.e. flowable, EC, grain, granule, capsule, etc.

Study of the phase behaviour of surfactants (which can be obtained using polarizing microscopy) is crucial in the selection of adjuvants. The interaction of the above units with the agrochemical is crucial in determining performance (e.g. solubilization). Similar interactions may also occur between the above structural units and the leaf surface (wax solubilization).

The application of an agrochemical, as a spray, involves a number of interfaces, where the interaction with the formulation plays a vital role. The first interface during application is that between the spray solution and the atmosphere (air) which governs the droplet spectrum, rate of evaporation, drift, etc. In this respect, the rate of adsorption of the surfactant and/or polymer at the air/liquid interface is of vital importance. This requires dynamic measurements of parameters such as surface tension which will give information on the rate of adsorption. The second interface is that between the impinging droplets and the leaf surface (with insecticides, the interaction with the insect surface may be important). The droplets impinging on the surface undergo a number of processes that determine their adhesion and retention and further spread on the target surface. The rate of evaporation of the droplet and the concentration gradient of the surfactant across the droplet governs the nature of the deposit formed.

8.2 Interactions at the air/solution interface and their effect on droplet formation

In a spraying process, a liquid is forced through an orifice (the spray nozzle) to form droplets by application of a hydrostatic pressure. When the latter is increased above a certain limit no separate drops are formed at all and a continuous jet issues from the orifice. At even higher hydrostatic pressures, the jet breaks into droplets in a phenomenon usually referred to as spraying. The process of break-up of jets (or liquid sheets) into droplets is the result of surface forces. The surface area and consequently the surface free energy (area × surface tension) of a sphere is smaller than that of a

less symmetrical body. Hence small liquid volumes of other shapes tend to give rise to smaller spheres. For example, a liquid cylinder becomes unstable and divides into two smaller droplets as soon as the length of the liquid cylinder is greater than its circumference. This occurs upon accidental contraction of the long liquid cylinder. A prolate spheroid tends to give two spherical drops when the length of the spheroid is greater than 3–9 times its width. A very long cylinder with radius r (as for example a jet) tends to divide into drops with a volume equal to $(9/2)\pi r^3$. Since the surface area of two unequal drops is smaller than that of two equal drops with the same total volume, the formation of a polydisperse spray is more probable.

The effect of surfactants and/or polymers on the droplet size spectrum of a spray can be, initially, described in terms of their effect on the surface tension. Since surfactants lower the surface tension of water, one would expect that their presence in the spray solution would result in the formation of smaller droplets. As a result of the low surface tension in the presence of surfactants, the total surface energy of the droplets produced on atomization is lower than that in the absence of surfactants. This implies that less mechanical energy is required to form the droplets when a surfactant is present. This leads to smaller droplets at the same energy input. However, the actual situation is not simple since one is dealing with a dynamic situation. In a spraying process, a fresh liquid surface is continuously being formed. The surface tension of that liquid depends on the relative ratio between the time taken to form the interface and the rate of adsorption of the surfactant from bulk solution to the air/liquid interface. The rate of adsorption of a surfactant molecule depends on its diffusion coefficient and its concentration (see below). Clearly, if the rate of formation of a fresh interface is much faster than the rate of adsorption of the surfactant, the surface tension of the spray liquid will not be far from that of pure water. Alternatively, if the rate of formation of the fresh surface is much slower than that of the rate of adsorption, the surface tension of the spray liquid will be close to that of the equilibrium value of the surface tension. The actual situation is somewhere in between and the rate of formation of a fresh surface is comparable to that of the rate of surfactant adsorption. In this case, the surface tension of the spray liquid will be in between that of a clean surface (pure water) and the equilibrium value of the surface tension which is reached at times larger than that required to produce the jet and the droplets. This shows the importance of measuring dynamic surface tension and the rate of surfactant adsorption.

The rate of surfactant adsorption may be described by applying Fick's first law. When concentration gradients are set up in the system, or when the system is stirred, then the diffusion to the interface may be expressed in terms of Fick's first law, i.e.,

$$\frac{\mathrm{d}\Gamma}{\mathrm{d}t} = \frac{D}{\delta}\frac{N_\mathrm{A}}{100}C(1-\theta), \tag{8.1}$$

where Γ is the surface excess (number of moles of surfactant adsorbed per unit area), t is the time, D is the diffusion coefficient of the surfactant molecule, δ is the thickness of the diffusion layer, N_A is the Avogadro constant and θ is the fraction of the

surface already covered by adsorbed molecules. Equation (8.1) shows that the rate of surfactant diffusion increases with increase of D and C. The diffusion coefficient of a surfactant molecule is inversely proportional to its molecular weight. This implies that shorter chain surfactant molecules are more effective in reducing the dynamic surface tension. However, the limiting surface tension reached by a surfactant molecule decreases with increase of its chain length and hence a compromise is usually made when selecting a surfactant molecule. Usually, one chooses a surfactant with a chain length of the order of 12 carbon atoms. In addition, the higher the surfactant chain length, the lower its cmc and hence lower concentrations are required when using a longer chain surfactant molecule. Again, one problem with longer chain surfactants is their high Krafft temperatures (which means they are only soluble at temperatures higher than ambient temperature). Thus, an optimum chain length is usually necessary for optimizing the spray droplet spectrum.

As mentioned above, the faster the rate of adsorption of surfactant molecules, the greater the effect on reducing the droplet size. However, with liquid jets there is an important factor that may enhance surfactant adsorption. Addition of surfactants reduces the surface velocity (which is in general lower than the mean velocity of flow of the jet) below that obtained with pure water. This results from surface tension gradients which can be explained as follows. Where the velocity profile is relaxing, the surface is expanding, i.e. it is newly formed, and might even approach the composition and surface tension of pure water. A little further downstream, appreciable adsorption of the surfactant will have occurred, giving rise to a back-spreading tendency from this part of the surface towards the cleaner surface immediately adjacent to the nozzle. This phenomenon is thus a form of the Marangoni effect, which reduces the surface velocity near the nozzle and induces some liquid circulation which accelerates the adsorption of the surfactant molecules by as much as ten times. This effect casts doubt on the use of liquid jets to obtain the rate of adsorption. Indeed, under conditions of jet formation, it is likely that the surface tension approaches its equilibrium value very closely. Thus, one should be careful when using dynamic surface tension values, as for example measured using the maximum bubble pressure method.

The influence of polymeric surfactants on the droplet size spectrum of spray liquids is relatively more complicated since adsorbed polymers at the air/liquid interface produce other effects than simply reducing the surface tension. In addition, polymeric surfactants diffuse very slowly to the interface and it is doubtful if they have an appreciable effect on the dynamic surface tension. In most agrochemical formulations, polymers are used in combination with surfactants and this makes the situation more complicated. Depending on the ratio of polymer to surfactant in the formulation, various effects may be envisaged. If the concentration of the polymer is appreciably greater than the surfactant and interaction between the two components is strong, the resulting "complex" will behave more like a polymer. On the other hand, if the surfactant concentration is appreciably higher than that of the polymer and interaction between the two molecules is still strong, one may end up with polymer–surfactant complexes

as well as free surfactant molecules. The latter will behave as free molecules and reduction in the surface tension may be sufficient even under dynamic conditions. However, the role of the polymer–surfactant "complex" could be similar to the free polymer molecules. The latter produce a viscoelastic film at the air-water interface and that may modify the droplet spectrum and the adhesion of the droplets to the leaf surface. In many agrochemical applications, high molecular weight materials such as polyacrylamide, polyethylene oxide or guar gum are sometimes added to the spray solution to reduce drift. It is well known that incorporation of high molecular weight polymers favours the formation of larger drops. The effect can be achieved at very low polymer concentrations when the molecular weight of the polymer is fairly high ($>10^6$). The most likely explanation of how polymers affect the droplet size spectrum is in terms of their viscoelastic behaviour in solution. High molecular weight polymers adopt spatial conformations in bulk solution, depending on their structure and molecular weight. Many flexible polymer molecules adopt a random coil configuration which is characterized by a root mean square radius of gyration, R_G. The latter depends on the molecular weight and the interaction with the solvent. If the polymer is in good solvent conditions, e.g. polyethylene oxide in water, the polymer coil becomes expanded and R_G can reach high values, of the order of several tens of nanometres. At relatively low polymer concentrations, the polymer coils are separated and the viscosity of the polymer solution increases gradually with increase of its concentration. However, at a critical polymer concentration, to be denoted by C^*, the polymer coils begin to overlap and a rapid increase in the viscosity of the solutions takes place, with further increase in the concentration above C^*. This concentration C^* is defined as the onset of the semi-dilute region. C^* decreases with increase in the molecular weight of the polymer and at very high molecular weights it can be as low as 0.01 %. Under this condition of polymer coil overlap, the spray jet opposes deformation and this results in the production of larger drops. This phenomenon can be applied successfully to reduce drift. Some polymers also produce conformations that approach a rod like or double helix structure. An example of this is xanthan gum which is used with many emulsions and suspension concentrates to reduce sedimentation. If the concentration of such polymer is appreciable in the formulation, then even after extensive dilution on spraying (usually by 100 to 200 fold) the concentration of the polymer in the spray solution may be sufficient to cause production of larger drops. This effect may be beneficial if drift is a problem. However, it may be undesirable if relatively small droplets are required for adequate adhesion and coverage. Again, the ultimate effect required depends on the application methods and the mode of action of the agrochemical. Fundamental studies of the various effects is required to arrive at optimum conditions. The effect of the various surfactants and polymers should be studied in spray application during the formulation of the agrochemical. In most cases, the formulation chemist concentrates on producing the best system for long term physical stability (shelf life). It is crucial to investigate the effect of the various formulation variables on the droplet spectrum, their adhesion, retention and spreading. In addition, simultaneous inves-

tigations should be made into the effects of the various surfactants on the penetration and uptake of the agrochemical.

One of the problems with many anti-drift agents is their shear degradation. At the high shear rates involved in spray nozzles (which may reach several thousand s^{-1}), the polymer chain may degrade into smaller units and this results in considerable reduction of the viscosity. This will have the effect of reducing the anti-drift effect. It is, therefore, essential to choose polymers that are stable at the high shear rates involved in a spraying process.

8.3 Spray impaction and adhesion

When a drop of a liquid impinges on a solid surface, e.g. a leaf, one of several states may arise depending on the conditions. The drop may bounce or undergo fragmentation into two or more droplets which in turn may bounce back and return to the surface with a lower kinetic energy. Alternatively, the drop may adhere to the leaf surface after passing through several stages, where it flattens, retracts, spreads and finally rests to form a hemispherical cap. In some cases, the droplet may not adhere initially but instead float as an individual drop for a fraction of a second or even several seconds and either adhere to the surface or leave it again. The most important parameters that determine which one of the above-mentioned stages is reached are the mass (volume) of the droplet, its velocity in flight and the distance between the spray nozzle and the target surface, the difference between the surface energy of the droplet in flight, E_0, and its surface energy after impact, E_s, and displacement of air between the droplet and the leaf.

20–50 µm diameter droplets do not usually undergo reflection if they are able to reach the leaf surface. These droplets have a low momentum and can only reach the surface if they travel in the direction of the air stream. On the other hand, large droplets of the order of a few thousand micrometres in diameter undergo fragmentation. 100–400 µm droplets, the range produced by most spray nozzles, may be reflected or retained depending on a number of parameters such as the surface tension of the spray solution, surface roughness and elasticity of the drop surface. A study by Brunskill [62] showed that 100 % adhesion is obtained for drops of 250 µm when the surface tension of the liquid was lowered (using methanol) to 39 N m^{-1}, whereas only 4 % adhesion occurred when the surface tension, γ, was 57 N m^{-1}. For any given spray solution (with a given surface tension), a critical droplet diameter exists below which adhesion is high and above which adhesion is low. The critical droplet diameter increases as the surface tension of the spray solution decreases. The viscosity of the spray solution has only a small effect on the adhesion of large drops, but with small droplets adhesion increases with increase of the viscosity. As expected, the percentage of adhered droplets decreases as the angle of incidence of the target surface increases.

A simple theory for bouncing and droplet adhesion has been formulated by Hartley and Brunskill [63] who considered an ideal case where no adhesion (short range) forces between the liquid and solid substrate exist and the liquid has zero viscosity. During impaction, the initially spherical droplet will flatten into an oblately spheroidical shape until the increased area has stored the kinetic energy as increased surface energy. This is often followed by an elastic recoil towards the spherical form and later beyond it with the long axis normal to the surface. During this process, energy will be transformed into upward kinetic energy and the drop may leave the surface in a state of oscillation between the spheroidal forms. This sequence was confirmed using high-speed flash illumination.

When the reflected droplet leaves in an elastically deformed condition, the coefficient of restitution must be less than unity since part of the translational energy is transformed to vibrational energy. Moreover, the distortion of droplets involves loss of energy as heat by operation of viscous forces. The effect of increasing the viscosity of the liquid is rather complex, but at a very high viscosity liquids usually have a form of elasticity operating during deformations of very short duration. Reduction of deformation as a result of increase of viscosity will affect adhesion.

As mentioned above, the adhesion of droplets is governed by the relative magnitude of the kinetic energy of the droplet in flight and its surface energy as it lands on the leaf surface. Since the kinetic energy is proportional to the third power of the radius (at constant droplet velocity) whereas the surface energy is proportional to the second power of the radius, one would expect that sufficiently small droplets will always adhere. However, this is not always the case since smaller droplets fall with smaller velocities. Indeed, the kinetic energy of sufficiently small drops, in the Stokesian range, falling at their terminal velocity, is proportional to the seventh power of the radius. In the 100–400 μm range, it is nearly proportional to the fourth power of the radius.

Consider a droplet of radius r (sufficiently small for gravity to be neglected) falling onto a solid surface and spreading with an advancing contact angle, θ_A, and having a spherical upper surface of radius R. The surface energy of the droplet in flight, Eo, is given by,

$$E_0 = 4\pi r^2 \gamma_{LA}, \tag{8.2}$$

where γ_{LA} is the liquid/air surface tension.

The surface energy of the spread drop is given by the following equation,

$$E_s = A_1 \gamma_{LA} + A_2 \gamma_{SL} - A_2 \gamma_{SA} \tag{8.3}$$

where A_1 is the area of the spherical air/liquid interface, A_2 is that of the plane circle of contact with the solid surface, γ_{SL} is the solid/liquid interfacial tension and γ_{SA} that of the solid/air interface.

From Young's equation,

$$\gamma_{SA} = \gamma_{SL} + \gamma_{LA} \cos\theta. \tag{8.4}$$

Therefore, the surface energy of the droplet spreading on the leaf surface is given by the equation,

$$E_s = \gamma_{LA}(A_1 - A_2 \cos\theta). \tag{8.5}$$

The volume of a free drop is $(4/3)\pi r^3$, whereas that of the spread drop is $\pi R^3 \times [(1 - \cos\theta) + (1/3)(\cos^3\theta)]$ so that,

$$\frac{4}{3}\pi r^3 = \pi R^3\left[(1 - \cos\theta) + \tfrac{1}{3}(\cos^3\theta - 1)\right] \tag{8.6}$$

and,

$$A_1 = 2\pi R^2(1 - \cos\theta), \tag{8.7}$$

$$A_2 = \pi R^2 \sin^2\theta. \tag{8.8}$$

Combining equations (8.5), (8.6), (8.7) and (8.8) one can obtain the minimum energy barrier between attached and free drop,

$$\frac{E_0 - E_s}{E_0} = 1 - 0.39[2(1 - \cos\theta) - \sin^2\theta\cos\theta][1 - \cos\theta + (1/3)(\cos^3\theta - 1)]^{-2/3} \tag{8.9}$$

A plot of $(E_0 - E_s)/E_0$ shows that this ratio decreases rapidly from its value of unity when $\theta = 0$ to a near zero value when $\theta > 160°$. This plot can be used to calculate the critical contact angle required for adhesion of water droplets, with a surface tension $\gamma = 72\,\mathrm{mN\,m^{-1}}$ at 20 °C, of various sizes and velocities. As an illustration, consider a water droplet of 100 µm diameter falling with its terminal velocity $v \approx 0.25\,\mathrm{m\,s^{-1}}$. The kinetic energy of the drop is 1.636×10^{-9} J, whereas its surface energy in flight is 2.26×10^{-9} J. The surface energy of the attached drop at which the kinetic energy is just balanced is 2.244×10^{-9} J. The contact angle at which this occurs can be obtained by calculating the fraction $(E_0 - E_s)/E_0$ and interpolating using the above-mentioned plot. This gives $(E_0 - E_s)/E_0 = 0.00723$ and $\theta \approx 160°$. Thus, providing droplets of this size form an angle that is less than 160°, they will stick to the leaf's surface. It is thus not surprising that droplets of this size do not need any surfactant for adhesion. For a 200 µm droplet with a velocity of $1\,\mathrm{m\,s^{-1}}$, the critical contact angle is 87° and this shows that in this case surfactants are required for adhesion. The higher the velocity of the drop, the lower the critical contact angle required for adhesion. With larger drops, this critical contact angle becomes smaller and smaller and this clearly shows the importance of surfactants for ensuring drop adhesion.

It should be mentioned, however, that the above calculations are based on "idealized" conditions, i.e. droplets falling on a smooth surface. Deviation is expected when dealing with practical surfaces such as leaf surfaces. The latter are rough, containing leaf hairs and wax crystals that are distributed in different ways depending on the nature of the leaf and climatic conditions. Under such conditions, the adhesion of droplets may occur at critical contact angle values that are either smaller or larger than those predicted from the above calculations. The critical θ values will certainly be determined by the topography on the leaf surface. As we will see later, the

definition and measurement of the contact angle on a rough surface are not straightforward. In spite of these complications, experimental results on droplet adhesion seem to support the predictions from the above simple theory. These experimental results showed little dependence of adhesion of spray droplets on surfactant concentration. Since with most spray systems the contact angles obtained were lower than the critical value for adhesion (except for droplets larger than 400 μm), in most circumstances surfactant addition had only a marginal effect on droplet adhesion. However, one should not forget that the surfactant in the spray solution determines the droplet size spectrum. The addition of surfactants will also certainly affect the adhesion of droplets moving at high velocities and on various plant species. The situation is further complicated by the dynamics of the process, which depend on the nature and concentration of the surfactant added. For fundamental investigations, measurements of the dynamic surface tension and contact angle is required both on model and practical surfaces. These measurements are now easy to perform due to the advance in instruments such as the maximum bubble pressure method for measurement of dynamic surface tension and high speed video equipment for measurement of the dynamic contact angle. Such techniques will enable the formulation chemist and the biologist to understand the role and the function of the surfactant in spray solutions.

8.4 Droplet sliding and spray retention

Many agrochemical applications involve high volume sprays, whereby the volume of the drops continue to grow in size with continuous spraying by impaction of more spray droplets upon them and by coalescence with neighbouring drops on the surface. During this process, the amount of spray retained steadily increases provided the liquid drops which are impacted are also retained. However, on further spraying, the drops continue to grow in size until they reach a critical value above which they begin to slide down the surface and "drop off", the so called "run-off" condition. At the point of "incipient run-off", the volume of the spray retained is a maximum. The retention at this point is governed by the movement of the liquid drops on the solid surface. Bikerman [64] stated that the percentage of droplets sticking to a plant after touching it should depend upon the tilt of the leaf, the size of the droplets and the contact angle at the plant leaf/droplet/air interface. However, this process is complicated and governed by many other factors [65] such as droplet spectrum, velocity of impacting droplets, volatility and viscosity of the spray liquid and ambient conditions.

Several authors [65] have tried to relate the resistance to movement of liquid drops on a tilted surface to the surface tension and the contact angles (advancing and receding) of liquid droplets with the solid surface. A detailed analysis was given by Furmidge [65], who obtained an expression of spray retention, R, in terms of γ_{LA} and θ,

i.e.,

$$R = k\left[\frac{\pi\gamma_{LA}(\cos\theta_R - \cos\theta_A)}{24\rho g \sin\alpha}\right]^{1/2}\left[\frac{(1-\cos\theta_A)^2(2+\cos\theta_A)}{\sin^3\theta_A}\right]^{1/2} \tag{8.10}$$

The value of k depends on the droplet spectrum, since it relates to the rate of build-up of critical droplets and their distribution. However, equation (8.10) does not take into account the flattening effect of the droplet on impact. Thus, equation (8.10) is only likely to be valid under conditions of low impaction velocity. In this case, retention is governed by the surface tension of the spray liquid, the difference between θ_A and θ_R (i.e. the contact angle hysteresis) and the value of θ_A.

Equation (8.10) can be further simplified by removing the constant terms and standardizing $\sin\alpha$ as equal to 1. A further simplification can be achieved by replacing the second term between square brackets on the right hand side of equation (8.10) by θ_M, and the arithmetic mean of θ_A and θ_R. In this way a retention factor, F, may be defined by the following simple expression,

$$F = \theta_M\left[\frac{\gamma_{LA}(\cos\theta_R - \cos\theta_A)}{\rho}\right]^{1/2}. \tag{8.11}$$

Equation (8.11) shows that F depends on γ_{LA}, the difference between θ_R and θ_A and θ_M. At any given value of θ_A and γ_{LA}, F increases rapidly with increase in $(\theta_A - \theta_R)$, reaches a maximum and then decreases. At any given $(\theta_A - \theta_R)$ and γ_{LA}, F increases rapidly with increase in θ_A (and also θ_M). In systems with the same contact angles, F increases with increase of γ_{LA} but the effect is not very large since $F \propto \gamma_{LA}^{1/2}$. Obviously, any variation in γ_{LA} is accompanied by a change in contact angles and hence one cannot investigate these parameters in isolation. In general, by increasing the surfactant concentration, γ_{LA}, θ_A and θ_R are reduced. The relative extent to which these three values are affected depends on surfactant nature, its concentration and the surface properties of the leaf. This is a very complex problem and predictions are almost impossible.

It should also be mentioned that the above treatment does not take into account the effect of surface roughness and the presence of hairs, which play a significant role. A difference in the amount of liquid retained of up to an order of magnitude may be encountered, at constant F values, between e.g. a hairy and a smooth leaf. Besides these large variations in the surface properties of various species of leaves, there are also variations within the same species depending on age, environmental conditions and position. However, contact angle measurements on leaf surfaces are not easy and one has to make several measurements and subject the results to statistical analysis. Thus, at best the measured F values can be used as a guideline for comparing various surface active agents on leaf surfaces of a particular species grown under standard conditions.

Several other factors affect retention, of which droplet size spectrum, droplet velocities and wind speed are probably the most important. Usually, retention increases

with reduction of droplet size, but is significantly reduced at high droplet velocities and wind speeds. The impact velocity effect becomes more marked as the receding contact angle decreases. Wind reduces the volume of spray that can be retained, particularly when θ_A and θ_R are fairly large because little force is required to remove the drop along the surface. As θ_A and θ_R become small, the wind effect becomes less significant and it becomes negligible when θ_A and θ_R are close to zero. The leaf's structure is also important, since less spray is lost due to wind movements from leaves with a very rough surface when compared to those with smooth leaves. Thus, care should be taken when results are obtained on plants grown under standard conditions, such as glass houses. These results should not be extrapolated to field conditions, since plants grown under normal environmental conditions may have surfaces that are vastly different from those grown in glass houses. In order to obtain a realistic picture of spray retention, measurements should be made on field-grown plants and the results obtained may be correlated to those obtained on glass house plants. In this case, it is possible to use glass house plants for selection of surfactants, if an allowance is made for the difference between the two sets of results.

8.5 Wetting and spreading

Another factor which can affect the biological efficacy of foliar spray application of agrochemicals is the extent to which the liquid wets, spreads and covers the foliage surface. This, in turn, governs the final distribution of the agrochemical over the area to be protected. The optimum degree of coverage in any spray application depends on the mode of action of the agrochemical and the nature of the pest to be controlled. With non-systemic agrochemicals, the cover required depends on the mobility or location of the pest. The more static the pest, the greater the need for complete coverage on those areas of the plant liable to attack. Under those conditions, good spreading of the liquid spray with maximum coverage is required. On the other hand, with systemic agrochemicals, satisfactory cover is ensured provided the spray liquid is brought into contact with those areas of the plant through which the agrochemical is absorbed. Since, as we will see later, high penetration requires high concentration gradients, an optimum situation may be required here, whereby one achieves adequate coverage of those areas where penetration occurs without too much spreading over the total leaf surface since this usually results in "thin" deposits. These "thin" deposits do not provide adequate "reservoirs", which are sometimes essential to maintain a high concentration gradient, thus enhancing penetration. In addition, thick deposits which are produced from droplets with limited spreading can increase the tenacity of the agrochemical and ensure longer term protection by the agrochemical. This situation may be required with many systemic fungicides.

Many leaf surfaces represent the most unwettable of known surfaces. This is due to the predominantly hydrophobic nature of the leaf surface, which is usually covered

with crystalline wax of straight chain paraffinic alcohols in the range 24–35 carbon atoms. The crystals may be less than 1 µm thick and only a few µm apart, giving the surface "microroughness" and the "real" area of the surface can be several times the "gross" (apparent) area. When a water drop is placed on a leaf surface, it takes the form of a spherical cap that is characterized by the contact angle θ. From the balance of tensions, one obtains equation (8.4) (Young's equation) which applies to a liquid drop on a smooth surface.

Wetting is sometimes simply assessed by the value of the contact angle; the smaller the angle the better the liquid is said to wet the solid. Complete wetting implies a contact angle of zero, whereas complete non-wetting dictates an angle of contact of 180°. However, contact angle measurements are not easy on real surfaces since a great variation in the value is obtained at various locations of the surface. In addition, it is very difficult to obtain an equilibrium value. This is due to the heterogeneity of the surface and its roughness. Thus, in most practical systems such as spray drops on leaf surfaces, the contact angle exhibit hysteresis, i.e. its value depends on the history of the system and varies according to whether the given liquid tends to advance across or recede from the leaf surface. The limiting angles achieved just prior to movement of the wetting line (or just after movement ceases) are known as the advancing and receding contact angles, θ_A and θ_R, respectively. For a given system, $\theta_A > \theta_R$ and θ can usually take any value between these two limits without discernable movement of the wetting line. Since smaller angles imply better wetting, it is clear that the contact angle always changes in such a direction as to oppose wetting line movement.

The use of contact angle measurements to assess wetting depends upon equilibrium thermodynamic arguments, which unfortunately do not reflect the real situation. In the practical situation of spraying, the liquid has to displace the air or another fluid attached to the leaf surface and hence measurement of dynamic contact angles, i.e. those associated with moving wetting lines is more appropriate. Such measurements require special equipment such as video cameras and image analysis and they should enable one to obtain a more accurate assessment of wetting by the spray liquid.

As mentioned above, the contact angle often undergoes hysteresis so that θ cannot be defined unambiguously by experiment. This hysteresis is accounted for by surface roughness, surface heterogeneity and metastable configurations. Surface roughness can be taken into account by introducing a term r to Young's equation, where r is the ratio of real to apparent surface area, i.e.,

$$r\gamma_{SA} = r\gamma_{SL} + \gamma_{LA}\cos\theta. \tag{8.12}$$

Thus, the contact angle on a rough surface is given by the expression,

$$\cos\theta = \frac{r(\gamma_{SA} - \gamma_{SL})}{\gamma_{LA}}. \tag{8.13}$$

In other words, the contact angle on a rough surface, θ, is related to that on a smooth surface, θ_0, by the equation,

$$\cos\theta = r\cos\theta_0. \tag{8.14}$$

Equation (8.14) shows that surface roughness increases the magnitude of $\cos\theta_0$, whether its value is positive or negative. If $\theta_0 < 90°$, $\cos\theta_0$ is positive and it becomes more positive as a result of roughness, i.e. $\theta < \theta_0$ or roughness in this case enhances wetting. In contrast, if $\theta_0 > 90°$, $\cos\theta_0$ is negative and roughness increases the negative value of $\cos\theta_0$, i.e. roughness results in $\theta > \theta_0$. This means that if $\theta_0 > 90°$ roughness makes the surface even more difficult to wet.

The influence of surface heterogeneity was analyzed by Cassie and Baxter [66]. The possibility of adopting metastable configurations as a result of surface roughness was suggested by Deryaguin [67]. He considered the wetting line to move in a series of thermodynamically irreversible jumps from one metastable configuration to the next.

In spite of the above complications, measurement of contact angles of spray liquids on leaf surfaces are still most useful in defining the wetting and spreading of the spray. A very useful index for measuring the spread of a liquid on a solid surface is Harkin's spreading coefficient, S, which is defined by the change in tension when solid/liquid and liquid/air interfaces are replaced by a solid/air interface. In other words, S is the work required to destroy a unit area each of the solid/liquid and liquid/air interfaces while forming a unit area of the solid/air interface, i.e.,

$$S = \gamma_{SA} - (\gamma_{SL} + \gamma_{LA}). \tag{8.15}$$

If S is positive, the liquid will usually spread until it completely wets the solid. If S is negative, the liquid will form a non-zero contact angle. This can be clearly shown if equation (8.15) is combined with Young's equation, i.e.,

$$S = \gamma_{LV}(\cos\theta - 1). \tag{8.16}$$

Clearly, if $\theta > 0$, S is negative and this implies only partial wetting. In the limit $\theta = 0$, S is equal to zero and this represents the onset of complete wetting. A positive S implies rapid spreading of the liquid on the solid surface. Indeed, by measuring the contact angle only, one can define a spread factor, SF, which is the ratio between the diameter of the area wetted on the leaf, D, and the diameter of the drop d, i.e.,

$$SF = \frac{D}{d}. \tag{8.17}$$

Provided θ is not too small ($> 5°$), the spread factor can be calculated from θ, i.e.,

$$SF = \left[\frac{4\sin^3\theta}{(1-\cos\theta)^2(2+\cos\theta)}\right]^{1/3}. \tag{8.18}$$

A plot of SF versus θ shows a rapid increase in SF when $\theta < 35°$. The most practical method of measuring the spread factor is to apply drops of known volume using

a micro-applicator on the leaf's surface. By using a tracer material, such as a fluorescent dye, one may be able to measure the spread area directly using for example image analysis. This area can be converted to an equivalent sphere, allowing D to be obtained.

Another useful concept for assessing the wettability of surfaces is that introduced by Zisman et al. [68], namely the critical surface tension of wetting, γ_c. These authors found that for a given surface and a series of related liquids such as n-alkanes, siloxanes or dialkyl ethers, $\cos\theta$ is a reasonably linear function of γ_{LA}. The surface tension at the point where the line cuts the $\cos\theta = 1$ axis is known as the critical surface tension of wetting, γ_c. It is the surface tension of a liquid that would just spread to give complete wetting.

Several authors have tried to relate the critical surface tension to the solid/liquid interfacial tension, or at least its dispersion component, $\gamma\, dS$. From the above discussion, it is clear that to enhance the wetting and spreading of liquids on leaf surfaces, one needs to lower the contact angle of the droplets. This is usually achieved by the addition of surfactants, which adsorb at various interfaces and modify the local interfacial tension. Since most leaf surfaces are nonpolar low energy surfaces, increase of surfactant concentration enhances wetting. This explains why most agrochemical formulations contain high concentrations of surfactants to enhance wetting and spreading. However, as we will see later, surfactants play other roles in deposit formation, distribution of the agrochemical on the target surface and enhancement of penetration of the chemical.

Although the role played by a surfactant is complex, these materials sometimes referred to as wetting agents or simply adjuvants need to be carefully selected for optimization of biological efficacy. To date, surfactants are still selected by the formulation chemist on the basis of a trial and error procedure. However, some guidelines may be applied to make this selection. The HLB system may be initially applied for choosing the most common wetting agents. The latter have HLB numbers between 7 and 9. Nonionic surfactants usually have two orders of magnitude lower critical micelle concentration (cmc) when compared with their ionic counter parts at the same alkyl chain length. Since the limiting value of the surface tension is reached at concentrations above the cmc, it is clear that many nonionic surfactants are more effective as wetting agents since after dilution of the formulation the concentration of the nonionic surfactant in the spray solution may be higher than its cmc. However, many nonionic surfactants with HLB numbers in the range 7–9 undergo phase separation at high concentrations and/or temperatures. This may limit their incorporation in the formulation at high concentrations. In some cases, the addition of a small amount of an ionic surfactant may be beneficial in reducing this phase separation and raising the cloud point of the nonionic surfactant. Thus, many agrochemical formulations contain complex mixtures of surfactants which are carefully arrived at by the formulation chemist. The composition of these mixtures is usually kept confidential.

Another important property of the surfactant selected for a given agrochemical is its effect on the leaf structure and the cuticle. Surfactants that cause significant damage to the leaf are described as phytotoxic and in many crops such damage must be avoided. This can sometimes limit the choice, since in some cases the best wetter may not be the best from the phytotoxicity point of view and a compromise must be made. This shows that selecting the surfactant can be difficult and requires careful investigation of many surface chemical properties as well as its interaction with the leaf surface and the cuticle. In addition, its effect on deposit formation and penetration of the agrochemical need to be separately investigated.

8.6 Evaporation of spray drops and depsoit formation

The object of spraying is often to leave a long-lasting deposit of particulate fungicide or insecticide or a residue able to penetrate the cuticle in the case of systemic pesticides and herbicides or to be transferred locally within the crop by its own slower evaporation. The form of residue left by evaporation of the carrier liquid depends to a large extent on the rate of evaporation and most importantly on the nature and concentration of surfactant and other ingredients in the formulations. Evaporation from a spray drop tends to occur most rapidly near the edges since these receive the necessary heat most rapidly from the air by conduction through the dry air surrounding the leaf. This results in a higher concentration of surfactant at the edge, causing surface tension gradients and convection (arising from the associated density difference). Surface tension gradients cause a Marangoni effect with liquid circulation within the drop that causes the particles to be preferentially deposited at the edge. Convection within the drop leads to preferential precipitation near the edge because the particles can first become “wedged” between the solid/liquid and liquid/air interface.

The type and composition of the spray deposit depends to a large extent on the type of formulation as well as the concentration and type of dispersing agent (for suspensions) or emulsifier (for emulsifiable concentrates and emulsions). Additives such as wetters, humectants and stickers also affect the nature of the deposit. It should also be mentioned that these may undergo some physical changes upon drying during the evaporation of a spray droplet containing dispersed particles or droplets. For example, the solid particles of a suspension may undergo recrystallization forming differently shaped particles which will affect the final form of the deposit. Both suspension particles and emulsion droplets may also undergo flocculation, coalescence and Ostwald ripening all of which affect the nature of the deposit. Following such changes during evaporation is not easy and requires special techniques such as microscopy and differential scanning calorimetry.

Another important factor in deposits is the tenacity of the resulting particles or droplets. Strong adhesion between the particles or droplets and the leaf surface is required to prevent removal of these particles or droplets by the rain. The adhesion

forces between a particle or droplet are determined by the van der Waals attraction and the area of contact between the particles and the surface. Several other factors may affect adhesion, namely electrostatic attraction, and chemical and hydrogen bonding. The area of contact between the particle and the surface is determined by its size and shape. It is obvious that by reducing the particle size of a suspension, one increases the total area of contact between them and the leaf surface, when compared with coarser particles of the same total mass. The shape of the particle also affects the area of contact. For example, flat or cube-like particles will have larger areas of contact when compared with needle shaped crystals of equivalent volume. Several other factors may affect adhesion such as the water solubility of the agrochemical. In general, the lower the solubility, the greater the rain fastness.

One of the most important factors that affects deposit formation is the phase separation that occurs during evaporation. Surfactants form liquid crystalline phases when their concentration exceeds a certain value that depends on the nature of the surfactant, the hydrocarbon chain length and the nature and length of the hydrophilic portion of the molecules. During evaporation, liquid crystals of very high viscosity such as hexagonal or cubic phases may be produced at first. Such highly viscous (and elastic structures) will incorporate any particles or droplets and they act as reservoirs for the chemical. As a result of solubilization of the chemical, penetration and uptake may be enhanced (see below). With further evaporation, the hexagonal and cubic phases may produce lamellar structures with lower viscosity than former phases. Such structures will affect the distribution of particles or droplets in the deposit. Thus, the choice of a particular surfactant for an agrochemical formulation necessitates study of its phase diagram in order to identify the nature of the liquid crystalline phases that are produced on increasing its concentration. The effect of temperature on the liquid crystalline structures is also important. Liquid crystalline structures "melt" above a critical temperature producing liquid phases that contain micelles. These liquid phases have much lower viscosity and hence the particles or droplets of the agrochemical within these liquid phases become mobile. The temperature at which such melting occurs depends on the structure of the surfactant molecule and hence the choice depends on the mode of action of the agrochemical and the environmental conditions encountered such as temperature and humidity. It should also be mentioned that the liquid crystalline structures will be affected by other additives in the formulation such the antifreeze and electrolytes. In addition, the particles or droplets of the agrochemical may affect the liquid crystalline structures produced and this requires a detailed study of the phase diagram in the presence of the various additives as well as in the presence of the agrochemical. Various methods may be applied for such investigations, such as polarizing microscopy, differential scanning calorimetry and rheology.

8.7 Solubilization and its effect on transport

Solubilization is the incorporation of an "insoluble" substance (usually referred to as the substrate) into surfactant micelles (the solubilizer). Solubilization may also be referred to as the formation of a thermodynamically stable, isotropic solution of a substance, normally insoluble or slightly soluble in water by the introduction of an additional amphiphilic component or components [69]. Solubilization can be determined by measuring the concentration of the chemical that can be incorporated in a surfactant solution while remaining isotropic as a function of its concentration. At concentrations below the cmc, the amount of chemical that can be incorporated into the solution increases slightly above its solubility in water. However, just above the cmc, the concentration of the chemical that can be incorporated in the micellar solution increases rapidly with further increase in surfactant concentration. This rapid increase, just above the cmc, is usually described as the onset of solubilization. One may differentiate three different locations of the substrate in the micelles. The most common location is in the hydrocarbon core of the micelle. This is particularly the case for a lipophilic nonpolar molecule as is the case with most agrochemicals. Alternatively, the substrate may be incorporated in between the surfactant chains of the micelle, i.e. by co-micellization. This is sometimes referred to as penetration in the palisade layer, in which one may distinguish between deep and short penetration. The third way of incorporation is by simple adsorption on the surface of the micelle. This is particularly the case with polar compounds.

Several factors affect solubilization of which the structure of the surfactant and solubilizate, temperature and addition of electrolyte are probably the most important. Generalizations about the manner in which the structural characteristics of the surfactant affect its solubilizing capacity are complicated by the existence of different solubilzation sites within the micelles. For deep penetration within the hydrocarbon core of the micelle, solubilization increases with an increase in the alkyl chain length of the surfactant. On the other hand, if solubilization occurs in the hydrophilic portion of the surfactant molecules, e.g. its polyethylene oxide chain, then the capacity increases with increase in the hydrophilic chain length. The solubilizate structure can also play a major role. For example, polarity and polarizability, chain branching, molecular size and shape and structure have been shown to have various effects. The temperature also has an effect on the extent of micellar solubilization, which is dependent on the structure of the solubilizate and of the surfactant. In most cases, solubilization increases with increase in temperature. This is usually due to the increase of the solubility of the solubilizate and increase of the micellar size with nonionic ethoxylated surfactants. Addition of electrolytes to ionic surfactants usually causes an increase in the micelle size and reduction in the cmc, and hence an increase in the solubilization capacity. Non-electrolytes which are capable of being incorporated in the micelle, e.g. alcohols, lead to an increase in the micelle size and hence to an increase in solubilization.

The presence of micelles will have significant effects on the biological efficacy of an insoluble pesticide. In the first instance, surfactants will affect the rate of solution of the chemical. Below the cmc, surfactant adsorption can aid wetting of the particles and consequently increases the rate of dissolution of the particles or agglomerates. Above the cmc, the rate of dissolution is affected as a result of solubilization. According to the Noyes–Whitney relation, the rate of dissolution is directly related to the surface area of the particles A and the saturation solubility C_s, i.e.,

$$\frac{dC}{dt} = kA(C_s - C), \tag{8.19}$$

where C is the concentration of the solute.

Higuchi [70] assumed that an equilibrium exists between the solute and solution at the solid/solution interface and that the rate of movement of the solute into the bulk is governed by the diffusion of the free and solubilized solute across a stagnant layer. Thus, the effect of surfactant on the dissolution rate will be related to the dependence of that rate on the diffusion coefficient of the diffusing species. However, experimental results have not confirmed this hypothesis and it was concluded that the effect of solute solubilization involves more steps than a simple effect on the diffusion coefficient. For example, it has been argued that the presence of surfactants may facilitate the transfer of solute molecules from the crystal surface into a solution, since the activation energy of this process was found to be lower in the presence of surfactant than its absence in water. On the other hand, Chan, Evans and Cussler [71] considered a multi-stage process in which surfactant micelles diffuse to the surface of the crystal, become adsorbed (as hemimicelles) and form mixed micelles with the solubilizate. The latter is dissolved and it diffuses away into bulk solution, removing the solute from the crystal surface. This multi-stage process, which directly involves surfactant micelles, will probably enhance the dissolution rate.

Apart from the above effect on dissolution rate, surfactant micelles also affect the membrane permeability of the solute. Solubilization can, under certain circumstances, help the transport of an insoluble chemical across a membrane. The driving force for transporting the substance through an aqueous system is always the difference in its chemical potential (or to a first approximation to the difference of its relative saturation) between the starting point and its destination. The principal steps involved are dissolution, diffusion or convection in bulk liquid and crossing of a membrane. As mentioned above, solubilization will enhance the diffusion rate by affecting transport away from the boundary layer adjacent to the crystal. It should be mentioned, however, that to enhance transport the solution should remain saturated, i.e. excess solid particles must be present since an unsaturated solution has a lower activity.

Diffusion in bulk liquid obeys Fick's first law, i.e.,

$$J_D = D\left(\frac{\partial C}{\partial x}\right), \tag{8.20}$$

where J_D is the flux of solute (amount of solute crossing a unit cross section in unit time), D is the diffusion coefficient and $(\partial C/\partial x)$ is the concentration gradient. The presence of the chemical in a micelle will lower D since the radius of a micelle is obviously greater than that of a single molecule. Since the diffusion coefficient is inversely proportional to the radius of the diffusing particle, D is generally reduced when the molecule is transported by a micelle. Assuming that the volume of the micelle is about 100 times greater than a single molecule, the radius of the micelle will only be about 10 times larger than that of a single molecule. Thus, D will be reduced by about a factor of 10 when the molecule diffuses within a micelle when compared with that of a free molecule. However, the presence of micelles increases the concentration gradient in direct proportionality to the increase in incorporation of the chemical by the micelle. This is because Fick's law involves the absolute concentration gradient, which is necessarily small as long as the solubility is small, and not its relative rate. If the saturation is represented by S, Fick's law may be written as,

$$J_D = D \times 100S\left(\frac{\partial \%S}{\partial x}\right), \tag{8.21}$$

where $(\partial \%S/\partial x)$ is the gradient in relative value of S. Equation (8.21) shows that for the same gradient of relative saturation, the flux caused by diffusion is directly proportional to saturation. Hence, solubilization will in general increase transport by diffusion, since it can increase the saturation value by many orders of magnitude (outweighing the reduction in D).

Solubilization also increases transport by convection since the flux of this process, J_C, is directly proportional to the velocity of the moving liquid and the concentration of the solute C. Moreover, one would expect that solubilization enhances transport through a membrane by an indirect mechanism. Since solubilization reduces the steps involving diffusion and convection in bulk liquid, it permits application of a greater fraction of the total driving force to transport through the membrane. In this way, solubilization accelerates the transport through the membrane, even if the resistance to this step remains unchanged. It should also be mentioned that enhancement of transport as a result of solubilization does not necessarily involve transport of any micelles. The latter are generally too large to pass through membranes.

The above discussion clearly demonstrates the role of surfactant micelles in the transport of agrochemicals. Since the droplets applied to foliage undergo rapid evaporation, the concentration of the surfactant in the spray deposits can reach very high values which allow considerable solubilization of the agrochemical. This will certainly enhance transport as discussed above. Since the life time of a micelle is relatively short, usually less than 1 ms, such units break up quickly releasing their contents near the site of action and produce a large flux by increasing the concentration gradient. However, there have been few more detailed systematic investigations into this effect and this should certainly be a topic of research in the future.

8.8 Interaction between surfactants, agrochemicals and target species

To select adjuvants that can be used for enhancement of biological efficacy, one has to consider the specific interactions that may take place between the surfactant, agrochemical and target species. This is usually described in terms of an activation process for uptake of the chemical into the plant. This mechanism is particularly important for systemic agrochemicals.

Several key factors may be identified in the uptake activation process:

(i) in the spray droplet;
(ii) in the deposit formed on the leaf surface;
(iii) in the cuticle before or during penetration;
(iv) in tissues underlying the site of application.

Four main sites were considered by Stock and Holloway [72] for increase of uptake of the agrochemical into a leaf:

(i) on the surface of the cuticle;
(ii) within the cuticle itself;
(iii) in the outer epidermal wall underneath the cuticle;
(iv) at the cell membrane of internal tissues.

The activator surfactant is initially deposited together with the agrochemical and it can penetrate the cuticle reaching other sites of action and hence the role of surfactant in the activation process can be very complex. The net effect of surfactant interactions at any of the sites of action is to enhance the mass transfer of an agrochemical from a solid or liquid phase on the outside of the cuticle to the aqueous phase of the internal tissues of the treated leaf. As discussed above, solubilization can play a major role in activating the transport of the agrochemical molecules. With many nonpolar systemic fungicides which are mostly applied as suspension concentrates, the presence of micelles can enhance the rate of dissolution of the chemical and this results in increased availability of the molecules. It also leads to an increase in the flux as discussed above.

It has been suggested that cuticular wax can be solubilized by surfactant micelles (by the same mechanism of solubilization of the agrochemical). However, no evidence has been presented (for example using SEM) to show the wax disruption by the micelles. Schonherr [73] has suggested that surfactants interact with the waxes of the cuticle and thus increase the fluidity of this barrier. This hypothesis is sometimes referred to as wax "plasticization" (similar to the phenomenon of glass transition temperature reduction of polymers by the addition of plasticizers). Some measurements of uptake using surfactants with various molecular weights and HLB numbers offer some support for this hypothesis.

Several other mechanisms have been suggested by Stock and Holloway [72] for uptake activation:

(i) Prevention of crystal formation in deposits. It is often assumed that the foliar uptake of an agrochemical from a crystalline deposit will be less than that from an amorphous one.

(ii) Retention of moisture in deposits by humectant action. The humectant theory has arisen mainly from the observation that the uptake of highly soluble chemicals is promoted by high EO surfactants such as Tween 20.

(iii) Promotion of uptake of solutions via stomatal infiltration. This hypothesis stemmed from the observation of rapid uptake of agrochemicals (within the first 10 minutes) when using superwetters such as Silwett L-77, which is capable of reducing the surface tension of water to values as low as 20 $mN\,m^{-1}$.

References

[1] Tadros T. Surfactants in agrochemicals. New York: Marcel Dekker; 1994.
[2] Tadros T. Colloids in agrochemicals. Germany: Wiley-VCH; 2009.
[3] Tadros T. Emulsions. Berlin: De Gruyter; 2016.
[4] Tadros T. Nanodispersions. Berlin: De Gruyter; 2016.
[5] Tadros T. Suspension concentrates. Berlin: De Gruyter; 2017.
[6] Tadros T. Applied surfactants. Berlin: De Gruyter; 2005.
[7] Tadros T. Introduction to surfactants. Berlin: De Gruyter; 2014.
[8] Tadros T. Handbook of colloid and interface science. Vol. 1 and 2. Berlin: De Gruyter; 2018.
[9] Becher DZ. Encyclopedia of emulsion technology. Vol. 2. New York: Marcel Dekker; 1985. Chapter 3.
[10] Beerbower A, Hill MW. Amer Cosmet Perfum. 1972;87:85.
[11] Qunick G, Weidermanns A. 1888;35:593.
[12] Lewis JB, Pratt HRC. Nature. 1953;171:1155.
[13] Garner FH, Nutt CW, Mohradi MF. Nature. 1955;175:603.
[14] Davis JT, Rideal EK. Interfacial phenomena. 2nd ed. New York: Academic Press; 1963.
[15] Hartung HA, Rice OK. J Colloid Interface Sci. 1955;10:436.
[16] Davis JT, Haydon DA. Proc Int Congr Surface Activity. 2nd ed. Vol. 1. London; 1961. p. 417.
[17] Kaminiski A, McBain JW. Proc Royal Society. 1949;A198:447.
[18] Ogino K, Ota M. Bull Chem Soc Japan, 1976;49:1187.
[19] Ogino K, Umetsu H. Bull Chem Soc Japan. 1978;51:1543.
[20] Overbeek J. Faraday Disc Chem Soc. 1978;65:7.
[21] Griffin WC. J. Cosmet Chemists. 1949;1:311. 1954;5:249.
[22] Becher P. In: Schick MJ, editor. Nonionic surfactants. New York: Marcel Dekker; 1987. (Surfactant Science Series; vol. 1)
[23] Davies JT. Proc Int Congr Surface Activity. 1959;1:426.
[24] Shinoda K. J Colloid Interface Sci. 1967;25:396.
[25] Shinoda K, Saito H. J Colloid Interface Sci. 1969;30:258.
[26] Sherman P. J Colloid Sci. 1955;10:63.
[27] Sherman P. J Soc Chem Ind. 1950;69.
[28] Asakura S, Oosawa F. J Polym Sci. 1958;33:245.
[29] Thompson W. Phil Mag. 1871;42:448.
[30] Lifshitz IM, Slesov VV. Sov Phys JETP. 1959;35:331.
[31] Wagner C. Z Electrochem. 1961;35:581.
[32] Higuchi WI, Misra J. J Pharm Sci. 1962;51:459.
[33] Walstra P. In: Becher P, editor. Encyclopedia of emulsion technology. Vol. 4. New York: Marcel Dekker; 1996.
[34] Deryaguin BV, Scherbaker RL. Kolloid Zh. 1961;23:33.
[35] Friberg S, Jansson PO, Cederberg E. J Colloid Interface Sci. 1976;55:614.
[36] Parfitt GD, editor. Dispersion of powders in liquids. London: Applied Science Publishers Ltd.; 1977.
[37] Tadros T, editor. Solid/liquid dispersions. London: Academic Press; 1987.
[38] Parfitt GD. Fundamental aspects of dispersions. In: Parfitt GD, editor. Dispersion of powders in liquids. London: Applied Science Publishers; 1973.
[39] Rideal EK. Phil Mag. 1922;44. 1152.
[40] Washburn ED. Phys Rev. 1921;17:273.
[41] Rhebinder PA. Colloid J. USSR. 1958;20:493.

https://doi.org/10.1515/9783110588002-010

[42] Smolders CA. Rec Trav Chim. 1961;80:650.
[43] Tadros T. Dispersions of powders in liquids and stabilization of suspensions. Germany: Wiley-VCH; 2012.
[44] Bachelor GK. J Fluid Mech. 1972;52:245.
[45] Buscall R, Goodwin JW, Ottewill RH, Tadros T. J Colloid Interface Sci. 1982;85:78.
[46] van Olphen H. Clay colloid chemistry. New York: Wiley; 1963.
[47] Norrish K. Disc Faraday Soc. 1954;18:120.
[48] Tadros T. Rheology of dispersions. Germany: Wiley-VCH; 2010.
[49] Deryaguin BV, Landau L. Acta Physicochim USSR. 1941;14:633.
[50] Verwey E, Overbeek J. Theory of stability of lyophobic colloids. Amsterdam: Elsevier; 1948.
[51] Hamaker HC. Physica (Utrecht). 1937;4:1058.
[52] Tadros T. Polymeric surfactants. Berlin: De Gruyter; 2017.
[53] Scher HB. Controlled-release delivery systems for pesticides. New York: Marcel Dekker; 1999.
[54] Kondo A. Microcapsule processing and technology. New York: Marcel Dekker; 1979.
[55] Morgan PW, Kvolek SL. J Polym Sci. 1947;2:90.
[56] Bunderberg de Jong HC. Complex colloid system. In: Ktuyt H, editor. Colloid science. Vol. 2. Amsterdam: Elsevier; 1949.
[57] Beetsma GB. In: Scher HB, editor. Controlled-release delivery systems for pesticides. New York: Marcel Dekker; 1999.
[58] Park DJ, Jackson WR, McKinnon IR, Marshall M. Controlled-release delivery systems for pesticides. New York: Marcel Dekker; 1999.
[59] Bahadir M, Pfister G. Controlled release formulations of pesticides. In: Bowers WS, Ebing W, Martin D, editors. Controlled release, biochemical effects of pesticides and inhibition of plant pathogenic fungi. Berlin: Springer-Verlag; 1990. p. 1–64.
[60] Woodford AR. Dispersible granules. In: Van Valkenberg W, Sugavanan B, Khetan SK, editors. Pesticide formulation. New Delhi, India: New Age International (P) Ltd.; 1998. Chapter 9.
[61] Wilkins RM, editor. Controlled delivery of crop protection agents. London: Taylor and Francis; 1990.
[62] Brunskill RT. Proceeding of the third weed conference. Association of British Manufacturers; 1956. p. 593.
[63] Hartley GS, Brunskill RG. Surface phenomena in chemistry and biology. New York: Pergamon Press; 1958. p. 214–223.
[64] Bikerman JJ. Ind Eng Chem. 1941;13:443.
[65] Furmidge C. J Colloid Interface Sci. 1962;17:309.
[66] Cassie ADB, Baxter S. Trans Faraday Soc. 1944;40:546.
[67] Deryaguin BV. CR Acad Sci USSR. 1946;51:361.
[68] Zisman WA. Adv Chem Ser. 1964;43.
[69] Attwood D, Florence AT. Surfactant systems. London: Chapman and Hall; 1983.
[70] Higuchi WI. J Pharm Sci. 1964;53:532. 1967;56:315.
[71] Chan AF, Evans DF, Cussler EL. AJ Chem. 1976;22:1006.
[72] Stock D, Hollaway PJ. Pesticide Sci. 1993;37:233.
[73] Schonherr J. Pesticide Sci. 1993;39:213.

Part II: **The formulation of paints and coatings**

9 Formulation of paints and coatings

9.1 Introduction

Paints or surface coatings are complex multi-phase colloidal systems that are applied as a continuous layer to a surface [1, 2]. A paint usually contains pigmented materials, which distinguishes it from clear films that are described as lacquers or varnishes. The main purpose of a paint or surface coating is to provide aesthetic appeal as well as to protect the surface. For example, motor car paint can enhance the appearance of the car body by providing colour and gloss and it also protects the car body from corrosion.

When considering a paint formulation, one must know the specific interaction between the paint components and substrates. This subject is of particular importance when considering the deposition and adhesion of the components to the substrate. The latter can be wood, plastic, metal, glass, etc. The interaction forces between the paint components and the substrate must be considered when formulating any paint. In addition, the method of application can vary from one substrate and another.

For many applications, more than one coat is applied to achieve a required property such as durability, strong adhesion to the substrate, opacity, colour, gloss, mechanical properties, chemical resistance, corrosion protection, etc. The first two or three coats (referred to as the primer and undercoat) are applied to seal the substrate and provide strong adhesion to the substrate. The topcoat provides the aesthetic appeal such as gloss, colour, smoothness, etc. This clearly explains the complexity of paint systems which require fundamental understanding of the processes involved, such as particle–surface adhesion, colloidal interaction between the various components, mechanical strength of each coating, etc.

The main objective of the present part is to consider the colloidal phenomena involved in a paint system, its flow characteristics or rheology, its interaction with the substrate and the main criteria that are needed to produce a good paint for a particular application.

To obtain a fundamental understanding of the above basic concepts one must consider first the paint components. Most paint formulations consist of disperse systems (solid in liquid dispersions). The disperse phase consists of primary pigment particles (organic or inorganic), which provide opacity, colour and other optical effects. These are usually in the submicron range. Other coarse particles (mostly inorganic) are used in the primer and undercoat to seal the substrate and enhance the adhesion of the top coat. The continuous phase consists of a solution of polymer or resin which provides the basis for a continuous film that seals the surface and protects it from the outside environment. Most modern paints contain latexes which are used as film formers. These latexes (with a glass transition temperature mostly below ambient temperature) coalesce on the surface and form a strong and durable film. Other components may be present in the paint formulation such as corrosion inhibitors, driers, fungicides, etc.

https://doi.org/10.1515/9783110588002-011

In this introductory chapter, I will give a brief account of the properties of the main components in a paint formulation, namely the disperse particles and the medium in which they are dispersed (the film formers and the solvent).

9.2 Dispersion particles

The primary pigment particles (normally in the submicron range) are responsible for the paint's opacity, colour and anti-corrosive properties. The principal pigment in use is titanium dioxide, due to its high refractive index. It is the pigment used to produce white paint. To produce maximum scattering, the particle size distribution of titanium dioxide has to be controlled within a narrow limit. Rutile with a refractive index of 2.76 is preferred over anatase, which has a lower refractive index of 2.55. To produce maximum scattering, the particle size distribution of titanium dioxide has to be controlled within 220–140 nm. Rutile provides the possibility of higher opacity than anatase and it is more resistant to chalking on exterior exposure. The surface of rutile is photoactive and it is surface-coated with silica and alumina in various proportions to reduce its photoactivity.

Coloured pigments may consist of inorganic or organic particles. For a black pigment, one can use carbon black, copper carbonate, manganese dioxide (inorganic) or aniline black (organic). For yellow, one can use lead, zinc, chromates, cadmium sulphide, iron oxides (inorganic) or nickel azo yellow (organic). For blue/violet, one can use ultramarine, prussian blue, cobalt blue (inorganic), phthalocyanin, indanthrone blue or carbazol violet (organic). For red, one can use red iron oxide, cadmium selenide, red lead, chrome red (inorganic), toluidine red or quinacridones (organic).

The colour of a pigment is determined by the selective absorption and reflection of the various wavelengths of visible light (400–700 nm) which impinges on it. For example, a blue pigment appears so because it reflects the blue wavelengths in the incident white light and absorbs the other wavelengths. Black pigments absorb all the wavelengths of incident light almost totally, whereas a white pigment reflects all the visible wavelengths.

The primary shape of pigmented particles is determined by its chemical nature, its crystalline structure (or lack of it) and the way the pigment is created in nature or made synthetically. Pigments as primary particles may be spherical, nodular, needle or rod-like, or plate like (lamellar).

The pigments are usually supplied in the form of aggregates (whereby the particles are attached at their faces) or agglomerates (where the particles are attached at their corners). When dispersed in the continuous phase, these aggregates and agglomerates must be dispersed into single units. This requires the use of an effective wetter/dispersant as well as the application of mechanical energy. This process of dispersion will be discussed in detail in Chapter 11.

In paint formulations, secondary pigments are also used. These are referred to as extenders, fillers and supplementary pigments. They are relatively cheaper than the primary pigments and they are incorporated in conjunction with the primary pigments for a variety of reasons such as cost effectiveness, enhancement of adhesion, reduction of water permeability, enhancement of corrosion resistance, etc. For example, in primers or undercoats (matt latex paint), coarse particle extenders such as calcium carbonate are added in conjunction with TiO_2 to achieve whiteness and opacity in a matt or semi-matt product. The particle size of extenders range from a submicron to a few tens of microns. Their refractive index is very close to that of the binder and hence they do not contribute to the opacity from light scattering. Most extenders used in the paint industry are naturally occurring materials such as barytes (barium sulphate), chalk (calcium carbonate), gypsum (calcium sulphate) and silicates (silica, clay, talc or mica). However, more recently synthetic polymeric extenders have been designed to replace some of the TiO_2. A good example is spindrift which consists of polymer beads that consist of spherical particles (up to 30 µm in diameter) that contain submicron air bubbles and a small proportion of TiO_2. The small air bubbles (< 0.1 µm) reduce the effective refractive index of the polymer matrix, thus enhancing the light scattering of TiO_2.

The refractive index (RI) of any material (primary or secondary pigment) is key to its performance. As is well known, the larger the difference in refractive index between the pigment and the medium in which it is dispersed, the greater the opacity effect. A summary of the refractive indices of various extenders and opacifying pigments is given in Tab. 9.1.

Tab. 9.1: Refractive indices (RI) of extenders and opacifying pigments.

Extender pigments	RI	Opacifying white pigments	RI
Calcium carbonate	1.58	Zinc sulphide	1.84
China clay	1.56	Zinc oxide	2.01
Talc	1.55	Zinc sulphide	2.37
Barytes	1.64	TiO_2 anatase	2.55
		TiO_2 rutile	2.76

The refractive index of the medium in which the pigment is dispersed ranges from 1.33 (for water) to 1.4–1.6 (for most film formers). Thus, rutile will give the highest opacity, whereas talc and calcium carbonate will be transparent in fully bound surface coatings. Another important fact that affects light scattering is the particle size and hence to obtain the maximum opacity from rutile an optimum particle size of 250 nm is required. This explains the importance of dispersing the powder in the liquid well, which can be achieved by a good wetting/dispersing agent as well as with the application of sufficient milling efficiency.

For coloured pigments, the refractive index of the pigment in the non-absorbing, or highly reflecting part of the spectrum, affects the performance as an opacifying material. For example, Pigment Yellow 1 and Arylamide Yellow G give lower opacity than Pigment Yellow 34 Lead Chromate. Most suppliers of coloured pigments attempt to increase the opacifying effect by controlling the particle size.

The nature of the pigment surface plays a very important role in its dispersion in the medium as well as its affinity to the binder. For example, the polarity of the pigment determines its affinity for alkyds, polyesters, acrylic polymers and latexes, which are commonly used as film formers (see below). In addition, the nature of the pigment surface determines its wetting characteristics in the medium in which it is dispersed (which can be aqueous or nonaqueous) as well as the dispersion of the aggregates and agglomerates into single particles. It also affects the overall stability of the liquid paint. Most pigments are surface treated by the manufacturer to achieve the optimum performance. As mentioned above, the surface of rutile particles is treated with silica and alumina in various proportions to reduce its photoactivity. If the pigment has to be used in a nonaqueous paint, its surface is also treated with fatty acids and amines to make it hydrophobic for incorporation in an organic medium. This surface treatment enhances the dispersibility of the paint, its opacity and tinting strength and its durability (glass retention, resistance to chalking and colour retention). It can also protect the binder in the paint formulation.

The dispersion of the pigment powder in the continuous medium requires several processes, namely wetting of the external and internal surface of the aggregates and agglomerates, separation of the particles from these aggregates and agglomerates by application of mechanical energy, displacement of occluded air and coating of the particles with the dispersion resin. It is also necessary to stabilize the particles against flocculation either by electrostatic double layer repulsion and/or steric repulsion. The process of wetting and dispersion of pigments will be described in detail in Section 11.3, whereas the eminence of colloid stability (lack of aggregation) will be discussed in Section 11.4.

9.3 Dispersion medium and film formers

The dispersion medium can be aqueous or nonaqueous depending on application. It consists of a dispersion of the binder in the liquid (which is sometimes referred to as the diluent). The term solvent is frequently used to include liquids that do not dissolve the polymeric binder. Solvents are used in paints to enable the paint to be made and they enable application of the paint to the surface. In most cases, the solvent is removed after application by simple evaporation and if the solvent is completely removed from the paint film it should not affect the paint film performance. However, in the early life of the film, solvent retention can affect hardness, flexibility and other film properties. In water-based paints, the water may act as a true solvent for some of

the components but it should be a nonsolvent for the film former. This is particularly the case with emulsion paints.

With the exception of water, all solvents, diluents and thinners used in surface coatings are organic liquids with low molecular weights. Two types can be distinguished, hydrocarbons (both aliphatic and aromatic) and oxygenated compounds such as ethers, ketones, esters, ether alcohols, etc. Solvents, thinners and diluents control the flow of the wet paint on the substrate to achieve a satisfactory smooth, even thin film, which dries in a predetermined time. In most cases, mixtures of solvents are used to obtain the optimum conditions for paint application. The main factors that must be considered when choosing solvent mixtures are their solvency, viscosity, boiling point, evaporation rate, flash point, chemical nature, odour and toxicity.

The solvent power or solvency of a given liquid or mixture of liquids determines the miscibility of the polymer binder or resin. It has also a big effect on the attraction between particles in a paint formulation, as will be discussed in detail in Chapter 11. A very useful parameter that describes solvency is the Hildebrand solubility parameter δ [3, 4], which is related to the energy of association of molecules in the liquid phase in terms of "cohesive energy density". The latter is simply the ratio of the energy required to vaporize 1 cm^3 of liquid ΔE_v to its molar volume V_m. The solubility parameter δ is simply the square root of that ratio,

$$\delta = \left(\frac{\Delta E_v}{V_m} \right). \tag{9.1}$$

Liquids with similar values of δ are miscible, whereas those with significant differences are immiscible. The solubility parameters of liquids can be determined experimentally by measuring the energy of vaporization. For polymers, one can determine the solubility parameter using an empirical approach by contacting the polymer with liquids with various δ values and observing whether or not dissolution occurs. The solubility parameter of the polymer is taken as the average of two δ values for two solvents that appear to dissolve the polymer. A better method is to calculate the solubility parameter from the "molar attraction constant" G of the constituent parts of the molecule [4],

$$\delta = \left(\frac{\rho \Sigma G}{M} \right), \tag{9.2}$$

where ρ is the density of the polymer and M is its molecular weight.

Hansen [5] extended Hildebrand's concept by considering three components for the solubility parameter, a dispersion component δ_d, a polar component δ_p, and a hydrogen bonding component δ_h,

$$\delta^2 = \delta_d^2 + \delta_p^2 + \delta_h^2. \tag{9.3}$$

Values of δ and its components are tabulated in the book by Barton [6].

As mentioned above, the dispersion medium consists of a solvent or diluent and the film former. The latter is also sometimes referred to as a "binder", since it functions by binding the particulate components together and this provides the continuous film-forming portion of the coating. The film former can be a low molecular weight polymer (oleoresinous binder, alkyd, polurethane, amino resins, epoxide resin, unsaturated polyester), a high molecular weight polymer (nitrocellulose, solution vinyls, solution acrylics), an aqueous latex dispersion (polyvinyl acetate, acrylic or styrene/butadiene) or a nonaqueous polymer dispersion (NAD). In this introductory chapter, I will only briefly describe film formers based on polymer solutions. The subject of polymer latexes and nonaqueous dispersions will be dealt with in Chapter 10. The polymer solution may exist in the form of a fine particle dispersion in nonsolvent. In some cases, the system may be a mixed solution/dispersion implying that the solution contains both single polymer chains and aggregates of these chains (sometimes referred to as micelles). A striking difference between a polymer that is completely soluble in the medium and that which contains aggregates of that polymer is the viscosity reached in both cases. A polymer that is completely soluble in the medium will show a higher viscosity at a given concentration compared to another polymer (at the same concentration) that produces aggregates. Another important difference is the rapid increase in the solution viscosity with increase in molecular weight for a completely soluble polymer. If the polymer makes aggregates in solution, increase in molecular weight of the polymer does not show a dramatic increase in viscosity.

The earliest film-forming polymers used in paints were based on natural oils, gums and resins. Modified natural products are based on cellulose derivatives such as nitrocellulose, which is obtained by nitration of cellulose under carefully specified conditions. Organic esters of cellulose such as acetate and butyrate can also be produced. Another class of naturally occurring film formers are those based on vegetable oils and their derived fatty acids (renewable resource materials). Oils used in coatings include linseed oil, soya bean oil, coconut oil and tall oil. When chemically combined into resins, the oil contributes flexibility and, with many oils, oxidative crosslinking potential. The oil can also be chemically modified, as for example the hydrogenation of castor oil that can be combined with alkyd resins to produce some specific coating properties.

Another early binder used in paints are the oleoresinous vehicles that are produced by heating oils and either natural or certain pre-formed resins together, so that the resin dissolves or disperses in the oil portion of the vehicle. However, these oleoresinous vehicles have bee replaced later by alkyd resins which are probably one of the first applications of synthetic polymers in the coating industry. These alkyd resins are polyesters obtained by reaction of vegetable oil triglycerides, polyols (e.g. glycerol) and dibasic acids or their anhydrides. These alkyd resins enhanced the mechanical strength, drying speed and durability over and above those obtained using the oleoresinous vehicles. The alkyds were also modified by replacing part of the dibasic acid

with a diisocyanate (such toluene diisocyanate, TDI) to produce greater toughness and quicker drying characteristics.

Another type of binder is based on polyester resins (both saturated and unsaturated). These are typically composed mainly of co-reacted di- or polyhydric alcohols and di- or tri-basic acid or acid anhydride. They have also been modified using silicone to enhance their durability.

More recently, acrylic polymers have been used in paints due to their excellent properties of clarity, strength and chemical and weather resistance. Acrylic polymers refer to systems containing acrylate and methylacrylate esters in their structure along with other vinyl unsaturated compounds. Both thermoplastic and thermosetting systems can be made, the latter are formulated to include monomers possessing additional functional groups that can further react to give crosslinks following the formation of the initial polymer structure. These acrylic polymers are synthesized by radical polymerization. The main polymer-forming reaction is a chain propagation step which follows an initial initiation process. A variety of chain transfer reactions are possible before chain growth ceases by a termination process.

The monomers used for preparation of acrylic polymers vary in nature and can generally be classified as "hard" (such as methylmethacrylate, styrene and vinyl acetate) or "soft" (such as ethyl acrylate, butyl acrylate, 2-ethyl hexyl acrylate). Reactive monomers may also have hydroxyl groups (such as hydroxy ethyl acrylate). Acidic monomers such as methacrylic acid are also reactive and may be included in small amounts in order that the acid groups may enhance pigment dispersion. The practical coating systems are usually copolymers of "hard" and "soft". The polymer hardness is characterized by its glass transition temperature, T_g. The T_g (K) of the copolymer can be estimated from the T_g of the individual T_g (K) of the homopolymers with weight fractions W_1 and W_2,

$$\frac{1}{T_g} = \frac{W_1}{T_{g1}} + \frac{W_2}{T_{g2}}. \tag{9.4}$$

The vast majority of acrylic polymers consist of random copolymers. By controlling the proportion of "hard" and "soft" monomers and the molecular weight of the final copolymer one can achieve the properties required for a given coating. As mentioned above, two types of acrylic resins can be produced, namely thermoplastic and thermosetting. The former have applications in automotive topcoats although they suffer from some disadvantages like cracking in cold conditions and this may require a process of plasticization. These problems can be overcome by using thermosetting acrylics which improve the chemical and alkali resistance. Also it allows one to use higher solid contents in cheaper solvents. Thermosetting resins can be self-cross linking or may require a co-reacting polymer or hardener.

9.4 Deposition of particles and their adhesion to the substrate

In a paint film, the pigment particles need to undergo a process of deposition to the surfaces (that is governed by long range forces such as van der Waals attraction and electrical double layer repulsion or attraction). This process of deposition is also affected by polymers (nonionic, anionic or cationic) which can enhance or prevent adhesion. Once the particles reach surface, they have to adhere strongly to the substrate. This process of adhesion is governed by short-range forces (chemical or nonchemical). The same applies to latex particles, which also undergo a process of deposition, adhesion and coalescence.

9.5 Flow characteristics (rheology) of paints

Control of the flow characteristics of paints is essential for its successful application. All paints are complex systems consisting of various components such as pigments, film formers, latexes and rheology modifiers. These components interact with each other and the final formulation becomes non-Newtonian, exhibiting complex rheological behaviour. The paint is usually applied in three stages, namely transfer of the paint from the bulk container, transfer of the paint from the applicator (brush or roller) to the surface to form a thin even film and flow-out of film surface, coalescence of polymer particles (latexes) and loss of the medium by evaporation. During each of these processes, the flow characteristics of the paint and its time relaxation produce interesting rheological responses. To understand the rheological behaviour of a paint system, one must start with a basic knowledge of rheology. This will be described in Chapter 13, which gives an account of the basic principles of rheology [7]. The subject of rheology modifiers, which are essential components of a paint formulation, will be briefly described. These modifiers are introduced for various reasons, such as maintenance of the long-term stability of the paint, ease of its application and the final characteristics of the film produced. A brief account of the main rheological characteristics of a paint formulation will be given.

10 Formulation of film formers

Emulsion polymers (latexes) are the most commonly used film formers in the coating industry. This is particularly the case with aqueous emulsion paints that are used for home decoration. These aqueous emulsion paints are applied at room temperature and the latexes coalesce on the substrate, forming a thermoplastic film. Sometimes functional polymers are used for cross linking in the coating system. The polymer particles are typically submicron (0.1–0.5 μm).

Generally speaking, there are two methods for preparation of polymer dispersions, namely emulsion and dispersion polymerization. In emulsion polymerization, a monomer is emulsified in a nonsolvent, commonly water, usually in the presence of a surfactant. A water-soluble initiator is added, and particles of polymer form and grow in the aqueous medium as the reservoir of the monomer in the emulsified droplets is gradually used up. In dispersion polymerization (which is usually applied for preparation of nonaqueous polymer dispersion, commonly referred to as nonaqueous dispersion polymerization, NAD), monomer, initiator, stabilizer (referred as protective agent) and solvent initially form a homogeneous solution. The polymer particles precipitate when the solubility limit of the polymer is exceeded. The particles continue to grow until the monomer is consumed. In suspension polymerization, the monomer is emulsified in the continuous phase using a surfactant or polymeric suspending agent. The initiator (which is oil-soluble) is dissolved in the monomer droplets and the droplets are converted into insoluble particles, but no new particles are formed.

Below, a description of both emulsion and dispersion polymerization is given, with particular reference to the control of their particle size and colloid stability which is greatly influenced by the emulsifier or dispersant used. Particular emphasis will be given to the effect of polymeric surfactants, which have recently been used for the preparation of emulsion polymers.

10.1 Emulsion polymerization

In emulsion polymerization, the monomer, e.g. styrene or methyl methacrylate, which is insoluble in the continuous phase, is emulsified using a surfactant that adsorbs at the monomer/water interface [8]. The surfactant micelles in bulk solution solubilize some of the monomer. A water-soluble initiator such as potassium persulphate $K_2S_2O_8$ is added and this decomposes in the aqueous phase, forming free radicals that interact with the monomers forming oligomeric chains. It has long been assumed that nucleation occurs in the "monomer swollen micelles". The reasoning behind this mechanism was the sharp increase in the rate of reaction above the critical micelle concentration and that the number of particles formed and their size depend to a large extent on the nature of the surfactant and its concentration (which determines

https://doi.org/10.1515/9783110588002-012

the number of micelles formed). However, this mechanism was later disputed and it was suggested that the presence of micelles means that excess surfactant is available and molecules will readily diffuse to any interface.

The most accepted theory of emulsion polymerization is referred to as the coagulative nucleation theory [9, 10]. A two-step coagulative nucleation model has been proposed by Napper et al. [9, 10]. In this process, the oligomers grow by propagation and this is followed by a termination process in the continuous phase. A random coil is produced which is insoluble in the medium and this produces a precursor oligomer at the θ-point. The precursor particles subsequently grow primarily by coagulation to form true latex particles. Some growth may also occur by further polymerization. The colloidal instability of the precursor particles may arise from their small size, and the slow rate of polymerization can be due to reduced swelling of the particles by the hydrophilic monomer [9, 10]. The role of surfactants in these processes is crucial since they determine the stabilizing efficiency and the effectiveness of the surface-active agent ultimately determines the number of particles formed. This was confirmed by using surface active agents of a different nature. The effectiveness of any surface active agent in stabilizing the particles was the dominant factor and the number of micelles formed was relatively unimportant.

A typical emulsion polymerization formulation contains water, 50 % monomer blended for the required glass transition temperature, T_g , surfactant (and often colloid), initiator, pH buffer and fungicide. Hard monomers with a high T_g used in emulsion polymerization may be vinyl acetate, methyl methacrylate or styrene. Soft monomers with a low T_g include butyl acrylate, 2-ethylhexyl acrylate, vinyl versatate and maleate esters. Most suitable monomers are those with low, but not too low, water solubility. Other monomers such as acrylic acid, methacrylic acid and adhesion promoting monomers may be included in the formulation. It is important that the latex particles coalesce as the diluent evaporates. The minimum film-forming temperature (MFFT) of the paint is a characteristic of the paint system. It is closely related to the T_g of the polymer but the latter can be affected by materials present such as surfactant and the inhomogeneity of the polymer composition at the surface. High T_g polymers will not coalesce at room temperature and in this case a plasticizer ("coalescing agent") such as benzyl alcohol is incorporated in the formulation to reduce the T_g of the polymer thus reducing the MFFT of the paint. Clearly, for any paint system one must determine the MFFT since, as mentioned above, the T_g of the polymer is greatly affected by the ingredients in the paint formulation.

Several types of surfactants can be used in emulsion polymerization:

- anionic such as sodium dedecyl sulphate (SDS);
- cationic such as dodecyl trimethyl ammonium chloride, $C_{12}H_{25}(CH_3)_3NCl$;
- zwitterionic such as betaine, lauryl amido propyl dimethyl betaine $C_{12}H_{25}CON(CH_3)_2CH_2COOH$;
- nonionic such as alcohol ethoxylates, alkyl phenol ethoxylates, fatty acid ethoxylates, monoalkaolamide ethoxylates, sorbitan ester ethoxylates, fatty amine

ethoxylates and ethylene oxide–propylene oxide copolymers (sometimes referred to as polymeric surfactants);
- multihydroxy products such as glycol esters, glycerol (and polyglycerol) esters, glucosides (and polyglucosides), sucrose esters.

The role of surfactants is two-fold, firstly to provide a locus for the monomer to polymerize and secondly to stabilize the polymer particles as they form. In addition, surfactants aggregate to form micelles (above the critical micelle concentration) and these can solubilize the monomers. In most cases, a mixture of anionic and nonionic surfactant is used for optimum preparation of polymer latexes. Cationic surfactants are seldom used, except for some specific applications where a positive charge is required on the surface of the polymer particles.

In addition to surfactants, most latex preparations require the addition of a polymer (sometimes referred to as a "protective colloid") such as partially hydrolyzed polyvinyl acetate (commercially referred to as polyvinyl alcohol, PVA), hydroxyethyl cellulose or a block copolymer of polyethylene oxide (PEO) and polypropylene oxide (PPO). These polymers can be supplied with various molecular weights or proportions of PEO and PPO. When used in emulsion polymerization, they can be grafted by the growing chain of the polymer being formed. They assist in controlling the particle size of the latex, enhance the stability of the polymer dispersion and control the rheology of the final paint.

A typical emulsion polymerization process involves two stages known as the seed stage and the feed stage. In the feed stage, an aqueous charge of water, surfactant, and colloid is raised to the reaction temperature (85–90 °C) and 5–10 % of the monomer mixture is added along with a proportion of the initiator (a water soluble persulphate). In this seed stage, the formulation contains monomer droplets stabilized by surfactant, a small amount of monomer in solution as well as surfactant monomers and micelles. Radicals are formed in solution from the breakdown of the intiator and these radicals polymerize the small amount of monomer in solution. These oligomeric chains will grow to some critical size, the length of which depends on the solubility of the monomer in water. The oligomers build up to a limiting concentration and this is followed by a precipitous formation of aggregates (seeds), a process similar to micelle formation, except in this case the aggregation process is irreversible (unlike surfactant micelles which are in dynamic equilibrium with monomers).

In the feed stage, the remaining monomer and initiator are fed together and the monomer droplets become emulsified by the surfactant remaining in solution (or by extra addition of surfactant). Polymerization proceeds as the monomer diffuses from the droplets, through the water phase, into the already forming growing particles. At the same time, radicals enter the monomer-swollen particles causing both termination and re-initiation of polymerization. As the particles grow, the remaining surfactant from the water phase is adsorbed onto the surface of particles to stabilize the polymer particles. The stabilization mechanism involves both electrostatic and steric

repulsion. The final stage of polymerization may include a further shot of initiator to complete the conversion.

According to the theory of Smith and Ewart [11] of the kinetics of emulsion polymerization, the rate of propagation R_p is related to the number of particles N formed in a reaction by the equation,

$$-\frac{d[M]}{dt} = R_p k_p N n_{av}[M], \tag{10.1}$$

where $[M]$ is the monomer concentration in the particles, k_p is the propagation arte constant and n_{av} is the average number of radicals per particle.

According to equation (10.1), the rate of polymerization and the number of particles are directly related to each other, i.e. an increase in the number of particles will increase the rate. This has been found for many polymerizations, although there are some exceptions. The number of particles is related to the surfactant concentration [S] by the equation [11],

$$N \approx [S]^{3/5}. \tag{10.2}$$

Using the coagulative nucleation model, Napper et al. [9, 10] found that the final particle number increases with increase in surfactant concentration with a monotonically diminishing exponent. The slope of $d(\log N_c)/d(\log t)$ varies from 0.4 to 1.2. At high surfactant concentration, the nucleation time will be long in duration since the new precursor particles will be readily stabilized. As a result, more latex particles are formed and eventually will outnumber the very small precursor particles at long times. The precursor/particle collisions will become more frequent and fewer latex particles are produced. The dN_c/dt will approach zero and over long times the number of latex particles remain constant. This shows the inadequacy of the Smith–Ewart theory which predicts a constant exponent (3/5) at all surfactant concentrations. For this reason, the coagulative nucleation mechanism has now been accepted as the most probable theory for emulsion polymerization. In all cases, the nature and concentration of surfactant used is very crucial and this is very important in the industrial preparation of latex systems.

Most reports on emulsion polymerization have been limited to commercially available surfactants, which in many cases are relatively simple molecules such as sodium dodecyl sulphate and simple nonionic surfactants. However, studies on the effect of surfactant structure on latex formation have revealed the importance of the structure of the molecule.

Block and graft copolymers (polymeric surfactants) are expected to be better stabilizers when compared to simple surfactants. The use of these polymeric surfactants in emulsion polymerization and the stabilization of the resulting polymer particles is discussed below.

Block copolymers are also used as stabilizers in emulsion polymerization. Most aqueous emulsion and dispersion polymerization reported in the literature are based

on a few commercial products with a broad molecular weight distribution and varying block compositions. The results obtained from these studies could not establish what effect the structural features of the block copolymer has on their stabilizing ability and effectiveness in polymerization. Fortunately, model block copolymers with well-defined structures could be synthesized and analyses of their role in emulsion polymerization have been carried out using model polymers and model latexes.

A series of well-defined A–B block copolymers of polystyrene-block–polyethylene oxide (PS–PEO) were synthesized [12] and used for emulsion polymerization of styrene. These molecules are "ideal" since the polystyrene block is compatible with the polystyrene formed and thus it forms the best anchor chain. The PEO chain (the stabilizing chain) is strongly hydrated with water molecules and it extends into the aqueous phase, forming the steric layer necessary for stabilization. However, the PEO chain can become dehydrated at high temperatures (due to the break of hydrogen bonds) thus reducing the effective steric stabilization. Thus, the emulsion polymerization should be carried out at temperatures well below the theta (θ)-temperature of PEO.

Another systematic study of the effects of block copolymer on emulsion polymerization was carried out using a block of poly(methylmethacrylate)-block–polyethylene oxide (PMMA–PEO) for the preparation of PMMA latexes. The ratio and molecular weight of PMMA to PEO in the block copolymer was varied. Ten different PMMA–PEO blocks were synthesized [13] with M_n for PMMA varying between 400 and 2,500. The M_w of PEO was varied between 750 and 5,000.

A summary of the effect of the molecular weight of PMMA and PEO blocks on the resulting latex is given in Tab. 10.1. Tab. 10.2 shows the effects of the total molecular weight of the diblock copolymer. The results of the systematic study (Tab. 10.1 and Tab. 10.2) of varying the PMMA and PEO block molecular weight, the % PEO in the chain as well as the overall molecular weight clearly show the effect of these factors on the resulting latex. For example, when using a block copolymer with 400 molecular weight of PMMA and 750 molecular weight of PEO (i.e. containing 65 wt% PEO) the resulting latex has fewer particles when compared with the other surfactants.

The most dramatic effects were obtained when the PMMA molecular weight was increased to 900 while keeping the PEO molecular weight (750) the same. This block copolymer contains only 46 wt% PEO and it became insoluble in water due to the lack of hydrophilicity. The latex produced was unstable and it collapsed at the early stage of polymerization. The PEO molecular weight of 750 is insufficient to provide effective steric stabilization. By increasing the molecular weight of PEO to 2,000 or 5,000 while keeping the PMMA molecular weight at 400 or 800 a stable latex was produced with a small particle diameter and large number of particles. The best results were obtained by keeping the molecular weight of PMMA at 800 and that of PEO at 2,000. This block copolymer gave the highest conversion rate, the smallest particle diameter and the largest number of particles (Tab. 10.2). It is interesting to note that by increasing the PEO molecular weight to 5,000 while keeping the PMMA molecular

Tab. 10.1: Effect of PMMA and PEO molecular weight in the diblock.

M_n PMMA	M_w PEO	wt% PEO	$R_p \times 10^4$ (mol l^{-1} s)	D (nm)	$N \times 10^{-13}$ (cm^{-3})
400	750	65	1.3	213	1.7
400	2000	83	1.5	103	14.7
400	5000	93	2.4	116	10.3
900	750	46	Unstable latex	—	—
800	2000	71	3.4	92	20.6
800	5000	86	3.2	106	13.5
1300	2000	61	2.4	116	10.3
1200	5000	81	4.6	99	16.6
1900	5000	72	3.4	110	11.4
2500	5000	67	2.2	322	0.4

Tab. 10.2: Effect of total molecular weight of the PMMA–PEO diblock.

M_w	wt% PEO	$R_p \times 10^4$ (mol l^{-1} s)	D (nm)	$N \times 10^{-13}$ (cm^{-3})
1150	65	1.3	213	1.7
2400	83	1.5	103	14.7
2800	71	3.4	92	20.6
3300	61	2.4	99	16.6
6200	81	4.6	99	16.6
6900	72	3.4	110	11.4
7500	67	2.2	322	0.4

weight at 800, the rate of conversion decreased, the average diameter increased and the number of particles decreased when compared with the results obtained using 2,000 molecular weight for PEO. It seems that when the PEO molecular weight is increased the hydrophilicity of the molecule increased (86 wt% PEO) and this reduced the efficiency of the copolymer. It seems that by increasing hydrophilicity of the block copolymer and its overall molecular weight the rate of adsorption of the polymer to the latex particles and its overall adsorption strength may have decreased. The effect of the overall molecular weight of the block copolymer and its overall hydrophilicity have a big effect on the latex production (Tab. 10.2). Increase of the overall molecular weight of the block copolymer above 6,200 resulted in a reduction in the rate of conversion, increase in the particle diameter and reduction in the number of latex particles. The worst results were obtained with an overall molecular weight of 7,500 while reducing the PEO wt% in which case particles with 322 nm diameter were obtained and the number of latex particles were significantly reduced.

The importance of the affinity of the anchor chain (PMMA) to the latex particles was investigated by using different monomers [12]. For example, when using styrene as the monomer the resulting latex was unstable and it showed the presence of coagulum. This can be attributed to the lack of chemical compatibility of the anchor

chain (PMMA) and the polymer to be stabilized, namely polystyrene. This clearly indicates that block copolymers of PMMA–PEO are not suitable for emulsion polymerization of styrene. However, when using vinyl acetate monomer, whereby the resulting poly(vinyl acetate) latex should have strong affinity to the PMMA anchor, no latex was produced when the reaction was carried out at 45 °C. It was speculated that the water solubility of the vinyl acetate monomer resulted in the formation of oligomeric chain radicals which could exist in solution without nucleation. Polymerization at 60 °C, which did nucleate particles, was found to be controlled by chain transfer of the vinyl acetate radical with the surfactant, resulting in broad molecular weight distributions

Emulsion polymerization of MMA using triblock copolymers was carried out with PMMA-block–PEO–PMMA using blocks with the same PMMA molecular weight (800 or 900) while varying the PEO molecular weight from 3,400 to 14,000 in order to vary the loop size. Although the rate of polymerization was not affected by the loop size, the particles with the smallest diameter were obtained with the 10,000 molecular weight PEO. Comparison of the results obtained using the triblock copolymer with those obtained using diblock copolymer (while keeping the PMMA block molecular weight the same) showed the same rate of polymerization. However, the average particle diameter was smaller and the total number of particles larger when using the diblock copolymer. This clearly shows the higher efficacy of the diblock copolymer when compared with the triblock copolymer.

Graft copolymers were also used as stabilizers in emulsion polymerization. The first systematic study of the effects of graft copolymers were carried out by Piirma and Lenzotti [13] who synthesized well-characterized graft copolymers with different backbone and side-chain lengths. Several grafts of poly(p-methylstyrene)-graft–polyethylene oxide, (PMSt)–$(PEO)_n$, were synthesized and used in styrene emulsion polymerization. Three different PMSt chain lengths (with molecular weights of 750, 2,000 and 5,000) and three different PEO chain lengths were prepared. In this way, the structure of the amphipathic graft copolymer could be changed in three different ways:

(i) three different PEO graft chain lengths;
(ii) three different backbone chain lengths with the same wt% PEO;
(iii) four different wt% PEO grafts.

Piirma and Lenzotti [13] first investigated the graft copolymer concentration required to produce the highest conversion rate, the smallest particle size and the largest number of latex particles. The monomer-to-water ratio was kept at 0.15 to avoid overcrowding of the resulting particles. They found that a concentration of 18 g/100 g monomer (2.7 % aqueous phase) was necessary to obtain the above results, after which further increase in graft copolymer concentration did not have any significant increase in rate of polymerization or increase in the number of particles used. Using the graft copolymer concentration of 2.7 % aqueous phase, the results showed an increase in the number of particles with increase in conversion reaching a steady value at about

35 % conversion. Obviously, before that conversion, new particles are still being stabilized from the oligomeric precursor particles, after which all precursor particles are assimilated by the existing particles. The small size of the latex produced, namely 30–40 nm, clearly indicates the efficiency with which this graft copolymer stabilizes the dispersion.

Three different backbone chain lengths of M_n 1,140, 4,270 and 24,000 were produced while keeping the same weight percent of PEO (82 %), which is equivalent to 3, 10 and 55 PEO chains per backbone respectively. The results showed that the rate of polymerization, particle diameter and number of particles was similar for the three cases. Since the graft copolymer concentration was the same in each case, it can be concluded that one molecule of the highest molecular graft is just as effective as 18 molecules of the lowest molecular weight graft in stabilizing the particles.

Four graft copolymers were synthesized with a PMSt backbone with M_w = 4,540 while increasing the wt% of PEO: 68, 73, 82 and 92 wt% (corresponding to 4.8, 6, 10 and 36 grafts per chain). The results showed a sharp decrease (by more than one order of magnitude) in the number of particles as the wt% of PEO increased from 82 to 94 %. The reason for this reduction in the number of particles is the increased hydrophilicity of the graft copolymer, which could result in desorption of the molecule from the surface of the particle. In addition, a graft with 36 side chains doest not leave enough space for anchoring by the backbone.

The effect of PEO side chain length on emulsion polymerization using graft copolymers was systematically studied by keeping the backbone molecular weight the same (1,380) while gradually increasing the PEO molecular weight of the side chains from 750 to 5,000. For example, by increasing M_w of PEO from 750 to 2,000 while keeping the wt% of PEO roughly the same (84 and 82 wt% respectively), the number of side chains in the graft decreases from 10 to 3. The results showed a decrease in the rate of polymerization as the number of side chain in the graft increases. This is followed by a sharp reduction in the number of particles produced. This clearly shows the importance of spacing of the side chains to ensure anchoring of the graft copolymer to the particle surface, which is stronger with the graft containing a smaller number of side chains. If the number of side chains for the PEO with M_w of 2,000 is increased from 3 to 9 (93 wt% of PEO) the rate of polymerization and number of particles decrease. Using a PEO chain with M_w of 5,000 (92 wt% PEO) and 3 chains per graft gives the same result as the PEO 2,000 with 3 side chains. Any increase in the number of side chains in the graft results in reduction in the rate of polymerization and the number of latex particles produced. This clearly shows the importance of spacing of the side chains of the graft copolymer.

Similar results were obtained using a graft copolymer of poly(methyl methacrylate-co-2-hydroxypropyl methacrylate)-graft–polyethylene oxide, PMMA(PEO)$_n$, for emulsion polymerization of methyl methacrylate. As with PMSt(PEO)$_n$ graft, the backbone molecular weight had little effect on the rate of polymerization or the

number of particles used. The molecular weight of the PEO side chains was varied at constant M_w of the backbone (10,000). Three PEO grafts with M_w of 750, 2,000 and 5,000 were used. Although the rate of polymerization was similar for the three graft copolymers, yet the number of particles was significantly lower with the graft containing PEO 750. This shows that this short PEO chain is not sufficient for stabilization of the particles. The overall content of PEO in the graft has also a big effect. Using the same backbone chain length while changing the wt% of PEO 200, it was found that the molecule containing 67 wt% PEO is not sufficient for stabilization of the particles when compared with a graft containing 82 wt% PEO. This shows that a high concentration of PEO in the adsorbed layer is required for effective steric stabilization. The chemical nature of the monomer also plays an important role. For example, stable latexes could be produced using PMSt$(PEO)_n$ graft but not with PMMA$(PEO)_n$ graft.

Recently, a novel graft copolymer of hydrophobically modified inulin (INUTEC® SP1) has been used in emulsion polymerization of styrene, methyl methacrylate, butyl acrylate and several other monomers [14]. All latices were prepared by emulsion polymerization using potassium persulphate as initiator. The z-average particle size was determined by photon correlation spectroscopy (PCS) and electron micrographs were also taken.

Emulsion polymerization of styrene or methylmethacrylate showed an optimum weight ratio of (INUTEC)/monomer of 0.0033 for PS and 0.001 for PMMA particles. The (initiator)/(monomer) ratio was kept constant at 0.00125. The monomer conversion was higher than 85 % in all cases. Latex dispersions of PS reaching 50 % and of PMMA reaching 40 % could be obtained using such low concentration of INUTEC® SP1. Fig. 10.1 shows the variation of particle diameter with monomer concentration.

The stability of the latexes was determined by determining the critical coagulation concentration (CCC) using $CaCl_2$. The CCC was low (0.0175–0.05 mol dm^{-3}) but this was higher than that for the latex prepared without surfactant. Post addition of INUTEC® SP1 resulted in a large increase in the CCC, as is illustrated in Fig. 10.2, which shows log W–log C curves (where W is the ratio between the fast flocculation rate constant to the slow flocculation rate constant, referred to as the stability ratio) at various additions of INUTEC® SP1.

As with the emulsions, the high stability of the latex when using INUTEC® SP1 is due to the strong adsorption of the polymeric surfactant on the latex particles and formation of strongly hydrated loops and tails of polyfructose that provide effective steric stabilization. Evidence for the strong repulsion produced when using INUTEC® SP1 was obtained from atomic force microscopy investigations [15] whereby the force between hydrophobic glass spheres and hydrophobic glass plate, both containing an adsorbed layer of INUTEC® SP1, was measured as a function of distance of separation both in water and in the presence of various Na_2SO_4 concentrations. In both cases, a strong repulsion was confirmed when the stabilizing layers started to overlap.

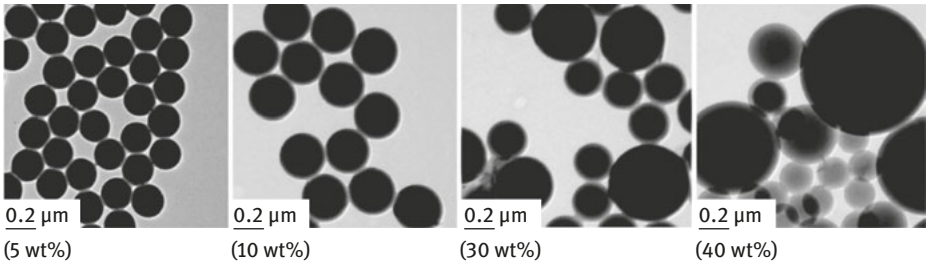

(5 wt%) (10 wt%) (30 wt%) (40 wt%)

(a) PS latexes

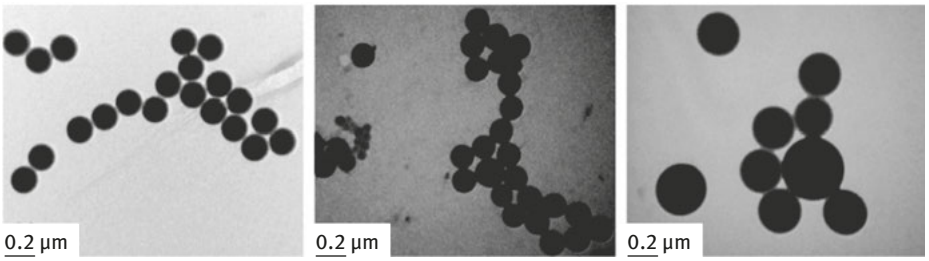

(10 wt%) (20 wt%) (30 wt%)

(b) PMMA latexes

Fig. 10.1: Electron micrographs of the latexes.

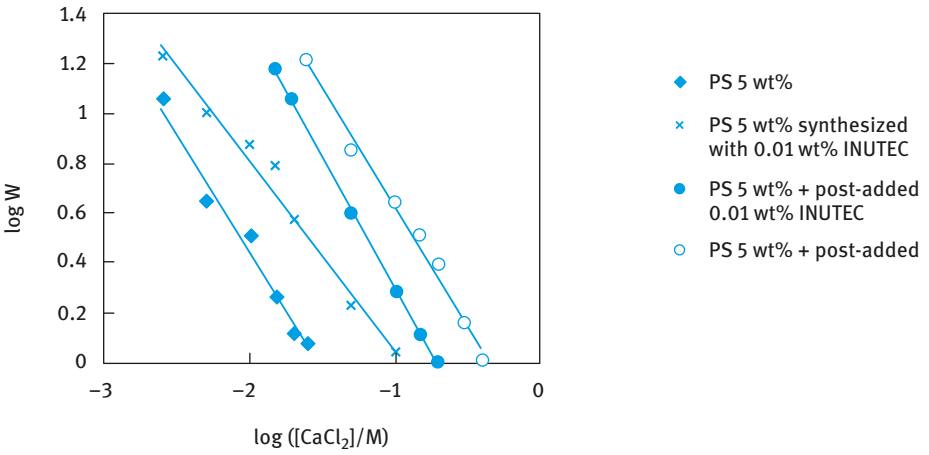

Fig. 10.2: Influence of post addition of INUTEC® SP1 on the latex stability.

10.2 Dispersion polymerization

This method is usually applied for the preparation of nonaqueous latex dispersions and hence it is referred to as NAD. This method has also been adapted to prepare aqueous latex dispersions by using an alcohol–water mixture.

In the NAD process, the monomer, normally an acrylic, is dissolved in a nonaqueous solvent, normally an aliphatic hydrocarbon and an oil-soluble initiator and a stabilizer (to protect the resulting particles from flocculation, sometimes referred to as "protective colloid") is added to the reaction mixture. The most successful stabilizers used in NAD are block and graft copolymers. These block and graft copolymers are assembled in a variety of ways to provide the molecule with an "anchor chain" and a stabilizing chain. The anchor chain should be sufficiently insoluble in the medium and has a strong affinity to the polymer particles produced. In contrast, the stabilizing chain should be soluble in the medium and strongly solvated by its molecules to provide effective steric stabilization. The length of the anchor and stabilizing chains has to be carefully adjusted to ensure strong adsorption (by multipoint attachment of the anchor chain to the particle surface) and a sufficiently "thick" layer of the stabilizing chain to prevent close approach of the particles to a distance where the van der Waals attraction becomes strong. Several configurations of block and graft copolymers are possible, as is illustrated in Fig. 10.3. Typical preformed graft stabilizers based on poly (12-hydroxy stearic acid) (PHS) are simple to prepare and effective in NAD polymerization. Commercial 12-hydroxystearic acid contains 8–15 % palmitic and stearic acids, which limits the molecular weight during polymerization to an average of 1,500–2,000. This oligomer may be converted to a "macromonomer" by reacting the carboxylic group with glycidyl methacrylate. The macromonomer is then copoly-

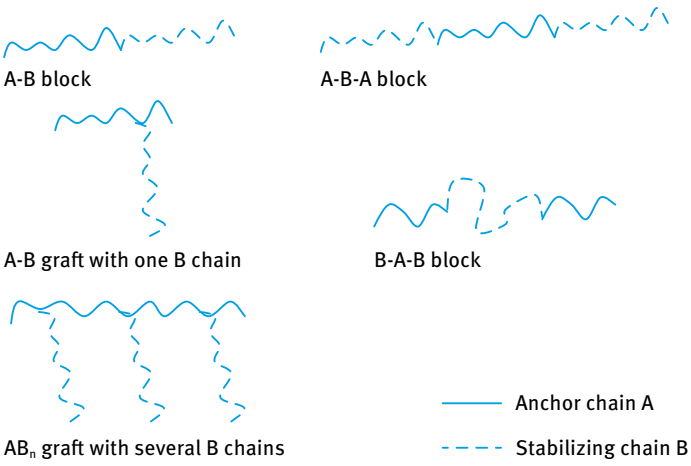

Fig. 10.3: Configurations of block and graft copolymers

merized with an equal weight of methyl methacrylate (MMA) or similar monomer to give a "comb" graft copolymer with an average molecular weight of 10,000–20,000. The graft copolymer contains on average 5–10 PHS chains pendent from a polymeric anchor backbone of PMMA. Thus a graft copolymer can stabilize latex particles of various monomers. The major limitation of the monomer composition is that the polymer produced should be insoluble in the medium used.

Several other examples of block and graft copolymers that are used in dispersion polymerization are given in Tab. 10.3, which also shows the continuous phase and disperse polymer that can be used with these polymers.

Tab. 10.3: Block and graft copolymers used in dispersion polymerization.

Polymeric surfactant	Continuous phase	Disperse polymer
Polystyrene-block–poly(dimethyl siloxane)	Hexane	Polystyrene
Polystyrene-block–poly(methacrylic acid)	Ethanol	Polystyrene
Polybutadiene-graft–poly(methacrylic acid)	Ethanol	Polystyrene
Poly(2-ethylhexyl acrylate)-graft–poly(vinyl acetate)	Aliphatic hydrocarbon	Poly(methyl methacrylate)
Polystyrene-block–poly(t-butylstyrene)	Aliphatic hydrocarbon	Polystyrene

Two main criteria must be considered in the process of dispersion polymerization:
(i) the insolubility of the formed polymer in the continuous phase;
(ii) the solubility of the monomer and initiator in the continuous phase.

Initially, dispersion polymerization starts as a homogeneous system but after sufficient polymerization, the insolubility of the resulting polymer in the medium forces them to precipitate. Initially polymer nuclei are produced which then grow to polymer particles. The latter are stabilized against aggregation by the block or graft copolymer that is added to the continuous phase before the process of polymerization starts. It is essential to choose the right block or graft copolymer which should have a strong anchor chain A and good stabilizing chain B as schematically represented in Fig. 10.3.

Dispersion polymerization may be considered a heterogeneous process which may include emulsion, suspension, precipitation and dispersion polymerization. In dispersion and precipitation polymerization, the initiator must be soluble in the continuous phase, whereas in emulsion and suspension polymerization the initiator is chosen to be soluble in the disperse phase of the monomer. A comparison of the rate of polymerization of methylmethacrylate at 80 °C for the three systems was given by

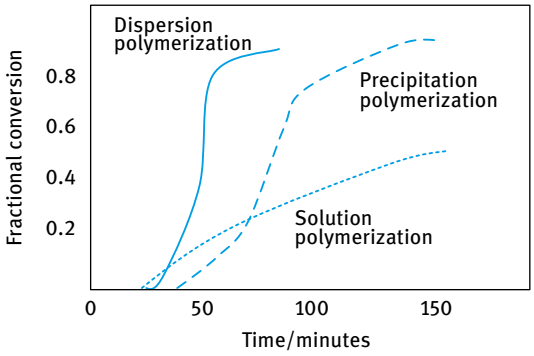

Fig. 10.4: Comparison of rates of polymerization.

Barrett and Thomas [16], as is illustrated in Fig. 10.4 The rate of dispersion polymerization is much faster than precipitation or solution polymerization. The enhancement of the rate in precipitation polymerization over solution polymerization has been attributed to the hindered termination of the growing polymer radicals.

Several mechanisms have been proposed to explain the mechanism of emulsion polymerization; however, no single mechanism can explain all happenings in emulsion polymerization. Barrett and Thomas [16] suggested that particles are formed in emulsion polymerization by two main steps:

(i) Initiation of monomer in the continuous phase and subsequent growth of the polymer chains until the latter become insoluble. This process clearly depends on the nature of the polymer and medium.
(ii) The growing oligomeric chains associate with each other, forming aggregates which below a certain size are unstable as they become stabilized by the block or graft copolymer added.

As mentioned before, this aggregative nucleation theory cannot explain all happenings in dispersion polymerization. An alternative mechanism based on Napper's theory [17] for aqueous emulsion polymerization can be adapted to the process of dispersion polymerization. This theory includes coagulation of the nuclei formed and not just association of the oligomeric species. Unstable precursor particles (nuclei) can undergo one of the following processes to become colloidally stable:

(i) homocoagulation, i.e. collision with other precursor particles;
(ii) growth by propagation, adsorption of stabilizer;
(iii) swelling with monomer.

The nucleation terminating events are diffusional capture of oligomers and heterocoagulation.

The number of particles formed in the final latex does not depend on particle nucleation alone, since other steps are involved which determine how many precursor particles created are involved in the formation of a colloidally stable particle. This

clearly depends on the effectiveness of the block or graft copolymer used in stabilizing the particles (see below).

In most cases, increase in polymeric surfactant concentration (at any given monomer amount) results in the production of a larger number of particles with smaller size. This is to be expected since the larger number of particles with smaller size (i.e. larger total surface area of the disperse particles) requires more polymeric surfactant for their formation. The molecular weight of the polymeric surfactant can also influence the number of particles formed. For example, Dawkins and Taylor [18] found that in dispersion polymerization of styrene in hexane, increasing the molecular weight of the block copolymer of polydimethyl siloxane-block–polystyrene resulted in the formation of smaller particles, which was attributed to the more effective steric stabilization by the higher molecular weight block.

A systematic study of the effect of monomer solubility and concentration in the continuous phase was carried out by Antl et al. [19]. Dispersion polymerization of methyl methacrylate in hexane mixed with a high boiling point aliphatic hydrocarbon was investigated using poly(12-hydoxystyearic acid)-glycidyl methacrylate block copolymer. They found that the methyl methacrylate concentration had a drastic effect on the size of the particles produced. When the monomer concentration was kept below 8.5 %, very small particles (80 nm) were produced and these remained very stable. However, between 8.5 and 35 % monomer the latex produced was initially stable but flocculated during polymerization. An increase in monomer concentration from 35 to 50 % results in the formation of a stable latex but the particle size increased sharply from 180 nm to 2.6 μm as the monomer concentration increased. The authors suggested that the final particle size and stability of the latex is strongly affected by increased monomer concentration in the continuous phase. The presence of monomer in the continuous phase increases the solvency of the medium for the polymer formed. In a good solvent for the polymer, the growing chain is capable of reaching higher molecular weight before it is forced to phase separate and precipitate.

NAD polymerization is carried out in two steps:

(i) Seed stage: the dilutent, a portion of the monomer, a portion of dispersant and initiator (azo or peroxy type) are heated to form an initial low-concentration fine dispersion.
(ii) Growth stage: the remaining monomer together with more dispersant and initiator are then fed over the course of several hours to complete the growth of the particles.

A small amount of transfer agent is usually added to control the molecular weight. Excellent control of particle size is achieved by proper choice of the designed dispersant and correct distribution of dispersant between the seed and growth stages. NAD acrylic polymers are applied in automotive thermosetting polymers and hydroxy monomers may be included in the monomer blend used.

Two main factors must be considered when considering the long-term stability of a nonaqueous polymer dispersion. The first and very important factor is the nature of the "anchor chain" A. As mentioned above, this should have a strong affinity to the produced latex and in most cases it can be designed to be "chemically" attached to the polymer surface. Once this criterion is satisfied, the second important factor in determining the stability is the solvency of the medium for the stabilizing chain B. As will be discussed in detail, the solvency of the medium is characterized by the Flory–Huggins interaction parameter χ. Three main conditions can be identified:

- $\chi < 0.5$ (good solvent for the stabilizing chain);
- $\chi > 0.5$ (poor solvent for the stabilizing chain);
- $\chi = 0.5$ (referred to as the θ-solvent).

Clearly, to maintain stability of the latex dispersion, the solvent must be better than a θ-solvent. The solvency of the medium for the B chain is affected by the addition of a nonsolvent and/or temperature changes. It is, therefore, essential to determine the critical volume fraction (CFV) of a nonsolvent above which flocculation (sometimes referred to as incipient flocculation) occurs. One should also determine the critical flocculation temperature at any given solvent composition below which flocculation occurs. The correlation between CFV or CFT and the flocculation of the nonaqueous polymer dispersion has been demonstrated by Napper [17], who investigated the flocculation of poly(methyl methacrylate) dispersions stabilized by poly(12-hydroxy stearic acid) or poly(n-lauryl methacrylate-co-glycidyl methacrylate) in hexane by adding a nonsolvent such as ethanol or propanol and cooling the dispersion. The dispersions remained stable until the addition of ethanol transformed the medium to a θ-solvent for the stabilizing chains in solution. However, flocculation did occur under conditions of slightly better than θ-solvent for the chains. The same was found for the CFT, which was 5–15 K above the θ-temperature. This difference was accounted for by the polydispersity of the polymer chains. The θ-condition is usually determined by cloud point measurements and the least soluble component will precipitate, first giving values that are lower than the CFV or higher than the CFT.

The process of dispersion polymerization has been applied in many cases by using completely polar solvents such as alcohol or alcohol–water mixtures [20, 21]. The results obtained showed completely different behaviour when compared with dispersion polymerization in nonpolar media. For example, results obtained by Lok and Ober [21] using styrene as monomer and hydroxypropyl cellulose as stabilizer showed a linear increase of particle diameter with increase in the weight percent of the monomer. There was no region in monomer concentration where instability occurred (as has been observed for the dispersion polymerization of methyl methacrylate in aliphatic hydrocarbons). Replacing water in the continuous phase with 2-methoxyethanol, Lok and Ober were able to grow large, monodisperse particles up to 15 μm in diameter. They concluded from these results that the polarity of the medium is the controlling factor in the formation of particles and their final size. The authors suggested

a mechanism in which the polymeric surfactant molecule grafts to the polystyrene chain, forming a physically anchored stabilizer (nuclei). These nuclei grow to form the polymer particles. Paine [22] carried out dispersion polymerization of styrene by systematically increasing the alcohol chain length from methanol to octadecanol and using hydroxypropyl cellulose as stabilizer. The results showed an increase in particle diameter with increase in number of carbon atoms in the alcohol, reaching a maximum when hexanol was used as the medium, after which there was a sharp decrease in the particle diameter with further increase in the number of carbon atoms in the alcohol. Paine explained his results in terms of the solubility parameter of the dispersion medium. The largest particles are produced when the solubility parameter of the medium is closest to those of styrene and hydroxpropyl cellulose.

11 Formulation of pigment dispersions for paint application

As mentioned in Chapter 9, a paint may be considered a colloidal dispersion of a pigment (the disperse phase) in a medium that may be aqueous or nonaqueous that contains a polymer (film former) and/or latex particles. The state of dispersion of a pigment in a paint is vital as it determines its optical properties (e.g. colour), flow properties (rheology), durability, opacity, gloss and storage stability. This chapter will deal with dispersion of a powder in a liquid.

11.1 Wetting of the bulk powder

Dispersion methods are used for the preparation of suspension of preformed particles. The term dispersion is used to refer to the complete process of incorporating the solid into a liquid such that the final product consists of fine particles distributed throughout the dispersion medium [23]. This is illustrated in Fig. 11.1.

It is essential in the dispersion process to wet both external and internal surfaces and displace the air entrapped between the particles. Wetting is achieved by the use of surface-active agents (wetting agents) of the ionic or nonionic type, which are capable of diffusing quickly (i.e. lower the dynamic surface tension) to the solid/liquid interface and displace the air entrapped by rapid penetration through the channels between the particles and inside any "capillaries". For wetting of hydrophobic powders into water, anionic surfactants, e.g. alkyl sulphates or sulphonates or nonionic surfactants of the alcohol or alkyl phenol ethoxylates are usually used.

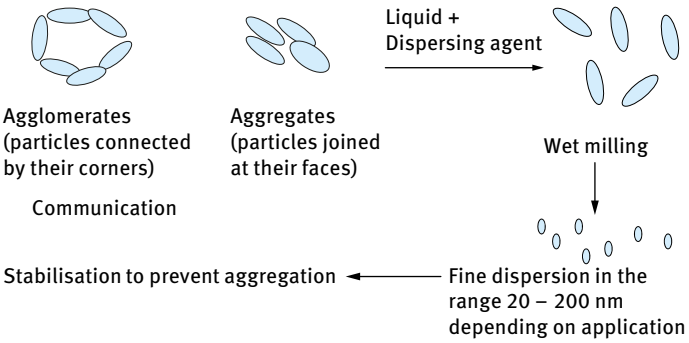

Fig. 11.1: Schematic representation of the dispersion process.

https://doi.org/10.1515/9783110588002-013

The process of the wetting of a solid by a liquid involves three types of wetting [23]:
- adhesion wetting W_a;
- immersion wetting W_i;
- spreading wetting W_s.

The work of dispersion W_d is the sum of W_a, W_i and W_s

$$W_d = W_a + W_i + W_s = 6\gamma_{SV} - \gamma_{SL} = -6\gamma_{LV}\cos\theta, \tag{11.1}$$

where γ_{SV} is the solid/vapour surface tension and γ_{SL} is the solid/liquid surface tension. Using Young's equation,

$$\gamma_{SV} = \gamma_{SL} + \gamma_{LV}\cos\theta, \tag{11.2}$$

where θ is the contact angle of a liquid drop on the substrate.

$$W_d = -\gamma_{LV}\cos\theta. \tag{11.3}$$

Equation (11.3) shows that when $\theta < 90°$, $\cos\theta$ is positive and the work of dispersion is negative, i.e. wetting is spontaneous.

The breaking of the aggregates and agglomerates is achieved by the use of high-speed stirrers (Ultra-Turrax or Silverson) and comminution (milling) of the resulting particles into smaller units is achieved by ball or bead milling.

Dispersion wetting W_d is given by the product of the external area of the powder, A, and the difference between γ_{SL} and γ_{SV} :

$$W_d = A(\gamma_{SL} - \gamma_{SV}) \tag{11.4}$$

Using Young's equation:

$$W_d = -A\gamma_{LV}\cos\theta \tag{11.5}$$

Thus, wetting of the external surface of the powder depends on the liquid surface tension and contact angle. As mentioned above, if $\theta < 90°$, $\cos\theta$ is positive and the work of dispersion is negative, wetting is spontaneous. The most important parameter that determines wetting of the powder is the dynamic surface tension, $\gamma_{dynamic}$ (i.e. the value at short times). As will be discussed later, $\gamma_{dynamic}$ depends both on the diffusion coefficient of the surfactant molecule as well as its concentration. Since wetting agents are added in sufficient amounts ($\gamma_{dynamic}$ is lowered sufficiently) spontaneous wetting is the rule rather than the exception.

Wetting of the internal surface requires penetration of the liquid into channels between and inside the agglomerates. The process is similar to forcing a liquid through fine capillaries. To force a liquid through a capillary with radius r, a pressure p is required that is given by,

$$p = -\frac{2\gamma_{LV}\cos\theta}{r} = \left[\frac{-2(\gamma_{SV} - \gamma_{SL})}{r\gamma_{LV}}\right]. \tag{11.6}$$

γ_{SL} has to be made as small as possible; rapid surfactant adsorption to the solid surface, i.e. low θ. When $\theta = 0$, $p \propto \gamma_{LV}$. Thus, for penetration into pores one requires a high γ_{LV}. Thus, wetting of the external surface requires a low contact angle θ and low surface tension γ_{LV}. Wetting of the internal surface (i.e. penetration through pores) requires a low θ but high γ_{LV}. These two conditions are incompatible and a compromise has to be made: $\gamma_{SV} - \gamma_{SL}$ must be kept at a maximum. γ_{LV} should be kept as low as possible but not too low.

The above conclusions illustrate the problem of choosing the best wetting agent for a particular powder. This requires measurement of the above parameters as well as testing the efficiency of the dispersion process.

For horizontal capillaries (gravity neglected), the depth of penetration l in time t is given by the Rideal–Washburn equation [24, 25],

$$l^2 = \left[\frac{r\gamma_{LV}\cos\theta}{2\eta}\right]t. \tag{11.7}$$

To enhance the rate of penetration, γ_{LV} has to be made as high as possible, θ as low as possible and η as low as possible.

For dispersion of powders into liquids, one should use surfactants that lower θ while not reducing γ_{LV} too much. The viscosity of the liquid should also be kept at a minimum. Thickening agents (such as polymers) should not be added during the dispersion process. It is also necessary to avoid foam formation during the dispersion process.

For a packed bed of particles, r may be replaced by r/k^2, where the effective radius of the bed and a k is the turtuosity factor, which takes into account the complex path formed by the channels between the particles, i.e.,

$$l^2 = \left(\frac{r\gamma_{LV}\cos\theta}{2\eta k^2}\right)t. \tag{11.8}$$

Thus, a plot of l^2 versus t gives a straight line and from the slope of the line one can obtain θ. The Rideal–Washburn equation can be applied to obtain the contact angle of liquids (and surfactant solutions) in powder beds. k should first be obtained using a liquid that produces zero contact angle.

The most effective wetting agent is the one that gives a zero-contact angle at the lowest concentration. For $\theta = 0$ or $\cos\theta = 1$, γ_{SL} and γ_{LV} have to be as low as possible. This requires quick reduction of γ_{SL} and γ_{LV} under dynamic conditions during powder dispersion (This reduction should normally be achieved in less than 20 s). This requires fast adsorption of the surfactant molecules both at the L/V and S/L interfaces. It should be mentioned that reduction of γ_{LV} is not always accompanied by simultaneous reduction of γ_{SL} and hence it is necessary to have information on both interfacial tensions, which means that measurement of the contact angle is essential in selection of wetting agents. The most commonly used wetting agents for hydrophobic solids are anionic or nonionic surfactants To achieve rapid adsorption, the wetting agent should

be either a branched chain with central hydrophilic group or a short hydrophobic chain with hydrophilic end group, e.g. Aerosol OT (diethylhexyl sulphosuccinate):

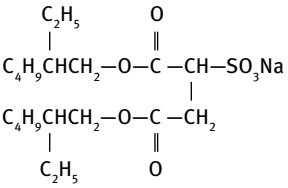

The above molecule has a low critical micelle concentration (cmc) of 0.7 g dm^{-3} and at above the cmc the water surface tension is reduced to ≈ 25 mN m^{-1} in less than 15 s.

An alternative anionic wetting agent is sodium dodecylbenzene sulphonate with a branched alkyl chain:

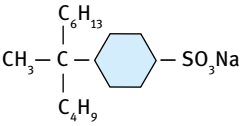

The above molecule has a higher cmc (1 g dm^{-3}) than Aerosol OT. It is also not as effective in lowering the surface tension of water, reaching a value of 30 mN m^{-1} at and above the cmc. It is, therefore, not as effective as Aerosol OT for powder wetting.

Several nonionic surfactants such as the alcohol ethoxylates can also be used as wetting agents. These molecules consist of a short hydrophobic chain (mostly C_{10}) which is also branched. A medium chain polyethylene oxide (PEO) mostly consisting of 6 EO units or lower is used. The above molecules also reduce the dynamic surface tension within a short time (< 20 s) and they have reasonably low cmc. One should always use the minimum amount of wetting agent to avoid interference with the dispersants that need to be added to maintain the colloid stability during dispersion and on storage.

Most processes of powder wetting work under dynamic conditions and improvement of their efficiency requires the use of surfactants that lower the liquid surface tension γ_{LV} under these dynamic conditions. The interfaces involved (particles separated from aggregates or agglomerates) are freshly formed and have only a small effective age of some seconds or even less than a millisecond.

The most frequently used parameter to characterize the dynamic properties of liquid adsorption layers is the dynamic surface tension (which is a time-dependent quantity). Techniques should be available to measure γ_{LV} as a function of time (ranging from a fraction of a millisecond to minutes and hours or days). It is, therefore, necessary to describe the dynamics of surfactant adsorption at a fundamental level.

The two most suitable techniques for studying adsorption kinetics are the drop volume method and the maximum bubble pressure method [23]. The first method can obtain information on adsorption kinetics during a time period ranging from a few seconds to some minutes. However, it has the advantage of measurement both at the air/liquid and liquid/liquid interfaces. The maximum bubble pressure method allows one to obtain measurements in the millisecond range, but it is restricted to the air/liquid interface. The drop volume technique is limited in its application. Under conditions of fast drop formation and larger tip radii, the drop formation shows irregular behaviour.

The maximum bubble pressure technique [23] is the most useful for measuring adsorption kinetics over short time periods, particularly if correction for the so-called "dead time", τ_d, is made. The dead time is simply the time required to detach the bubble after it has reached its hemispherical shape. A schematic representation of the principle of maximum bubble pressure is shown in Fig. 11.2, which shows the evolution of a bubble at the tip of a capillary. The figure also shows the variation of pressure p in the bubble with time.

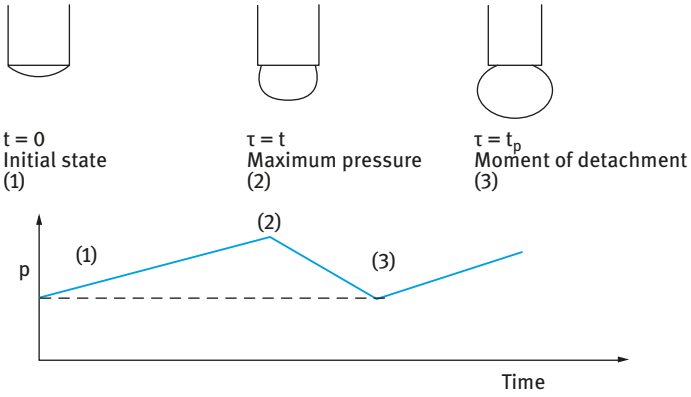

Fig. 11.2: Scheme of bubble evolution and pressure change with time.

At $t = 0$ (initial state), the pressure is low (note that the pressure is equal to $2\gamma/r$; since r of the bubble is large, p is small). At $t = \tau$ (smallest bubble radius that is equal to the tube radius), p reaches a maximum. At $t = \tau_b$ (detachment time), p decreases since the bubble radius increases. The design of a maximum bubble pressure method for high bubble formation frequencies (short surface age) requires the following:

(i) measurement of bubble pressure;
(ii) measurement of bubble formation frequency;
(iii) estimation of surface lifetime and effective surface age.

The first problem can be easily solved if the system volume (which is connected to the bubble) is large enough in comparison with the bubble separating from the capillary. In this case, the system pressure is equal to the maximum bubble pressure. The use of an electric pressure transducer for measuring bubble formation frequency presumes that pressure oscillations in the measuring system are distinct enough and this satisfies (ii). Estimation of the surface lifetime and effective surface age, i.e. (iii), requires estimation of the dead time τ_d. A schematic representation of the set-up for measuring the maximum bubble pressure and surface age is shown in Fig. 11.3.

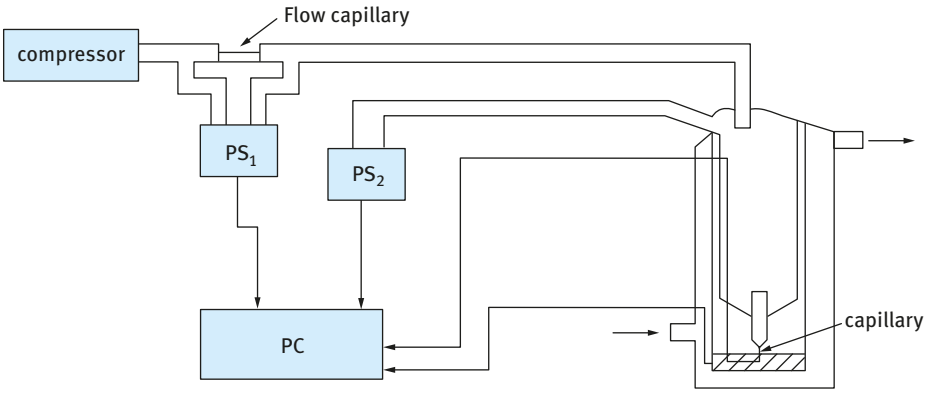

Fig. 11.3: Maximum bubble pressure apparatus.

The air coming from a micro-compressor first flows through the flow capillary. The air flow rate is determined by measuring the pressure difference at both ends of the flow capillary with the electric transducer PS1. Thereafter, the air enters the measuring cell and the excess air pressure in the system is measured by a second electric sensor PS2. A sensitive microphone is placed in the tube which leads the air to the measuring cell.

The measuring cell is equipped with a water jacket for temperature control, which simultaneously holds the measuring capillary and two platinum electrodes, one of which is immersed in the liquid under study and the second of which is situated exactly opposite to the capillary and controls the size of the bubble. The electric signals from the gas-flow sensor PS1 and pressure transducer PS2, the microphone and the electrodes, as well as the compressor are connected to a personal computer which operates the apparatus and acquires the data.

The value of τ_d, equivalent to the time interval necessary to form a bubble of radius R, can be calculated using Poiseuille's law,

$$\tau_d = \frac{\tau_b L}{Kp}\left(1 + \frac{3r_{ca}}{2R}\right). \tag{11.9}$$

K is given by Poiseuille's law,

$$K = \frac{\pi r^4}{8\eta l}, \tag{11.10}$$

where η is the gas viscosity, l is the length, L is the gas flow rate and r_{ca} is the radius of the capillary.

The calculation of dead time τ_d can be simplified when taking into account the existence of two gas flow regimes for the gas flow leaving the capillary: bubble flow regime when $\tau > 0$ and jet regime when $\tau = 0$ and hence $\tau_b = \tau_d$. A typical dependence of p on L is shown in Fig. 11.4. On the right-hand side of the critical point, the dependence of p on L is linear in accordance with Poiseuille law. Under these conditions,

$$\tau_d = \tau_b \frac{L p_c}{L_c p}, \tag{11.11}$$

where L_c and p_c are related to the critical point, and L and p are the actual values of the dependence left from the critical point.

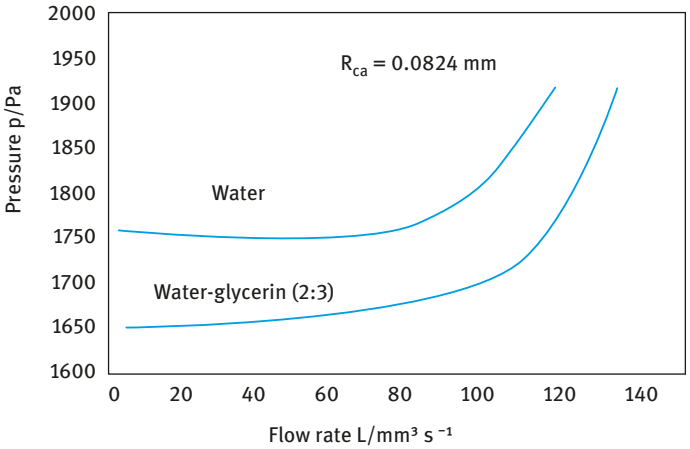

Fig. 11.4: Dependence of p on gas flow rate L at 30 °C.

The surface life-time can be calculated from,

$$\tau = \tau_b - \tau_d = \tau_b \left(1 - \frac{L p_c}{L_c p}\right). \tag{11.12}$$

The critical point in the dependence of p and L can be easily located and is included in the software of the computer connected to the apparatus.

The surface tension value in the maximum bubble pressure method is calculated using the Laplace equation,

$$p = \frac{2\gamma}{r} + \rho h g + \Delta p, \tag{11.13}$$

where ρ is the density of the liquid, g is the acceleration due to gravity, h is the depth the capillary is immersed in the liquid and Δp is a correction factor to allow for hydrodynamic effects.

11.2 Breaking of aggregates and agglomerates (deagglomeration)

As mentioned above, all pigments are supplied as powders consisting of aggregates (where the particles are connected by their surfaces) or agglomerates (where the particles are connected by their corners). For example, pigmentary titanium dioxide mostly exists in powder form as loose agglomerates of several tens of μm in diameter. These pigments are surface coated by the manufacturer for two main reasons. First, the surface coating reduces the cohesive forces of the powder, thus assisting the deagglomeration process. Second, the coating (SiO_2 and Al_2O_3) decativates the surface of the rutile pigment (by reducing the photochemical activity), which otherwise accelerates the degradation of the resin on weathering.

The "grinding stage" in mill base manufacture is not a comminution stage but a dispersion process of the pigment agglomerates, whereby the latter are separated into "single" primary particles. However, some of the primary particles may consist of sinters of TiO_2 crystals produced during the surface coating stage. To separate the particles in an aggregate or agglomerate, one requires the use of a wetting/dispersing system. As mentioned above, the wetting agent, which is usually a short chain surfactant molecule, can seldom prevent the reaggregation of the primary particles after the dispersion process. Thus, to prevent the reaggregation of particles, a dispersing agent is required. The dispersing agent may replace the wetting agent at the S/L interface or become co-adsorbed with the wetting agent. The dispersant produces an effective repulsive barrier upon close approach of the particles. This repulsive barrier is particularly important for concentrated pigment dispersions (that may contain more than 50 % by volume of solids).

The main criteria for an effective dispersant are [23]:

(i) Strong adsorption or "anchoring" to the particle surface.

(ii) High repulsive barrier. The stabilizing chain A of the dispersant must provide an effective repulsive barrier to prevent flocculation by van der Waals attraction. Three main mechanisms of stabilization can be considered: Electrostatic, as for example produced by ionic surfactants Steric, as produced by nonionic polymeric surfactants of the A–B, B–A–B, A–B–A or AB_n graft copolymers (where A is the "anchor" chain and B is the "stabilizing" chain). Electrosteric, as produced by polyelectrolytes.

(iii) Strong solvation of the stabilizing B chain, i.e. it should be in a good solvent condition, i.e. very soluble in the medium and strongly solvated by its molecules. Solvation of the chain by the medium is determined by the chain/solvent (Flory–

Huggins) interaction parameter χ. In good solvent conditions, $\chi < 0.5$ and hence the mixing or osmotic interaction is positive (repulsive). χ should be maintained at < 0.5 under all conditions, e.g. low and high temperature, in the presence of electrolytes and other components of the formulation such as addition of anti-freeze (mostly propylene glycol).

(iv) Reasonably thick adsorbed layer. The adsorbed layer thickness of the B chains, usually described by a hydrodynamic value δ_h (i.e. the thickness δ plus any contribution from the solvation shell), should be sufficiently large to prevent the formation of a deep minimum which may result in flocculation (although reversible) and increase the viscosity of the suspension. A value of $\delta_h > 5$ nm is usually sufficient to prevent the formation of a deep minimum.

As mentioned above, the polymeric surfactants that are most effective as dispersants are those of the A–B, B–A–B block and AB_n or BA_n graft types. A the "anchor chain" is chosen to be highly insoluble in the medium and has a strong affinity to the surface. Examples of A chains for hydrophobic solids are polystyrene (PS), polymethylmethacrylate (PMMA), poly(propylene oxide) (PPO) or alkyl chains provided these have several attachments to the surface. The B stabilizing chain has to be soluble in the medium and strongly solvated by its molecules. The B chain/solvent interaction should be strong, giving a Flory–Huggins parameter $\chi < 0.5$ under all conditions. Examples of B chains are polyethylene oxide (PEO), polyvinyl alcohol (PVA) and polysaccharides (e.g. polyfructose). Several examples of commercially available B–A–B block copolymers are available**:** B–A–B Block copolymers of PEO and PPO: Pluronics. Several molecules of PEO–PPO–PEO are available with various proportions of PEO and PPO. The commercial name is followed by a letter L (liquid), P (paste) and F (flake). This is followed by two numbers that represent the composition. The first digit represents the PPO molar mass and the second digit represents the % PEO. Pluronic F68 (PPO molecular mass 1,508–1,800 + 80 % or 140 mol EO). Pluronic L62 (PPO molecular mass 1,508–1,800 + 20 % or 15 mol EO). In many cases, two Pluronics with high and low EO content are used together to enhance the dispersing power.

Graft copolymers of the AB_n type are also available, for example AB_n graft copolymer based on polymethylmethacrylate (PMMA) back bone (with some polymethacrylic acid) on which several PEO chains (with average molecular weight of 750) are grafted:

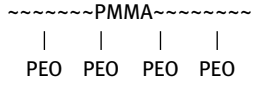

It is a very effective dispersant particularly for high solids content suspensions. The graft copolymer is strongly adsorbed on hydrophobic surfaces with several attachment points by the small PMMA loops of the backbone and a strong steric barrier is obtained by the highly hydrated PEO chains in aqueous solutions.

A novel BA_n graft has been recently synthesized, namely INUTEC® SP1, consisting of Inulin, a linear polyfructose chain B (with degree of polymerization > 23), on which several alkyl chains have been grafted:

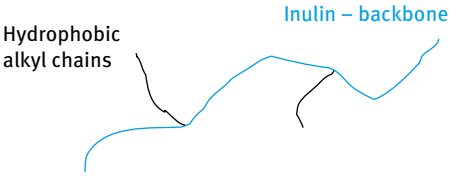

The polymeric surfactant adsorbs with multi-point attachment with several alkyl chains.

Another commercially available "blocky" copolymer is partially hydrolyzed polyvinyl acetate, commercially referred to as polyvinyl alcohol (PVA). The molecule contains short blocks of polyvinyl acetate (PVAc) which form the anchor chains to the hydrophobic surface leaving several loops and tails of PVA chains which are strongly hydrated to give an effective steric barrier:

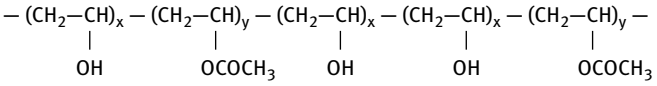

Several commercial PVA grades are available with molecular weights in the range 20,000–100,000 and acetate content in the range 4–12 %. The molecule is designated by two numbers representing the degree of hydrolysis and viscosity of 4 % solution (which gives a rough estimate of molecular weight. For example, Moviol 88/10 refers to a degree of hydrolysis of 88 % (12 % acetate groups) and a viscosity of 10 mPa s of 4 % solution.

Several methods can be applied to assess and select dispersants [23]:

(i) Adsorption isotherms. These are by far the most quantitative methods for aseessment of the dispersing power. Known amounts of solids (m grams) with a surface area A ($m^2\,g^{-1}$) are equilibrated at constant temperature with dispersant solutions with various concentrations C_1. The bottles containing the various dispersions are rotated for several hours till equilibrium is reached. The particles are removed from the dispersant solution by centrifugation and/or filtration through millipore filters. The dispersant concentration in the supernatant liquid C_2 is analytically determined by a suitable technique that can measure low concentrations.

The amount of adsorption Γ (mg m^{-2} or mol m^{-2}) is calculated:

$$\Gamma = \frac{(C_1 - C_2)}{mA}. \tag{11.14}$$

A plot of Γ versus C_2 gives the adsorption isotherm. Two types of isotherms can be distinguished: a Langmuir type for reversible adsorption of surfactants and a high affinity isotherm for irreversible adsorption of polymeric surfactants. In both cases, a plateau adsorption value Γ_∞ is reached at a given value of C_2. In general, the value of Γ_∞ is reached at lower C_2 for polymeric surfactant adsorption when compared with small molecules. The high affinity isotherm obtained with polymeric surfactants implies that the first added molecules are virtually completely adsorbed and this process is irreversible. The irreversibility of adsorption is checked by carrying out a desorption experiment. The suspension at the plateau value is centrifuged and the supernatant liquid is replaced by water. After redispersion, the suspension is centrifuged again and the concentration of the polymeric surfactant in the supernatant liquid is analytically determined. For lack of desorption, the above concentration will be very small indicating that the polymer remains on the particle surface.

(ii) Measurement of dispersion and particle size distribution. An effective dispersant should result in complete dispersion of the powder into single particles. In addition, upon wet milling (comminution), smaller particle distribution should be obtained. The efficiency of dispersion and reduction of particle size can be understood from the behaviour of the dispersant. Strong adsorption and an effective repulsive barrier prevent any aggregation during the dispersion process. It is necessary in this case to include the wetter (which should be kept at the optimum concentration). Adsorption of the dispersant at the solid/liquid interface results in lowering of γ_{SL} and this reduces the energy required for breaking the particles into smaller units. In addition, by adsorption in crystal defects, crack propagation occurs (the Rehbinder effect) and this results in the production of smaller particles. Several methods may be applied for measurement of the particle size distribution, e.g. optical microscopy, which is by far the most valuable tool for a qualitative or quantitative examination of the dispersion. Information on the size, shape, morphology and aggregation of particles can be conveniently obtained with minimum time required for sample preparation. However, optical microscopy has some limitations, e.g. the minimum size that can be detected. The practical lower limit for accurate measurement of particle size is 1.0 μm, although some detection may be obtained down to 0.3 μm. Image contrast may not be good enough for observation particularly when using a video camera which is mostly used for convenience. The contrast can be improved by decreasing the aperture of the iris diaphragm but this reduces the resolution. Three main attachments to the optical microscope are possible, namely phase contrast, differential interference contrast (DIC) and polarized light microscopy. The optical microscope can be used to observe dispersed particles and flocs. Particle sizing can be carried out using manual, semi-automatic or automatic image analysis techniques.

Electron microscopy utilizes an electron beam to illuminate the sample. The electrons behave as charged particles which can be focused by annular electrostatic or electromagnetic fields surrounding the electron beam. Due to the very short wavelength of electrons, the resolving power of an electron microscope exceeds that of an

optical microscope by ≈ 200 times. Two main types of electron microscopes are used, namely transmission (TEM) and scanning (SEM).

Confocal laser scanning microscopy (CLSM) is a very useful technique for identification of dispersions. It uses a variable pinhole aperture or variable width slit to illuminate only the focal plane by the apex of a cone of laser light. Out-of-focus items are dark and do not distract from the contrast of the image. As a result of extreme depth discrimination (optical sectioning), the resolution is considerably improved (up to 40 % when compared with optical microscopy). The CLSM technique acquires images by laser scanning or uses computer software to subtract out-of-focus details from the in-focus image. Images are stored as the sample is advanced through the focal plane and this allows one to construct three-dimensional images.

Scattering techniques are by far the most useful methods for characterizing dispersions and in principle they can give quantitative information on the particle size distribution, floc size and shape. The only limitation of the methods is the need to use sufficiently dilute samples to avoid interference such as multiple scattering, which makes interpretation of the results difficult. However, recently back scattering methods have been designed to allow one to measure the sample without dilution. In principle, one can use any electromagnetic radiation such as light, X-ray or neutrons but in most industrial labs only light scattering is applied (using lasers).

Scattering techniques can be conveniently divided into the following classes:

(i) time-average light scattering, static or elastic scattering;
(ii) turbidity measurements, which can be carried out using a simple spectrophotometer;
(iii) light diffraction technique;
(iv) dynamic (quasi-elastic) light scattering, usually referred to as photon correlation spectroscopy (PCS) – this is a rapid technique that is very suitable for measuring submicron particles or droplets (nano-size range);
(v) back scattering techniques that are suitable for measuring concentrated samples.

The light diffraction technique is a rapid and nonintrusive technique for determining particle size distribution in the range of 2–300 μm with good accuracy for most practical purposes. By combining light diffraction with forward light scattering, it is possible to increase the particle size range to the submicron region. In this way, one can measure the particle size distribution in the range of 0.1 to 300 μm. Light diffraction gives an average diameter over all particle orientations as randomly oriented particles pass the light beam. A collimated and vertically polarized laser beam illuminates a particle dispersion and generates a diffraction pattern with the undiffracted beam in the centre. The energy distribution of diffracted light is measured by a detector consisting of light sensitive circles separated by isolating circles of equal width. The angle formed by the diffracted light increases with decreasing particle size. The angle-dependent intensity distribution is converted by Fourier optics into a spatial intensity distribution. The spatial intensity distribution is converted into a set of photocurrents and the par-

ticle size distribution is calculated using a computer. Several commercial instruments are available, e.g. Malvern Mastersizer (Malvern, UK), Horriba (Japan) and Coulter LS Sizer (USA).

Photon correlation spectroscopy (PCS) or dynamic light scattering PCS is a technique that utilizes Brownian motion to measure particle size. As a result of the Brownian motion of dispersed particles, the intensity of scattered light undergoes fluctuations that are related to the velocity of the particles. Since larger particles move less rapidly than smaller ones, the intensity fluctuation (intensity versus time) pattern depends on particle size and this allows one to obtain the size distribution. In a system where the Brownian motion is not interrupted by sedimentation or particle–particle interaction, the movement of particles is random. Thus to apply the PCS technique one must make sure that sedimentation does not occur during the measurement and the system is dilute enough to avoid particle–particle interaction. The intensity fluctuation of the scattered light is measured using a photomultiplier and information on particle motion is obtained using a digital correlator. PCS allows one to measure the diffusion coefficient D of the particles that is related to the particle radius R by the Stokes–Einstein equation,

$$D = kT/6\pi\eta R, \tag{11.15}$$

where k is the Boltzmann constant, T is the absolute temperature and η is the viscosity of the medium.

PCS is a rapid, absolute, non-destructive and rapid method for particle size measurements. It has some limitations; the main disadvantage is the poor resolution of particle size distribution. Also it suffers from the limited size range (absence of any sedimentation) that can be accurately measured.

The back-scattering technique is based on the use of fibreoptics, sometimes referred to as fibreoptic dynamic light scattering (FODLS) and it allows one to measure at high particle number concentrations. FODLS employs either one or two optical fibres. Alternatively, fibre bundles may be used. The exit port of the optical fibre (optode) is immersed in the sample and the scattered light in the same fibre is detected at a scattering angle of 180° (i.e. back-scattering). This technique is suitable for on-line measurements during the manufacture of a suspension. Several commercial instruments are available, e.g. Lesentech (USA).

11.3 Wet milling (cominution)

The primary dispersion (sometimes referred to as the mill base) may then be subjected to a bead milling process to produce nanoparticles, which are essential for some coating applications. Subdivision of the primary particles into much smaller units in the nano-size range (10–100 nm) requires the application of intense energy. In some cases, high pressure homogenizers (such as the Microfluidizer, USA) may be sufficient to produce nanoparticles. This is particularly the case with many organic pigments. In some

cases, the high pressure homogenizer is combined with the application of ultrasound to produce nanoparticles.

Milling or cominution (the generic term for size reduction) is a complex process and there is little fundamental information on its mechanism. To break down single crystals or particles into smaller units, mechanical energy is required. This energy in a bead mill is supplied by impaction of the glass or ceramic beads with the particles. As a result, permanent deformation of the particles and crack initiation results. This will eventually lead to the fracture of particles into smaller units. Since the milling conditions are random, some particles receive impacts far in excess of those required for fracture whereas others receive impacts that are insufficient to fracture process. This makes the milling operation grossly inefficient and only a small fraction of the applied energy is used in cominution. The rest of the energy is dissipated as heat, vibration, sound, interparticulate friction, etc.

The role of surfactants and dispersants on the grinding efficiency is far from being understood. In most cases the choice of surfactants and dispersant is made by trial and error until a system is found that gives the maximum grinding efficiency. Rehbinder [26] investigated the role of surfactants in the grinding process. As a result of surfactant adsorption at the solid/liquid interface, the surface energy at the boundary is reduced and this facilitates the process of deformation or destruction. The adsorption of surfactants at the solid/liquid interface in cracks facilitates their propagation. This mechanism is referred to as the Rehbinder effect.

Several factors affect the efficiency of dispersion and milling:

(i) volume concentration of dispersed particles (i.e. the volume fraction);
(ii) nature of the wetting/dispersing agent;
(iii) concentration of wetter/dispersant (which determines the adsorption characteristics).

To optimize the dispersion/milling process, these parameters need to be systematically investigated. From the wetting performance of a surfactant and contact angle measurements, one can establish the nature and concentration of the wetting agent. The nature and concentration of dispersing agent required is determined by adsorption isotherm and rheological measurements.

Once the concentration of wetting/dispersing agent is established, dispersions are prepared at various volume fractions, keeping the ratio of wetting/dispersing agent to the solid content constant. Each system is then subjected to a dispersion/milling process, keeping all parameters constant:

(i) speed of the stirrer (normally one starts at lower speed and gradually increases the speed in increments at fixed time);
(ii) volume and size of beads relative to the volume of the dispersion (an optimum value is required);
(iii) speed of the mill.

The change of average particle size with time of grinding is established using for example the Mastersizer. Fig. 11.5 shows a schematic representation of the reduction of particle size with grinding time in minutes using a typical bead mill at various volume fractions. The presentation in Fig. 11.5 is only schematic and is not based on experimental data. It shows the expected trend. When the volume fraction ϕ is below the optimum (in this case, the relative viscosity of the dispersion is low) one requires a long time to achieve size reduction. In addition, the final particle size may be large and outside the nano-range. When ϕ is above the optimum value, the dispersion time is prolonged (due to the relatively high relative viscosity of the system) and the grinding time is also longer. In addition, the final particle size is larger than that obtained at the optimum ϕ. At the optimum volume fraction, the dispersion and grinding times are shorter and the final particle size is also smaller.

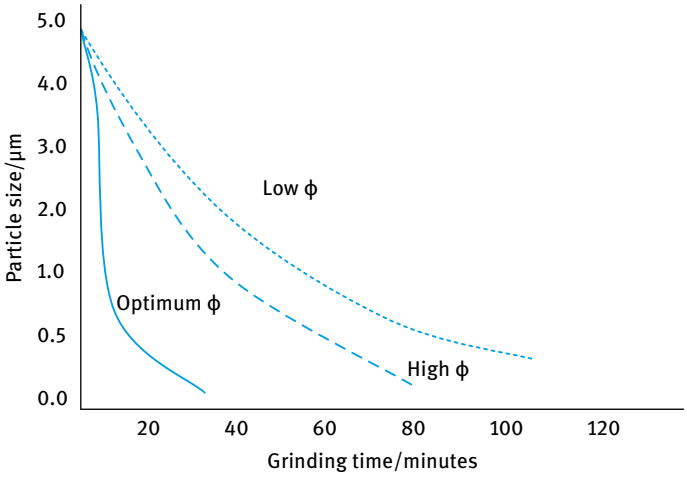

Fig. 11.5: Variation of particle size with grinding time in a typical bead mill.

For preparation of nano-dispersions, bead mills are commonly used. The beads are mostly made of glass or ceramics (which are preferred due to minimum contamination). The operating principle is to pump the premixed, preferably predispersed (using a high speed mixer), millbase through a cylinder containing a specified volume of say ceramic beads (normally 0.5–1 mm diameter to achieve nano-size particles). The dispersion is agitated by a single or multi-disc rotor. The disc may be flat or perforated. The millbase passing through the shear zone is then separated from the beads by a suitable screen located at the opposite end of the feedport. Generally speaking, bead mills may be classified to two types:

(i) vertical mills with open or closed top;
(ii) horizontal mills with closed chambers.

The horizontal mills are more efficient and the most commonly used one are: Netzsch (Germany) and Dyno Mill (Switzerland). These bead mills are available in various sizes from 0.5 to 500 l. The factors affecting the general dispersion efficiency are known reasonably well (from the manufacturer). The selection of the right diameter of the beads is important for maximum utilization. In general, the smaller the size of the beads and the higher their density the more efficient the milling process.

The centrifugal force transmitted to the grinding beads at the tip of the rotating disc increases considerably by its weight. This applies greater shear to the mill base. This explains why the more dense beads are more efficient in grinding. The speed transmitted to the individual chambers of the beads at the tip of the disc assumes that speed and the force can be calculated. The centrifugal force F is simply given by

$$F = \frac{\upsilon^2}{rg}, \tag{11.16}$$

where υ is the velocity, r is the radius of the disc and g is the acceleration due to gravity.

11.4 Colloid stabilization of paint dispersions

The colloid stabilization of the disperse phase in any paint formulation is essential during preparation of the pigment dispersion in order to prevent any particle reaggregation. Colloid stability is also very important for the long-term storage of a paint formulation. Aggregation of particles leads to poor performance of the paint, such as its opacity, colour, durability, etc. The colloid stability of any disperse system is determined by the balance between attractive [27] (van der Waals) and repulsive forces. The latter can be of two types:

(i) electrostatic double layer repulsion resulting from the presence of a charge on the particle surface [28, 29];
(ii) steric repulsion [30] arising from the presence of adsorbed nonionic surfactants or polymers.

In some cases, a combination of electrostatic and steric repulsion (referred to as electrosteric) occurs as for example when using polyelectrolytes for stabilization. In this section, I will first describe electrostatic double layer repulsion and van der Waals attraction, and their combination, which lead to the general theory of colloid stability. The factors that affect colloid stability, such as addition of electrolytes, will be described in terms of well-known theories of flocculation. This will be followed by a section on the adsorption and conformation of polymeric surfactants at the solid/liquid interface. This is key to understanding how these polymeric surfactants can stabilize the particles against aggregation. Finally, the interaction between particles containing an adsorbed layer will be discussed and the factors responsible for steric stabilization will also be considered.

11.4.1 Electrostatic double layer repulsion

A great variety of processes occur to produce a surface charge, e.g. surface ions that have such a high affinity to the surface of the particles that they may be taken as part of the surface, e.g. H^+ and OH^- on oxides (titania or silica). In some cases, specifically adsorbed ions (that have non-electrostatic affinity to the surface) "enrich" the surface but may not be considered as part of the surface, e.g. bivalent cations on oxides, cationic and anionic surfactants on most surfaces. These adsorbed ions produce a surface charge σ_0 that is compensated by unequal distribution of counter ions (opposite in charge to the surface) and co-ions (same sign as the surface) which extend to some distance from the surface forming an electrical double layer schematically represented by Gouy and Chapman [31, 32].

The double layer extension depends on the electrolyte concentration and valency of the counter ions,

$$\left(\frac{1}{\kappa}\right) = \left(\frac{\varepsilon_r \varepsilon_0 kT}{2n_0 Z_i^2 e^2}\right)^{1/2}. \tag{11.17}$$

ε_r is the permittivity (dielectric constant); 78.6 for water at 25 °C. ε_0 is the permittivity of free space. k is the Boltzmann constant and T is the absolute temperature. n_0 is the number of ions per unit volume of each type present in bulk solution and Z_i is the valency of the ions. e is the electronic charge.

Values of $(1/\kappa)$ for a 1 : 1 electrolyte (e.g. KCl) are given in Tab. 11.1.

Tab. 11.1: Values of $(1/\kappa)$ for a 1 : 1 electrolyte at 25 °C.

C (mol dm^{-3})	10^{-5}	10^{-4}	10^{-3}	10^{-2}	10^{-1}
$(1/\kappa)$ (nm)	100	33	10	3.3	1

The double layer extension increases with decrease in electrolyte concentration. Stern [3] introduced the concept of the non-diffuse part of the double layer for specifically adsorbed ions, the rest being diffuse in nature.

When charged, colloidal particles in a dispersion approach each other such that the double layers begin to overlap (particle separation becomes less than twice the double layer extension), and repulsion occurs. The individual double layers can no longer develop without restriction, since the limited space does not allow complete potential decay [28, 29].

For two spherical particles of radius R and surface potential ψ_0 and condition $\kappa R < 3$, the expression for the electrical double layer repulsive interaction is given by,

$$G_{el} = \frac{4\pi\varepsilon_r\varepsilon_0 R^2 \psi_0^2 \exp -(\kappa h)}{2R + h}, \tag{11.18}$$

where h is the closest distance of separation between the surfaces.

The above expression shows the exponential decay of G_{el} with h. The higher the value of κ (i.e. the higher the electrolyte concentration), the steeper the decay. This means that at any given distance h, the double layer repulsion decreases with the increase of electrolyte concentration.

In addition to the double layer repulsion, the particles also show van der Waals attraction, which is given by the following expression for two spheres (at small h) [27],

$$G_A = -\frac{A_{11(2)}R}{12h} \tag{11.19}$$

where $A_{11(2)}$ is the effective Hamaker constant of two identical particles with Hamaker constant A_{11} in a medium with Hamaker constant A_{22}. When the particles are dispersed in a liquid medium, the van der Waals attraction has to be modified to take into account the medium effect.

The effective Hamaker constant for two identical particles 1 and 1 in a medium 2 is given by,

$$A_{11(2)} = A_{11} + A_{22} - 2A_{12} = (A_{11}^{1/2} - A_{22}^{1/2})^2 \tag{11.20}$$

Equation (11.20) shows that two particles of the same material attract each other unless their Hamaker constant exactly matches each other. The Hamaker constant of any material is given by,

$$A = \pi q^2 \beta_{ii}, \tag{11.21}$$

where q is the number of atoms or molecules per unit volume.

In most cases, the Hamaker constant of the particles is higher than that of the medium. G_A decreases with increase of h. At very short distances, Born repulsion appears.

Combination of G_{el} and G_A results in the well-known theory of stability of colloids (DLVO theory) [28, 29],

$$G_T = G_{el} + G_A. \tag{11.22}$$

A plot of G_T versus h is shown in Fig. 11.6, which represents the case at low electrolyte concentrations, i.e. strong electrostatic repulsion between the particles.

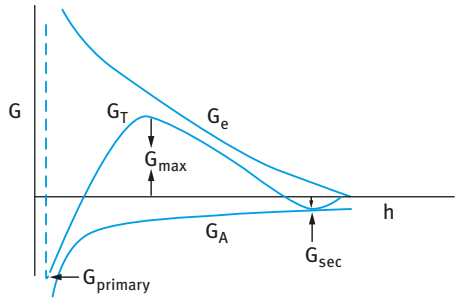

Fig. 11.6: Schematic representation of the variation of G_T with h according to the DLVO theory.

G_{el} decays exponentially with h, i.e. $G_{el} \to 0$ as h becomes large. $G_A \propto 1/h$, i.e. G_A does not decay to 0 at large h. At long distances of separation, $G_A > G_{el}$, resulting in a shallow minimum (secondary minimum). At very short distances, $G_A \gg G_{el}$, resulting in a deep primary minimum. At intermediate distances, $G_{el} > G_A$, resulting in energy maximum G_{max}, whose height depends on ψ_0 (or ψ_d) and the electrolyte concentration and valency. At low electrolyte concentrations ($< 10^{-2}$ mol dm^{-3} for a 1:1 electrolyte), G_{max} is high ($> 25kT$) and this prevents particle aggregation into the primary minimum. The higher the electrolyte concentration (and the higher the valency of the ions), the lower the energy maximum. Under some conditions (depending on electrolyte concentration and particle size), flocculation into the secondary minimum may occur. This flocculation is weak and reversible. By increasing the electrolyte concentration, G_{max} decreases until, at a given concentration, it vanishes and particle coagulation occurs.

The condition for kinetic stability is $G_{max} > 25kT$. When $G_{max} < 5kT$, flocculation occurs. Two types of flocculation kinetics may be distinguished: Fast flocculation with no energy barrier and slow flocculation when an energy barrier exists. Fast flocculation kinetics was treated by Smoluchowki [33], who considered the process to be represented by second order kinetics and the process is simply diffusion controlled. Slow flocculation kinetics was treated by Fuchs [34], who related the rate constant k to the Smoluchowski rate by the stability ratio constant W,

$$W = \frac{k_0}{k}. \tag{11.23}$$

W is related to G_{max} by the following expression [35],

$$W = \frac{1}{2} k \exp\left(\frac{G_{max}}{kT}\right). \tag{11.24}$$

Since G_{max} is determined by the salt concentration C and valency, one can derive an expression relating W to C and Z [35],

$$\log W = -2.06 \times 10^9 \left(\frac{R\gamma^2}{Z^2}\right) \log C, \tag{11.25}$$

where γ is a function that is determined by the surface potential ψ_0,

$$\gamma = \left[\frac{\exp(Ze\psi_0/kT) - 1}{\exp(Ze\psi_0/kT) + 1}\right]. \tag{11.26}$$

Plots of $\log W$ versus $\log C$ are shown in Fig. 11.7. The condition $\log W = 0$ ($W = 1$) is the onset of fast flocculation. The electrolyte concentration at this point defines the critical flocculation concentration CFC. Above the CFC, $W < 1$ (due to the contribution of van der Waals attraction which accelerates the rate above the Smoluchowski value).

Below the CFC, $W > 1$ and it increases with decrease of electrolyte concentration. The above figure also shows that the CFC decreases with increase of valency in accordance with the Schulze–Hardy rule.

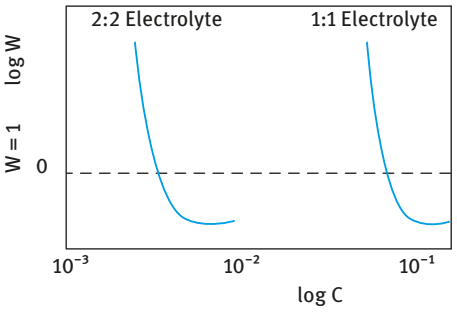

Fig. 11.7: log W–log C curves for electrostatically stabilized dispersions.

Another mechanism of flocculation is that involving the secondary minimum (G_{min}), which is a few kT units. In this case, flocculation is weak and reversible and hence one must consider both the rate of flocculation (forward rate k_f) and deflocculation (backward rate k_b). In this case, the rate or decrease of particle number with time is given by the expression,

$$-\frac{dn}{dt} = -k_f n^2 + k_b n. \tag{11.27}$$

The backward reaction (break-up of weak flocs) reduces the overall rate of flocculation.

The two main criteria for stabilization are:

(i) high surface or stern potential (zeta potential), high surface charge;
(ii) low electrolyte concentration and low valency of counter and co-ions.

One should ensure that an energy maximum in excess of $25kT$ should exist in the energy–distance curve. When $G_{max} \gg kT$, the particles in the dispersion cannot overcome the energy barrier, thus preventing coagulation. In some cases, particularly with large and asymmetric particles, flocculation into the secondary minimum may occur. This flocculation is usually weak and reversible and may be advantageous for preventing the formation of hard sediments.

11.4.2 Steric repulsion

This is obtained by using polymeric surfactants of the block and graft polymer types described in Chapter 10. Understanding the adsorption and conformation of polymeric surfactants at interfaces is key to knowing how these molecules act as stabilizers. Most basic ideas on adsorption and conformation of polymers have been developed for the solid/liquid interface [36].

The process of polymer adsorption is fairly complicated; It involves polymer/surface interaction, polymer/solvent interaction and surface/solvent interaction as well as the configuration (conformation) of the polymer at the solid/liquid interface.

The polymer/surface interaction is described in terms of adsorption energy per segment χ^s. The polymer/solvent interaction is described in terms of the Flory–Huggins interaction parameter χ. The polymer configuration is described by sequences of:

- trains, segments in direct contact with the surface;
- loops, segments in between the trains that extend into the solution;
- tails, ends of the molecules that also extend into solution.

A schematic representation of the various polymer configurations is given in Fig. 11.8.

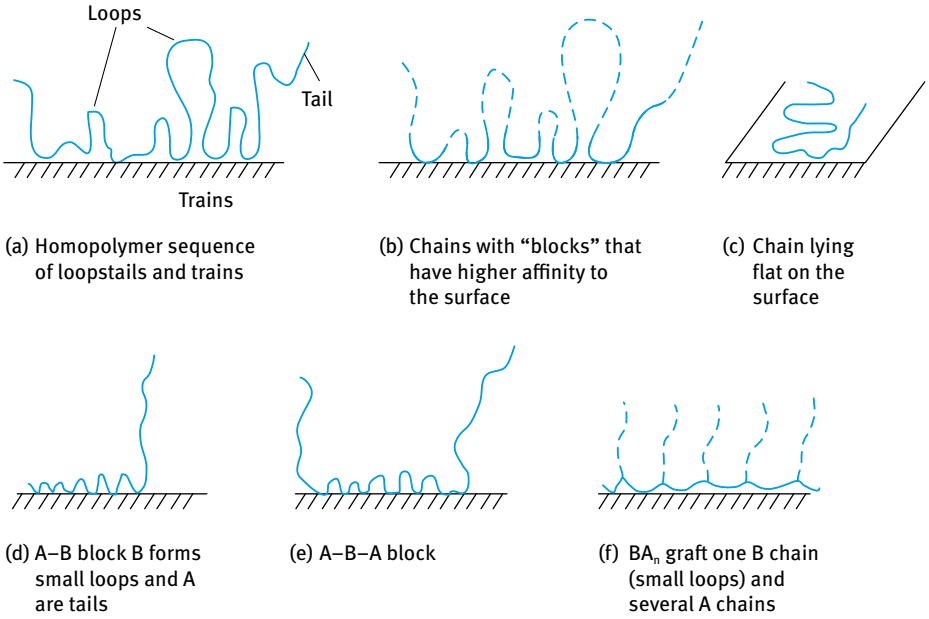

Fig. 11.8: Various conformations of macromolecules on a plane surface.

Homopolymers, e.g. poly(ethylene oxide) (PEO) or polyvinyl pyrrolidone (PVP), have a train–loop–tail configuration. For adsorption to occur, a minimum energy of adsorption per segment χ^s is required. When a polymer molecule adsorbs on a surface, it loses configurational entropy and this must be compensated by an adsorption energy χ^s per segment. The minimum value of χ^s can be very small ($< 0.1kT$) since a large number of segments per molecule are adsorbed. For a polymer with, for example, 100 segments where 10 % of these are in trains, the adsorption energy per molecule now reaches $1kT$ (with $\chi^s = 0.1kT$). For 1,000 segments, the adsorption energy per molecule is now $10kT$.

Homopolymers are not the most suitable for stabilization of dispersions. For strong adsorption, one needs the molecule to be "insoluble" in the medium and have strong affinity ("anchoring") to the surface. For stabilization, one needs the molecule

to be highly soluble in the medium and strongly solvated by its molecules; this requires a Flory–Huggins interaction parameter of less than 0.5. The above opposing effects can be resolved by introducing "short" blocks into the molecule which are insoluble in the medium and have a strong affinity to the surface, as illustrated in Fig. 11.8 (b). An example is partially hydrolyzed polyvinyl acetate (88 % hydrolyzed, i.e. with 12 % acetate groups), usually referred to as polyvinyl alcohol (PVA),

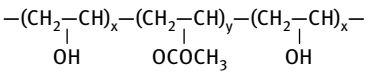

The above requirements are better satisfied using A–B, A–B–A and BA_n graft copolymers. B is chosen to be highly insoluble in the medium and it should have high affinity to the surface. This is essential to ensure strong "anchoring" to the surface (irreversible adsorption). A is chosen to be highly soluble in the medium and strongly solvated by its molecules. The Flory–Huggins parameter χ can be applied in this case. For a polymer in a good solvent, χ has to be lower than 0.5; the smaller the χ value the better the solvent for the polymer chains. Examples of B for a hydrophobic particles in aqueous media are polystyrene and polymethylmethacrylate. Examples of A in aqueous media are polyethylene oxide, polyacrylic acid, polyvinyl pyrollidone and polysaccharides. For nonaqueous media such as hydrocarbons, the A chain(s) could be poly(12-hydroxystearic acid).

For a full description of polymer adsorption one needs to obtain information on the following:

(i) The amount of polymer adsorbed Γ (in mg or mol) per unit area of the particles. It is essential to know the surface area of the particles in the suspension. Nitrogen adsorption on the powder surface may give this information (by application of the BET equation) provided there will be no change in area on dispersing the particles in the medium. For many practical systems, a change in surface area may occur on dispersing the powder, in which case one has to use dye adsorption to measure the surface area (some assumptions have to be made in this case).

(ii) The fraction of segments in direct contact with the surface, i.e. the fraction of segments in trains p:

$$p = \frac{\text{number of segments in direct contact with the surface}}{\text{total number}}.$$

(iii) The distribution of segments in loops and tails, $\rho(z)$, which extend in several layers from the surface.

$\rho(z)$ is usually difficult to obtain experimentally although recently application of small angle neutron scattering could obtain such information. An alternative and useful parameter for assessing "steric stabilization" is hydrodynamic thickness, δ_h (thickness

of the adsorbed or grafted polymer layer plus any contribution from the hydration layer). It is important to obtain the adsorption parameters as a function of the important variables of the system:

(i) Solvency of the medium for the chain which can be affected by temperature, addition of salt or a nonsolvent. The Flory–Huggins interaction parameter χ could be separately measured.
(ii) The molecular weight of the adsorbed polymer.
(iii) The affinity of the polymer to the surface as measured by the value of χ^s, the segment–surface adsorption energy.
(iv) The structure of the polymer. This is particularly important for block and graft copolymers.

When two particles, each with a radius R and containing an adsorbed polymer layer with a hydrodynamic thickness δ_h, approach each other to a surface–surface separation distance h that is smaller than $2\delta_h$, the polymer layers interact with each other, resulting in two main situations [30, 36]:

(i) The polymer chains may overlap with each other.
(ii) The polymer layer may undergo some compression.

In both cases, there will be an increase in the local segment density of the polymer chains in the interaction region. The real situation is perhaps in between the above two cases, i.e. the polymer chains may undergo some interpenetration and some compression.

Provided the dangling chains (the A chains in A–B, A–B–A block or BA_n graft copolymers) are in a good solvent, this local increase in segment density in the interaction zone will result in strong repulsion as a result of two main effects:

(i) Increasing osmotic pressure in the overlap region as a result of the unfavourable mixing of the polymer chains, when these are in good solvent conditions. This is referred to as osmotic repulsion or mixing interaction and it is described by a free energy of interaction G_{mix}.
(ii) Reduction of the configurational entropy of the chains in the interaction zone; this entropy reduction results from the decrease in the volume available for the chains when these either overlap or are compressed. This is referred to as volume restriction interaction, or entropic or elastic interaction and it is described by a free energy of interaction G_{el}.

The combination of G_{mix} and G_{el} is usually referred to as the steric interaction free energy, G_s, i.e.,

$$G_s = G_{mix} + G_{el}. \tag{11.28}$$

The sign of G_{mix} depends on the solvency of the medium for the chains. If in a good solvent, i.e. the Flory–Huggins interaction, parameter χ is less than 0.5, then G_{mix} is

positive and the mixing interaction leads to repulsion (see below). In contrast, if $\chi > 0.5$ (i.e. the chains are in a poor solvent condition), G_{mix} is negative and the mixing interaction becomes attractive. G_{el} is always positive and hence in some cases one can produce stable dispersions in a relatively poor solvent (enhanced steric stabilization).

Combination of G_{mix} and G_{el} with G_A (the van der Waals attractive energy) gives the total free energy of interaction G_T (assuming there is no contribution from any residual electrostatic interaction), i.e.,

$$G_T = G_{mix} + G_{el} + G_A. \tag{11.29}$$

A schematic representation of the variation of G_{mix}, G_{el}, G_A and G_T with surface–surface separation distance h is shown in Fig. 11.9.

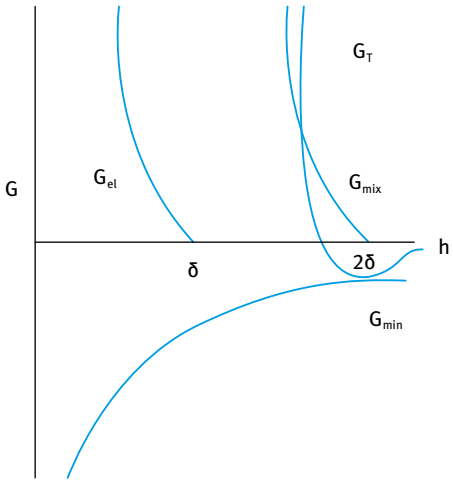

Fig. 11.9: Energy–distance curves for sterically stabilized systems.

G_{mix} increases very sharply with decrease of h when $h < 2\delta$. G_{el} increases very sharply with decrease of h when $h < \delta$. G_T versus h shows a minimum, G_{min}, at separation distances comparable to 2δ. When $h < 2\delta$, G_T shows a rapid increase with decrease in h.

The depth of the minimum depends on the Hamaker constant A, the particle radius R and the adsorbed layer thickness δ. G_{min} increases with increases of A and R. At a given A and R, G_{min} increases with decrease in δ (i.e. with decrease of the molecular weight, M_w, of the stabilizer. This is illustrated in Fig. 11.10 which shows the energy–distance curves as a function of δ/R. The larger the value of δ/R, the smaller the value of G_{min}. In this case, the system may approach thermodynamic stability as is the case with nano-dispersions.

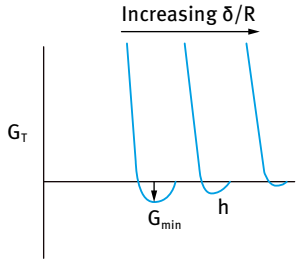

Fig. 11.10: Variation of G_{min} with δ/R.

Several criteria must be satisfied for effective steric stabilization:

(i) The particles should be completely covered by the polymer (the amount of polymer should correspond to the plateau value). Any bare patches may cause flocculation either by van der Waals attraction (between the bare patches) or by bridging flocculation (whereby a polymer moleculae will become simultaneously adsorbed on two or more particles).

(ii) The polymer should be strongly "anchored" to the particle surfaces, to prevent any displacement during particle approach. This is particularly important for concentrated suspensions. For this purpose, A–B, A–B–A block and BA_n graft copolymers are the most suitable where the chain B is chosen to be highly insoluble in the medium and has a strong affinity to the surface. Examples of B groups for hydrophobic particles in aqueous media are polystyrene and polymethylmethacrylate.

(iii) The stabilizing chain A should be highly soluble in the medium and strongly solvated by its molecules. Examples of A chains in aqueous media are poly(ethylelene oxide) and poly(vinyl alcohol).

(iv) δ should be sufficiently large (> 5 nm) to prevent weak flocculation.

Three main types of flocculation for sterically stabilized dispersions may be distinguished:

(i) Weak flocculation. This occurs when the thickness of the adsorbed layer is small (usually < 5 nm), particularly when the particle radius and Hamaker constant are large.

(ii) Depletion flocculation. This is obtained by the addition of a "free" (non-adsorbing) polymer into the continuous phase [37]. At a critical concentration or volume fraction of free polymer, ϕ_p^+, weak flocculation occurs, since the free polymer coils are "squeezed out" from between the droplets.

(iii) Incipient flocculation, which occurs when the solvency of the medium is reduced to become worse than θ-solvent (i.e. $\chi > 0.5$). This is illustrated in Fig. 11.11 where χ was increased from < 0.5 (good solvent) to > 0.5 (poor solvent).

When $\chi > 0.5$, G_{mix} becomes negative (attractive), which when combined with the van der Waals attraction at this separation distance gives a deep minimum causing flocculation. In most cases, there is a correlation between the critical flocculation point and

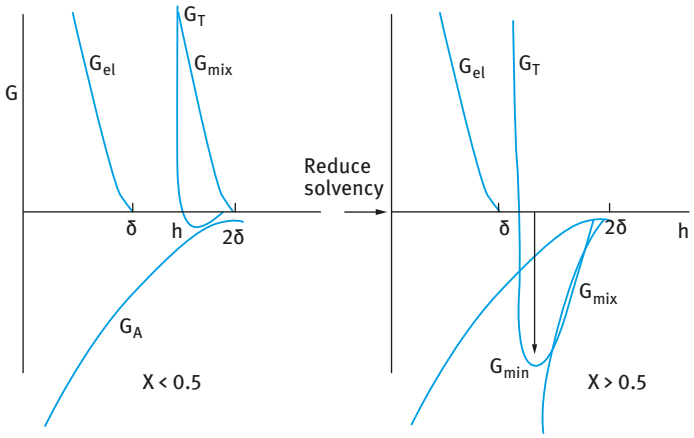

Fig. 11.11: Influence of reduction in solvency on the energy–distance curves for sterically stabilized dispersions.

the θ condition of the medium. Good correlation is found in many cases between the critical flocculation temperature (CFT) and θ-temperature of the polymer in solution (with block and graft copolymers one should consider the θ-temperature of the stabilizing chains A) [30, 36]. Good correlation is also found between the critical volume fraction (CFV) of a nonsolvent for the polymer chains and their θ-point under these conditions. However, in some cases such correlation may break down, and this is particularly the case for polymers which adsorb by multi-point attachment. This situation has been described by Napper [28], who referred to it as "enhanced" steric stabilization. Thus by measuring the θ-point (CFT or CFV) for the polymer chains (A) in the medium under investigation (which could be obtained from viscosity measurements) one can establish the stability conditions for a dispersion before its preparation. This procedure also helps in designing effective steric stabilizers such as block and graft copolymers.

12 Enhancement of particle deposition and adhesion in paints and coatings

The deposition of particles to surfaces is an important process in paint and coating applications, since it governs the paint or coating film properties. Two main types of particles must be considered, namely the latex particles (that may be considered as emulsions) that determine film formation and the pigment particles such as TiO_2 and other coloured pigments. Particle deposition is followed by their adhesion and it is essential to have uniform deposition (without any flocculation) to ensure that the final adhered film has the required properties such as gloss, durability, etc. Particle deposition is determined by long rage forces, namely van der Waals attraction, electrostatic repulsion or attraction and the presence of adsorbed or grafted surfactants, polymers or polyelectrolytes (referred to as steric interaction). Particle surface adhesion is governed by short-range forces that may include chemical and nonchemical bonds. In this chapter, I will discuss the role of van der Waals attraction and electrostatic repulsion (or attraction) on particle deposition and this is followed by description of particle/surface adhesion.

12.1 Particle deposition

As mentioned before, particle deposition is governed by the long-range van der Waals attraction and electrostatic repulsion or attraction. The van der Waals attraction between a particle of radius R and a flat surface separated by a distance h is given by the expression,

$$G_{\mathrm{VDW}}(h) = -\frac{A_{12}}{6}\left[\frac{R}{h} + \frac{R}{h+2R} \ln \frac{h}{h+2R}\right], \tag{12.1}$$

where A_{12} is the effective Hamaker constant. For a particle and surface with Hamaker constants A_{11} and A_{22} separated by a medium with Hamaker constant A_{33}, the effective Hamaker constant A_{12} is given by the expression,

$$A = (A_{11}^{1/2} - A_{33}^{1/2})(A_{22}^{1/2} - A_{33}^{1/2}). \tag{12.2}$$

For very small h, equation (12.1) reduces to,

$$G_{\mathrm{VDW}}(h) = -\frac{A_{12}R}{6h}. \tag{12.3}$$

Equation (12.3) shows that the interaction of a sphere with a thick plate has a geometric factor that is twice that of two similar spheres.

For a sphere and a flat plate, the repulsive interaction at $\kappa a < 5$ and weak overlap is twice that estimated for two similar spheres (assuming constant potential ψ),

$$G_{\mathrm{el}}^{\psi} = 4\pi\varepsilon_{\mathrm{r}}\varepsilon_0 R\psi_{\mathrm{d}}^2 \exp(-\kappa h). \tag{12.4}$$

https://doi.org/10.1515/9783110588002-014

For close approach and large κa,

$$G_{el}^{\psi} = 4\pi\varepsilon_r\varepsilon_0 R\psi_d^2 \ln[1 + \exp(-\kappa h)], \tag{12.5}$$

where ε_r is the permittivity (dielectric constant); 78.6 for water at 25 °C, ε_0 is the permittivity of free space. k is the Boltzmann constant and T is the absolute temperature. ψ_d is the Stern potential (that can be equated to the measured zeta potential) and κ is the reciprocal Debye length ($1/\kappa$ is the extension of the electrical double layer given by equation (11.17)).

Combination of G_A with G_{el} gives an energy–distance curve schematically represented by Fig. 11.5. The energy–distance curve is characterized by two minima, a shallow secondary minimum (weak and reversible attraction) and a primary deep minimum (strong and irreversible attraction).

Particles deposited under conditions of secondary minimum will be weakly attached, whereas particles deposited under conditions of primary minimum will be strongly attached. At intermediate distances of separation, an energy maximum is obtained whose height depends on the surface or zeta potential, electrolyte concentration and valency of the ions. This maximum prevents particle deposition.

The magnitude of the energy minima and the energy maximum depends on electrolyte concentration and valency. This is illustrated in Fig. 12.1 for a 1 : 1 electrolyte (e.g. NaCl) at various concentrations.

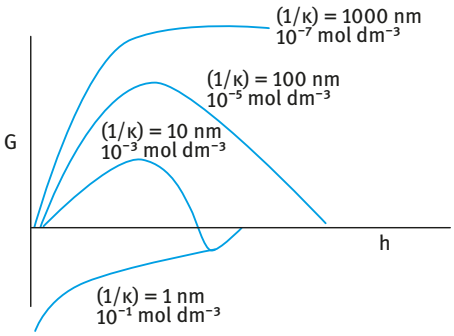

Fig. 12.1: G_T–h curves at various NaCl concentrations.

It can be seen that G_{max} decreases with increase in NaCl concentration and eventually it disappears at 10^{-1} mol dm^{-3}. Thus, particle deposition for particles with the same sign as the surface will increase with increase in electrolyte concentrations.

The above trend was confirmed by Hull and Kitchener [38] using a rotating disc coated with a negative film and negative polystyrene latex particles.

The number of polystyrene particles deposited was found to increase with increase in NaCl concentration, reaching a maximum at $C_{NaCl} > 10^{-1}$ mol dm^{-3}. The ratio of the maximum number of particles deposited N_{max} to the number deposited at any other NaCl concentration N_d (the so-called stability ratio W) was calculated

and plotted versus NaCl concentration,

$$W = \frac{N_{max}}{N_d}. \tag{12.6}$$

Fig. 12.2 shows this plot, which clearly shows that W decreases with increase in NaCl concentration reaching a minimum above 10^{-3} mol dm^{-3}, whereby maximum deposition occurs. Similar results were obtained by Tadros [39] using a rotating cylinder apparatus and the results are shown in Fig. 12.3.

It can be concluded from the above results that deposition of particles on substrates of the same sign will increase with increase in electrolyte concentration. However, the situation with oppositely charged surface to the particles being deposited is very different. In this case, attraction between oppositely charged surfaces will occur, a phenomenon referred to as heteroflocculation. This is schematically illustrated in Fig. 12.4 for positively charged polystyrene latex particles on a negative surface – both surfaces were covered by a nonionic polymer layer.

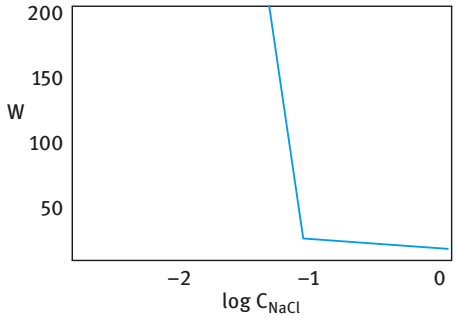

Fig. 12.2: Variation of W with log C_{NaCl} using a rotating disc.

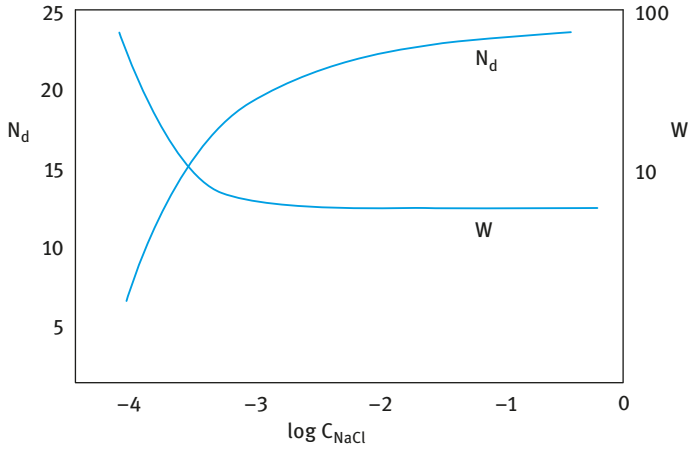

Fig. 12.3: N_d and W versus C_{NaCl} using a rotating cylinder.

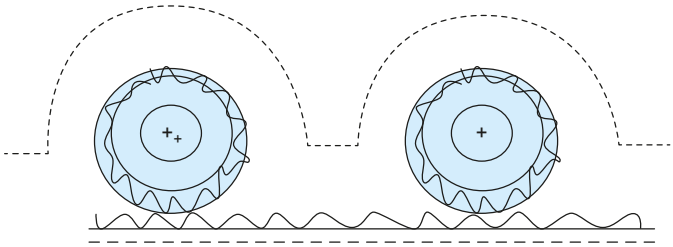

Fig. 12.4: Deposition of positively charged particles on negatively charged surface.

The effect of addition of electrolyte in this case will be opposite to that observed with surfaces of the same charge. Attraction between oppositely charged double layers will be higher at lower electrolyte concentrations. In other words, addition of electrolyte in this case will decrease deposition.

The effect of polymers and polyelectrolytes (bot natural and synthetic) on particle deposition is important in most paint formulations. These materials are used as thickening agents, film formers, resinuous powder and humectants. For example, thickening agents, sometimes referred to as rheology modifiers, are used in many paint formulations to maintain the product stability.

In many formulations, polymers and surfactants are present and interaction between them can produce remarkable effects. Several structures can be identified and the aggregates produced can have profound effects on particle deposition. With many paint formulations, polymers are added and these are mostly polyelectrolytes with cationic charges, which are essential for strong attachment to the negatively charged surface.

For convenience, I will consider the effect of three classes of polymers on particle deposition separately, namely nonionic polymers, anionic polyelectrolytes and cationic polyelectrolytes. Nonionic polymers can be of the synthetic type such as polyvinylpyrrolidone or natural such as many polysaccharides. The role of nonionic polymers in particle deposition depends on the manner in which they interact with the surface and the particle to be deposited. With many high molecular weight polymers, the chains adopt conformation forming loops and tails that may extend several nm from the surface. If there is not sufficient polymer to fully cover the surfaces, bridging may occur resulting in enhancement of deposition. In contrast, if there is sufficient polymer to cover both surfaces, the loops and tails provide steric repulsion resulting in reduction of deposition.

One may be able to correlate particle deposition to the adsorption isotherm. Under conditions of incomplete coverage, i.e. well before the plateau value is reached, particle deposition is enhanced. Under conditions of complete coverage, one observes reduction in deposition and at sufficient coverage deposition may be prevented altogether. This is schematically shown in Fig. 12.5, which shows the correlation between the adsorption isotherm and particle surface deposition.

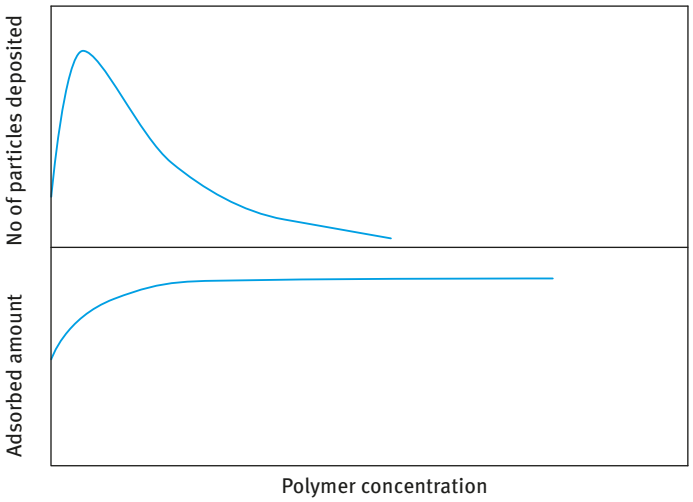

Fig. 12.5: Correlation between particle deposition and polymer adsorption.

The most commonly used nonionic polymers in paints are polysaccharide based. Polysaccahrides perform a number of functions in paints: rheology modifiers, suspending agents and emulsifying agents.

Polysaccharides are sometimes referred to as "polyglycans" or "hydrocolloids". The majority of polysaccharides are comprised primarily of six-membered cyclic structures known as pyranose ring (five carbon atoms and one oxygen atom). Many polysaccharides form helices, which is a tertiary spatial configuration, arranged to minimize the total energy of the polysaccharide (e.g. xanthan gum).

The behaviour of polysaccharides is critically influenced by the nature of the substituent groups bound to the individual monosaccharides (natural or synthetic). Anionic charges may also occur in natural polysaccharides and this will have a big influence on the adsorption and conformation of the polymer chain. The effect of polysaccharides on particle deposition is rather complex and it depends on the structure of the molecule and interaction with other ingredients in the formulation.

Many paint formulations contain anionic polymers mostly of the polyacrylate and polysaccharide type. The role of the anionic polymers is particle deposition is complex since these polyelectrolytes interact with ions in the formulation, e.g. Ca^{+} as well as with the surfactants used. Two of the most commonly used anionic polysaccharides are carboxymethylcellulose and caboxymthylechitin, obtained by carboxymethylation of cellulose and chitin, respectively. Several naturally occurring anionic polysaccharides exist, namely alginic acid, pectin, carragenans, xanthan gum, hyaluronic acidic and gum excudates (gum arabic, karaya, traganth, etc.). Crosslinking sites that occur when a polyvalent cation (e.g. Ca^{+}) causes inter-polysaccharide binding are called "junction zones".

The above complexes, which may produce colloidal particles, will have a big influence on the deposition of other particles in the formulation. They may enhance binding, simply by a cooperative effect in which the polysaccharide complexly interacts with the particles and increases the attraction to the surface. The pH of the whole system plays a major role since it affects the dissociation of the carboxylic groups.

Many of the anionic polysaccharides and their complexes affect the rheology of the system and this has a pronounced effect on particle deposition. Any increase in the viscosity of the system will reduce the flux of the particles to the surface and this may reduce particle deposition. This reduction may be offset by specific interactions between the particles and the polyanion or its complex.

Polycationic polyelectrolytes have a pronounced effect on particle deposition due to their interaction with the substrate and the particles. One of the earliest polycationic polymer is polyethyleneimine (PEI), which was used in some paint formulations. Later, an important class of cellulosic polycationic polymers were introduced with the trade name "Polymer JR" (Amerchol corporation). Another synthetic polycationic polymers from Calgon corporation are Merquat 100 (based on dimethyldiallyl amine chloride) and Merquat 550 (based acrylamide/dimthyldiallylamine chloride).

Several naturally occurring polycationic polymers exist such as chitosan (polyglycan with cationic charges), which is positively charged at pH < 7, cationic hydroxyethyl cellulose and cationic guar gum. These polycationic polymers interact with anionic surfactants present in the formulation and at a specific surfactant concentration a rapid increase in the viscosity of the solution is observed. At higher surfactant concentrations, precipitation of the polymer–surfactant complex occurs and at even higher surfactant concentrations, repeptization may occur.

Clearly, the above interactions will have pronounced effects on particle deposition. In the absence of any other effects, addition of cationic polyelectrolytes can enhance particle deposition either by simple charge neutralisation or "bridging" between the particle and the surface. At high polyelectrolyte concentrations, when there is sufficient molecules to coat both particle and surface, repulsion may occur resulting in reduction in deposition.

However, the above effects are complicated by the interaction of the polycationic polymer with surfactants in the formulation and this complicates the prediction of particle deposition. Investigations of the interactions that take place between the polycation, surfactants and other ingredients in the formulation are essential before a complete picture on particle deposition is possible.

12.2 Particle–surface adhesion

Adhesion is the force necessary to separate adherents; it is governed by short-range forces [40, 41]. Adhesion is more complex than deposition and more difficult to measure. No quantitative theory is available that can describe all adhesion phenomena:

Chemical and nonchemical bonds operate. Adequate experimental techniques for measuring adhesion strength are still lacking.

When considering adhesion, one must consider elastic and non-elastic deformation that may take place at the point of attachment. The short-range forces could be strong, e.g. primary bonds or intermediate, e.g. hydrogen and charge transfer bonds.

In 1934, Deryaguin [40, 41] considered the force of adhesion F in terms of the free energy of separation of two surfaces $[G(h_\infty) - G(h_0)]$ from a distance h_0 to infinite separation distance h_∞ – for the simple case of parallel plates,

$$-\int_{h_0}^{\infty} F \, \mathrm{d}h = G(h_\infty) - G(h_0). \tag{12.7}$$

F is made of three contributions,

$$F = F_\mathrm{m} + F_\mathrm{c} + F_\mathrm{e}. \tag{12.8}$$

F_m is the molecular component and it is made of two components, an elastic deformation component F_S and a surface energy component F_H,

$$F_\mathrm{m} = F_\mathrm{S} + F_\mathrm{H} \tag{12.9}$$

F_c is the component that depends on prior electrification. F_e is the electrical double layer contribution.

When a sphere adheres to a plane surface, elastic deformation occurs and one can distinguish the radius of the adhesive area r_0.

A schematic representation of elastic deformation is shown in Fig. 12.6.

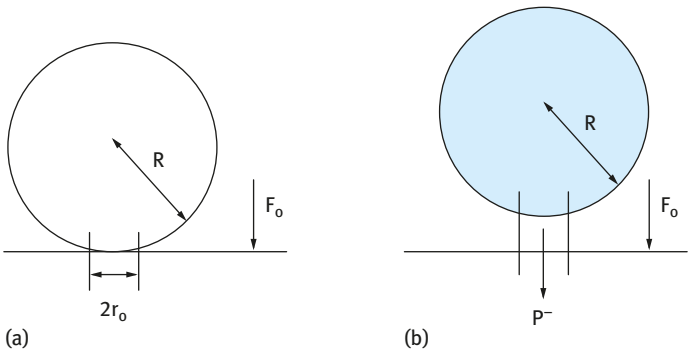

Fig. 12.6: Elastic deformation on adhesion of a sphere to a plane surface.

Usually $r_0/R \ll 1$, where R is the particle radius. The adhesive area can be calculated from a knowledge of the time dependence of the modulus of the sphere and the time dependence of the hardness of the plate.

Two approaches may be applied to consider the process of adhesion:

(i) Fox and Zisman's [42] critical surface tension approach; This approach was initially used to obtain the critical surface tension of wetting of liquid on solid substrates. Fox and Zisman [42] found that a plot of $\cos\theta$ (where θ is the contact angle of a liquid drop on the substrate) versus γ_{LV} (the liquid surface tension) for a number of related liquids gives a straight line which when extrapolated to $\cos\theta = 1$ gives the critical surface tension of wetting γ_c. This is shown in Fig. 12.7 for a number of solids.

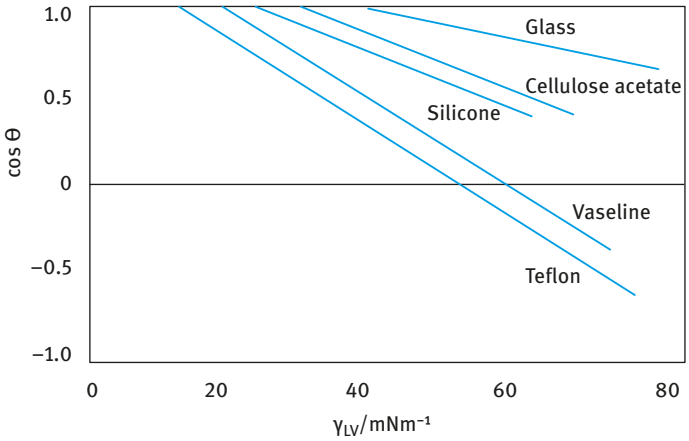

Fig. 12.7: cos θ versus γ_{LV} for a number of substrates.

A liquid with $\gamma_{LV} < \gamma_c$ will provide complete wetting of the substrate. Surfaces with high $\gamma_c > 40\,\text{mN m}^{-1}$ and small slopes are high energy surfaces (e.g. glass and cellulose). Surfaces with low very γ_c ($< 22\,\text{mN m}^{-1}$) and high slope are low energy surfaces, e.g. Teflon. Hydrocarbon surfaces such as vaseline produce intermediate values ($\gamma_c \approx 30\,\text{mN m}^{-1}$). This approach could also be applied for adhesion of "soft" particles to solid substrates. One can define three surface tensions:

- γ_{PL} (particle/liquid);
- γ_{PS} (particle/surface);
- γ_{SL} (solid/liquid).

The Helmholtz free energy of adhesion ΔF is given by the following expression,

$$\Delta F = (\gamma_{PS} - \gamma_{PL} - \gamma_{SL})\pi r_0^2 \tag{12.10}$$

For adhesion to occur ΔF should be negative. If ΔF is positive, no adhesion occurs.

(ii) Neuman's equation of state approach [43]. Neuman simplified the analysis by using a simple equation of state approach. He showed that a plot of $\gamma_{LV}\cos\theta$ versus γ_{LV} gives a smooth curve as is illustrated in Fig. 12.8. This simple analysis allows one to obtain γ_S from a single contact angle measurement.

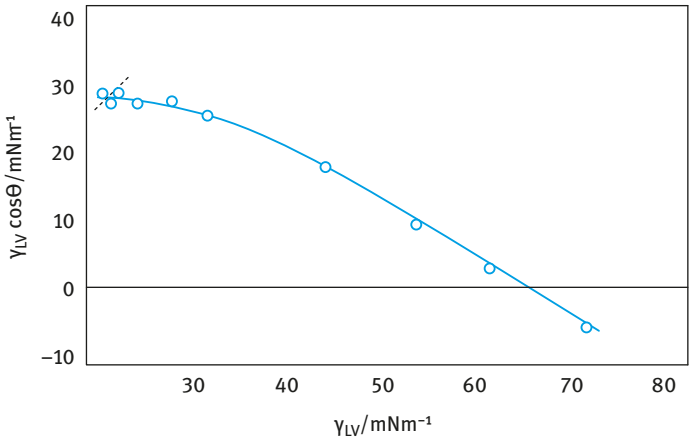

Fig. 12.8: Plot of $\gamma_{LV} \cos \theta$ versus γ_{LV}.

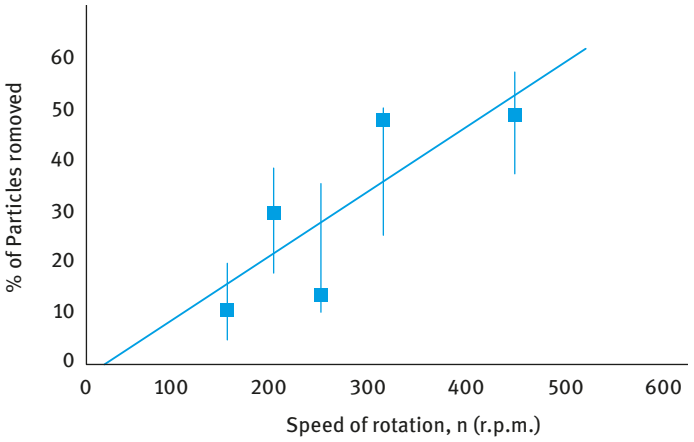

Fig. 12.9: Percent of particles removed versus speed of rotation.

Two experimental methods can be applied for measurement of particle–surface adhesion:

(i) Centrifugal method (Krupp, 1966). The centrifugal force required to remove a particle is given by the expression [44],

$$F_c = \frac{4}{3}\pi a^3(\rho_p - \rho_w)(\omega^2 x + g), \tag{12.11}$$

where a is the particle radius, ρ_p is the particle density, ρ_w is the density of water, ω is the centrifuge speed, x is the distance from the rotor and g is the acceleration due to gravity. To remove small particles from substrates one needs to apply very high g values (as high as 10^7). Thus this method is of little practical application.

(ii) Hydrodynamic method (Visser, 1976). A rotating cylinder apparatus is used and after the particles are deposited on the inner cylinder, the speed is increased [45]. The percent of detachment is measured (microscopically) as a function of the speed of rotation. The hydrodynamic force required to remove 50 % of the particles is taken as a measure of the force of adhesion.

This method was applied by Tadros [46] in 1980 to measure the force of adhesion of polystyrene latex on polyethylene. The results are shown in Fig. 12.9, which shows the percent of particles removed versus the speed of rotation of the cylinder. From knowledge of the hydrodynamic force required for particle removal, one could calculate the force of adhesion. The force of adhesion could be compared with the attractive force calculated from the Hamaker equation. The results showed that the force of adhesion was about two orders of magnitude lower than the theoretical value calculated from the van der Waals attraction.

It was concluded from the above results that the latex particles are not perfectly smooth ("hairy" surface) and hence not in intimate contact with the surface.

13 Control of the rheology of paint formulations

As mentioned in Chapter 9, paints are complex colloidal dispersions of solid and "liquid" (latex) particles that are dispersed in a liquid medium (continuous phase) which could be aqueous or nonaqueous depending on the applications. The continuous phase also contains various rheological modifiers which could be polymers or inert fine solid particles. The interaction between the various components in a paint formulation results in a non-Newtonian system with complex rheological behaviour. Control of paint rheology is essential for successful utilization of the paint. Whatever application technique is used, e.g. a spray gun, brush, roller, etc., three stages must be considered when considering the rheology of a paint [47]:

(i) transfer of the paint from the bulk container to the applicator;
(ii) transfer of the paint to the surface to form a thin and even film, i.e. film formation;
(iii) flow-out of the film surface, coalescence of the polymer latex particles and loss of the medium by evaporation.

Each of these processes requires accurate control of the rheological characteristics.

In the bulk container, the paint should be of sufficiently low viscosity so that it can be readily utilized in the applicator. For application by a brush or a hand roller, the paint should readily penetrate the spaces between the bristles of a brush or the porous surface of the roller. The paint is then held by capillary/surface tension forces during the transfer to the surface to be painted. Control of the brush loading is crucial in any paint application. If the brush loading is too high, the total weight of the paint becomes sufficient to overcome the capillary forces, leading to paint drip or run-off the brush, clearly an undesirable result. In contrast, if the brush-load is too low, this results in a thin paint film, or a non-uniform film with thicker film over a smaller surface area . To achieve the optimum film thickness one should control the flow-out properties as will be discussed below. Increasing brush-loading may be achieved by increasing the bulk paint viscosity or by introducing rheology modifiers. The latter are the most preferred option, since these rheology modifiers produce a shear thinning system, whereby the viscosity of the paint is rapidly reduced during application thus reducing the mechanical effort required to spread into a film. The recovery of the viscosity after application prevents dripping or running of the paint. In addition, these rheology modifiers produce high residual viscosity thus preventing sedimentation of particles in the paint.

In industrial applications such as spraying or roller-coating, control of the paint rheology is crucial. In spraying, the viscosity of the bulk paint must be low enough to allow the paint to be pumped through the fine jet of the spray gun with minimal application of pressure. In most cases, the paint is thinned from the higher-solids bulk immediately before application and during such short period, settling of the particles is less of a problem. The rheology of the diluted paint has a big influence on the droplet

https://doi.org/10.1515/9783110588002-015

spectrum of the sprayed paint [47]. One should avoid the formation of small spray droplets which may undergo drift on application. The use of rheological modifiers is essential to produce the optimum droplet size distribution in the spray.

In the roller-coating process, the pint must be considerably thicker than that used in spray processes. The paint should be able to flow under gravity or low pumping energy to the surface of the application roller, where it may be spread to an even layer by the action of doctor blade or another roller. In this case, the mechanical work required to cause the paint to flow is much less important. However, the paint must be viscous enough to prevent it running off or being thrown of the roller by centrifugal force.

In both spraying and roller-coating applications, the fluid flow rate and operating speed are very high and in this case both high stresses and high shear rates operate in the process. One should also note that the paint remains in the spray gun or the "nip" between the rollers for a very short time and hence a steady state is never reached. In this case, only transient or high-frequency rheological measurements are likely to produce relevant rheological parameters. Shear rates as high as $10^5\ s^{-1}$ can be reached in high speed rollers. At such high shear rates and in the presence of high molecular weight polymers in the paint formulation, a high extensional viscosity (which can be several orders of magnitude higher than the shear viscosity) can develop. The extensional viscosity of "thickened" water-based emulsion paints influence the application properties such as tracking, spattering, etc. One would expect that such a high extensional viscosity might interfere with the process of filament or jet rupture to form spray droplets [48].

The next process that must be considered in paint application is film formation. The loading and transfer of the paint by a brush or a roller from the bulk container to the surface to be painted is followed by regular movement of the brush or roller over the surface to transfer the load of the paint from the brush to the surface and spread it out in an even layer. During this process, hand pressure on the brush causes shearing and compression of the brush bristles or fibres of the rubber foam or fibrous mat typically covering the surface of a hand roller. The flow processes involved are very complex and very difficult to analyze. However, some attempts have been made to calculate the range of shear rates involved in paint brush applications. Ranges of $15–30\ s^{-1}$ were estimated for brush dipping and $2{,}500–10{,}000\ s^{-1}$ for brush spreading [49, 50].

The third and most important step of paint application is that of flow-out or leveling of the paint film which involves latex coalescence and loss of medium by evaporation. This has a major influence on colour uniformity, hiding power as well as major flow faults such as sagging and slumping [51, 52]. Unfortunately, there is still a lack of understanding of the relevant theological parameters that affect these processes. There may be some correlation between elastic recovery and surface irregularity flow-out (leveling). Both pigment dispersions (mill bases) as well as the final paint formulation show viscoelastic behaviour [53, 54]. This clearly demonstrates the importance of dynamic (oscillatory) measurements in the assessment of leveling properties.

Solvent evaporation during application will have a major effect on the rheological properties as well as the surface tension at the wet film/air interface. Evaporation results in increase in the disperse volume fraction as well as a cooling effect at the film's surface. Both effects lead to a tangential surface shearing force. It has been argued that the hydrostatic pressure gradient in a paint film is insufficient to explain the leveling effect. Whilst surface tension tends to produce a flat surface, irrespective of the substrate surface profile underneath, the surface tension gradient developing over the wet film tends to produce a uniform film thickness, i.e. the surface profile of the paint film mirrors exactly the surface profile of the substrate.

Solvent evaporation also leads to gradients in the solvent concentration through the film as well as across the surface. This leads to density gradients which with the surface tension gradients could contribute to circularly patterns being set up in the wet paint film. This may lead to the formation of Bernard cell patterns commonly observed at the surface of boiling or rapidly evaporating bulk liquid samples.

The complexity of the rheology of the applied paint film is shown by its viscoelastic behaviour as well as the nonlinear and time-dependent effects arising from the high shear during application. In addition, due to the concentration gradients through the film thickness, the rheology will also vary through the depth of the film. Rough calculations showed that the operative forces in leveling are in the range of 3–5 Pa and in sagging is about 0.8 Pa at the surface of a typical paint film. The shear rates for leveling processes in paint films are in the range 10^{-3}–5×10^{-1}. Since the shear stress resulting from gravitational and surface tension forces control the flow in leveling and sagging, it is important to carry out constant stress (creep) measurements when considering the relation between paint rheology and its flow characteristics. Measurement of shear rates seem to be irrelevant in this case.

From the above discussion, one can summarize the desirable rheological characteristics of a paint formulation. The latter should have a sufficiently low viscosity to facilitate its transfer to the applicator. However, it should also have a sufficiently high residual (zero shear) viscosity to prevent particle sedimentation and sufficiently high modulus to prevent separation (syneresis). This requires the use of an appropriate rheology modifier, which produces a "gel" structure that is easily "broken" during transfer from the bulk container. Because of the high shear rates and short time scales involved in the transfer process, both elasticity and extensional flow processes may modify the pattern of surface irregularities on the paint film. The paint must remain low in viscosity for a sufficient time for the surface irregularities to flow out to an acceptable extent. However, while the viscosity is low, the paint may flow on vertical surfaces under the influence of gravity. If the film thickness (film depth) builds up too much, sagging may become noticeable to the observer and lumps of thickened paint may result in an irregular film, which is undesirable. To prevent this from occurring, the initial low viscosity must be followed by a sharp rise in viscosity either by solvent evaporation and/or elastic recovery. The drying film becomes immobilized and sagging is prevented.

Several techniques can be applied for studying paint rheology. During the early stages of paint formulation, i.e. during research and development, one must carry out carefully controlled rheological methods. The results from these controlled experiments can be applied to arrive at the optimum composition of a given paint formulation. Once the latter is established, much simpler methods must be used for quality control of the paint during manufacture. In this chapter, I will start with the simple methods for quality control. This is then followed by a comprehensive list of the rheological methods that can be applied during the research and development stage.

The simple methods that can be used for quality control of a paint must be fast, reliable and convenient to apply during paint manufacture. Three methods can be applied, namely measuring the flow through constrictions, measuring the speed of an object moving through the paint or measuring the relative speed of motion in a finite sample; the moving object can be shaped in the form of a spindle which is made to rotate in a fixed volume of the paint. Below, a brief description of the three methods is given. This is followed by a section on measurement of rheology during flow-out (leveling).

Flow through constrictions is best illustrated by the Ford cup, which has been extensively used in the paint industry [47]. A known volume of the paint is held within a vertical cylindrical cup whose bottom has a short capillary of controlled length and diameter. The paint is released to flow through the hole in the bottom of the cup (usually by the operator releasing his finger) and the time for the paint to flow out of the cup is measured with a stop-watch. The flow end point is normally taken as the point at which the continuous liquid jet breaks up into drops. However, this simple technique suffers from several disadvantages. First, because the liquid height varies during the test, the gravity force driving the liquid through the capillary also varies. Since the paint is non-Newtonian, the viscosity results can be misleading. Second, since the capillary is short, stable flow conditions within the capillary are not obtained. This effect together with the entry and exit errors may affect the result, particularly if the paint is elastic in nature. Third, the presence of abrasive particles in the paint may lead to wear of the metal capillary. It is, therefore, necessary to frequently check the Ford cup using Newtonian liquids (e.g. silicone oils) of known viscosity.

Measuring the speed of an object moving through the paint is best illustrated by the Hoeppler-type viscometer whereby a solid ball of varying density serves as the object. The fall of the ball can be electrically timed between two contacts and the time is a measure of the consistency of the material.

Perhaps the most useful (and commonly used) method for studying paint rheology is based on measuring the relative speed of motion of a spindle rotating in a fixed volume of paint as is illustrated by the Brookfield viscometer. Several spindles and rotation speeds are used to cover a wide range of viscosity. However, a limited range of shear rates are possible when using the Brookfield viscometer. An alternative instrument that is widely used in the paint industry is the Stormer viscometer, which has a paddle as a rotational member.

Measurement of film flow-out (leveling and sagging) is perhaps the most difficult methods for direct measurement of paint film rheology during flow-out (leveling). This is due to the fact that the rheology of paint film material is extremely complex as it is not only viscoelastic but extremely nonlinear. In addition, the rheology of a paint film can change rapidly with time due to solvent evaporation, increase in solids volume fraction and rheological structure recovery. The paint film may also become inhomogeneous in composition through the film depth. For these reasons, it is essential to have rapid methods for following the paint film rheology during flow-out. Several methods can be applied:

(i) Impact method (bouncing ball), where a 0.5 cm diameter steel ball (weight 0.5 g) is dropped on to a 1.25 cm thick glass slab coated with the paint under test [56]. The rebound height is measured as a function of time as the film dries. Initially, the bound height decreases with time, since the viscosity of the film increases owing to solvent loss. Consequently, the energy dissipated by the film during the impact of the ball with the glass also increases and this results in a sharp decrease of the rebound height in this early stage of drying. However, as the film cures (either by autoxidation or "lacquer-type" drying), the film develops some elasticity and the rebound height increases. A schematic representation of the rebound height with drying time is given in Fig. 13.1. Using for example the ball momentum and energy losses, it is not easy to derive a relationship between rebound height and film viscosity. This is due to the additional factors such as the hydrodynamic force (which prevents the ball from actually touching the substrate surface) as well as the paint elasticity effects at the short times of impact (in the region of few tenths of a millisecond). In spite of these drawbacks, the method is simple and one can use paint films on different substrates (glass, metal, wood, etc.) and balls of different size.

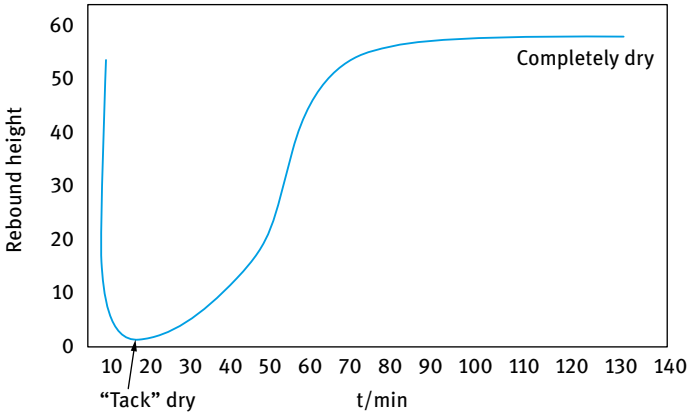

Fig. 13.1: Variation of rebound height with time for a 200 µm refinish paint film on glass.

(ii) Impedance method at high frequency; the mechanical impedance of an elastic shear wave propagating through a medium is changed by the presence of a viscoelastic layer at the surface of the medium. If the elastic wave is completely damped in this layer, the change in the characteristic impedance can be related to the rheological parameters of the layer material. This method can be applied to follow the changes in the paint-film rheology during drying and curing. Pulses of high frequency oscillations (in the region of 2–100 MHz) are generated by means of a suitably-excited piezoelectric crystal attached to the support medium [57]. After propagation through the support, the attenuated pulses are again transformed into electrical signals by a piezoelectric crystal attached to the support. This is schematically shown in Fig. 13.2. The phase angle and attenuation of the received pulses are measured and changes in their values are used to compare the rate changes in drying and curing of different paint films. Unfortunately, this technique is limited to measurement of the film properties during only a limited part of the total drying/curing process. In addition, the adhesion of the drying paint film to the substrate can have a big influence on the results.

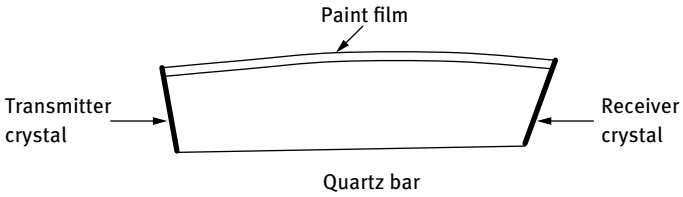

Fig. 13.2: Schematic representation of the impedance technique.

(iii) Rheological techniques for research and development of a paint system. The basic principles of rheological methods and the techniques that can be applied for their investigation were described in detail in Chapter 14 of Vol. 1.

In this section, a brief description of the methods that can be applied for a paint formulation is given. Essentially, three main rheological methods can be applied:

(i) steady state shear stress–shear rate measurements with particular attention to time effects (thixotropy);
(ii) transient methods: application of constant strain and following the relaxation of the stress with time (stress relaxation measurements) or application of constant stress and following the change of strain with time (creep measurements);
(iii) dynamic (oscillatory) measurements.

Apart from these methods, two main investigations relevant to paint systems must be considered:

(iv) normal force measurements;
(v) elongational viscosity measurements.

(i) Steady state shear stress–shear rate measurements

Here one applies different, constant rates of shear to the material and measures the resulting stress [58–61]. To calculate the shear stress–shear rate relationship one should have a well-defined geometry, the most common being the concentric cylinder, the cone and plate and the parallel plate configurations. Most paint systems exhibit pseudoplastic behaviour as is illustrated in Fig. 13.3 whereby the stress σ and viscosity η are plotted as a function of shear rate $\dot{\gamma}$.

The above curve shows the shear thinning behaviour of the system. It shows two plateau (Newtonian) regions at low and high shear rate ranges. The low shear rate plateau region gives the residual (sometimes referred to as "zero shear rate") viscosity $\eta(0)$ whereas the high shear rate plateau region gives the lowest viscosity that is reached with a shear thinning system, sometimes referred to as η_∞. These two regions are separated by the shear thinning regime whereby the viscosity decreases with increase of shear rate. The residual viscosity $\eta(0)$ is an important parameter that determines particle sedimentation. A minimum value is needed to prevent sedimentation. The critical shear rate above which a paint shows shear thinning behaviour is an important parameter that controls the transfer of paint to applicator. This critical shear rate should not be too high otherwise the transfer of the paint from the container (which requires a low viscosity) becomes very difficult. The high shear rate viscosity η_∞ determines the flow of the paint on the substrate.

Several models have been suggested to analyze the flow curves of pseudoplastic systems and these were described in Chapter 14 of Vol. 1.

(i) Power law fluid model:

$$\sigma = k\dot{\gamma}^n, \tag{13.1}$$

where k is the consistency index and n is the shear thinning index; $n < 1$.

By fitting the experimental data to equation (13.1), one can obtain k and n. The viscosity at a given shear rate can be calculated as,

$$\eta = \frac{\sigma}{\dot{\gamma}} = \frac{k\dot{\gamma}^n}{\dot{\gamma}} = k\dot{\gamma}^{n-1}. \tag{13.2}$$

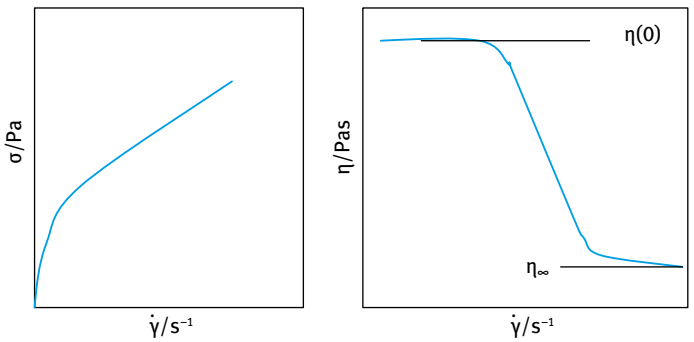

Fig. 13.3: Stress–shear rate and viscosity–shear rate relationship for a pseudoplastic system.

(ii) Herschel–Bulkley general model; many systems show a dynamic yield value followed by shear thinning behaviour. The flow curve can be analyzed using the Herschel–Bulkley equation [62]:

$$\sigma = \sigma_\beta + k\dot{\gamma}^n. \tag{13.3}$$

When $\sigma_\beta = 0$, equation (13.3) reduces to the power fluid model. The Herschel–Bulkley equation fits most flow curves with a good correlation coefficient and hence it is the most widely used model.

(iii) The Casson model, which is a semi-empirical linear parameter model that has been applied to fit the flow curves of many paints and printing ink formulations [63],

$$\sigma^{1/2} = \sigma_C^{1/2} + \eta_C^{1/2}\gamma^{1/2}. \tag{13.4}$$

Thus a plot of $\sigma^{1/2}$ versus $\dot{\gamma}^{1/2}$ should give a straight line from which σ_C and η_C can be calculated from the intercept and slope of the line. One should be careful when using the Casson equation since straight lines are only obtained from the results above a certain shear rate.

(iv) The Cross equation can be used to analyze the flow curve of shear thinning systems that show a limiting viscosity $\eta(0)$ in the low shear rate regime and another limiting viscosity $\eta(\infty)$ in the high shear rate regime [64]. These two regimes are separated by a shear thinning behaviour as schematically shown in Fig. 13.4

$$\frac{\eta - \eta(\infty)}{\eta(0) - \eta(\infty)} = \frac{1}{1 + k\gamma^n}, \tag{13.5}$$

where k is the consistency index and n is the shear thinning index.

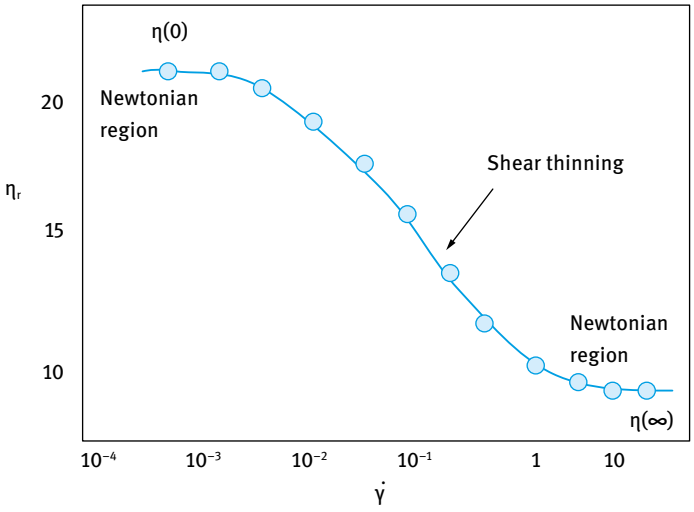

Fig. 13.4: Viscosity versus shear rate for a shear thinning system.

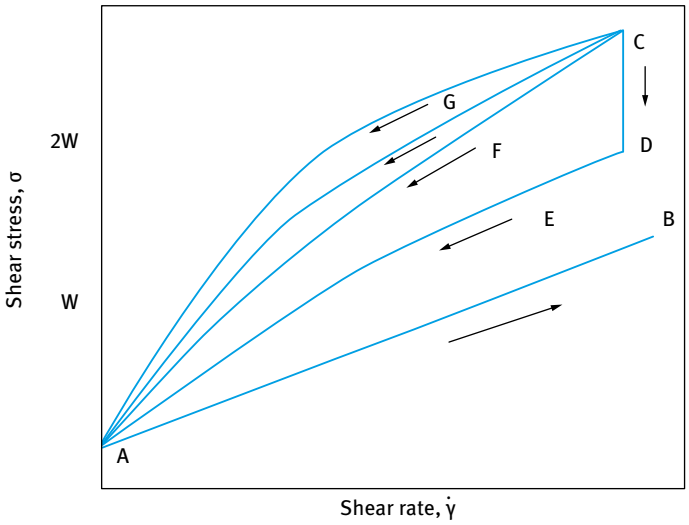

Fig. 13.5: Schematic representation of thixotropic paint.

Most paints show thixotropic behaviour in addition to being pseudoplastic. Thixotropy was first defined as an isothermal, reversible sol-gel-sol transition. This implies that the paint decreases in viscosity on shear (which is essential for ease of spreading and coating on the substrate), but builds up when the shearing process is stopped. Control of the time required for build up of viscosity is essential for producing a paint film with the desirable properties. If the viscosity build-up is too fast one may produce a film with the brush marks of the applicator. If the viscosity build-up is too slow, dripping and sagging may occur.

A schematic representation of the thixotropic behaviour of a paint is shown schematically in Fig. 13.5. If the flow could be measured without stirring (i.e. without breaking the structure) the curve AB could be produced [65]. However, when increasing the rate of shear from 0 to $2W$, breakdown of the structure occurs resulting in curve AC. While a continuous shear rate of $2W$ is applied over a period of time, the consistency of the paint decreases continuously from C to D, where it reaches a constant value, the lowest it can experience at the given shear rate of $2W$. Only a higher shear rate will be able to decrease the consistency further. If the shear is discontinued at point D, the build-up in the consistency of the paint to regain its original structure will follow along curve E, F or G, depending on the time which the particular paint requires for the building-up process.

Generally speaking, two methods can be applied to study thixotropy in a paint formulation. The first and most commonly used procedure is the loop test whereby the shear rate is increased continuously and linearly in time from zero to some maximum value and then decreased to zero in the same way [60]. This is illustrated in Fig. 13.6. The main problem with this procedure is the difficulty of interpreting the results. The

nonlinear approach used is not ideal for developing loops because by decoupling the relaxation process from the strain one does not allow for the recovery of the material. However, the loop test gives the qualitative behaviour of the paint thixotropy. An alternative method for studying thixotropy is to apply a step change test, whereby the paint is suddenly subjected to a constant high shear rate and the stress is followed as a function of time whereby the structure breaks down and an equilibrium value is reached (14). The stress is further followed as a function of time to evaluate the rebuilding of the structure. A schematic representation of this procedure is shown in Fig. 13.7.

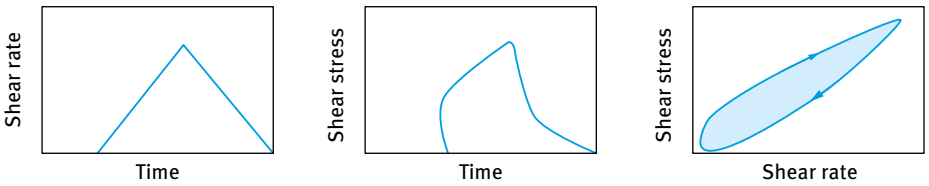

Fig. 13.6: Loop test for studying thixotropy.

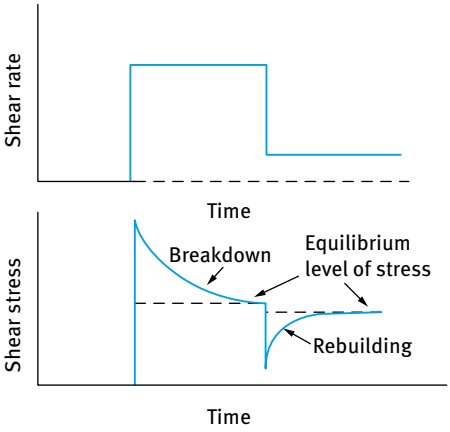

Fig. 13.7: Step change test for studying thixotropy.

Application of the above tests for a highly elastic paint is not straightforward since there are contributions to the stress growth and decay from viscoelasticity. The occurrence of thixotropy implies that the flow must be taken into account when making predictions of flow behaviour.

(ii) Transient methods for studying paint rheology

Two transient methods can be applied to study paint rheology:

(i) stress relaxation after sudden application of strain;

(ii) strain relaxation after sudden application of stress (creep measurements).

Both these techniques were described in detail in Chapter 14 of Vol. 1 and here only a brief summary will be given [66].

In the stress relaxation method, a constant strain γ is applied within a very short period (that must be much smaller than the relaxation time of the sample) and the stress σ is followed immediately as a function of time.

For a viscoelastic liquid (e.g. many paint systems), the stress decreases exponentially with time t and reaches zero at infinite time. If the stress is divided by the applied constant strain one obtains the stress relaxation modulus $G(t)$ which is related to the instantaneous modulus by the following expression,

$$G(t) = \frac{\sigma(t)}{\gamma} = \frac{\sigma(0)}{\gamma} \exp\left(-\frac{t}{\tau_m}\right) = G(0) \exp\left(-\frac{t}{\tau_m}\right). \tag{13.6}$$

For a viscoelastic solid, the modulus reaches a limiting value G_e after a long time (sometimes referred to as the equilibrium modulus). In this case, equation (13.6) has to be modified to account for G_e

$$G(t) = G(0) \exp\left(-\frac{t}{\tau_m}\right) + G_e. \tag{13.7}$$

Note that according to equation (13.6), $t = \tau_m$ when $\sigma(t) = \sigma(0)/e$ or when $G(t) = G(0)/e$. This shows that stress relaxation can be used to obtain the relaxation time for a viscoelastic liquid.

In the constant stress (creep) method, a stress σ is applied on the system (that may be placed in the gap between two concentric cylinders or a cone and plate geometry) and the strain (relative deformation) γ or compliance J ($= \gamma/\sigma$, Pa^{-1}) is followed as a function of time for a period of t. At $t = t$, the stress is removed and the strain γ or compliance J is followed for another period t. This procedure is referred to as "creep measurement". From the variation of J with t when the stress is applied and the change of J with t when the stress is removed (in this case J changes sign) one can distinguish between viscous, elastic and viscoelastic response (Chapter 14 of Vol. 1).

For viscoelastic response (which occurs in most paint systems) the following trend is observed: at $t = 0$, J shows a sudden increase and this is followed by slower increase for the time applied. When the stress is removed, J changes sign and J shows an exponential decrease with increase of time (creep recovery) but it does not reach 0 as with the case of an elastic response.

The compliance $J(t)$ is given by two components, an elastic component Je that is given by the reciprocal of the instantaneous modulus and a viscous component J_v that is given by $t/\eta(0)$,

$$J(t) = \frac{1}{G(0)} + \frac{t}{\eta(0)}. \tag{13.8}$$

The Maxwell relaxation time τ_M is given by,

$$\tau_M = \frac{\eta(0)}{G(0)}. \tag{13.9}$$

For a viscoelastic solid, complete recovery occurs and the system is characterized by a Kelvin retardation time τ_k that is also given by the ratio of $\eta(0)/G(0)$.

The Berger model (Maxwell + Kelvin) represents most practical paints consisting of a Maxwell element and a Kelvin element. The modulus of the spring in the Maxwell element is G_1 and the viscosity in the dash-pot is η_1. The Maxwell relaxation time is η_1/G_1. The modulus of the spring in the Kelvin element is G_2 and the viscosity in the dash-pot is η_2. The Kelvin retardation time is η_2/G_2. The Berger model gives an instantaneous elastic response from G_1 and a continuous viscous response from η_1.

More complex models can also be introduced: The generalized Maxwell model introduces several elements with different relaxation times. The generalized Kelvin model also consists of several Kelvin elements with different retardation times.

In creep experiments, one starts with a low applied stress (below the critical stress σ_{cr}, see below) at which the system behaves as a viscoelastic solid with complete recovery. The stress is gradually increased and several creep curves are obtained. Above σ_{cr}, the system behaves as a viscoelastic liquid showing only partial recovery. Fig. 13.8 shows a schematic representation of the variation of compliance J with time t at increasing σ (above σ_{cr}). From the slopes of the lines, one can obtain the viscosity η_σ at each applied stress. A plot of η_σ versus σ is shown in Fig. 13.9. This shows a limiting vis-

Creep measurements (constant stress) can be used to obtain the residual or zero shear viscosity

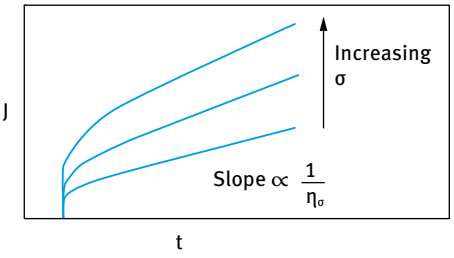

Fig. 13.8: Creep curves at increasing applied stress.

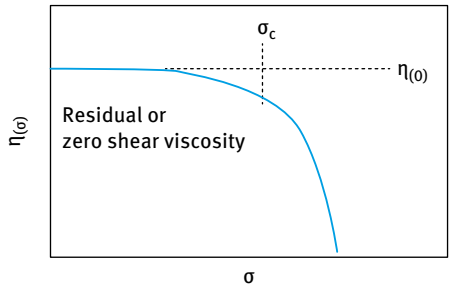

Critical stress is a useful parameter (related to yield stress) as denotes the stress at which structure "breaks down"

Fig. 13.9: Variation of viscosity with applied stress.

cosity $\eta(0)$ below σ_{cr} and above σ_{cr} the viscosity shows a sharp decrease with further increase in σ. $\eta(0)$ is referred to as the residual or zero shear viscosity, which is an important parameter for predicting sedimentation. σ_{cr} is the critical stress above which the structure "breaks down". It is sometimes referred to as the "true" yield stress.

(iii) Dynamic (oscillatory) technique

This is the response of the material to an oscillating stress or strain. When a sample is constrained in, say, a cone and plate or concentric cylinder assembly, an oscillating strain at a given frequency ω (rad s^{-1}) ($\omega = 2\pi\nu$, where ν is the frequency in cycles s^{-1} or Hz) can be applied to the sample. After an initial start-up period, a stress develops in response to the applied strain, i.e. it oscillates with the same frequency. The change of the sine waves of the stress and strain with time can be analyzed to distinguish between elastic, viscous and viscoelastic response. Analysis of the resulting sine waves can be used to obtain the various viscoelastic parameters as discussed below.

Three cases can be considered:

- Elastic response whereby the maximum of the stress amplitude is at the same position as the maximum of the strain amplitude (no energy dissipation). In this case, there is no time shift between stress and strain sine waves.
- Viscous response whereby the maximum of the stress is at the point of maximum shear rate (i.e. the inflection point) where there is maximum energy dissipation. In this case the strain and stress sine waves are shifted by $\omega t = \pi/2$ (referred to as the phase angle shift δ which in this case is 90°).
- Viscoelastic response: In this case the phase angle shift δ is greater than 0 but less than 90°.

Let us consider the case of a viscoelastic system. The frequency ω is in rad s^{-1} and the time shift between strain and stress sine waves is Δt. The phase angle shift δ is given by (in dimensionless units of radians),

$$\delta = \omega\,\Delta t. \tag{13.10}$$

As discussed in Chapter 14 of Vol. 1,

- for a perfectly elastic solid, $\delta = 0$;
- for a perfectly viscous liquid, $\delta = 90°$;
- for a viscoelastic system, $0 < \delta < 90°$.

The ratio of the maximum stress σ_0 to the maximum strain γ_0 gives the complex modulus $|G^*|$,

$$|G^*| = \frac{\sigma_0}{\gamma_0}. \tag{13.11}$$

$|G^*|$ can be resolved into two components, namely the storage (elastic) modulus G' (the real component of the complex modulus) and the loss (viscous) modulus G'' (the

imaginary component of the complex modulus),

$$|G^*| = G' + \mathrm{i}G'', \tag{13.12}$$

where i is the imaginary number that is equal to $(-1)^{1/2}$. The complex modulus can be resolved into G' and G'' using vector analysis and the phase angle shift δ as described in Chapter 14 of Vol. 1,

$$G' = |G^*| \cos \delta \tag{13.13}$$

$$G'' = |G^*| \sin \delta \tag{13.14}$$

$$\tan \delta = \frac{G''}{G'}. \tag{13.15}$$

Dynamic viscosity η',

$$\eta' = \frac{G''}{\omega}. \tag{13.16}$$

Note that $\eta \to \eta(0)$ as $\omega \to 0$.

Both G' and G'' can be expressed in terms of frequency ω and Maxwell relaxation time τ_m by,

$$G'(\omega) = G\frac{(\omega\tau_\mathrm{m})^2}{1 + (\omega\tau_\mathrm{m})^2}, \tag{13.17}$$

$$G''(\omega) = G\frac{\omega\tau_\mathrm{m}}{1 + (\omega\tau_\mathrm{m})^2}. \tag{13.18}$$

In oscillatory techniques, one has to carry two types of experiments, namely strain sweep, where the frequency ω is kept constant (say 1 Hz or 6.28 rad s^{-1}) and G^*, G' and G'' are measured as a function of strain amplitude and frequency sweep where the strain is kept constant (in the linear viscoelastic region) and G^*, G' and G'' are measured as a function of frequency.

In the strain sweep experiments, G^*, G' and G'' remain constant up to a critical strain γ_cr. This is the linear viscoelastic region where the moduli are independent of the applied strain. Above γ_cr, G^* and G' start to decrease whereas G'' starts to increase with further increase in γ_0. This is the nonlinear region. γ_cr may be identified with the critical strain above which the structure starts to "break down". It can also be shown that above another critical strain, G'' becomes higher than G'. This is sometimes referred to as the "melting strain" at which the system becomes more viscous than elastic.

In the oscillatory sweep experiments, the strain γ_0 is fixed in the linear region (taking a mid-point, i.e. a strain that is not too low, where the results may show some "noise" and which is far from γ_cr) and G^*, G' and G'' are then measured as a function of frequency (a range of 10^{-3}–10^2 rad s^{-1} may be chosen depending on the instrument and operator patience). One can identify a characteristic frequency ω^* at which $G' = G''$ (the "crossover point") which can be used to obtain the Maxwell relaxation time τ_m,

$$\tau_\mathrm{m} = \frac{1}{\omega^*}. \tag{13.19}$$

In the low frequency regime, i.e. $\omega < \omega^*$, $G'' > G'$. This corresponds to a long-duration experiment (time is reciprocal to frequency) and hence the system can dissipate energy as viscous flow. In the high frequency regime, i.e. $\omega > \omega^*$, $G' > G''$. This corresponds to a short time experiment where energy dissipation is reduced. At sufficiently high frequencies, $G' \gg G''$. At such a high frequency, $G'' \to 0$ and $G' \approx G^*$. The high frequency modulus $G'(\infty)$ is sometimes referred to as the "rigidity modulus" where the response is mainly elastic. For a viscoelastic solid G' does not become zero at low frequency. G'' still shows a maximum at intermediate frequency.

The cohesive energy density E_c, which is an important parameter for identification of the "strength" of the structure in a dispersion can be obtained from the change of G' with γ_0,

$$E_c = \int_0^{\gamma_{cr}} \sigma \, d\gamma, \tag{13.20}$$

where σ is the stress in the sample, given by,

$$\sigma = G'\gamma. \tag{13.21}$$

$$E_c = \int_0^{\gamma_{cr}} G'\gamma_{cr} \, d\gamma = \frac{1}{2}\gamma_{cr}^2 G'. \tag{13.22}$$

Note that E_c is given in J m^{-3}.

(iv) Normal force

Normal stresses may be responsible for the flow behaviour of some paint formulations. The most well-known and certainly the most dramatic effect is the rod-climbing phenomenon, referred to as the "Weissenberg effect". It is observed when a rotating rod is dipped into a squat vessel containing an elastic liquid. Whereas a Newtonian liquid would be forced to the rim of the vessel by inertia, and thus produce a free surface that is higher at the rim than near the rod, the elastic liquid produces a free surface that is much higher near the rod. The Weissenberg effect may be viewed as a direct consequence of normal stress, which acts like a hoop stress around the rod. This stress causes the liquid to "strangle" the rod and hence move along it.

Consider for example if a material possessing both elasticity and viscosity is placed in the gap between parallel plates. If the upper plate is moved at a constant velocity υ (or shear rate $\dot{\gamma}$), then due to the presence of elasticity (resistance to continuous deformation exerted by the material) the total force exerted on the moving plate is at an angle to the direction of motion. This total force can be resolved into its components, which include a force parallel to and in the same plane as the plate, as well as a component in a plane vertical to the plane of motion and at right angles to the direction of motion. The latter is the normal force. In practical terms, the normal force tries to push the plates apart while there is motion. In practical instruments,

the moving plate must be either held rigidly in the vertical plane, or it can be allowed to move and kept in position by applying an equal and opposite restoring force to counteract the normal force. This approach allows one to measure the normal force.

(v) Extensional (elongational) viscosity

The importance of measurement of viscosity under extensional conditions is well-known in the area of fibre formation, i.e. strongly spinnable materials. However, it has been recognized that measurement of extensional viscosity is of direct relevance in many other areas such as ink-jet printers, roll mills, blade coating, curtain coating, emulsions, suspensions, etc. Thus, measuring the extensional viscosity of paint systems could be important for several applications. With many polymer solutions, the extensional viscosity can be several orders of magnitude higher than the shear viscosity. The same may apply to some paint systems, which contain high molecular weight polymers (rheology modifiers). Unfortunately, measuring extensional viscosity is not easy, although recently some manufacturers have designed special instruments for such experiments.

14 Application of rheological techniques to paint formulations

Any change in the physical or chemical characteristics of a paint formulation is directly reflected in its flow characteristics or rheology. These changes can occur as a result of aging, temperature changes, application of shear, type of dispersion, extent of grinding and mixing as well as addition of special surfactants for some applications. Below a summary is given of the possible physical changes that may occur and their evaluation using rheological techniques.

The aging of paint (during storage) can cause an increase or decrease in consistency. This change in consistency could be due to flocculation that may result from desorption of the dispersant during storage or simply by temperature fluctuations. Some chemical changes may also occur as a result of the reaction between the solid and liquid phases. The change in consistency can be followed by measuring the flow curves at various intervals of time, as is illustrated in Fig. 14.1. This presentation illustrates that the consistency of the paint increases on storage which is most likely due to flocculation. The flow curves can be analyzed using the models described above. Using these models one can calculate the yield value and the viscosity as a function of storage time. Both parameters show an increase with increase in storage time.

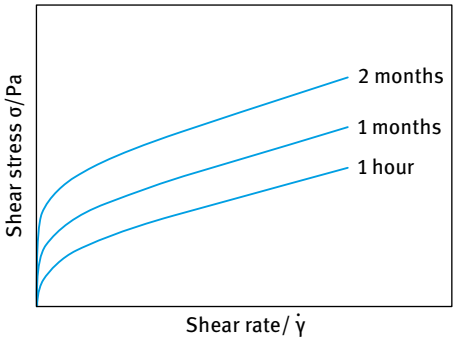

Fig. 14.1: Schematic representation of the change in the flow curve of a paint system at various times.

Another important investigation is to follow the thixotropic behaviour of the paint during storage. As mentioned above, thixotropy can be investigated using the thixotropic loop or the step change method. Any flocculation will also be accompanied by change in the thixotropic behaviour. Clearly, a physically stable paint should show no change in its rheological behaviour during storage for a period of at least least 6 months and also at various temperatures to which the paint system will be subjected.

A more sensitive method for following the change in consistency on storage is constant stress or creep measurements. As discussed above, these measurements allow one to obtain the residual (or zero shear) viscosity $\eta(0)$ as well as the critical stress

https://doi.org/10.1515/9783110588002-016

σ_{cr} above which the structure breaks down. Any increase in $\eta(0)$ and σ_{cr} indicates flocculation of the paint on storage.

A third, sensitive method for following the changes in consistency during storage is the dynamic (oscillatory) method that was described above. By following the change of elastic modulus and cohesive energy during storage, one can obtain information on the flocculation of the paint.

The consistency or the viscosity η of most paint formulations decreases with increase of temperature. However, in some cases the viscosity may increase with increase in temperature when the latter reaches a critical value. In most cases, this is due to sudden flocculation of the paint above a critical temperature (referred to as the critical flocculation temperature, CFT). This flocculation may result from decrease of solvency of the chains to worse than θ-solvent above a critical temperature. Alternatively, the flocculation may occur as a result of desorption of the dispersant at high temperature due to the sudden increase of its solubility.

Due to the above changes in the state of the paint with change of temperature, the viscosity–temperature relationship seldom follows an Arrhenius plot (which shows a linear relationship between $\log \eta$ versus $(1/T)$, where T is the absolute temperature).

A rapid technique for studying the effect of temperature changes on the flocculation of a paint formulation is to carry out temperature sweep experiments, running the samples from, for example, 5–50 °C. The trend in the variation of σ_β and η_{pl} with temperature can quickly give an indication on the temperature range at which a paint remains stable (in that temperature range, σ_β and η_{pl} remain constant).

Most paint formulations consist of a mixture of suspension particles (pigments) and emulsion droplets (latex particles that are liquid-like at room temperature) referred to as suspoemulsions. The continuous medium with viscosity η_0 may simply be an aqueous phase in which several ingredients are dissolved or could be nonaqueous (oil) that may consist of two or more miscible oils. For non-Newtonian systems (which is the case with paint systems), some empirical equations can be established to relate the plastic viscosity η_{pl} and yield value σ_β to the volume fraction of the disperse phase ϕ [66],

$$\eta_{pl} = (\eta_0 + A)\exp(B\phi), \tag{14.1}$$

$$\sigma_\beta = M\exp(n\phi). \tag{14.2}$$

B, M and n are related to particle size, shape and surface. A is independent of particle size but may depend on particle shape and surface. A may be related to particle–particle interaction in the dispersion.

Equations (14.1) and (14.2) predict a linear relationship between $\log \eta_{pl}$ or $\log \sigma_\beta$ and ϕ. This is illustrated in Fig. 14.2 and 14.3, which also show the effect of the average particle diameter (volume to surface ratio d_{32}) of the pigment (20). The smaller the size, the higher the slope. This is illustrated in Fig. 14.4, which shows the variation of the exponents B and n with particle diameter. It is clear that both B and n increase with decrease of d_{32}.

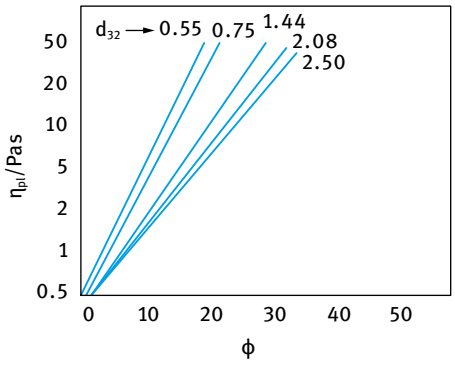

Fig. 14.2: Variation of log η_{pl} with ϕ for leaded ZnO suspensions with different particle diameters d_{32}.

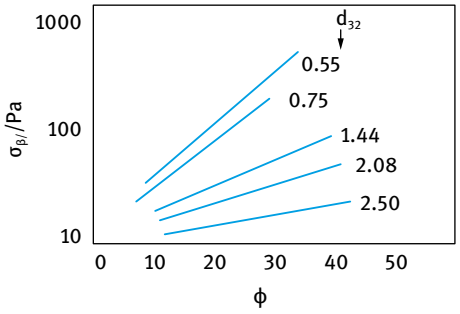

Fig. 14.3: Variation of the yield value σ_β with volume fraction ϕ for ZnO suspensions at various particle diameters d_{32}.

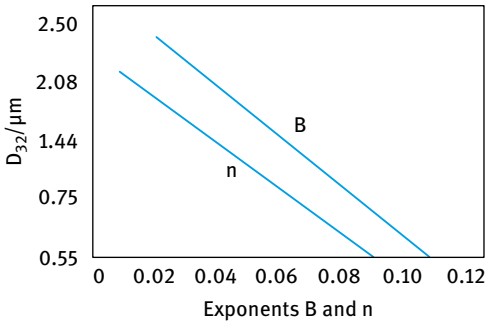

Fig. 14.4: Variation of exponents B and n with average particle diameter d_{32}.

Dispersing agents (mostly polymeric surfactants) are also added to stabilize the particles against aggregation. Both materials affect the viscosity and yield value of the final paint dispersion by adsorption at the solid/liquid interface. The main purpose of wetters and dispersants is to produce "better dispersion" by causing deaggregation and deflocculation. Deaggregation is a mechanical or chemical separation of single particles in an aggregate. The aggregate consisting of these unit particles is "glued"

together thus preventing the liquid from penetrating into the aggregated mass and thus surrounding each unit particle. Deflocculation, on the other hand, can only be affected by the use of a dispersing agent. The mechanical force does not change the state of flocculation. A flocculate is a "loose" but connected structure of particles, whereby the particles are far enough apart to permit the liquid to surround them. However, the particles are sufficiently close to each other with strong van der Waals attraction. Thus, the dispersion will not flow until enough shearing stress is applied to overcome these attractive forces. This shearing stress is proportional to the yield value. A dispersant that is strongly adsorbed to the particle surface and provides sufficient repulsive forces can overcome the van der Waals attraction, thus causing a marked reduction in the yield value.

It should be mentioned that controlled flocculation of a pigment dispersion can be desirable to prevent settling and formation of hard sediments and to control the surface finish of a coating. For pigments dispersed in oil, small quantities of a polar liquid such as alcohol, glycerol and butanol, are used as flocculating agents. For hydrophilic pigments suspended in aqueous media, oils and oil-soluble agents, such as lecithin, can induce flocculation.

In general, increase in the viscosity of a dispersion results in an increase in the efficiency of milling. This is schematically represented in Fig. 14.5 for a three-roller mill, which shows the variation of milling time with the plastic viscosity of the dispersions measured using a rotational viscometer [47].

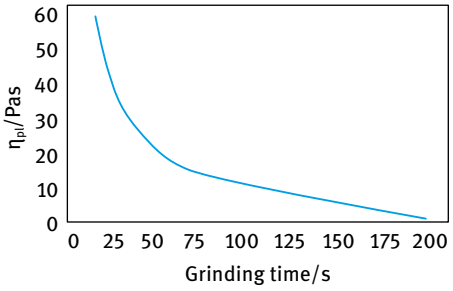

Fig. 14.5: Schematic representation of the effect of dispersion viscosity on grinding time.

It should be mentioned that the trend shown in Fig. 14.5 gives only an indication since the operational viscosity in the three-roller mill is not the same as the plastic viscosity measured using a rotational viscosity. Apparently, the yield value does not affect the grinding efficiency, as long as it is low enough so that the material flows readily from the feed rollers.

In ball milling, the viscosity of the dispersion also plays an important role. A practical viscosity for good operation depends on the nature of the balls. When using steel ball mills, a high viscosity (up to 20 Pa s) can be used. With pebble and porcelain ball mills, a lower viscosity is required since the weight of the grinding medium is lower. It should also be mentioned that the viscosity measured before mixing is substantially

different from that which exists during the mixing operation. The flow properties of the dispersion during the process of grinding change as a result of increase in temperature, increase inwetting, increased degree of aggregation and improved interaction between the solid and liquid phases.

Microscopic investigations showed an increase in deaggregation during milling and this was accompanied by increase in colour strength [67]. This is schematically illustrated in Fig. 14.6, which shows the change of plastic viscosity, yield value and colour strength for a carbon black dispersion in mineral oil. Because the shear rate is much higher during milling than the maximum value measured in a rotational viscometer (usually of the order of 1,000 s^{-1}), the viscosity of a pseudoplastic plastic material will decrease substantially, while its yield value may increase during milling. The viscosity of a thixotropic dispersion will decrease substantially, while its yield value may increase during milling. Thus, to evaluate the grinding performance the consistency of the dispersion at the operational grinding conditions and at different steps of processing has to be determined. This may require measurement of the viscosity at much higher shear rates than encountered with rotational viscometers, as for example determined using capillary viscometers (which can operate at much higher shear rates).

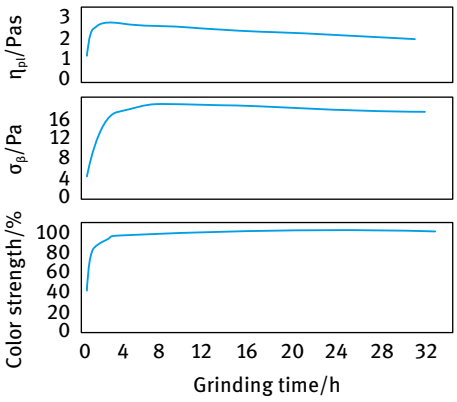

Fig. 14.6: Change in flow properties on colour strength of carbon black suspensions in mineral oil as a function of ball milling time.

From the above discussion, it is clear that rheology is perhaps one of the most powerful techniques for paint evaluation during its formulation as well as in its manufacture. Before a paint is manufactured, its application is known and it is essential to control its flow properties for best operation and application. To control the flow properties of the paint, a rheometer must be selected to make flow measurements, which permits good interpretation of the flow properties of the paint.

This allows the manufacturer to decide whether two batches of the same material or of different materials will have equal flow behaviour under all conditions of operational application. The manufacturer could also predict from these flow measurements whether there is any difference in physical properties on paint application.

In the preoperational stage, physical effects which occur in manufacturing and storing, such as temperature effects, evaporation, mixing procedures and shelf life must be studied. These physical effects can be correlated to the flow characteristics of the paint formulation. This allows one to achieve a more efficient and better controlled operation in manufacture and application.

To date, many paint manufacturers use one-point measurement for measurement of the consistency. This for example can be carried out using a simple Brookfield viscometer using one spindle at a given rpm. This one-point measurement can be misleading [47]. To illustrate this point let us consider three systems, namely Newtonian, Bingham plastic and pseudoplastic with thixotropy as is illustrated in Fig. 14.7.

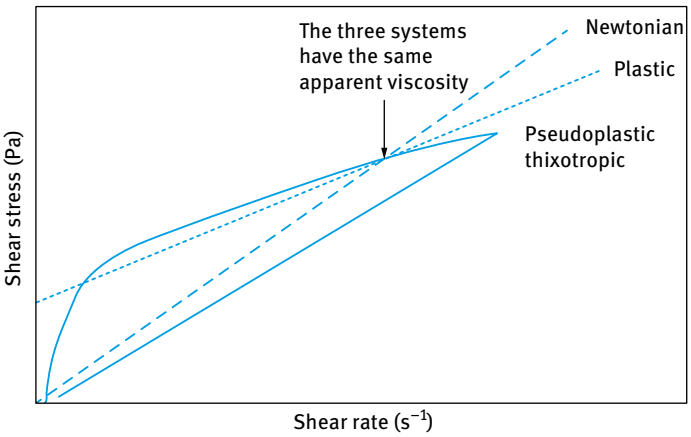

Fig. 14.7: Schematic representation of the flow behaviour of Newtonian, plastic and pseudoplastic (thixotropic) systems.

At a specific shear rate, all three systems show the same apparent viscosity although their flow behaviours (using the full shear-stress curves) are significantly different [47]. These systems show entirely different behaviour on application at the shear rate at which the apparent viscosity is the same. A study of the flow curves indicates that the Newtonian system will flow at extremely low shear rates, whereas the plastic and thixotropic system will show reluctance to do so because of their yield values. This is clearly reflected in the final film properties. Once the yield value is overcome, the viscosity of the paint may become even lower than that of a Newtonian system. At the operational high shear rates, all three systems show different viscosities.

Since most paints are pumped through pipes during manufacture and in application, it is essential to analyze their flow behaviour in pipes. Two types of flow behaviour must be considered:

(i) laminar flow, whereby distinct layers of material pass each other;
(ii) turbulent flow, whereby no distinct layers are observed and all layers mix with one another, forming eddy currents, swirls and vortices.

Whether the flow is laminar or turbulent depends on the dimensionless Reynolds number *Re* that is given by the following equation,

$$Re = \frac{\upsilon l \rho}{\eta}, \tag{14.3}$$

where υ is the mean velocity, x is an instrument length parameter, ρ is the density and η is the viscosity. For laminar flow, $Re \leq 2{,}000$ whereas for turbulent flow $Re \geq 2{,}000$. Thus, when the shear rate exceeds a critical value, the laminar flow changes to turbulent flow. This is reflected in the flow curve, which shows an apparent increase in shear stress above a critical shear rate. This does not mean that the viscosity of the material increases with increase of shear rate (as is the case with dilatant systems) but it indicates that with increasing shear rate the degree of turbulence increases, since part of the increased stress is used to increase the number of eddy currents rather than to increase the flow of the bulk material.

Turbulent flow in pipes, where l is replaced by the mean pipe diameter D, can occur when the Reynolds number exceeds 2,000. Empirical equations have been established for turbulent flow of Newtonian materials [68, 69]:

– For smooth pipes,

$$\frac{1}{\sqrt{f}} = 2\log\left(\frac{Re}{\sqrt{f}}\right) - 0.8. \tag{14.4}$$

– For rough pipes,

$$\frac{1}{\sqrt{f}} = 2\log\left(\frac{D}{2k}\right). \tag{14.5}$$

f is the friction factor that is given by,

$$f = \frac{2DP}{\rho L \upsilon^2} = \frac{64}{Re}, \tag{14.6}$$

where k is the grain diameter that indicates surface roughness, P is the pressure in the pipe and L is the entire length of the pipe.

Thus, for turbulent flow in smooth pipes the flow velocity depends on the Reynolds number and hence on the viscosity.

The pressure that is necessary to pump a material through a pipeline system at a given flow rate depends on the pressure loss in the total pipeline system. Pressure losses are incurred through the viscous resistance of the material in the straight pipeline and in the pipeline transitions such as bends, valves, elbows, pipe expansions and contractions. The viscous losses in the straight pipe lines are frequently large compared to the pipe transitions, so that the latter can sometimes be neglected.

The pressure loss for an entire pipe line system is given by [68, 69],

$$\Delta P = \rho \frac{\upsilon^2}{2}\left[\frac{L}{D}f + C_{\mathrm{L}}\right], \tag{14.7}$$

where C_{L} is the sum of all pressure loss coefficients obtained from all pipe line transitions in the pipe line system.

The flow of Newtonian materials in pipe lines under laminar flow is well understood and is given by Poiseuille's equation,

$$\eta = \frac{\pi R^4 P}{8QL}, \tag{14.8}$$

where Q is the volumetric flow ($m^3\,s^{-1}$) and R is the pipe radius.

In turbulent flow, the flow for Newtonian systems is given by equations (14.4) and (14.5).

The flow of non-Newtonian materials (as is the case with paints) in pipelines is not as well understood. However, Buckingham [70] derived the following equation for evaluating the plastic viscosity of a Bingham plastic system from the flow curve in a capillary viscometer (assuming end effects, kinetic energy effects and slippage flow are absent),

$$\eta_{\text{pl}} = \frac{\pi P R^4}{8QL}\left[1 - \frac{8L\sigma_\beta}{3RP} + \frac{1}{3}\left(\frac{2L\sigma_\beta}{RP}\right)^4\right]. \tag{14.9}$$

Equation (14.9) can be used to determine the laminar flow of plastic materials in pipe lines, where R is the pipe radius. For pseudoplastic and dilatant materials, the power law equation can be used,

$$\eta = k\dot{\gamma}^{n-1}, \tag{14.10}$$

where k is the consistency index and n is the shear thinning index ($n < 1$ for pseudoplastic materials).

For a Bingham plastic in laminar flow the friction factor f is given by,

$$f = \frac{64}{Re}\frac{Pl}{8s}, \tag{14.11}$$

where Pl is the plasticity number that is given by,

$$Pl = \frac{\sigma_\beta D}{U\upsilon}, \tag{14.12}$$

where U is the coefficient of plastic viscosity and υ is the velocity.

s is the ratio of yield value to the shear stress at the wall. Since s is a function of Pl, the friction factor for Bingham plastics is fully determined from Re and Pl.

For pseudoplastic materials in laminar flow, the friction factor is given by [68, 69],

$$f = \frac{64}{Re}\left(\frac{3+N}{4}\right), \tag{14.13}$$

where $N = 1/n$. Thus, the friction factor for pseudoplastic materials is fully determined from Re and N.

The shear rate in the pipe line for the flow of pseudoplastic materials is given by [68, 69],

$$\dot{\gamma} = \frac{2\upsilon(N+3)}{D}. \tag{14.14}$$

The apparent viscosity that is to be used in the Reynolds number has to be measured in the viscometer at the pipeline shear rate. This can be obtained by fitting the flow curve to the power law relationship given by equation (13.1).

In turbulent non-Newtonian flow, the friction factor is a unique function of the Reynolds number. For Bingham plastic systems, the Reynold number is calculated by using the plastic viscosity since it remains constant with increasing shear rates. For pseudoplastic flow, the Reynolds number is calculated by using an estimated apparent viscosity that is obtained by extrapolation to infinite shear rate.

15 Examples of the flow properties of some commercial paints

Most commercial paints have flow characteristics similar to thixotropic plastic materials [71–73]. Typical examples of the flow characteristics of some paints are given in Tab. 15.1.

The above results were obtained at the same shear rate (using a Stormer-type concentric cylinder and they clearly show similar flow characteristics with viscosities of less than 0.4 Pa s and yield values not exceeding 12 Pa).

The rheological behaviour of a paint and a lacquer during and after application determines the smoothness and perfection of the resulting film surface. Paints are applied by brushing, dipping, flow coating and spraying. The flow-out of the material between the time of application and drying always determines the characteristics of the finished surface. The time required for flow-out of oils of different viscosities on a non-porous surface depends on the layer thickness, as is illustrated in Tab. 15.2.

The above results show that leveling to a smoother film takes less time with lower viscosity paints and for films with greater thicknesses. However, one should remember that the film viscosity continues to increase while drying and leveling proceed. Generally speaking, the flow-out is usually complete in about 1 min if the viscosity does not exceed 0.1 Pa s. Most paints require longer flow-out time since the viscosity is higher than 0.1 Pa s at 1 min after deposition.

Tab. 15.1: Flow properties of some commercial paints.

Product	η (Pa s)	σ_β (Pa)	Degree of thixotropy
Enamel, gloss	0.14–0.39	0–3	Nil to slight
Enamels, semi-gloss	0.10–0.35	5–12	slight
Flat or matte paints	0.06–0.10	2–10	Slight to marked
Wall, water-dispersible	0.02–0.14	1–10	Slight to marked
Primers, metal	0.03–0.12	0–10	Nil to marked
Varnishes	0.09–0.29	0	Nil

Tab. 15.2: Approximate time of leveling of oil films on a non-porous substrate as a function of viscosity and film thickness.

η (Pa s)	Leveling time (min)	Film thickness (mm)
< 0.05	< 1	0.5–5.0
0.20	5	0.5
0.20	< 0.5	$\gg 0.5$
1.0	> 120	0.5
1.0	10	$\gg 0.5$

https://doi.org/10.1515/9783110588002-017

The shear rate produced by brushing paints on a surface was estimated to range from 130 to 260 s^{-1}. This value can be obtained by determining the shear rate at which the order of apparent viscosities of thyrotrophic paints exhibiting entirely different flow behaviour coincide with the order of ease of flow indicated by practical brushing. Alternatively, the shear rate can be calculated by assuming that the brushing velocity is 0.2 ms^{-1} for a distance between the substrate and the brush of about 0.001 m (this gives a shear rate of 200 s^{-1}). However, other authors have assumed much higher shear rates (about 100 times higher). Various other investigators have tried to correlate the flow behaviour of paints with their brushing behaviour. In general, paints have good brushing properties if the plastic viscosity ranges from 0.2 to 0.5 Pa s and the yield value from 40 to 140 Pa. Both the plastic viscosity and yield value increase with increase of solvent evaporation (particularly for nonaqueous paints based on volatile solvents. This is illustrated in Tab. 15.3 for brushed black enamel paint [71].

Tab. 15.3: Change in flow properties of a brushed black enamel.

Time (min)	η_{pl} (Pa s)	σ_β (Pa)	Type of flow
0	0.19	0	Newtonian
2.5	1.4	2.4	Plastic
5.0	3.0	52.0	Thyrotrophic plastic
7.5	16.7	620.0	Thixotropic plastic

A paint is considered to have good brushing properties when all brush marks disappear during the drying process. This might be achieved by rapid flow-out caused by low viscosity and low yield value or by taking advantage of the thixotropic behaviour of the paint. Low viscosity and low yield value often lead to sag marks and "curtains", since the low consistency causes the paint to continue to flow after application until drying is sufficiently advanced. Sagging can also appear if the film is applied in a layer that is too thick. The thixotropic properties have the advantage of giving the paint the low operational consistency needed for initial flow-out in order to prevent the brush marks and to obtain good leveling. At the same time, they provide the paint with a mechanism for increasing the consistency by means of the thixotropic build-up of the structure that can be effective immediately after application. However, a too rapid thixotropic build-up can be detrimental because leveling and flow-out are not instantaneous. It has been shown [26, 27] that thixotropic paints which decrease in consistency rapidly with increase of shear rate but rebuild the structure slowly exhibit the best leveling characteristics. A too rapid increase in thixotropic structure can produce poor leveling.

The viscosity of paints and lacquers that are applied by spraying (using for example a spray-gun) range from 0.04 to 0.12 Pa s. For hot sprays that are applied at about 75 °C, the viscosity should be adjusted to about 0.2 Pa s at room temperature, so that

it will be less than 0.1 Pa s at the spraying temperature. The viscosity of hot plastic paints that are sprayed at temperatures around 150 °C should be less than 0.15 Pa s. The viscosity of the paint is usually adjusted by addition of solvent. The viscosity of the bulk paint has to be this low for spray-operations because it will substantially increase when the solvent evaporates during the spraying process (from the time it leaves the spray nozzle to the time when it hits the substrate on which it is to be coated). The increase in viscosity depends on the solvent volatility.

When applying a paint by spraying, the droplet size of the spray will greatly influence the appearance of the finished surface. A fine spray will produce a glossy surface, whereas a coarse spray will give a matte finish, unless leveling occurs before drying is completed. The drop size of the spray depends on the physical properties of the paint such as its surface tension, its viscosity and density. Other parameters such as the flow rate, the relative velocities of the liquid and air also affect the spray droplet spectrum.

References

[1] Lambourne R, editor. Paint and surface coating. Chichester: Ellis Horwood; 1987.
[2] Tadros T. Colloids in paints. Germany: Wiley-VCH; 2010.
[3] Hildebrand JH, Scott R. The solubility of non-electrolytes. 3rd ed. New York: Reinhold; 1950.
[4] Hildebrand JH, Scott R. Regular solutions. Englewood Cliffs, NJ: Princeton Hall; 1962.
[5] Hansen CM. J. Paint Technology. 1967;39(505):104. 1967;39(511):505.
[6] Barton AFM. Handbook of solubility parameters. New York: CRC Press; 1983.
[7] Tadros T. Rheology of dispersions. Germany: Wiley VCH; 2010.
[8] Blakely DC. Emulsion polymerization. London: Elsevier, Applied Science; 1975.
[9] Litchi G, Gilbert RG, Napper DH. J Polym Sci. 1983;21:269.
[10] Feeney PJ, Napper DH, Gilbert RG. Macromolecules. 1984;17:2520. 1987;20:2922.
[11] Smith WV, Ewart RH. J Chem Phys. 1948;16:592.
[12] Piirma I. Polymeric surfactants. New York: Marcel Dekker; 1992.
[13] Piirma I, Lenzotti JR. Br Polymer J. 1959;21:45.
[14] Nestor J, Esquena J, Solans C, Levecke B, Booten K, Tadros T. Langmuir. 2005;21:4837.
[15] Nestor J, Esquena K, Solans C, Luckham PF, Levecke B, Tadros T. J Colloid Interface Sci. 2007;311:430.
[16] Barrett KEJ, Thomas HR. J Polymer Sci, Part A1. 1969;7:2627.
[17] Napper DH. Polymeric stabilization of colloidal dispersions. London: Academic Press; 1983.
[18] Dawkins JV, Taylor G. Polymer. 1987;20:171.
[19] Antl I, Goodwin JW, Hill RD, Ottewill RH, Owen SM, Papworth S, Waters JA. Colloids Surf. 1986;1:67.
[20] Barrett KEJ, editor. Dispersion polymerization in organic media. Chichester: John Wiley & Sons, Ltd; 1975.
[21] Lok KP, Ober CK. Can. J. Cjem. 1985;63:209.
[22] Paine AJ. J. Polymer Sci. Part A. 1990;28:2485.
[23] Tadros T. Dispersion of powders in liquids and stabilization of suspensions. Germany: Wiley-VCH; 2012.
[24] Rideal EK. Phil Mag. 1922;44:1152.
[25] Washburn ED. Phys Rev. 1921;17:273.
[26] Rehbinder PA. Colloid J. USSR. 1958;20:493.
[27] Hamaker HC. Physica. 1937;4:1058.
[28] Deryaguin BV, Landau L. Acta Physicochim. USSR. 1941;14:633.
[29] Verwey EJW, Overbeek J. Theory of stability of lyophobic colloids. Amsterdam: Elsevier; 1948.
[30] Napper DH. Polymeric stabilization of colloidal dispersions. London: Academic Press; 1983.
[31] Gouy G. J. Phys. 1910;9(4): 457. Ann Phys. 1917;7(9):129.
[32] Chapman DL. Phil Mag. 1913;25(6):475.
[33] Smoluchowski MV. Z Phys Chem. 1927;92:129.
[34] Fuchs N. Z Physik. 1936;89:736.
[35] Reerink H, Overbeek J. Disc Faraday Soc. 1954;18:74.
[36] Tadros T. Polymeric surfactants. Berlin: De Gruyter; 2017.
[37] Asakura A, Oosawa F. J Chem Phys. 1954;22:1235. J Polymer Sci. 1958;93:183.
[38] Hull M, Kitchener SA. Trans Faraday Soc. 1969;65:3039.
[39] Tadros T. Unpublished results.
[40] Deyaguin BV, Smilga VP. Proc Intern Congr Surface Activity 3r, Cologne, II, Dec. B; 1960. p. 349.
[41] Deryaguin BV. Kolloid Z. 1934;69:155.
[42] Fox HW, Zisman WA. J Colloid Sci. 1952;109(7):428.

https://doi.org/10.1515/9783110588002-018

[43] Neuman AW. Advances Colloid and Interface Sci. 1974;4:105.
[44] Krupp H. Advances Colloid Interface Sci. 1967;1:111.
[45] Visser J. J Colloid Interface Sci. 1970;34:26.
[46] Tadros T. Unpublished results.
[47] Strivens TA. In: Lambourne R, editor. Paint and surface coatings. Chichester: Ellis Horwood; 1987.
[48] Glass JE. Coatings Technol. 1978;50:56.
[49] Patton TC. Paint flow and pigment dispersion. New York: Wiley-Interscience; 1979.
[50] Kuge Y. Coating Technol. 1983;55:59.
[51] Smith NPD, Orchard SE, Rhind-Tutt A. J Oil and Colloid Chemistry Assoc. 1961;44:618.
[52] Pearson JAR. J Fluid Mech. 1960;7:481.
[53] Savage MD. J Fluid Mech. 1977;80:473.
[54] Glass JE. Oil Col Chem Assoc. 1975;58:169.
[55] Dodge JS. J Paint Technol. 1972;44:72.
[56] Snow CI. Official Digest. 1957;392:907.
[57] Myers RR. J Polym Science C. 1971;35:3.
[58] van Wazer JR, Lyons JW, Kim KY, Cowell RE. Viscosity and flow measurements. New York: Interscience Publishers; 1983.
[59] Whorlow RW. Rheological techniques. New York: John Wiley and Sons; 1980.
[60] Barnes HA, Hutton JF, Walters K. An introduction to rheology. Amsterdam: Elsevier; 1989.
[61] Goodwin JW, Hughes RW. Rheology for chemists. Cambridge: Royal Society of Chemistry Publication; 2000.
[62] Herschel WH, Bulkley R. Proc Amer Soc Test Materials. 1926;26:621. Kolloid Z. 1926;39:291.
[63] Casson N. In: Mill CC, editor. Rheology of disperse systems. New York: Pergamon Press; 1959. p. 84–104.
[64] Cross MM. J Colloid Interface Sci. 1965;20:417.
[65] Weltman RN. In: Eirich FR, editor. Rheology. Vol. 3. Cambridge: Academic Press; 1960. Chapter 6.
[66] Ferry JD. Viscoelastic properties of polymers. New York: John Wiley & Sons; 1980.
[67] Fischer EK. Ind Eng Chem. 1941;33:1465.
[68] Rouse H, Howe JW. Basic mechanics of fluids. New York: Wiley; 1953.
[69] da C. Andrade EK. Viscosity and plasticity. New York: Chemica Publishing; 1952.
[70] Buckingham E. Proc Am Soc Testing Materials. 1921;21:1154.
[71] Fischer EK. J Colloid Sci. 1950;5:271.
[72] Saunders B. J Oil & Colour Chemists. 1948;31:95.
[73] Jarret MED. J Oil & Colour Chemists. 1948;31:337.

Part III: **The formulation of food colloids**

16 Introduction to the formulation of food colloids

Many foods are colloidal systems containing a dispersed phase of particles, droplets or air bubbles of various kinds dispersed in a liquid medium (the continuous phase) that are stabilized by surfactants and/or polymers. The particles or droplets may aggregate, i.e. stay very close to each other for a much longer time than would be the case in the absence of attractive forces. The dispersed phase or the continuous phase may also become semi-solid or solid as a result of crystallization (e.g. in ice cream or butter) or through gelation, as with meat pastes or dairy deserts. The aggregation and gelation phenomena determine the rheological properties of the system, i.e. the consistency and appearance of the product. In addition, such rheological properties also determine the physical stability/instability of the product, as reflected in a change in consistency or loss of homogeneity. All these phenomena are determined by the interfacial properties of the surfactant and/or polymer used for the preparation of the food colloid. The interfacial properties of these surfactant and/or polymer films are very important in formulating such systems and maintaining their long-term physical stability. Naturally occurring surfactants such as lecithin from egg yolk and various proteins from milk are used for the preparation of many food products such as mayonnaise, salad creams, dressings, deserts, etc. Later, polar lipids such as monoglycerides were introduced as emulsifiers for food products. More recently, synthetic surfactants such as sorbitan esters and their ethoxylates and sucrose esters have been used in food emulsions. For example, esters of monostearate or mono-oleate with organic carboxylic acids, e.g. citric acid are used as antispattering agents in margarine for frying. The particles may remain as individual units suspended in the medium, but in most cases aggregation of these particles takes place, forming three-dimensional structures, generally referred to as "gels". As mentioned above, aggregation phenomena determine the appearance, rheology and physical stability of food colloids. These aggregation structures are determined by the interaction forces between the particles, which are controlled by the relative magnitudes of attractive (van der Waals forces) and repulsive forces. The latter can be electrostatic or steric in nature depending on the composition of the food formulation. It is clear that the repulsive interactions will be determined by the nature of the surfactant/polymer present in the formulation. Such surfactants can be ionic or polar in nature, or they may be polymeric in nature. The latter are sometimes added not only to control the interaction between particles or droplets in the food formulation, but also to control the consistency (rheology) of the system. Many food formulations contain mixtures of surfactants (emulsifiers) and hydrocolloids. The interaction between the surfactant and polymer molecule plays a major role in the overall interaction between the particles or droplets, as well as the bulk rheology of the whole system. Such interactions are complex and require fundamental studies of their colloidal properties. Many food products contain proteins that are used as emulsifiers. The interaction between proteins and hydrocolloids is

https://doi.org/10.1515/9783110588002-019

also very important in determining the interfacial properties and bulk rheology of the system. In addition, the proteins can also interact with the emulsifiers present in the system and this interaction requires particular attention.

A special class of stabilization of foams and emulsions is produced by particulate materials that accumulate at the interface (referred to as Pickering foams or emulsions). This requires an appropriate balance of interfacial free energies such that the particles are wetted preferentially by the continuous phase. A typical food product in which the air phase is stabilized by particles is whipped cream, in which the fat particles adhere to the air bubbles during the whipping process, forming a protective layer and preventing bubble coalescence.

It should be mentioned that application of the colloid theory to foods is not straightforward. Colloid science typically considers the interaction between two identical homogeneous particles (sometimes referred to as "hard-spheres"), whereas most foods contain many particles, varying in size, heterogeneity, deformability and making up a considerable volume fraction. Most foods also contain proteins with complex structures that may adsorb at the interface between the particles or droplets and the medium.

In Chapter 17, the interaction between food grade agent surfactants and water will be described, and the structure of the liquid crystalline phases will be highlighted. Some examples of the binary phase diagrams of the monogylceride–water systems, and the ternary phase diagrams of oil-surfactant-water systems will be given [1]. The role of liquid crystalline phases in the stabilization of emulsions will also be described. Chapter 18 will deal with proteins, which are used in many food emulsions [2]. A brief description of the structure of casein micelles and their primary and secondary structures will be given. These systems are widely used in many food products. A section will be devoted to the interfacial phenomena in food colloids, in particular their dynamic properties and the competitive adsorption of various components at the interface. The interaction between proteins and polysaccharides in food colloids will be briefly described. This is followed by discussion of the interaction between polysaccharides and surfactants. Chapter 19 will deal with surfactant association structures, microemulsions and emulsions in food [3]. Chapter 20 will describe the effect of food surfactants on the interfacial and bulk rheology of food emulsions. The formation of aggregation networks and the application of fractal concepts will then be considered. Chapter 21 will deal with foam stabilization and destabilization of foams in food systems. The last chapter will discuss the application of rheology in studying food texture and mouthfeel.

It should be mentioned that the structures of many food emulsions and foams is complex and in many cases several phases may exist. Such structures may exist under non-equilibrium conditions and the state of the system may depend to a large extent on the process used for preparing the system, its prehistory and the conditions to which it is subjected. It is not surprising, therefore, that fundamental studies of such systems are not easy to carry out and in many cases one is content with some

qualitative observations. However, due to the great demand for the production of consistent food products and the introduction of new recipes, a great deal of fundamental understanding of the physical chemistry of such complex systems is required.

17 Interaction between food-grade agent surfactants and water and structure of the liquid crystalline phases

A review on this subject has been published by Krog et al. [1], to which the reader should refer to for more details. As discussed by these authors, food grade surfactants are, in general, not soluble in water, but they can form association structures in aqueous media that are liquid crystalline in nature. Three main liquid crystalline structures may be distinguished, namely the lamellar phase, the hexagonal phase and the cubic phase. Fig. 17.1 shows a model of the crystalline state of a surfactant which forms a lamellar phase (Fig. 17.1 (a)).

When dispersed in water above its Krafft temperature (T_c) it produces a lamellar mesophase (Fig. 17.1 (b)) with a thickness d_a of the bilayer, a thickness d_w of the water layer. The lamellar layer thickness d is simply $d_a + d_w$. These thicknesses can be determined using low angle X-ray diffraction. The surface area per molecule of surfactant is denoted by S. The lamellar mesophase can be diluted with water and it has almost infinite swelling capacity provided the lipid bilayers contain charged molecules and the water phase has a low ion concentration [4]. These diluted lamellar phases may form liposomes (multilamellar vesicles), which are spherical aggregates with internal lamellar structures [5]. Under the polarizing microscope, the lamellar structures exhibit an "oil-streaky" texture.

When the surfactant solution containing the lamellar phase is cooled below the Krafft temperature of the surfactant, a gel phase is formed, as is schematically shown

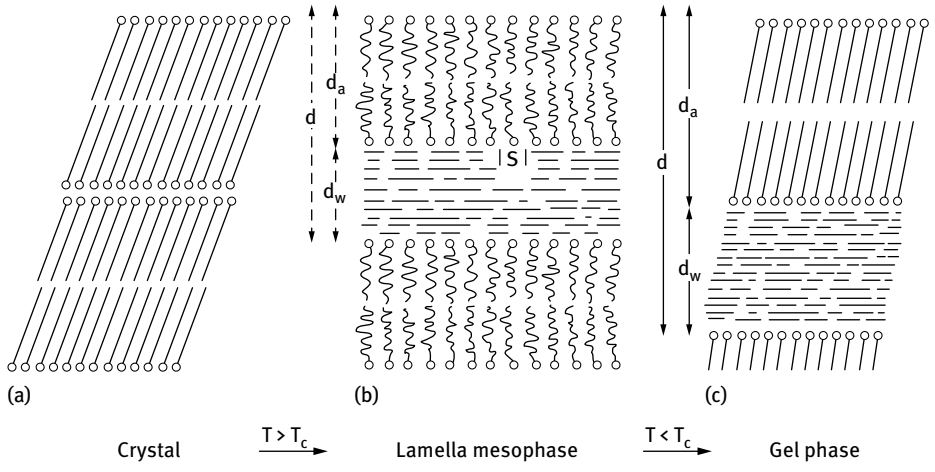

Fig. 17.1: Schematic representation of lamellar liquid crystalline structures.

https://doi.org/10.1515/9783110588002-020

in Fig. 17.1 (c). The crystalline structure of the bilayer is now similar to that of the pure surfactant and the aqueous layer with thickness d_w is the continuous phase of the gel.

The hexagonal mesophase structure is periodic in two dimensions and it exists in two modifications, hexagonal I and hexagonal II. The structure of the hexagonal I phase consists of cylindrical aggregates of surfactant molecules with the polar head groups oriented towards the outer (continuous) water phase and the surfactant hydrocarbon chains filling out the core of the cylinders. These structures show a fan-like or angular texture under the polarizing microscope (see lecture on concentrated surfactant solutions). The hexagonal II phase consists of cylindrical aggregates of water in a continuous medium of surfactant molecules with the polar head groups oriented towards the water phase and the hydrocarbon chains filling out the exterior between the water cylinders. This phase shows the same angular texture under the polarizing microscope as the hexagonal I phase. Whereas the hexagonal I phase can be diluted with water to produce micellar (spherical) solutions, the hexagonal II phase has a limited swelling capacity (usually not more than 40 % water in the cylindrical aggregates).

The viscous isotropic cubic phase, which is periodic in three dimensions, is produced with monogylceride–water systems at chain lengths above C_{14}. This isotropic phase was shown to consist of a bicontinuous structure, consisting of a lamellar bilayer, which separates two water channel systems [6, 7]. The cubic phase behaves as a very viscous liquid phase, which can accommodate up to ≈ 40 % water.

Of the above liquid crystalline structures, the lamellar phase is the most important for food applications. As we will see later, these lamellar structures are very good stabilizers for food emulsions. In addition, they can be diluted with water, forming liposome dispersions which are easy to handle (pumpable liquids) and they interact with water soluble components such as amylose in starch particles. When the hexagonal and cubic phases are formed, by contrast, they create problems in food processing due to their highly viscous nature (viscous particles may block filters).

17.1 Binary phase diagrams

Typical binary (surfactant + water) phase diagrams of monoglycerides are shown in Fig. 17.2 for three molecules with decreasing Krafft temperature (1-monopalmitin, 1-mono-elaidin and 1-mono-olein). With 1-monopalmitin, the dominant mesophase is the lamellar (neat) phase, which swells to a maximum water layer thickness, d_w, of 2.1 nm at 40 % water. At higher water content (> 60 %), a disperse phase is produced in the temperature range 55–68 °C, whereas above 68 °C a cubic phase in equilibrium with water is formed. With the mono-elaidin–water phase diagram (Fig. 17.2 (b)), the lamellar region becomes smaller, whereas the cubic phase region becomes larger, when compared with the monopalmitin–water phase diagram. The temperature at which the lamellar phase is formed (Krafft point) is decreased from 55 to 33 °C.

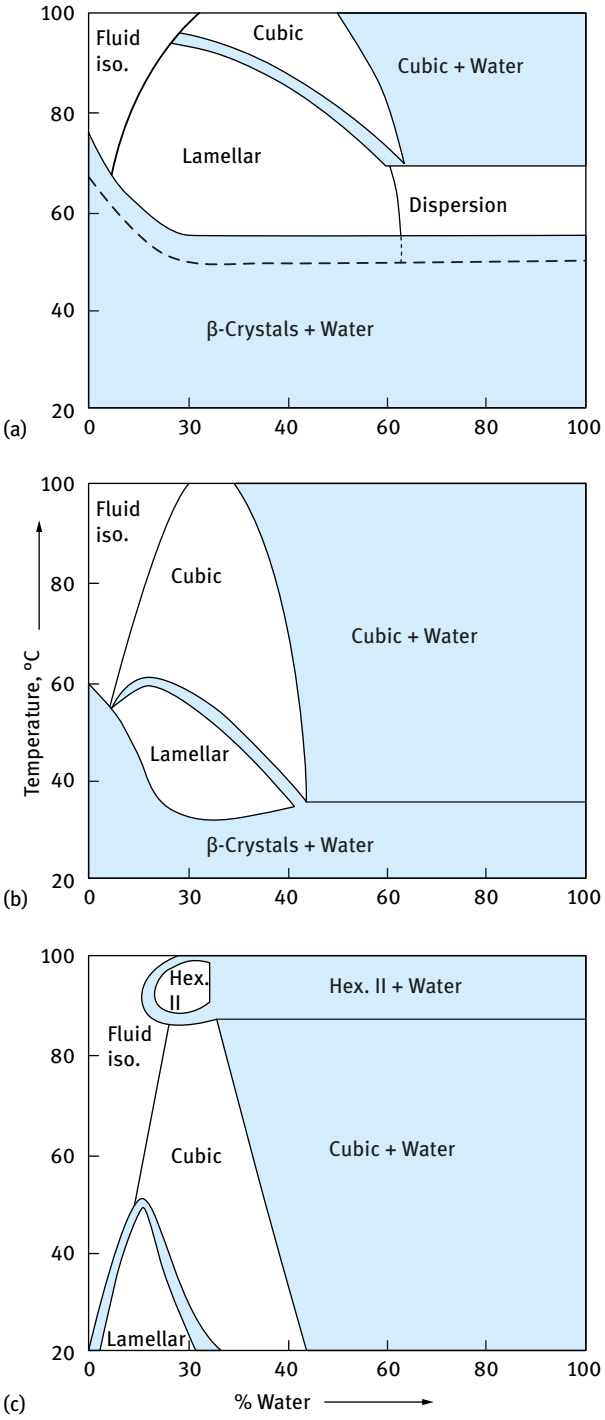

Fig. 17.2: Binary phase diagrams of pure 1-monoglycerides in water: (a) 1-monopalmitin; (b) mono-elaidin; (c) mono-olein.

At higher water concentrations (> 40 %), the mono-elaidin forms a cubic phase in equilibrium with bulk water. The mono-olein–water phase diagram shows the formation of lamellar liquid crystalline structure at room temperature (20 °C) at water content between 2 and 20 %. At higher water concentrations, a cubic phase is formed which exists in equilibrium with water above 40 % water. If the temperature of the cubic phase is increased above 90 °C, a hexagonal II phase is produced, which may contain up to 25 % water in the cylindrical aggregates.

Commercial distilled monoglycerides from edible fats (lard, tallow or vegetable oils) exhibit similar mesophase formations to pure monoglycerides. This is illustrated in Fig. 17.3, which shows the binary phase diagram of saturated, distilled monoglycerides based on hydrogenated lard (monopalmitin/monostearin ratio 30 : 65)

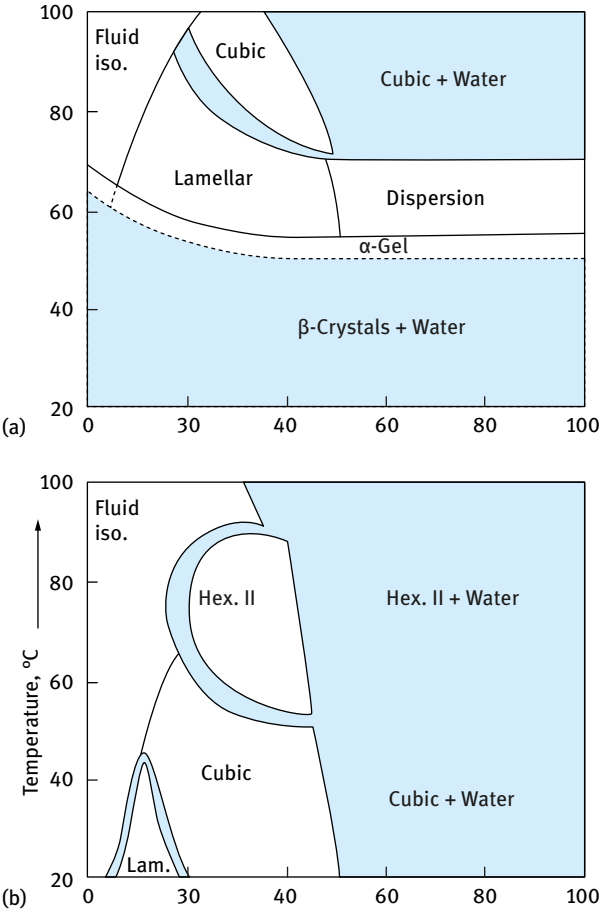

Fig. 17.3: Binary-phase diagrams of commercial, distilled saturated monoglycerides (a) and unsaturated monoglycerides (b).

(Fig. 17.3 (a)) and unsaturated, distilled monoglycerides based on sunflower oil containing 21 % mono-olein, 68 % monolinolein and 11 % saturated (C_{16}/C_{18}) monoglycerides (Fig. 17.3 (b)).

The phase regions may differ in size depending on the purity and fatty acid composition of the commercial monoglycerides. As mentioned above, the continuous swelling of the lamellar phase in the water rich region of the phase diagram is controlled by the charge of the lipid, which can be obtained by neutralization of the free fatty acid in the monoglyceride (by adding sodium bicarbonate or sodium hydroxide). The formation of charged RCOO- molecules in the lipid bilayer of the lamellar phase increases swelling by water, owing to the electric repulsion effect. This has been confirmed using low angle X-ray diffraction methods to measure the water thickness. This is illustrated in Fig. 17.4, which sows the X-ray data of lamellar phases on fully hydrogenated lard (C_{16}/C_{18} 35 : 65) in distilled water at 60 °C.(a) without neutralization and (b) with neutralization of the free fatty acids present (0.8 %).

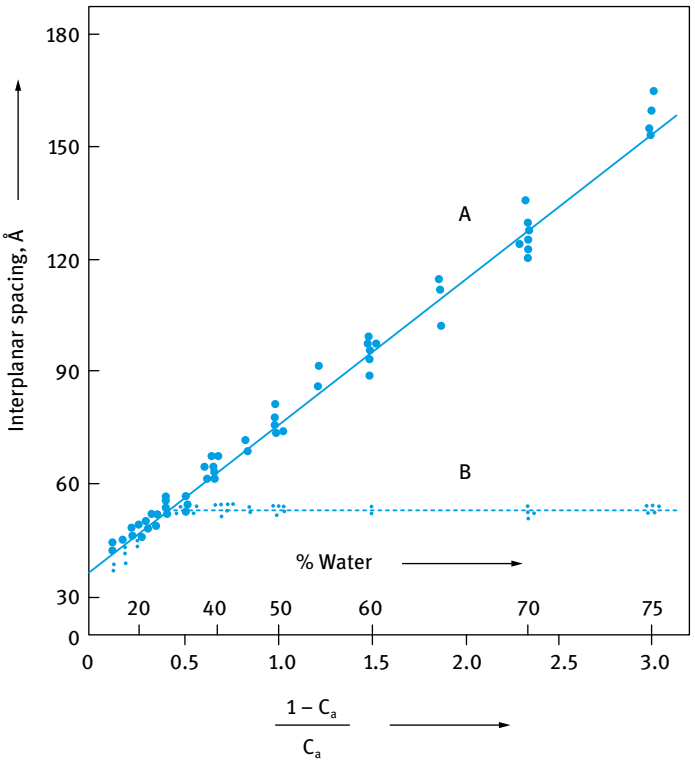

Fig. 17.4: X-ray data of monoglyceride–water lamellar phases at 60 °C: A, with neutralized free fatty acid; B, without neutralization.

It can be seen from Fig. 17.4 that without neutralization, maximum swelling occurs at 30 % water corresponding to a water layer thickness (d_w) of 1.6 nm. After neutralization of the free fatty acid with 1 mol dm^{-3} NaOH, the swelling is strongly increased. At a water concentration of 75 %, the lamellar phase has a water layer thickness (d_w) of 11.6 nm between the lipid layers. At higher water concentrations (> 95 %), these neutralized monoglycerides form transparent dispersions (liposomes).

The phase diagram of pure soybean lecithin–water system is shown in Fig. 17.5. The excess water region, relevant to emulsions based on this surfactant, consists of a dispersion of the lamellar liquid crystalline phase in the form of liposomes.

When a liquid-crystalline mesophase of a surfactant–water system is cooled below the Krafft point, a gel is formed. In the gel state, the lipid bilayers are separated by alternating water layers like in the lamellar phase. The hydrocarbon bilayers are solidified into an α-crystal form with a hexagonal subcell backing (short spacing 0.415 nm) and they are tilted 54° toward the water layer. A gel of distilled monoglycerides containing 75 % (w/w) water and approximately 0.5 % neutralized fatty acids shows X-ray

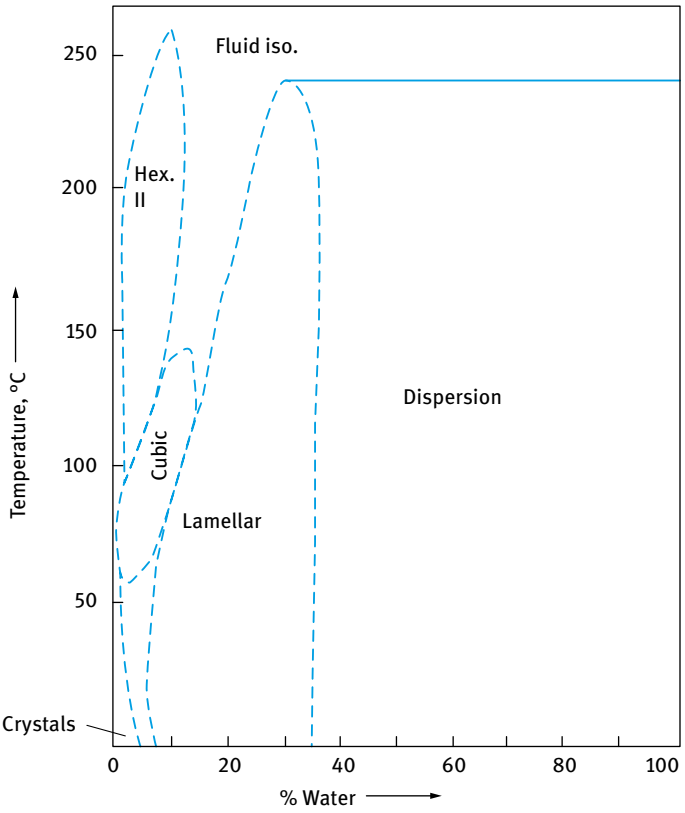

Fig. 17.5: Binary phase diagram of soybean lecithin–water system.

diffraction Bragg spacings of about 23 nm corresponding of a water layer thickness (d_w) of 17.5 nm and a lipid bilayer thickness (d_a) of 5.5 nm. The specific surface in contact with water is 2.2 nm in the gel phase. Fig. 17.6 shows the X-ray data of a gel phase.

The gel phase is very sensitive to electrolytes in water; 0.05 % (w/w) NaCl is enough to prevent swelling of the monoglyceride gel containing 70 % water which corresponds to a decrease in the water thickness (d_w) from 13.6 nm to about 0.9 nm. Gel phases of monoglycerides with other surfactants such as propylene glycol monostearate or polysorbate 60 containing 50–70 % water are used as aerating agents in cakes and other food products.

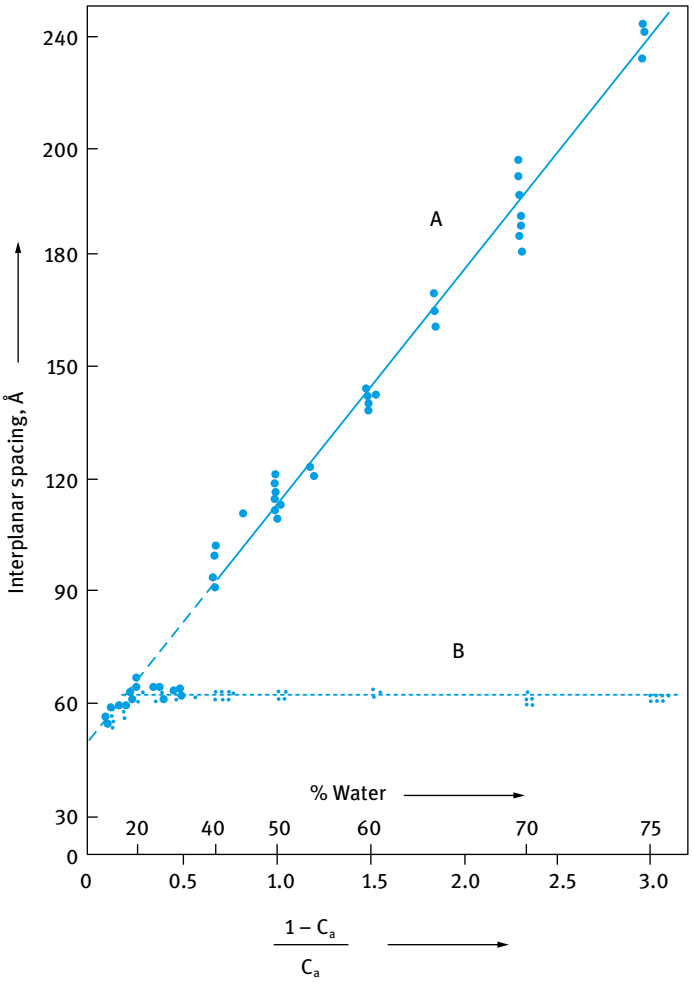

Fig. 17.6: X-ray data of monoglyceride–water gel phases at 25 °C: A, with neutralized free fatty acid; B, without neutralization.

17.2 Ternary phase diagrams

A typical ternary phase diagram of soybean oil (triglyceride), sunflower oil monoglyceride and water at 25 °C [8] is shown in Fig. 17.7. It clearly shows the L_C phase and the inverse micellar (L_2) phase. This inverse micellar phase is relevant to the formation of water-in-oil emulsions. The interfacial tension between the micellar L_2 phase and water is ≈ 1–2 mN m^{-1} and that between the L_2 and oils is even lower. It is proposed that the L_2 phase forms an interfacial film during emulsification, and the droplet size distribution should then be expected to be related mainly to the interfacial and rheological properties of the L_2 phase.

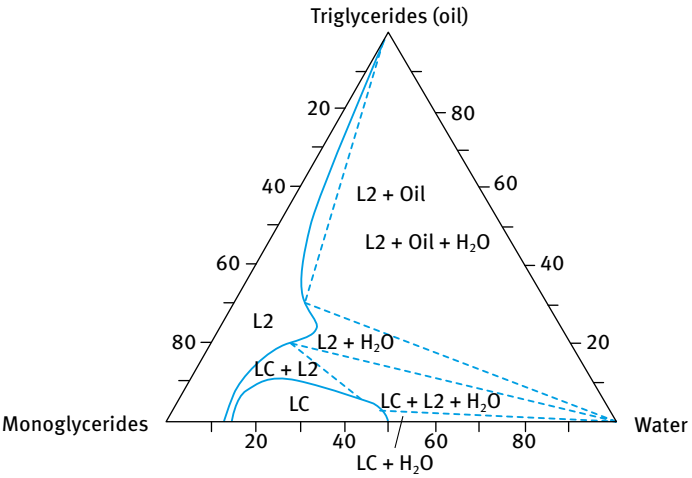

Fig. 17.7: Ternary phase diagram of soybean oil–sunflower oil monoglyceride and water.

17.3 Monolayer formation

The formation of a monomolecular film of the emulsifier at the oil/water (O/W) interface is a crucial factor in the emulsification process. Experimentally, it is easier to study lipid monolayers at the air/water (A/W) interface compared to the O/W interface. However, recently, studies at the O/W interface became possible using drop profile techniques. The results showed similar trends as observed at the A/W interface. As an illustration, Fig. 17.8 shows the variation of the film pressure π with concentration of pure 1-mono-olein spread on the water surface at 20 °C.

The results of Fig. 17.8 show a steep rise of surface pressure at a critical surfactant concentration (≈ 10^{-6} mol dm^{-3}) and this concentration corresponds to the highest monomer concentration in bulk solution. Above 10^{-6} mol dm^{-3}, the lipid monomers begin to associate. Surface pressure measurements at the air-water interface showed

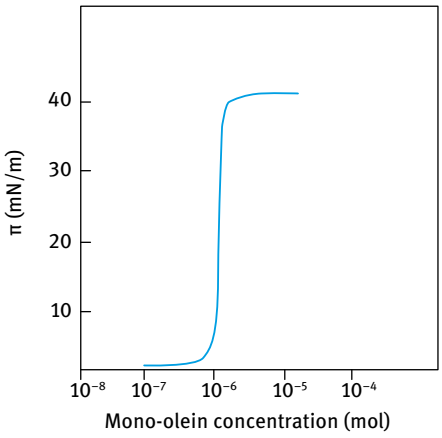

Fig. 17.8: Surface film pressure (π) versus concentration of pure 1-mono-olein spread on the water surface at 20 °C.

that the lipid molecules begin to associate to form a cubic structure. Monoglycerides of saturated fatty acids associate to form lamellar liquid crystalline phase or the gel phase at low concentrations. These condensed layers form at the oil–water interface at and above the critical temperature T_c, which is the temperature used for emulsification. These liquid crystalline phases play a major role in emulsion stabilization. It is necessary to have enough polar lipids to form a stabilizing film at the O/W interface, and this is not possible until the maximum of monomer concentration in the bulk is exceeded.

Hydrophilic emulsifiers, which in bulk form micellar solutions, exhibit a different monolayer behaviour. The interfacial tension γ shows a linear decrease with log concentration until the critical micelle concentration is reached after which γ remains virtually constant with further increase in surfactant concentration. However, most surfactants used in food emulsions do not form micellar solutions.

One of the most informative techniques for studying monolayer formation that are relevant to emulsification is to measure the surface pressure as a function of molecular area using a surface balance (Langmuir trough). In this method, the surfactant film is spread at the A/W or O/W interface between two barriers placed in the Langmuir trough. One of the barriers is fixed whereas the second can be moved to reduce the area occupied by the film. The surface or interfacial tension γ is monitored using a Wilhelmy plate, which can be attached to a microbalance thus measuring the force and hence calculating γ. In this way, surface pressure (π)–area/molecule (A) isotherms can be established. As an illustration, Fig. 17.9 shows the π–A isotherms (at 25 °C) for pure 1-monomyristin at the A/W interface. It can be seen that π shows a gradual increase with decrease of A reaching a plateau at $\approx 27\ \mathrm{mN\ m^{-1}}$ where a monolayer with liquid hydrocarbon chains, referred to as form I, can coexist with a monolayer with liquid crystalline chains, referred to as form II. The cross sectional area per molecule at this pressure of form I is 2.85 $\mathrm{nm^2}$ (28.5 $\mathrm{Å^2}$), which is in good agreement with that of the lamellar liquid crystalline phase. The molecular surface area at this transition of

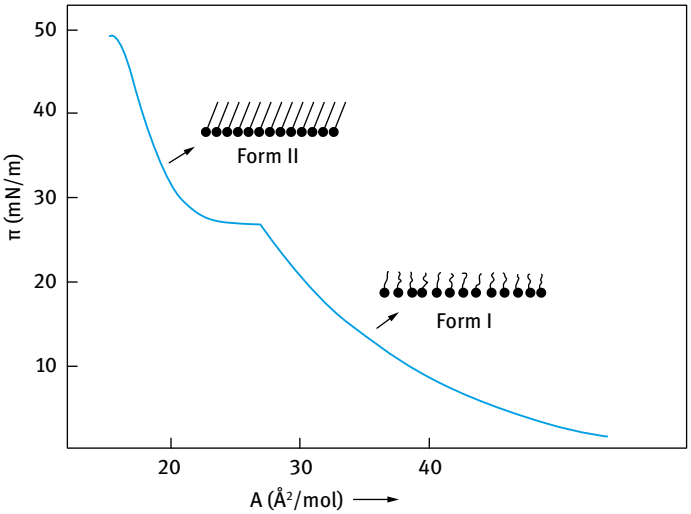

Fig. 17.9: π–A isotherm of pure 1-monomyristin at 25 °C.

form II is 2.25 nm^2, which is identical to that of the liquid crystalline structure in the gel phase.

The variation of the transition between form I and form II with temperature is shown in Fig. 17.10. The pressure of the transition plateau increases with temperature, and above a temperature of 42 °C no solid condensed monolayer (form II) is formed. This temperature also agrees with the temperature of transition from the crystalline state to the lamellar liquid crystalline state in the aqueous system of monomyristin.

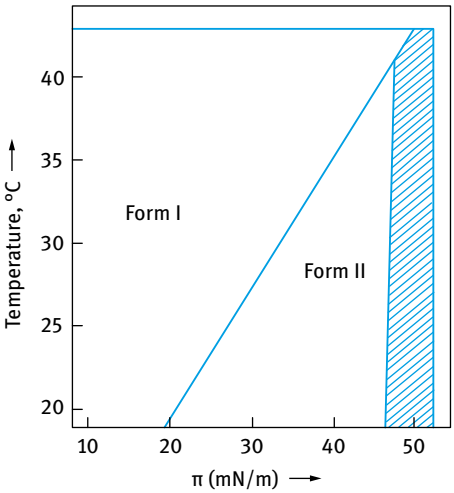

Fig. 17.10: Phase changes of 1-monomyristin monolayers at the A/W interface as a function of temperature. The shaded area shows the region above the collapse of the monolayer.

The corresponding relations between temperatures and monolayer film pressure of forms I and II in the case of monoelaidin is shown in Fig. 17.11. Monoelaidin, having a trans double bond, exhibits monolayers with liquid crystalline chains (form II) up to about 30 °C. The relation between the monolayer transitions and the corresponding bilk phase transition in the binary phase diagram of monoelaidin/water (Fig. 17.2 (b)) is thus very close. Mono-olein shows only monolayers with liquid chains (form I) at all temperatures between 0 and 100 °C, which is in agreement with the phase diagram of mono-olein/water shown in Fig. 17.2 (c).

The equilibrium surface pressure of the α-crystal form of monomyristin was also followed as a function of temperature, and it was found to have the same value as the plateau pressure at the transition from I to form II. One can then assume that the monolayer formed when excess of the α-crystal form is present has the structure illustrated as form II in Fig. 17.11. The agreement between molecular areas and transition temperatures indicates that the hydrocarbon chain structure of monolayer forms I and II is identical to that of the liquid crystalline phases and the α-crystalline gel phase, respectively.

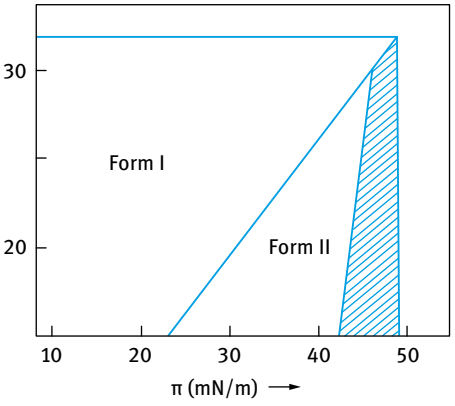

Fig. 17.11: Phase changes of 1-monoelaidin at the A/W interface as a function of temperature. The shaded area shows the region above collapse of the monolayer.

The liquid crystalline state of the monolayer, which is always formed at a temperature above the existence of the crystalline monolayer, possesses ideal rheological properties. The monolayer with liquid hydrocarbon chains (form I) can thus vary its curvature and cross-sectional area per molecule over wide ranges. Under certain conditions, however, it is possible to crystallize the monolayer after the emulsion has been formed.

17.4 Liquid crystalline phases and emulsion stability

A maximum in emulsion stability is obtained when three phases exist in equilibrium, and it was therefore proposed that the lamellar liquid crystalline phase stabilizes the emulsion by forming a film at the O/W interface. This film provides a barrier against coalescence. This is illustrated in Fig. 17.12, which shows that the lamellar liquid crystalline phase exhibits a hydrophobic surface towards the oil and a hydrophilic surface towards the water. These multilayers cause a significant reduction in the attraction potential and they also produce a viscoelastic film with much higher viscosity than that of the oil droplet. In other words, the multilayers produce a form of "mechanical barrier" against coalescence.

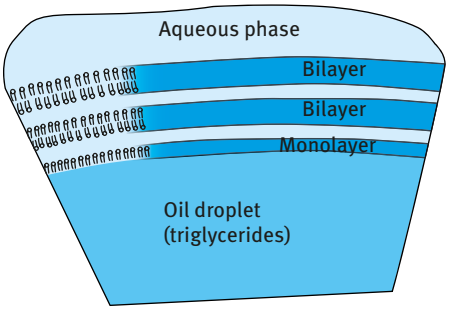

Fig. 17.12: Schematic representation of the lamellar liquid crystalline structure at the oil/water interface.

The rheological properties of monolayers of binary surfactant mixtures has been related to emulsion stability as will be discussed in Chapter 19 and to the structural properties of the lamellar liquid crystalline phases formed by the surfactant in water. It was suggested that the emulsifier molecules adsorbed at the O/W interface will adopt the same hydrocarbon chain structure as they have in the bimolecular lipid layer of lamellar mesophases. Other liquid crystalline phases than the lamellar phase can also occur at the O/W interface. Fluctuations of interfacial tension at the dodecane/water interface with a sodium sulphonate surfactant has been observed and this was attributed to the formation of a liquid crystalline phase of the hexagonal type at the interface. As mentioned above, the enhanced emulsion stability in the presence of lipid multilayers at the interface is related to the reduced attraction potential. In addition, the multilayer viscosity is considerably higher than that of the oil phase. Also, the lamellar liquid crystalline phase results in a repulsive force that is usually referred to as hydration force (see below).

Another important repulsive force that occurs when the surfactant film contains charged molecules, e.g. on addition of sodium stearate to lecithin, is the double layer repulsion arising from these ionogenic groups. An obvious consequence of the presence of charged chains is the increased distance between the surfactant bilayers.

The transition between the lamellar liquid crystalline phase and the gel phase can be utilized to stabilize the emulsion, provided the actual gel phase is stable. If an aqueous dispersion of the emulsifier is first formed, and the emulsification is then performed under cooling, an emulsion is formed with the gel phase forming the O/W interface. Such an emulsion has a much higher stability when compared with that produced with the lamellar phase at the O/W interface. This is probably due to the higher mechanical stability of the crystalline lipid bilayers compared to bilayers with liquid chain conformation.

Another repulsive force between the lipid bilayers in water is the hydration force, which is a short range force with exponential falloff. This is related to repulsion between dipoles and induced dipoles. It is quite obvious that the hydration force will tend to inhibit coalescence of emulsion droplets with a multilayer structure as schematically shown in Fig. 17.12.

18 Formulation of food emulsions using proteins and protein/polysaccharides and polysaccharide/surfactants

18.1 Protein structure

A protein is a linear chain of amino acids that assumes a three-dimensional shape dictated by the primary sequence of the amino acids in the chain. The side chains of the amino acids play an important role in directing the way in which the protein folds in solution. The hydrophobic (nonpolar) side chains avoid interaction with water, while the hydrophilic (polar) side chains seek such interaction. This results in a folded globular structure with the hydrophobic side chains inside and the hydrophilic side chains outside [9]. The final shape of the protein (helix, planar or "random coil") is a product of many interactions which form a delicate balance [10, 11]. These interactions and structural organizations are briefly discussed below.

Three levels of structural organisation have been suggested:

(i) primary structure referring to the amino acid sequence;
(ii) secondary structure, denoting the regular arrangement of the polypeptide back bone;
(iii) tertiary structure, as the three-dimensional organization of globular proteins.

A quaternary structure consisting of the arrangement of aggregates of the globular proteins may also be distinguished. The regular arrangement of the protein polypeptide chain in the secondary structure is determined by the structural restrictions. The C–N bonds in the peptide amide groups have a partial double bond character that restricts the free rotation about the C–N bond. This influences the formation of secondary structures. The polypeptide backbone forms a linear group, if successive peptide units assume identical relative orientations. The secondary structures are stabilized by hydrogen bonds between peptide amide and carbonyl groups. In the α-helix, the C=O bond is parallel to the helix axis and a straight hydrogen bond is formed with the N-H group and this is the most stable geometrical arrangement. The interaction of all constituent atoms of the main chain, which are closely packed together, allows the van der Waals attraction to stabilize the helix. This shows that the α-helix is the most abundant secondary structure in proteins. Several other structures may be identified and these are designated as π-helix, β-sheet, etc.

The classification of proteins is based on the secondary structures: α-proteins with α-helix only, e.g. myoglobin, β-proteins mainly with β-sheets, e.g. immunoglobin, α+β proteins with α-helix and β-sheet region that exist apart in the sequence, e.g. lysozome. The protein structure is stabilized by covalent disulphide bonds and a complexity of non-covalent forces, e.g. electrostatic interactions, hydrogen bonds,

https://doi.org/10.1515/9783110588002-021

hydrophobic interactions and van der Waals forces. Both the average hydrophobicity and the charge frequency (parameter of hydrophobicity) are important in determining the physical properties such as solubility of the protein. The latter can be expressed as the equilibrium between hydrophilic (protein-solvent) and hydrophobic (protein-protein) interactions. Protein denaturation can be defined as the change in the native conformation (i.e. in the region of secondary, tertiary and quaternary structure) which takes place without change in the primary structure, i.e without splitting of the peptide bonds. Complete denaturation may correspond to totally unfolded protein. When the protein is formed, the structure produced adopts the conformation with the least energy. This structure is referred to as the native or naturated form of the protein. Modification of the amino side chains or their hydrolysis may lead to different conformations. Similarly, addition of molecules that interact with the amino acids may cause conformational changes (denaturation of the protein). Proteins can be denaturated by adsorption at interfaces, as a result of hydrophobic interaction between the internal hydrophobic core and the nonpolar surfaces.

Many examples of proteins that were used in interfacial adsorption studies may be quoted: Small and medium size globular proteins, e.g. those present in milk such as β-lactoglobulin, α-lactoalbumin and serum albumin, and egg white, e.g. lysozyme and ovalalbumin. At pH values below the isoelectric point (4.2–4.5), these proteins associate to form dimers, trimers and higher aggregates. α-lactoalbumin is stabilized by Ca^{+} against thermal unfolding. X-ray analysis of lysozyme showed that all charged and polar groups are located at the surface, whereas the hydrophobic groups are buried in the interior. Bovine serum albumin (which represents about 5 % of whey proteins in bovine milk) forms a triple domain structure, which includes three very similar structural domains, each consisting of two large double loops and one small double loop. Below pH 4, the molecule becomes fully uncoiled within the limits of its disulphide bonds. Ovalbumin, the major component of egg white, is a monomeric phosphoglycoprotein with a molecular weight of 43 kDa. During storage of eggs, even at low temperatures, ovalbumin is modified by SH/SS exchange into a variant with greater heat stability, called s-ovalbumin.

These protein forming micelles, namely casein is the major protein fraction in bovine milk (about 80 % of the total milk protein). Several components may be identified, namely αs,1- and αs,2-caseins, β-casein and κ-casein. A protolytic breakdown product of β-casein is γ-casein. Similarly to ovalbumin, caseins are phosphoproteins. Large spherical casein micelles are formed by association of αs-, β- and κ-casein in the presence of free phosphate and calcium ions. The molecules are held together by electrostatic and hydrophobic interactions. The αs- and β-caseins are surrounded by the flexible hydrophilic κ-casein, which forms the surface layer of the micelle. The high negative charge of the κ-casein prevents collapse of the micelle by electrostatic repulsion. The micelle diameter varies between 50 and 300 nm.

Several oligomeric plant storage proteins can be identified. They are classified according to their sedimentation behaviour in the analytical ultracentrifuge, namely 11S,

7S and 2S proteins. Both 11S and 7S proteins are oligomeric globular proteins. The 11S globulins are composed of 6 non-covalently linked subunits, each of which contains a disulphide bridged pair of a rather hydrophilic acidic 30–40 kDa α-polypeptide chain and a more hydrophilic basic 20 kDa β-polypeptide chains. The molar mass and size of the protein as well as its shape depends on the nature of the plant from which it is extracted. These plant proteins can be used as emulsifying and foaming agents.

18.2 Interfacial properties of proteins at the liquid/liquid interface

Since proteins are used as emulsifying agents for oil-in-water emulsions, it is important to understand their interfacial properties, in particular the structural change that may occur on adsorption. The properties of protein adsorption layers differ significantly from those of simple surfactant molecules. In the first place, surface denaturation of the protein molecule may take place resulting in unfolding of the molecule, at least at low surface pressures. Secondly, the partial molar surface area of proteins is large and can vary depending on the conditions for adsorption. The number of configurations of the protein molecule at the interface exceeds that in bulk solution, resulting in a significant increase of the non-ideality of the surface entropy. Thus, one cannot apply thermodynamic analysis, e.g Langmuir adsorption isotherm, for protein adsorption. The question of reversibility versus irreversibility of protein adsorption at the liquid interface is still subject to a great deal of controversy. For that reason, protein adsorption is usually described using statistical mechanical models. Scaling theories proposed by de Gennes [12] could also be applied.

A schematic representation of protein structures at a fluid interface is shown in Fig. 18.1 which illustrates the effect of increasing protein concentration [13].

One of the most important investigations of protein surface layers is to measure their interfacial rheological properties (e.g. their viscoelastic behaviour). Several techniques can be applied to study the rheological properties of protein layers, e.g. using constant stress (creep) or stress relaxation measurements. At very low protein concentrations, the interfacial layer exhibits Newtonian behaviour, independent of pH and ionic strength. At higher protein concentrations, the extent of surface coverage increases and the interfacial layers exhibit viscoelastic behaviour revealing features of solid-like phases. Above a critical protein concentration, protein-protein interactions become significant, resulting in a "two-dimensional" structure formation. The dynamics of formation of protein layers at the liquid-liquid interface should be considered in detail when one applies the protein molecules as stabilizers for emulsions. Several kinetic processes must be considered:

- solubilization of nonpolar molecules resulting in the formation of associates in the aqueous phase;
- diffusion of solutes from bulk solution to the interface;

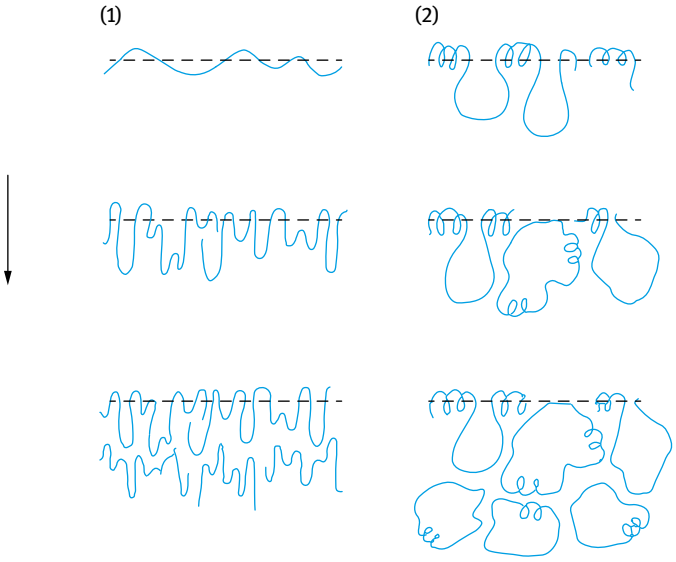

Fig. 18.1: Schematic representation of protein structure at a fluid interface: (i) flexible, random coil; (ii) globular highly structured proteins. The arrow denotes increasing protein concentration.

- adsorption of the molecules at the interface;
- orientation of the molecules at the liquid–liquid interface;
- formation of aggregation structures, etc.

18.3 Proteins as emulsifiers

When a protein is used as an emulsifier, it may adopt various conformations depending on the interaction forces involved. The protein may adopt a folded or unfolded conformation at the oil/water interface. In addition, the protein molecule may interpenetrate in the lipid phase to various degrees. Several layers of proteins may also exist. The protein molecule may bridge one drop interface to another. The actual structure of the protein interfacial layer may be complex, combining any or all of the above possibilities. For these reasons, measurement of protein conformations at various interfaces still remains a difficult task, even when using several techniques such as UV, IR and NMR spectroscopy as well as circular dichroism [14]. At an oil/water interface, the assumption is usually made that the protein molecule undergoes some unfolding and this accounts for the lowering of the interfacial tension on protein adsorption. As mentioned above, multilayers of protein molecules may be produced and one should take into account the intermolecular interactions as well as the interaction with the lipid (oil) phase. Proteins act in a similar way to polymeric stabilizers (steric stabilization). However, the molecules with compact structures may precipitate to form

small particles which accumulate at the oil/water interface. These particles stabilize the emulsions (sometimes referred to as Pickering emulsions) by a different mechanism. As a result of the partial wetting of the particles by the water and the oil, they remain at the interface. The equilibrium location at the interface provides stability since their displacement into the dispersed phase (during coalescence) results in an increase in the wetting energy.

From the above discussion, it is clear that proteins act as stabilizers for emulsions by different mechanisms depending on their state at the interface. If the protein molecules unfold and form loops and tails, they provide stabilization in a similar way to synthetic macromolecules. On the other hand, if the protein molecules form globular structures, they may provide a mechanical barrier that prevents coalescence. Finally, precipitated protein particles that are located at the oil/water interface provide stability as a result of the unfavourable increase in the wetting energy on their displacement. It is clear that in all cases, the rheological behaviour of the film plays an important role in the stability of the emulsions.

18.4 Protein–polysaccharide interactions in food colloids

Proteins and polysaccharides are present nearly in all food colloids [15]. The proteins are used as emulsion and foam stabilizers, whereas the polysaccharide acts as a thickener and also assists in water-holding. Both proteins and polysaccharides contribute to the structural and textural characteristics of many food colloids through their aggregation and gelation behaviour. Several interactions between proteins and polysaccharides may be distinguished, ranging from repulsive to attractive interactions. The repulsive interactions may arise from excluded volume effects and/or electrostatic interaction. These repulsive interactions tend to be weak except at very low ionic strength (expanded double layers) or with anionic polysaccharides at pH values above the isoelectric point of the protein (negatively charged molecules). The attractive interaction can be weak or strong and either specific or non-specific. A covalent linkage between protein and polysaccharide represents a specific strong interaction. A non-specific protein–polysaccharide interaction may occur as a result of ionic, dipolar, hydrophobic or hydrogen bonding interaction between groups on the biopolymers. Strong attractive interaction may occur between positively charged protein (at a pH below its isoelectric point) and an anionic polysaccharide.. In any particular system, the protein–polysaccharide interaction may change from repulsive to attractive as the temperature or solvent conditions (e.g. pH and ionic strength) change.

Aqueous solutions of proteins and polysaccharides may exhibit phase separation at finite concentrations. Two types of behaviour may be recognized, namely coacervation and incompatibility. Complex coacervation involves spontaneous separation into solvent-rich and solvent-depleted phases. The latter contains the protein–polysaccharide complex which is caused by non-specific attractive protein–poly-

saccharide interaction, e.g. opposite charge interaction. Incompatibility is caused by spontaneous separation into two solvent rich phases, one composed of predominantly protein and the other predominantly polysaccharide. Depending on the interactions, a gel formed from a mixture of two biopolymers may contain a coupled network, an interpenetrating network or a phase separated network. In food colloids, the two most important proteinaceous gelling systems are gelatin and casein micelles. An example of a covalent protein–polysaccharide interaction is that produced when gelatin reacts with propylene glycol alginate under mildly alkaline conditions. Non-covalent non-specific interaction occurs in mixed gels of gelatin with sodium alginate or low-methoxy pectin. In food emulsions containing protein and polysaccharide, any of the mentioned interactions may take place in the aqueous phase of the system. This results in specific structures with desirable rheological characteristics and enhanced stability. The nature of the protein–polysaccharide interaction affects the surface behaviour of the biopolymers and the aggregation properties of the dispersed droplets.

Weak protein–polysaccharide interactions may be exemplified by a mixture of milk protein (sodium casinate) and a hydrocolloid such as xanthan gum. Sodium casinate acts as the emulsifier and xanthan gum (with a molecular weight in the region of 2×10^6 Da) is widely used as a thickening agent and a synergistic gelling agent (with locust bean gum). In solution, xanthan gum exhibits pseudoplastic behaviour that is maintained over a wide range of temperatures, pH and ionic strengths. Xanthan gum at concentrations exceeding 0.1 % inhibits creaming of emulsion droplets by producing a gel-like network with a high residual viscosity. At lower xanthan gum concentrations (< 0.1 %) creaming is enhanced as a result of depletion flocculation. Other hydrocolloids such as carboxymethylcellulose (with a lower molecular weight than xanthan gum) are less effective in reducing creaming of emulsions.

Covalent protein–polysaccharide conjugates are sometimes used to avoid any flocculation and phase separation that is produced with weak non-specific protein–polysaccharide interactions. An example of these conjugates is that produced with globulin–dextran or bovine serum albumin–dextran. These conjugates produce emulsions with smaller droplets and narrower size distribution and they stabilize the emulsion against creaming and coalescence.

The effect of protein–polysaccharide interaction on emulsion stability was investigated by Dickinson [15] for the two cases of weak and strong protein–polysaccharide interactions. For the case of weak interaction, Dickenson [6] investigated the effect of addition of xanthan gum on 10 % mineral oil/water emulsions stabilized by 0.5 % caseinate at pH 7. The results are illustrated in Fig. 18.2 which shows plots of serum layer thickness H versus storage time.

In the absence of xanthan gum, visual inspection shows no serum separation. However, ultrasound velocity scanning showed the existence of an oil-depleted serum layer a few mm thick after 72 h. The emulsion, containing 0.125 wt% xanthan gum in the aqueous phase, showed no discernible serum separation over the observational

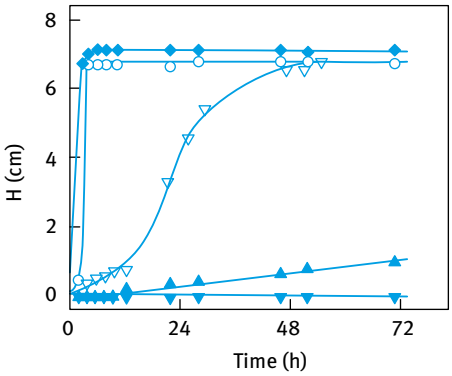

Fig. 18.2: Creaming of 10 % mineral oil/water emulsions stabilized with 0.5 % caseinate at pH 7 as a function of xanthan gum addition. ▼, 0 wt% and ≥ 0.125 wt%; ⧫, 0.025 wt%; ○, 0.05 wt%; ▽, 0.0625 wt%; ▲, 0.1 wt%.

time scale. In contrast, in the emulsions containing xanthan gum concentrations of 0.025 and 0.05 wt% the rate of serum separation at the bottom of the sample was rapid.

The emulsion stability is determined by the relative contributions of protein–polysaccharide and polysaccharide–polysaccharide interactions. The inhibition of creaming at xantham concentrations ≥ 0.125 wt% is due to immobilization of dispersed oil droplets in a weak gel-like network with a high low-stress viscosity (Chapter 14 of Vol. 1). Above 0.25 wt% xanthan gum, there is no serum or cream layer detectable ultrasonically after storage for several weeks. At low xanthan concentrations (below the gelation threshold) enhancement of creaming is attributed to depletion flocculation of the protein coated emulsion with non-adsorbing polysaccharide (Chapter 9 of Vol. 1).

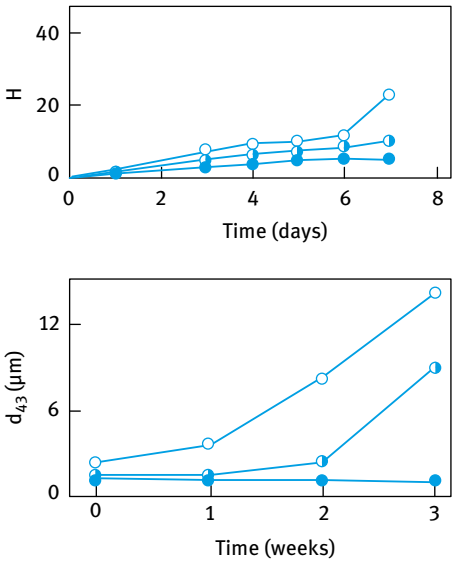

Fig. 18.3: Stability of 10 vol % n-tetradecane and 0.5 wt% protein. ●, conjugate; ○, 11S globulin; half open, simple mixture of 11S globulin and dextran T 40.

The stabilization of emulsions by strong protein-polysaccharide complexes that form conjugates by covalent bonding has been investigated by Dickinson [15] using dextran and 115 globulin or bovine serum albumin (BSA) proteins at a molar ratio R = 3. The complexes were prepared by dry heating at 60 °C for three weeks. The emulsions prepared using the BSA–dextran conjugate generates droplets with a narrower size distribution than with 11S globulin or BSA alone or in simple admixture with the polysaccharide. The stability of the emulsion was investigated by following the serum height H and mass mean droplet diameter d_{43} as a function of time. The results are shown in Fig. 18.3, which shows a comparison of emulsions prepared using 11S globulin alone, a simple mixture of 11S globulin and dextran T40 and the conjugate.

The results of Fig. 18.3 indicate that the emulsions made with the globulin–dextran conjugate (R = 3) have good stability with respect to creaming and coalescence.

18.5 Polysaccharide–surfactant interactions

One of the most important aspects of polymer–surfactant systems is their ability to control stability and rheology over a wide range of compositions [15]. The basic mechanism involved is illustrated in Fig. 18.4, which shows surfactant molecules associating with polymer chains in micelle-like clusters [15]. In dilute solutions, contraction of the polymer chains can result due to the association of a micelle with two parts of a polymer chain, while for semi-dilute or concentrated solutions, crosslinking of different polymer chains is expected.

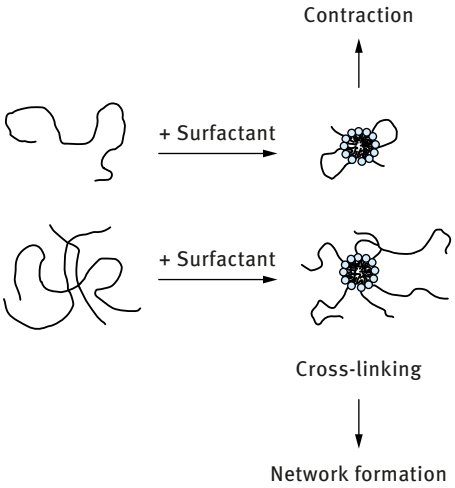

Fig. 18.4: Schematic representation of association of surfactant molecules with polymer chains.

Surfactant molecules that bind to a polymer chain generally do so in clusters that closely resemble the micelles formed in the absence of polymer [16]. If the polymer is less polar or contains hydrophobic regions or sites, there is an intimate contact between the micelles and polymer chain. In such a situation, the contact between one surfactant micelle and two polymer segments will be favourable. The two segments can be in the same polymer chain or in two different chains, depending on the polymer concentration. For a dilute solution, the two segments can be in the same polymer chain, whereas in more concentrated solutions the two segments can be in two polymer chains with significant chain overlap. The crosslinking of two or more polymer chains can lead to network formation and dramatic rheological effects.

Surfactant–polymer interaction can be treated in different ways, depending on the nature of the polymer. A useful approach is to consider the binding of surfactant to a polymer chain as a co-operative process. The onset of binding is well-defined and can be characterized by a critical association concentration (CAC). The latter decreases with increase in the alkyl chain length of the surfactant. This implies an effect of polymer on surfactant micellization. The polymer is considered to stabilize the micelle by short- or long-range (electrostatic interaction. The main driving force for surfactant self-assembly in polymer–surfactant mixtures is generally the hydrophobic interaction between the alkyl chains of the surfactant molecules. Ionic surfactants often interact significantly with both nonionic and ionic polymers. This can be attributed to the unfavourable contribution to the energetics of micelle formation from the electrostatic effects and their partial elimination due to charge neutralization or lowering of

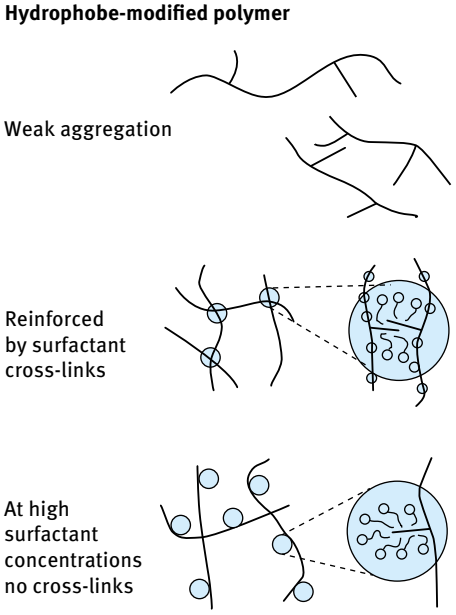

Fig. 18.5: Schematic representation of interaction between hydrophobically modified polymer chains and surfactant micelles.

the charge density. For nonionic surfactants, there is little to gain in forming micelles in the presence of a polymer and hence the interaction between nonionic surfactants and polymers is relatively weak. However, if the polymer chain contains hydrophobic segments or groups, e.g. with block copolymers, the hydrophobic polymer–surfactant interaction will be significant.

For hydrophobically modified polymers (such as hydrophobically modified hydroxyethyl cellulose or polyethylene oxide), the interaction between the surfactant micelles and the hydrophobic chains on the polymer can result in the formation of cross links, i.e. gel formation. This is schematically represented in Fig. 18.5. However, at high surfactant concentrations, there will be more micelles that can interact with the individual polymer chains and the cross links will be broken.

The above interactions are manifested in the variation of viscosity with surfactant concentration. Initially, the viscosity shows an increase with increase in surfactant concentration, reaching a maximum and then decreases with further increase in surfactant concentration. The maximum is consistent with the formation of crosslinks and the decrease after that indicates destruction these cross links (Fig. 18.5).

19 Surfactant association structures, microemulsions and emulsions in food

A typical phase diagram of a ternary system of water, ionic surfactant and long chain alcohol (cosurfactant) is shown in Fig. 19.1. The aqueous micellar solution A solubilizes some alcohol (spherical normal micelles), whereas the alcohol solution dissolves huge amounts of water, forming inverse micelles, B. These two phases are not in equilibrium with each other, but are separated by a third region, namely the lamellar liquid crystalline phase. These lamellar structures and their equilibrium with the aqueous micellar solution (A) and the inverse micellar solution (B) are the essential elements for both microemulsion and emulsion stability [17–19].

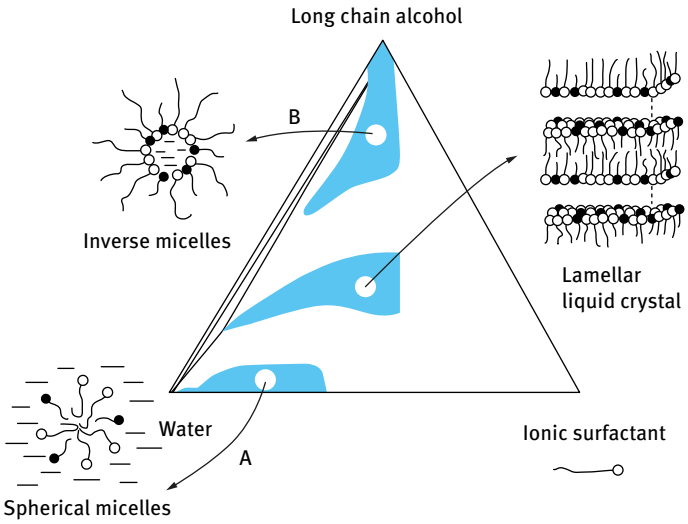

Fig. 19.1: Ternary phase diagram of water, an anionic surfactant and long chain alcohol (cosurfactant).

Microemulsions are thermodynamically stable and they form spontaneously (primary droplets a few nm in size), whereas emulsions are not thermodynamically stable since the interfacial free energy is positive and dominant in the total free energy. This difference can be related to the difference in bending energy between the two systems [19]. In microemulsions containing very small droplets, the bending energy (negative contribution) is comparable to the stretching energy (positive contribution) and hence the total surface free energy is extremely small ($\approx 10^{-3}$ mN m^{-1}). With macroemulsions, on the other hand, the bending energy is negligible (small curvature of the large emulsion drops) and hence the stretching energy dominates the total surface free

https://doi.org/10.1515/9783110588002-022

energy, which is now large and positive (a few mN m^{-1}). The microemulsion may be related to the micellar solutions A and B shown in Fig. 19.1. A W/O microemulsion is obtained by adding a hydrocarbon to the inverse micellar solution B, whereas an O/W microemulsion emanates from the aqueous micellar solution A. These microemulsion regions are in equilibrium with the lamellar liquid crystalline structure. To maximize the microemulsion region, the lamellar phase must be destabilized, for example by the addition of a relatively short chain alcohol such as pentanol. In contrast, for a macroemulsion, with its large radius, the parallel packing of the surfactant/cosurfactant is optimal and hence the cosurfactant should be of chain length similar to that of the surfactant.

From the above discussion, it is clear that a surfactant/cosurfactant combination for a microemulsion is of little use in stabilizing an emulsion. This is a disadvantage when a multiple emulsion of the W/O/W type is to be formulated, whereby the W/O system is a microemulsion. This problem has been resolved by Larsson et al. [20], who used a surfactant combination to stabilize the microemulsion and a polymer to stabilize the emulsion.

The formulation of food systems as microemulsions is not easy, since addition of triglycerides to inverse micellar systems results in a phase change to a lamellar liquid crystalline phase. The latter has to be destabilized by other means than adding cosurfactants, which are normally toxic. An alternative approach to destabilizing the lamellar phase is to use a hydrotrope, a number of which are allowed in food products.

As discussed in Chapter 16, for emulsion stabilization in food systems lamellar liquid crystalline structures are ideal. Friberg and coworkers [21, 22] attributed the enhanced stability of emulsions formed with mixtures of surfactants to the formation of three-dimensional structures, namely, liquid crystals. These structures can form, for example, in a three-component system of surfactant, alcohol and water, as illustrated in Fig. 19.2. The lamellar liquid crystalline phase, denoted by N (neat phase), in the phase diagram is particularly important for stabilizing the emulsion against coalescence. In this case, the liquid crystals "wrap" around the droplets in several layers, as will be illustrated below. These multilayers form a barrier against coalescence as will be discussed below. Friberg et al. [12] have given an explanation in terms of the reduced attractive potential energy between two emulsion droplets, each surrounded by a layer of liquid crystalline phase. They have also considered changes in the hydrodynamic interactions in the interdroplet region; this affects the aggregation kinetics.

Friberg et al. [21] have calculated the effect on the van der Waals attraction of the presence of a liquid crystalline phase surrounding the droplets. A schematic representation of the flocculation and coalescence of droplets with and without a liquid crystalline layer is shown in Fig. 19.3.

The upper part of Fig. 19.3 (A to F) represents the flocculation process when the emulsifier is adsorbed as a monomolecular layer. The distance d between the water droplets decrease to a distance m at which film ruptures and the droplets coalesce; m is chosen to correspond to the thickness of the hydrophilic layers in the liquid crys-

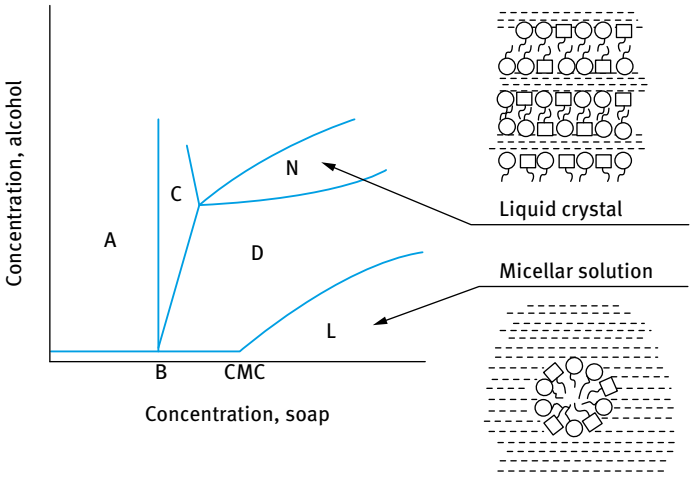

Fig. 19.2: Phase diagram of surfactant–alcohol–water system.

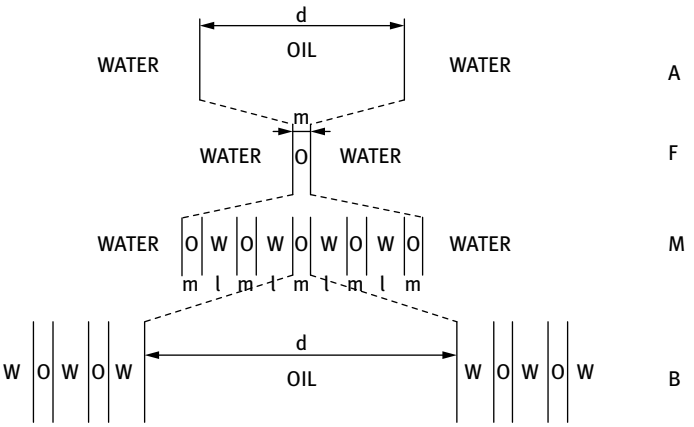

Fig. 19.3: Schematic representation of flocculation and coalescence in the presence and absence of liquid crystalline phases.

talline phase. This simplifies the calculations and facilitates comparison with the case in which the liquid crystalline layer is adsorbed around the droplets.

The flocculation process for the case of droplets covered with liquid crystalline layers is illustrated in the lower part of Fig. 19.3 (B to M). The oil layer between the droplets thins to thickness m. The coalescence process which follows involves the removal of successive layers between the droplets until a thickness of one layer is reached (F); the final coalescence step occurs in a similar manner to the case for a monomolecular layer of adsorbed surfactant.

For case A, the van der Waals attraction is given by the expression,

$$G_A = -\frac{A}{12\pi d^2}, \tag{19.1}$$

where A is the effective Hamaker constant,

$$A = (A_{11}^{1/2} - A_{22}^{1/2})^2, \tag{19.2}$$

where A_{11} and A_{22} are the Hamaker constants of the two phases.

For case B, G_B can be obtained from the algebraic summation of this expression for the aqueous layer on each side of the central layer. The ratio G_B/G_A is then given by,

$$\frac{G_B}{G_A} = d^2\left\{\sum_{p=0}^{n}\sum_{q=0}^{n}[d+(p+q)(l+m)]^{-2} + \sum_{p=0}^{n-1}\sum_{q=0}^{n-1}[d+2l+(p+q)(l+m)]^{-2} - \sum_{p=0}^{n}\sum_{q=0}^{n-1}[2(d+l)+(p+q)(l+m)]^{-2}\right\}, \tag{19.3}$$

where l and m are the thicknesses of the water and oil layers, n is the number of water layers (which is equal to the number of oil layers) and p and q are integers.

The free energy change associated with coalescence (i.e. M → F) is calculated from the variation of the van der Waals interaction across the droplet walls. This treatment reflects the energy change associated with the layers squeezed out from the interdroplet region. The problem is circumvented by assuming that these displaced layers adhere to the enlarged droplets so that their free energy is not significantly changed in the process. In this manner, the ratio of the interaction energies in the states F and M is obtained from summation of the van der Waals interactions from the individual layers on the water parts, i.e.,

$$\frac{G_M}{G_F} = m^2\left\{\sum_{p=0}^{n}[(m+p)(m+l)]^{-2} - \sum_{p=0}^{n}[(p+l)(m+l)]^{-2}\right\}. \tag{19.4}$$

To illustrate the relative importance of the van der Waals attraction energy, calculations were made using the above expressions, for the case of flocculation (i.e. A and B) and for the case of coalescence (i.e. F and M). The results are given in Fig. 19.4 (a) and (b), respectively.

Fig. 19.4 (a) shows that the influence of liquid crystalline layers around the droplets on the flocculation process is insignificant. In contrast, the effect on the free energy change is quite significant. For example, with nine layers on each droplet and a layer thickness of reasonable magnitude ($l = m = 5$ nm), the total van der Waals interaction is reduced to only 10 % of its original value for the coalescence process in the case of the layer structure. This is to be compared with 98 % in the case of two droplets at the same distance, but separated by the oil phase instead of the liquid crystalline

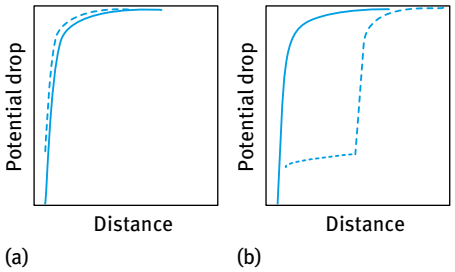

Fig. 19.4: van der Waals potential energy–distance curves for flocculation (a) and coalescence (b) in the presence (---) and absence (—) of liquid crystalline phases.

phase. Even more important are the extremely small changes in attraction energy after removal of the first layers. The first layers give a drop corresponding to 1.5 % of the total van deer Waals interaction energy (A to F). The last layer, before the state F is reached, corresponds to 78 % of the total van deer Waals energy. It seems, therefore, that the presence of a liquid crystalline phase has a pronounced influence on the distance dependence of the van deer Waals energy, leading to a drastic reduction in the force of attraction between the emulsion droplets.

A schematic representation of the role of liquid crystalline phases in reducing emulsion coalescence is shown in Fig. 19.5.

The process of coalescence occurs in two stages: first, the layers of the liquid crystals are removed two by two and the terminal stage is the disruption of the final belayed of the structure. The initiation of the flocculation process leads to very small energy changes and good stability is assumed as long as the liquid crystal remains adsorbed. This adsorption is the result of its structure. At the interface, the final layer towards the aqueous phase terminates with the polar group, while the layer towards the oil finishes with the methyl layer. In this manner, the interfacial free energy is a minimum.

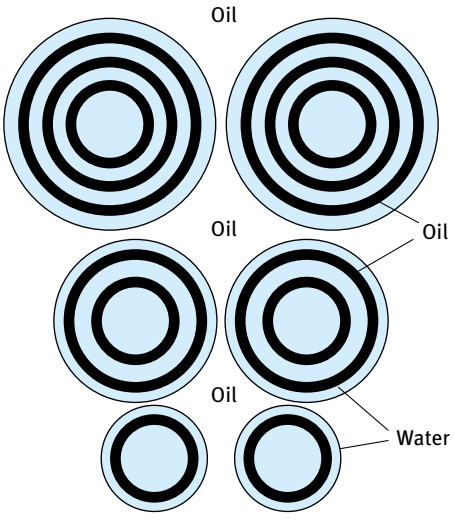

Fig. 19.5: Schematic representation of emulsions containing liquid crystalline structures.

20 Rheology of food emulsions

20.1 Interfacial rheology

It has long been argued that interfacial rheology, namely interfacial viscosity and elasticity, play an important role in emulsion stability. This is particularly the case with mixed surfactant films (which may also form liquid crystalline phases) and polymers such as hydrocolloids and proteins that are commonly used in food emulsions.

A fluid interface in equilibrium exhibits an intrinsic state of tension that is characterized by its interfacial tension γ which is given by the change in free energy with area of the interface, at constant composition n_i and temperature T,

$$\gamma = \left(\frac{\partial G}{\partial A}\right)_{n_i,T} \tag{20.1}$$

The unit for γ is energy per unit area (mJ m^{-2}) or force per unit length (mN m^{-1}) which are dimensionally equivalent. Adsorption of surfactants or polymers lowers the interfacial tension and this produces a two-dimensional surface pressure π that is given by,

$$\pi = \gamma_0 - \gamma, \tag{20.2}$$

where γ_0 is the interfacial tension of the "clean" interface (before adsorption) and γ that after adsorption.

The interface is considered to be a macroscopically planer, dynamic fluid interface. Thus, the interface is regarded as a two-dimensional entity independent of the surrounding three-dimensional fluid. The interface is considered to correspond to a highly viscous insoluble monolayer and the interfacial stress σ_s acting within such a monolayer is sufficiently large compared to the bulk-fluid stress acting across the interface and in this way one can define an interfacial shear viscosity η_s,

$$\sigma_s = \eta_s \dot{\gamma}, \tag{20.3}$$

where $\dot{\gamma}$ is the shear rate. η_s is given in surface Pa s (N m^{-1} s) or surface poise (dyne cm^{-1} s). It should be mentioned that the surface viscosity of a surfactant-free interface is negligible and it can reach high values for adsorbed rigid molecules such as proteins.

Many surface viscometers utilize torsional stress measurements upon a rotating ring, disk or knife edge (shown schematically in Fig. 20.1) within or near to the liquid/liquid interface [23]. This type of viscometer is moderately sensitive; with a disk viscometer, the interfacial shear viscosity can be measured in the range $\eta_s \geq 10^{-2}$ surface Pa s. The disk is rotated within the plane of the interface with angular velocity ω. A torque is exerted upon the disk of radius R by both the surfactant film with surface viscosity η_s and the viscous liquid (with bulk viscosity η) that is given by the expression,

$$M = (8/3)R^3\eta\omega + 4\pi R^2\eta_s\omega. \tag{20.4}$$

https://doi.org/10.1515/9783110588002-023

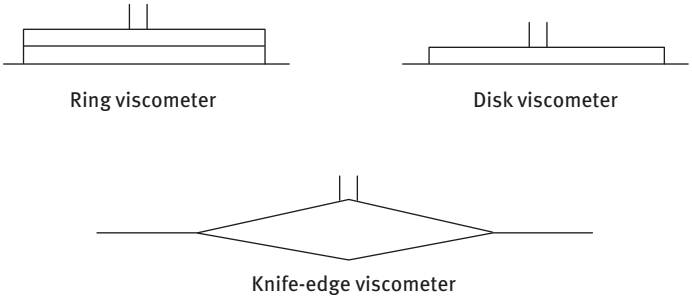

Fig. 20.1: Schematic representation of surface viscometers.

The interfacial dilational (Gibbs) elasticity ε, which is an important parameter in determining emulsion stability (reduction of coalescence during formation), is given by the following equation,

$$\varepsilon = \frac{\mathrm{d}\gamma}{\mathrm{d}\ln A}, \tag{20.5}$$

where $\mathrm{d}\gamma$ is the change in interfacial tension during expansion of the interface by an amount $\mathrm{d}A$ (referred to as interfacial tension gradient resulting from non-uniform surfactant adsorption on expansion of the interface). One of the most convenient methods for measuring ε is to use a Langmuir trough with two moving barriers for expansion and compression of the interface. Another method for measurement of ε is to use the oscillating bubble technique and other instruments that are commercially available.

A useful method for measuring ε is the pulsed drop method [24]. Rapid expansion of a droplet at the end of a capillary from a radius r_1 to r_2 is obtained by the application of pressure. The pressure drop within the droplet is measured as a function of time using a sensitive pressure transducer. From the pressure drop, one can obtain the interfacial tension as a function of time. The Gibbs dilational elasticity is determined from values of the time-dependent interfacial tension. Measurement can be made as a function of frequency, as is illustrated in Fig. 20.2 for stearic acid at the decane-water interface at pH = 2.5.

Measuring the dilational viscosity is more difficult than measuring the interfacial shear viscosity. This is due to the coupling between dilational viscous and elastic components. The most convenient method for measuring dilational viscosity is the maximum bubble pressure technique, which can be only applied at the air/water interface. According to this technique, the pressure drop across the bubble surface at the instant when the bubble possesses a hemi-spherical shape (corresponding to the maximum pressure) is due to a combination of bulk viscous, surface tension and surface dilational viscosity effects and this allows one to obtain the interfacial dilational viscosity.

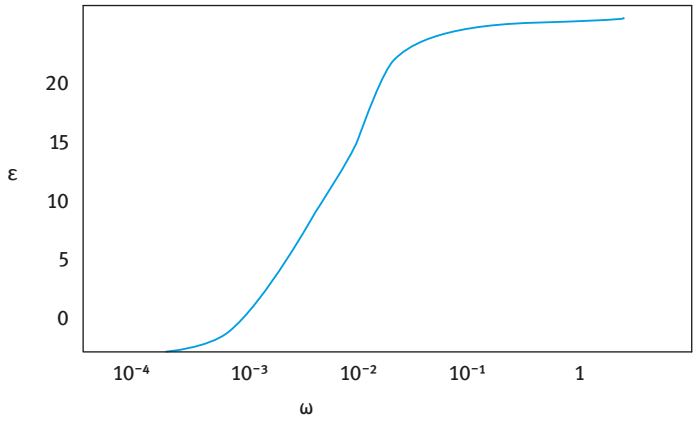

Fig. 20.2: Gibbs dilational elasticity versus frequency.

Most adsorbed surfactant and polymer coils at the oil–water (O/W) interface show non-Newtonian rheological behaviour. The surface shear viscosity η_s depends on the applied shear rate, showing shear thinning at high shear rates. Some films also show Bingham plastic behaviour with a measurable yield stress. Many adsorbed polymers and proteins show viscoelastic behaviour and one can measure viscous and elastic components using sinusoidally oscillating surface dilation. For example, the complex dilational modulus ε^* obtained can be split into an "in-phase" (the elastic component ε') and "out-of-phase" (the viscous component ε'') components. Creep and stress relaxation methods can be applied to study viscoelasticity.

20.2 Correlation between emulsion stability and interfacial rheology

20.2.1 Mixed surfactant films

Prins et al. [25] found that a mixture of sodium dodecyl sulphate (SDS) and dodecyl alcohol give a more stable O/W emulsion when compared to emulsions prepared using SDS alone. This enhanced stability is due to the higher interfacial dilational elasticity ε for the mixture when compared to that of SDS alone. Interfacial dilational viscosity did not play a major role since the emulsions are stable at high temperature whereby the interfacial viscosity becomes lower. This correlation is not general for all surfactant films since other factors such as thinning of the film between emulsion droplets (which depends on other factors such as repulsive forces) can also play a major role.

20.2.2 Protein films

Biswas and Haydon [26] found some correlation between the viscoelastic properties of protein (albumin or arabinic acid) films at the O/W interface interface and the stability of emulsion drops against coalescence. Viscoelastic measurements were carried out using creep and stress relaxation measurements (using a specially designed interfacial rheometer). A constant torque or stress σ (mN m^{-1}) was applied and the deformation γ was measured as a function of time for 30 min. After this period, the torque was removed and γ (which changes sign) was measured as a function of time to obtain the recovery curve. The results are illustrated in Fig. 20.3. From the creep curves, one can obtain the instantaneous modulus G_0 (σ/γ_{inst}) and the surface viscosity η_s from the slope of the straight line (which gives the shear rate) and the applied stress. G_0 and η_s are plotted versus pH as shown in Fig. 20.4. Both show increase with increase in pH, reaching a maximum at pH $\approx$ 6 (the isoelectric point of the protein) at which the protein molecules show maximum rigidity at the interface.

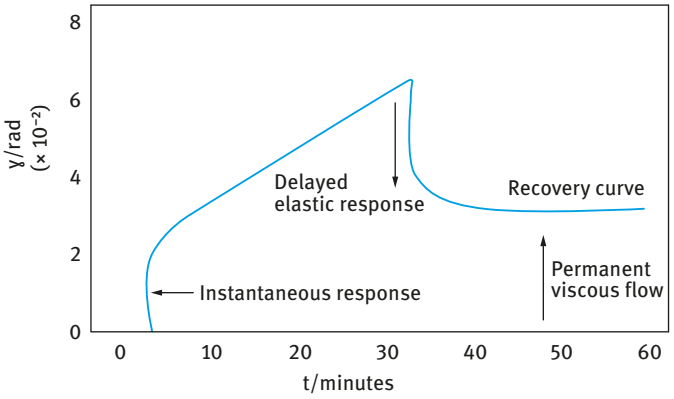

Fig. 20.3: Creep curve for protein film at the O/W interface.

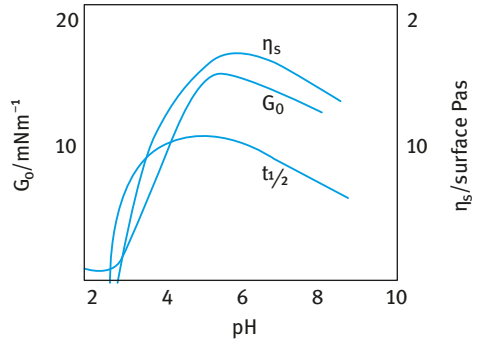

Fig. 20.4: Variation of $t_{1/2}$, G_0 and η_s with pH.

The stability of the emulsion was assessed by measuring the residence time t of several oil droplets at a planer O/W interface containing the adsorbed protein. Fig. 20.4 shows the variation of $t_{1/2}$ (time taken for half the number of oil droplets to coalesce with the oil at the O/W interface) with pH. Good correlation between $t_{1/2}$, G_0 and η_s is obtained.

Biswas and Haydon [26] derived a relationship between coalescence time τ and surface viscosity η_s, instantaneous modulus G_0 and adsorbed film thickness h,

$$\tau = \eta_s \left[3C' \frac{h^2}{A} - \frac{1}{G_0} - \phi(t) \right], \tag{20.6}$$

where $3C'$ is a critical deformation factor, A is the Hamaker constant and $\phi(t)$ is the elastic deformation per unit stress.

Equation (20.6) shows that τ increases with increase of η_s but most importantly it is directly proportional to h^2. These results show that viscoelasticity is necessary but not sufficient for ensuring stability against coalescence. To ensure stability of an emulsion, one must make sure that h is large enough and film drainage is prevented.

20.3 Bulk rheology of emulsions

For rigid (highly viscous) oil droplets dispersed in a medium of low viscosity such as water, the relative viscosity η_r of a dilute (volume fraction $\phi \leq 0.01$) O/W emulsion of non-interacting droplets causes them to behave as "hard-spheres" (similar to suspensions). In this case, η_r is given by the Einstein equation [27],

$$\eta_r = 1 + [\eta]\phi, \tag{20.7}$$

where $[\eta]$ is the intrinsic viscosity that is equal to 2.5 for hard-spheres.

For droplets with low viscosity (comparable to that of the medium) the transmission of tangential stress across the O/W interface, from the continuous phase to the dispersed phase causes liquid circulation in the droplets. Energy dissipation is less than that for hard spheres and the relative viscosity is lower than that predicted by the Einstein equation. For an emulsion with viscosity η_i for the disperse phase and η_0 for the continuous phase,

$$[\eta] = 2.5 \left(\frac{\eta_i + 0.4\eta_0}{\eta_i + \eta_0} \right). \tag{20.8}$$

Clearly when $\eta_i \gg \eta_0$, the droplets behave as rigid spheres and $[\eta]$ approaches the Einstein limit of 2.5. In contrast, if $\eta_i \ll \eta_0$ (as is the case for foams), $[\eta] = 1$. In the presence of viscous interfacial layers, equation (20.8) is modified to take into account the surface shear viscosity η_s and surface dilational viscosity μ_s,

$$[\eta] = 2.5 \left(\frac{\eta_i + 0.4\eta_0 + \xi}{\eta_i + \eta_0 + \xi} \right), \tag{20.9}$$

$$\xi = \frac{(2\eta_s + 3\mu_s)}{R}, \tag{20.10}$$

where R is the droplet radius.

When the volume fraction of droplets exceeds the Einstein limit, i.e. $\phi > 0.01$, one must take into account the effect of Brownian motion and interparticle interactions. The smaller the emulsion droplets, the more important the contribution of Brownian motion and colloidal interactions. Brownian diffusion tends to randomize the position of colloidal particles, leading to the formation of temporary doublets, triplets, etc. The hydrodynamic interactions are of longer range than the colloidal interactions and they come into play at relatively low volume fractions ($\phi > 0.01$) resulting in ordering of the particles into layers and tending to destroy the temporary aggregates caused by the Brownian diffusion. This explains the shear thinning behaviour of emulsions at high shear rates.

For the volume fraction range $0.01 < \phi < 0.2$, Batchelor [28] derived the following expression for a dispersion of hydrodynamically interacting hard spheres,

$$\eta_r = 1 + 2.5\phi + 6.2\phi^2 + \vartheta\phi^3. \tag{20.11}$$

The second term in equation (20.11) is the Einstein limit, the third term accounts for hydrodynamic (two-body) interaction, while the fourth term relates to multi-body interaction.

At higher volume fractions ($\phi > 0.2$), η_r is a complex function of ϕ and the η_r–ϕ curve is schematically shown in Fig. 20.5. This curve is characterized by two asymptotes, $[\eta]$ the intrinsic viscosity and ϕp the maximum packing fraction.

A good, semi-empirical equation that fits the curve is given by Dougherty and Krieger [29, 30],

$$\eta_r = \left(1 - \frac{\phi}{\phi_p}\right)^{-[\eta]\phi_p}. \tag{20.12}$$

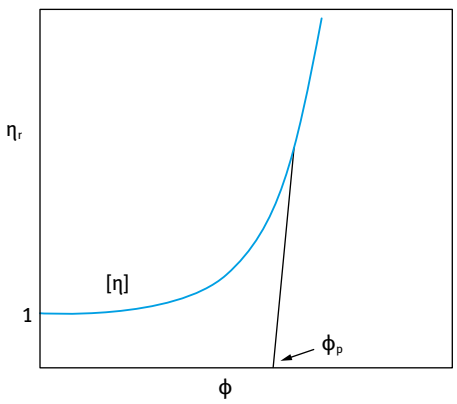

Fig. 20.5: η_r–ϕ curve.

20.4 Formation of networks

One of the important factors that affect the rheology of food emulsions is the presence of "networks" that are produced by the droplets or by the thickeners. These "networks" or "gels" control the consistency of the product and hence its acceptability to the customer. This can be illustrated from the work of van den Tempel [31] and Papenhuizen [32], who studied "gels" consisting of 25 % glyceryl stearate in paraffin oil (a model system for margarine). Creep experiments at various stress values showed an increase in strain (shear) γ, under constant stress τ, with time t. The data could be fitted empirically to an equation of the form,

$$\gamma = \frac{\tau}{G_1} + \frac{\tau}{G_2} \log t, \tag{20.13}$$

where G_1 and G_2 are the "rapid" and "retarded" elastic moduli respectively. The results could be explained by postulating two types of bonds between the particles in a network. The primary bonds (crystal bridges) were assumed to remain unbroken, whereas the secondary bonds (assumed to be due to van der Waals bonds) were broken under the influence of a stress and will reform in another relaxed position. The latter process gives rise to a retarded elastic behaviour. The relaxation of the reversible bonds causes an increasing part of the stress to be carried out by the irreversible bonds. Steady-state stress–strain measurements, carried out at low shear rates, showed a rapid increase in stress, reaching a maximum that was followed by a decrease, reaching an equilibrium value at large deformation. This is schematically illustrated in Fig. 20.6. This behaviour was explained by assuming that the network structure was destroyed to such an extent that only non-interacting aggregates of particles remained. The only effect of the agglomerates was immobilization of the liquid.

The above behaviour at low and larger deformation has been analyzed using a network model, in which the particles were assumed to be connected by van der Waals forces. The network was considered to consist of agglomerates of particles connected by chains. This is illustrated in Fig. 20.7, in which the network structure is

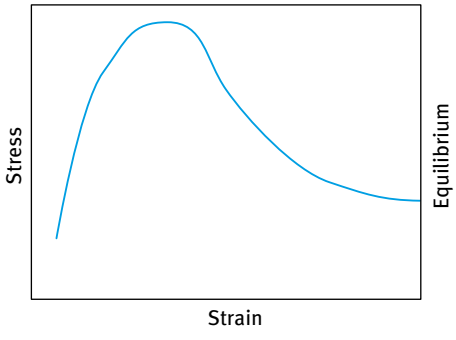

Fig. 20.6: Steady-state stress–strain relationship (at low shear rate).

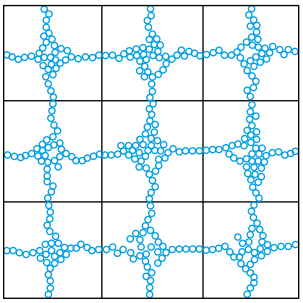

Fig. 20.7: Model of a network structure of a flocculated structure.

subdivided into small volume elements of characteristic size L, each consisting of one agglomerate. During the deformation process, stretching or tensile forces are applied to the network chain. These forces will increase distance between the rheological units (agglomerate or single particle). If this force reaches a critical value, the bond may break depending on the time available. However, in large deformation, reformation of the bonds may also occur. This is due to compression, i.e. deformation in the lateral direction.

Using the above model, Papenhuizen [32] derived an expression for the viscosity coefficient, η_{I}, resulting from purely hydrodynamic effects, i.e.,

$$\eta_{\mathrm{I}} = \frac{\eta_0 \phi a}{H}, \tag{20.14}$$

where η_0 is the viscosity of the medium, ϕ is the volume fraction, a is the radius of the particles (assumed to be spherical) and H is the distance between two spheres.

Papenhuizen [32] derived an expression for the viscosity coefficient, η_{II}, resulting from the presence of an agglomerate. He considered the force required to move an agglomerate consisting of a large number of particles through a stationary viscous medium at a certain speed. Such a flow problem is similar to determining the velocity of a viscous liquid flowing through a stationary porous plug under the influence of a pressure gradient, e.g using Darcy's law [33] and the Kozney–Carman equation [34]. Proceeding in this manner, the following expression for η_{II} was derived,

$$\eta_{\mathrm{II}} = \frac{CS^2}{2^{1/2}} \left(\frac{\phi}{1-\phi} \right)^2 \eta_0 L^2, \tag{20.15}$$

where C is a constant, equal to 5 for spheres, S is the surface area, equal to $3/a$ for spheres. Equation (20.15) shows that η_{II} depends on S and hence on particle size. Large particles have small S resulting in a low value for η_{II}, whereas small particles give rise to a large value of η_{II}. The latter is also proportional to the square of the volume fraction of the disperse phase. This shows the importance of particle size and volume fraction in controlling the viscosity (consistency) of a food emulsion system.

20.5 Rheology of microgel dispersions

Many food colloids are thickened with elastic micro-networks of polymeric materials, eg. gelatinised starch granules. The rheology of these systems is determined by particle swelling and deformability. Evans and Lips [35] developed a theory for the elasticity of microgel dispersions and this theory was tested using dispersions of Sephadex particles (spherical crosslinked dextran moieties). However, when using non-retrograded starch dispersions, deviation from theoretical predictions was obtained. This was attributed to the presence of solubilised amylose. The effect of addition of dextran on the elasticity of Sephadex dispersions was also investigated. The results could be explained by polymer particle bridging or depletion flocculation. However, it was could concluded that bridging is unlikely since Sephadex and dextran are chemically similar. Thus, addition of dextran to the dispersion was assumed to cause depletion flocculation, which provides an attractive component to the pair potential.

20.6 Fractal nature of the aggregated network

Considerable progress in describing the structure of aggregated particles has been made using the concept of fractals [36]. The complex structure of the aggregates is characterized by a single fractal dimension D, which describes a relation between the number N of particles in the aggregate and its typical radius R: $N \approx R^D$; the higher the value of D, the more compact the aggregate structure. Fractal growth models have been successfully studied for two limited regimes of fractal aggregation:

(i) diffusion-limited (or fast) aggregation characterized by $D = 1.7–1.8$;
(ii) reaction-limited (or slow) aggregation characterized by $D = 2.0–2.1$.

The fractal nature of the aggregates has important consequences for the rheology of dispersions. For example, the fractal theory predicts a scaling law for the elastic modulus G' versus volume fraction ϕ in the form $G' \approx \phi^n$ with $n = (3 + x)/(3 - D)$, where x is the backbone fractal dimension that varies between 1 and 1.3. This concept has been applied by Vreeker et al. [37] for dispersions containing 0.5 % glycerol stearate in olive or paraffin oil. The fat crystals were obtained by rapid cooling of the melt from 90 to 2 °C, after which the dispersion temperature was increased to 25 °C. At this temperature, rapid aggregation of the fat crystals was observed. The scattered light intensity $I(q)$ for the glycerol tristearate aggregates in olive or paraffin oil was measured as a function of the scattering vector q. Plots of $I(q)$ versus q gave a straight line, indicating the fractal nature of the fat aggregates. The fractal dimension D was calculated from the slope of the line and this was found to be 1.7; $I(q) \approx q - D$. This low value is characteristic of aggregates with a very open structure. This is consistent with a diffusion-limited aggregation dominated by attractive forces. However, aggregates with a low fractal dimension are sensitive to spontaneous restructuring or ageing ef-

fects. D was found to increase from 1.7 to 2.0 over several days of storage. Measurement of the elastic modulus G' versus (% w/w) solid fat content (for glycerol tristearate in paraffin oil) also showed a straight line when log G' was plotted versus log (% w/w) and this gave $D = 2.0$ which compares well with the value obtained from light scattering for dilute dispersions. Log-log plots of yield value σ_β versus solid fat content (% w/w) also gave a straight line and this gave $D = 1.9$.

21 Foam formulations in food

Many food products require the formation of foam. Whipping cream and bread dough are the most common of these foods. In the first case, the air bubbles are stabilized by fat crystals that adhere to the air bubbles during the whipping process, forming a protective layer and preventing bubble coalescence. In the latter case, the bread quality is determined by a high bread volume and a fine crumb structure. This quality can be realized if, during mixing, many small gas bubbles are occluded and held in the dough during fermentation and baking. Thus, dough may be considered as a foam. Processes that cause instability in the foam structure are dispropotionation (Ostwald ripening) and the coalescence of the air bubbles [38]. The surface rheological properties, as well as the bulk rheological properties, may contribute to the loss of the gas cells by these processes.

In this chapter, I will consider both processes of foam stability and instability. This was discussed in detail in Chapter 3 of Vol. 2 and only a summary is given here.

21.1 Foam stability

The structure of a foam formed by, for example, shaking a surfactant solution in a cylindrical vessel is shown schematically in Fig. 21.1.

In the lower part of the column, the bubbles are spherical (so-called kugelschaum) and of small size with a relatively low gas volume fraction. In this case, the liquid film separating the gas bubbles is relatively thick. As the liquid drains out of the foam, the bubbles distort to form polyhedra (polyederschaum) that consists of plane-parallel

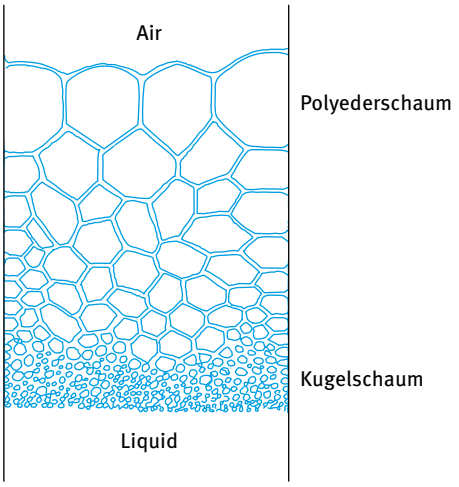

Fig. 21.1: Schematic representation of foam structure.

https://doi.org/10.1515/9783110588002-024

films joined by channels referred to as plateau borders. In the case, the gas volume fraction is relatively high and the liquid film thickness is relatively small [38].

A summary of the forces responsible for foam stability is given below (Chapter 3 of Vol. 2). As with most disperse systems, all foams are thermodynamically unstable This is due to the high interfacial free energy $\Delta A\gamma$ (where ΔA is the increase in interfacial area when producing the foam bubbles and γ is the surface tension) that exceeds the entropy of dispersion $T\Delta S$ (where T is the absolute temperature and ΔS is the increase in entropy in forming a large number of air bubbles. Thus, the free energy of formation of a foam ΔG,

$$\Delta G = \Delta A\gamma - T\Delta S \tag{21.1}$$

is positive and foam formation is non-spontaneous and the resulting foam is thermodynamically unstable.

For convenience, foams are classified according to the kinetics of their breakdown [38]:

(i) Unstable (transient) foams whose lifetime lasts for only seconds. These are generally produced using "mild" surfactants, e.g. short chain alcohols, aniline, phenol, pine oil, short chain undissociated fatty acid. Most of these compounds are sparingly soluble and may produce a low degree of elasticity.
(ii) Metastable ("permanent") foams whose lifetime lasts for hours or days. These metastable foams are capable of withstanding ordinary disturbances (thermal or Brownian fluctuations). They can collapse from abnormal disturbances (evaporation, temperature gradients, etc.).

The above metastable foams are produced from surfactant solutions near or above the critical micelle concentration (cmc). The stability is governed by the balance of surface forces (see below). The film thickness is comparable to the range of intermolecular forces. In the absence of external disturbances, these foams may stay stable indefinitely. They are produced using proteins, long chain fatty acids or solid particles. Gravity is the main driving force for foam collapse, directly or indirectly through the Plateau border. Thinning and disruption may be opposed by surface tension gradients at the air/water interface. Alternatively the drainage rate may be decreased by increasing the bulk viscosity of the liquid (e.g. addition of glycerol or polymers). Stability may be increased in some cases by the addition of electrolytes that produce a "gel network" in the surfactant film. Foam stability may also be enhanced by increasing the surface viscosity and/or surface elasticity. High packing of surfactant films (high cohesive forces) may also be produced using mixed surfactant films or surfactant/polymer mixtures.

For investigation of foam stability, one must consider the role of the Plateau border under dynamic and static conditions, which was discussed in detail in Chapter 3 of Vol. 2. One should also consider foam films with intermediate life times, i.e. between unstable and metastable foams.

Gravity is the main driving force for film drainage. Gravity can act directly on the film or through capillary suction in the plateau borders. As a general rule, the rate of drainage of foam films may be decreased by increasing the bulk viscosity of the liquid from which the foam is prepared. This can be achieved by adding glycerol or high molecular weight poly(ethylene oxide). Alternatively, the viscosity of the aqueous surfactant phase can be increased by addition of electrolytes that form a "gel" network (liquid crystalline phases may be produced). Film drainage can also be decreased by increasing the surface viscosity and surface elasticity. This can be achieved, for example, by addition of proteins, polysaccharides and even particles. These systems are applied in many food foams.

Several theories have been proposed to explain foam stability [38].

(i) Surface viscosity and elasticity theory. The adsorbed surfactant film is assumed to control the mechanical-dynamical properties of the surface layers by virtue of its surface viscosity and elasticity. This concept may be true for thick films (> 100 nm) whereby intermolecular forces are less dominant (i.e. foam stability under dynamic conditions). Surface viscosity reflects the speed of the relaxation process, which restores the equilibrium in the system after imposing a stress on it. Surface elasticity is a measure of the energy stored in the surface layer as a result of an external stress. The viscoelastic properties of the surface layer is an important parameter; e.g. with foams prepared using proteins. Some correlations have been found between surface viscosity, elasticity and foam stability, e.g. when adding lauryl alcohol to sodium lauryl sulphate, which tends to increase the surface viscosity and elasticity.

(ii) Gibbs–Marangoni effect theory [39]. The Gibbs coefficient of elasticity, ε, was introduced as a variable resistance to surface deformation during thinning:

$$\varepsilon = 2\left(\frac{\mathrm{d}\gamma}{\mathrm{d}\ln A}\right) = -2\left(\frac{\mathrm{d}\gamma}{\mathrm{d}\ln h}\right), \tag{21.2}$$

where $\mathrm{d}\ln h$ is the relative change in lamella thickness, ε is the "film elasticity of compression modulus" or "surface dilational modulus" and ε is a measure of the ability of the film to adjust its surface tension in an instant stress. In general, the higher the value of ε the more stable the film is. ε depends on surface concentration and film thickness. For a freshly produced film to survive, a minimum ε is required.

The main deficiency of the early studies on Gibbs elasticity was that it was applied to thin films and the diffusion from the bulk solution was neglected. In other words, the Gibbs theory applies to the case where there is insufficient surfactant molecules in the film to diffuse to the surface and lower the surface tension. This is clearly not the case with most surfactant films. For thick lamella under dynamic conditions, one should consider diffusion from the bulk solution, i.e. the Marangoni effect. The Marangoni effect tends to oppose any rapid displacement of the surface (Gibbs effect) and may provide a temporary restoring force to "dangerous" thin films. In fact, the Marangoni effect is superimposed on the Gibbs elasticity, so that the effective restoring force is a function of the rate of extension, as well as the thickness. When the

surface layers behave as insoluble monolayers, then the surface elasticity has its greatest value and is referred to as the Marangoni dilational modulus, ε_m.

The Gibbs–Marangoni effect explains the maximum foaming behaviour at intermediate surfactant concentrations. At low surfactant concentrations (well below the cmc), the greatest possible differential surface tension will only be relatively small and little foaming will occur. At very high surfactant concentration (well above the cmc), the differential tension relaxes too rapidly because of the supply of surfactant, which diffuses to the surface. This causes the restoring force to have time to counteract the disturbing forces and produces a dangerously thinner film and poor foaming. It is the intermediate surfactant concentration range that produces maximum foaming.

(iii) Surface forces theory (disjoining pressure π). This operates under static (equilibrium) conditions in relatively dilute surfactant solutions ($h < 100$ nm). In the early stages of formation, foam films drain under the action of gravitation or capillary forces. Provided the films remain stable during this drainage stage, they may approach a thickness in the range of 100 nm. At this stage, surface forces come into play, i.e. the range of the surface forces now becomes comparable to the film thickness. Deryaguin et al. [40, 41] introduced the concept of disjoining pressure, which should remain positive to slow down further drainage and film collapse. This is the principle of formation of thin metastable (equilibrium) films. In addition to the Laplace capillary pressure, three additional forces can operate at surfactant concentration below the cmc: electrostatic double layer repulsion π_{el}, van der Waals attraction π_{vdW} and steric (short range) forces π_{st},

$$\pi = \pi_{el} + \pi_{vdW} + \pi_{st}. \tag{21.3}$$

In the original definition of disjoining pressure by Deryaguin [40, 41], he only considered the first two terms on the right-hand side of equation (21.3). At low electrolyte concentrations, double layer repulsion predominates and π_{el} can compensate for the capillary pressure, i.e. $\pi_{el} = P_c$. This results in the formation of an equilibrium free film, which is usually referred to as the thick common film CF (≈ 50 nm thickness). This equilibrium metastable film persists until thermal or mechanical fluctuations cause rupture. The stability of the CF can be described in terms of the theory of colloid stability due to Deryaguin, Landau [42], Verwey and Overbeek [43] (DLVO theory).

The critical thickness value at which the CF ruptures (due to thickness perturbations) fluctuates and an average value h_{cr} may be defined. However, an alternative situation may occur as h_{cr} is reached and instead of rupturing a metastable film (high stability) may be formed with a thickness $h < h_{cr}$. The formation of this metastable film can be experimentally observed through the formation of "islands of spots" which appear black in light reflected from the surface. This film is often referred to a "first black" or "common black" film. The surfactant concentration at which this "first black" film is produced can be 1–2 orders of magnitude lower than the cmc. Further thinning can cause an additional transformation into a thinner stable region (a stepwise transformation). This usually occurs at high electrolyte concentrations, and leads to the

formation of a second, very stable, thin black film usually referred to as a Newton secondary black film, with a thickness in the region of 4 nm. Under these conditions, the short range steric or hydration forces control the stability and this provided the third contribution to the disjoining pressure, π_{st}, described in equation (21.3). Fig. 21.2 shows a schematic representation of the variation of disjoining pressure π with film thickness h, which shows the transition from the common film to the common black film and to the Newton black film. The common black film has a thickness in the region of 30 nm, whereas the Newton black film has a thickness in the region of 4–5 nm, depending on electrolyte concentration.

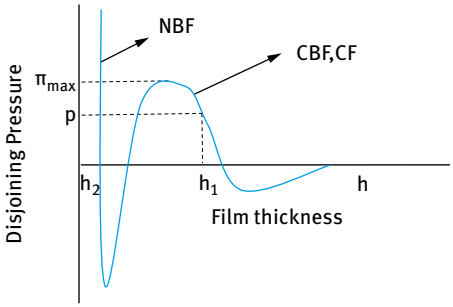

Fig. 21.2: Variation of disjoining pressure with film thickness.

Several investigations were carried out to study the above transitions from common film to common black film and finally to Newton black film. For sodium dodecyl sulphate, the common black films have thicknesses ranging from 200 nm in very dilute system to about 5.4 nm. The thickness depends strongly on electrolyte concentration and the stability may be considered to be caused by the secondary minimum in the energy distance curve. In cases where the film thins further and overcomes the primary energy maximum, it will fall into the primary minimum potential energy sink, where very thin Newton black films are produced. The transition from common black films to Newton black films occurs at a critical electrolyte concentration which depends on the type of surfactant.

The rupture mechanisms of thin liquid films were considered by de Vries [44] and by Vrij and Overbeek [45]. It was assumed that thermal and mechanical disturbances (having a wave-like nature) causes film thickness fluctuations (in thin films) leading to rupture or coalescence of bubbles at a critical thickness. Vrij and Overbeek [45] carried out a theoretical analysis of the hydrodynamic interfacial force balance, and expressed the critical thickness of rupture in terms of the attractive van der Waals interaction (characterized by the Hamaker constant A), the surface or interfacial tension γ and disjoining pressure. The critical wavelength, λ_{crit}, for the perturbation to grow (assuming the disjoining pressure just exceeds the capillary pressure) was determined. Film collapse occurs when the amplitude of the rapidly growing perturbation

was equal to the thickness of the film. The critical thickness of rupture, h_{cr}, was defined by the following equation,

$$h_{crit} = 0.267\left(\frac{a_f A^2}{6\pi\gamma\Delta p}\right)^{1/7}, \tag{21.4}$$

where a_f is the area of the film.

Many poorly foaming liquids with thick film lamella are easily ruptured, e.g. pure water and ethanol films (with thicknesses between 110 and 453 nm). Under these conditions, rupture occurs through the increase in disturbances, which may lead to thinner sections. Rupture can also be caused by spontaneous nucleation of vapour bubbles (forming gas cavities) in the structured liquid lamella. An alternative explanation for the rupture of relatively thick aqueous films containing low levels of surfactants is the hydrophobic attractive interaction between the surfaces that may be caused by bubble cavities [46, 47].

(iv) Stabilisation by micelles (high surfactant concentrations > cmc). At high surfactant concentrations (above the cmc), micelles of ionic or nonionic surfactants can produce organised molecular structures within the liquid film [21, 22]. This will provide an additional contribution to the disjoining pressure. Thinning of the film occurs through a stepwise drainage mechanism, referred to as stratification. The ordering of surfactant micelles (or colloidal particles) in the liquid film due to the repulsive interaction provides an additional contribution to the disjoining pressure and this prevents thinning of the liquid film.

(v) Stabilization by lamellar liquid crystalline phases. This is particularly the case with nonionic surfactant that produce lamellar liquid crystalline structure in the film between the bubbles [48]. These liquid crystals reduce film drainage as a result of the increase in the viscosity of the film. In addition, the liquid crystals act as a reservoir of surfactant of the optimal composition to stabilize the foam.

(vi) Stabilization of foam films by mixed surfactants. A combination of surfactants give slower drainage and improved foam stability. For example, mixtures of anionic and nonionic surfactants or anionic surfactant and long chain alcohol produce much more stable films than the single components. This could be attributed to several factors. For example, addition of a nonionic surfactant to an anionic surfactant causes a reduction in the cmc of the anionic. The mixture can also produce lower surface tension compared to the individual components. The combined surfactant system also has a high surface elasticity and viscosity when compared with the single components.

(vii) Stabilization by solid particles. The mechanism involves particles adsorbing at the air/liquid interface, as Fig. 21.3 illustrates schematically [49].

The foam stabilization by particles requires an appropriate balance of the interfacial free energies such that the particles are wetted preferentially by the continuous phase. The contact angle θ between the three interfaces defines the ability of the particle to stabilize or destabilize the foam. θ in Fig. 21.3 should lie between 0 and 90°.

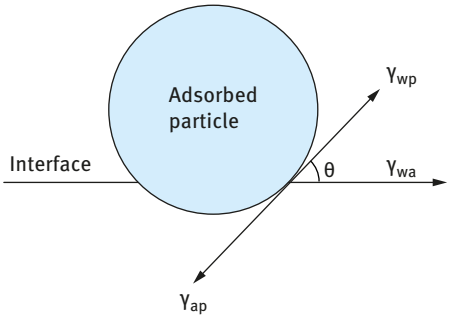

Fig. 21.3: Schematic representation of a particle adsorbing at the air/water interface. γ_{ap}, γ_{wp} and γ_{wa} are the tensions at the air/particle, water/particle and water/air interfaces respectively. θ is the contact angle between the three interfaces.

The most effective stabilization occurs when θ is in the range 60–70°. If θ is too close to 90°, physical perturbation at the interface can lead to destabilization.

A classical food product in which the air bubbles are stabilized by particles is whipping cream. Fat particles adhere to the air bubbles during the whipping process, forming a protective layer and preventing bubble coalescence. Stability of the whipped cream is described in terms of the interfacial energies between air, fat and aqueous phases. Increasing the particle/water and air/water interfacial tension increases adhesion of the particles to the air bubbles and so enhances stability. This can be achieved in practice by using oil or water-soluble surfactants.

21.2 Foam destabilization

Several factors can affect the foam stability of many food products. It is well known that the presence of particles from which surface active materials can spread at the air/water interface has a destabilizing effect in aqueous foams. A good example is the poor foaming behaviour of whole milk compared to skim milk, the destabilizing effect of egg yolk on the foaming of egg white and the detrimental effect of milk fat on bear foam. A schematic representation of film breakage as a result of a material from a particle spreading on the film surface [50] is shown in Fig. 21.4.

The factors that are responsible for film breakage are considered in terms of spreading of the surface-active material that is obtained from the particle on the foam film and the movement of the liquid in the same direction. This radial movement causes a local thinning of the film, resulting in its ultimate collapse when liquid has been squeezed away, as represented in Fig. 21.4. The film collapse increases with increase of the size of the spreading particle.

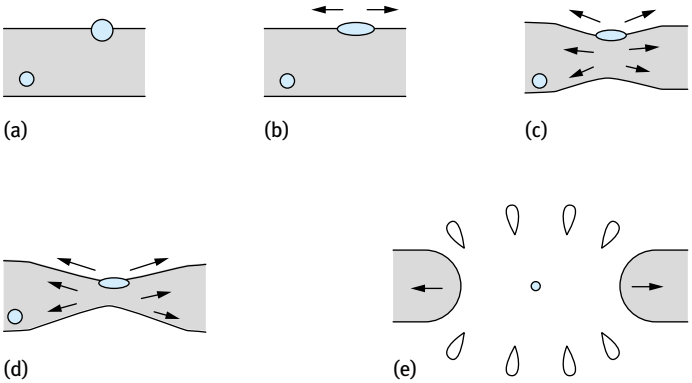

Fig. 21.4: Schematic representation of film breakage by a particle spreading over the film surface: (a) particle making contact with the surface; (b)–(d) particle spreading over the surface; (e) film breakage.

Another mechanism of foam destabilization is due to Ostwald ripening, which was discussed in detail in Chapter 10 of Vol. 1. This process, referred to as disproportionation, results from the difference in Laplace pressure Δp, given by equation (21.5), between small and large droplets,

$$\Delta p = \frac{2\gamma}{r}, \tag{21.5}$$

where γ is the surface tension and r is the bubble radius.

It is clear from equation (21.5) that Δp is higher for a smaller bubble when compared to a larger one. As a result, gas will diffuse from the smaller bubbles to the larger ones, resulting in a shift of the bubble size distribution to larger sizes. The large foam bubbles are more susceptible to film collapse and this causes foam instability. Assuming that the gas transport through the liquid takes place by diffusion and taking the bigger gas bubbles to be infinitely large, de Vries [51] derived an equation for the bubble size r as a function of time t,

$$r^2 = r_0^2 - \left(\frac{4RT}{p_0}\right)\left(\frac{DS\gamma}{\delta}\right)t, \tag{21.6}$$

where r_0 is the bubble radius at $t = 0$, R is he gas constant, T is the absolute temperature, p_0 is the atmospheric pressure, D is the diffusion coefficient of the gas in the liquid, S is its solubility in the liquid and δ is the thickness of the diffusion layer over which diffusion takes place.

Most gas bubble surfaces in food are viscoelastic, which means that the surface tension of the shrinking bubble γ is less than the equilibrium value γ_0. The surface property involved in this case is the surface dilational viscosity η_s given by,

$$\eta_s = \frac{(\gamma - \gamma_0)}{(\mathrm{d}\ln A/\mathrm{d}t)} = \frac{(\gamma - \gamma_0)}{2(\mathrm{d}\ln r/\mathrm{d}t)}, \tag{21.7}$$

where A is the surface area.

With most practical systems, η_s is strongly dependent on the rate of compression of the film, i.e. the surface behaviour is non-Newtonian. For a system such as milk or beer, the surface behaviour can be described by a power law relationship (Chapter 14 of Vol. 1),

$$\log \eta_s = m \log\left(\frac{\mathrm{d} \ln A}{\mathrm{d}t}\right) + n. \tag{21.8}$$

Typical values of m and n for skim milk are $m = -0.995$, $n = -2.4$. The negative value of m indicates the shear thinning behaviour of the surfaces, i.e. the surface dilational viscosity decreases with increase of the rate of compression (the shear rate). Combining equations (21.6), (21.7) and (21.8),

$$r\,\mathrm{d}r = -\left(\frac{2RT}{p_0}\right)\left(\frac{DS\gamma}{\delta}\right)\mathrm{d}t, \tag{21.9}$$

and this gives the following differential equation,

$$2\alpha C\left(\frac{\mathrm{d}r}{\mathrm{d}\tau}\right)^{m+1} + r^{m+2}\left(\frac{\mathrm{d}r}{\mathrm{d}\tau}\right) - \alpha\gamma_0 r^{m+1} = 0, \tag{21.10}$$

where,

$$\alpha = \frac{2RTDS}{\delta p_0}, \tag{21.11}$$

$$C = 2^m 10^n. \tag{21.12}$$

To account for the fact that $\mathrm{d} \ln A/\mathrm{d}t$ is negative, a new variable τ is introduced such that $\tau = -1$.

The differential equation (21.10) has been solved numerically and Fig. 21.5 shows the calculated bubble size as a function of time. Three points are particularly noteworthy:

(i) In the early stage of the disproportionation process, the bubble behaviour is close to that described by de Vries [51] (equation (21.6)), implying that $r \approx t^{1/2}$. This corresponds to the part of the curve in Fig. 21.5 which is concave downwards.

(ii) The quantity τ does not itself appear in equation (21.10), which means that curves of $r(t)$ are congruent to one another, i.e. they can be superimposed by shifting parallel to the x-axis.

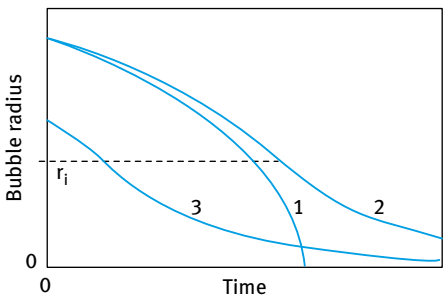

Fig. 21.5: Bubble radius as a function of time: curve 1, surface tension remains constant; curves 2 and 3, surface has a dilational viscosity for two initial bubble radii. Radius r_i corresponds to the inflection point.

(iii) If r approaches zero, it follows from equation (21.10) that dr/dt also approaches zero, and so the curve has to change somewhere from being concave downwards to concave upwards. This indicates a fundamental difference from the behaviour of the de Vries equation, where $dr/dt \to \infty$ as $r \to 0$ indicating that the bubble implodes. The inflection point in Fig. 21.5 indicates the slowing down of the disproportionation process and it is, therefore, worthwhile to investigate which parameters determines its process.

Differentiating equation (21.10) with respect to τ leads to the following expression for $d \ln r/dt$ at the inflection point,

$$\left(\frac{d \ln r}{dt}\right) = \left[\frac{\gamma_0}{2C(m+2)}\right]^{1/m+1}. \tag{21.13}$$

The bubble radius and surface tension at the inflection point are given by,

$$r_i^2 = \left[\frac{\alpha\gamma_0(m+1)}{(m+2)}\right]\left[\frac{2C(m+2)}{\gamma_0}\right]^{1/m+1}, \tag{21.14}$$

$$\gamma_i = \frac{(m+1)\gamma_0}{(m+2)}. \tag{21.15}$$

For beer, typical values of the parameters are such as to give $(d \ln r/dt) = -6.4 \times 10^3\ s^{-1}$, $r_i = 45$ nm (CO_2) or 6.3 nm (N_2), $\gamma_0 = 45\ mN\ m^{-1}$. From these results, it appears that the disproportionation process can only be slowed down when the bubbles are extremely small. The slowing down is to be understood only in a relative sense, since the absolute value of $d \ln r/dt$ at the inflection point is still large, indicating that small bubbles cannot exist for long. One should note that the surface tension of the bubble at the inflection point is extremely low and according to equation (21.15) its value depends on the parameter m. It should also be noted that the "stiffness" of the surface, as given by the value of η_s is only moderate. η_s as given by equation (21.8) is moderate, being equal to $13.6\ mN\ m^{-1}$ with $d \ln A/dt = 1\ s^{-1}$. For a bubble with η_s one order of magnitude higher i.e. $136\ mN\ m^{-1}$ with $d \ln A/dt = 1\ s^{-1}$, this is simply realized by taking $n = -0.865$. Using the values of γ_0 and m previously mentioned, the following values at the inflection point are obtained: $(d \ln r/dt) = -1.9 \times 10^{-6}\ s^{-1}$, $r_i = 2.6$ mm (CO_2) or 0.36 mm (N_2) and $\gamma_i = 3.9\ mN\ m^{-1}$. Thus, for this more rigid surface, the inflection point is found at a much larger bubble size, and the rate at which the bubble size decreases is extremely low at the inflection point. At first sight, it seems unexpected that a larger dilational viscosity is required to stabilize a bigger bubble because the driving force for disproportionation, as given by the Laplace pressure, is smaller for a bigger bubble than a smaller one. Due to the non-Newtonian behaviour, the much lower compression rate of the bigger bubble requires a higher value of η_s in order to reach the required low surface tension of ca $4\ mN\ m^{-1}$. In the same way, it can be understood that r_i is smaller for N_2 than for CO_2. In order to realize the same low surface tension at the same rate of surface compression, the rate of transport of poorly soluble

N_2 must be considerably higher than for CO_2. This implies that the Laplace pressure of the N_2 bubble must be higher, which under conditions of constant surface tension can only be realized with a smaller bubble radius.

22 Food rheology and mouthfeel

22.1 Introduction

As mentioned in Chapter 16, food systems are complex multiphase products that may contain dispersed components such as solid particles, liquid droplets or gas bubbles. The continuous phase may also contain colloidally dispersed macromolecules such as polysaccharides, protein and lipids. These systems are non-Newtonian, exhibiting complex rheology, which is usually plastic or pseudopolastic (shear thinning). Complex structural units are produced as a result of the interaction between the particles of the disperse phase as well as interaction with the polymers that are added to control the properties of the system such as its creaming or sedimentation as well as the flow characteristics. The control of rheology is important not only during processing but also for control of texture and sensory perception [38].

22.2 Rheological measurements

For adequate investigation of food rheology, it is essential to carry out well-defined rheological experiments. These experiments fall into two main categories, namely steady state shear stress–shear rate measurements and the possible time effects (thixotropy), low deformation measurements of constant stress (creep) and dynamic (oscillatory). During the flow process, both viscous (shear and normal) and inertial stresses act on the fluid matrix. The flow stresses tend to impede or influence the interactions of the structural components. Above a critical stress, flow-induced structuring may occur. The structural states may be of a reversible or irreversible nature. These structural changes influence the rheological behaviour of the fluid system and consequently the flow process itself is affected.

The above structural changes can have a significant effect on the technical performance of the food product. Problems of creaming or sedimentation and phase separation are directly related to the rheological characteristics. It is, therefore, crucial to control the rheology of the food product to avoid problems during manufacture, during storage and sensory perception of the product.

The sensory perception of food texture is significantly dependent on the structure of the system (e.g. the nature of the three dimensional units produced and the nature of the “gel” produced in the system) as well as its rheological behaviour. In a multiphase food product, such as an oil-in-water emulsion that contains surfactants for emulsification and polysaccharides that are added to reduce creaming, it is essential to relate the structure of the system to its rheology. This allows one to define the quality of the product in terms of its sensorial function (texture and consistency) as well as its technical function such as flow, dosing and storage stability.

https://doi.org/10.1515/9783110588002-025

To achieve the above objectives, it is essential to understand the colloid-chemical properties of the system as well as its flow characteristics under various conditions. Many food products (e.g. yoghurt) can be compared with the microstructure of particulate gels. The structure is formed from a continuous colloidal network, which holds the product together and gives rise to its characteristic properties. A colloidal network can be formed from particles linked together forming strands, enveloping pores and/or droplets, inclusions, etc. The size and shape of the particles, strands and pores may vary, thus creating different product properties.

During mastication, the structure breaks down and the sensory perception of the texture reflects this breakdown process. Various subjective tests for sensory evaluation are used, e.g. manual texture (touching) by a light pressure with forefinger, visual texture, mouthfeel during manipulation of the sample in the mouth. In order to relate the rheological characteristics of the product to the above sensory evaluation, it is essential to carry out experiments under various deformation conditions.

Two main type of measurements are required:

(i) Steady state measurements of shear stress versus shear rate relationship to distinguish between the various responses: Newtonian, plastic, pseudoplastic and dilatant. Particular attention is given to time effects during flow (thixotropy and negative thixotropy).
(ii) Viscoelastic behaviour, stress relaxation, constant stress (creep) and oscillatory measurements.

In steady state measurements, one applies a constant and increasing shear rate, γ (s^{-1}), on the sample (which may be placed in concentric cylinder, cone and plate or parallel plate platens) and the stress σ (Pa) is simultaneously measured. For Newtonian systems, the stress increases linearly with increase in shear rate and the slope of the shear stress–shear rate curve gives the Newtonian viscosity η (which is independent of the applied shear rate),

$$\sigma = \eta\gamma. \tag{22.1}$$

For a non-Newtonain system, as is the case with most food colloids, the stress–shear rate gives a pseudoplastic curve and the system is shear thinning, i.e. the viscosity decreases with increase of shear rate. In most cases, the shear stress–shear rate curve can be fitted with the Herschel–Bulkley equation,

$$\sigma = \sigma_\beta + k\gamma^n, \tag{22.2}$$

where σ_β is the yield stress (which gives a measure of the "structure" in the system, e.g its gel strength), k is the consistency index and n is the shear thinning index.

By fitting the experimental data to the above equation, one can obtain σ_β, k and n. The viscosity at any shear rate can then be calculated,

$$\eta = \frac{\sigma}{\gamma} = \frac{\sigma_\beta + k\gamma^n}{\gamma}. \tag{22.3}$$

Most food colloids show reversible time dependence of viscosity, i.e. thixotropy. If the system is sheared at any constant shear rate for a certain period of time, the viscosity shows a gradual decrease with increase of time. When the shear is removed, the viscosity returns to its initial value. This phenomenon can be understood from consideration of the structure of the multiphase food colloid that contains particles and/or droplets, surfactants, hydrocolloids, etc. On shearing the sample, this structure is "broken down". When the shear is removed, the structure recovers within a certain time scale that depends on the sample. Thixotropy is investigated by applying sequences of shear stress–shear rates within well defined time periods. If the shear rate is applied within a short period, e.g. increasing from 0 to 500 s^{-1} in one minute, then when reducing the shear rate from 500 to 0 s^{-1} the structure of the sample cannot be recovered within this time scale. In this case, the shear stress shear rate curves (the up and down curves) show large hysteresis, i.e. a large thixotropic loop is produced. By increasing the time of shear (e.g. 5 min for the up curve and 5 min for the down curve), the loop closes. In this way, one can investigate the thixotropy of the sample.

In constant stress (creep) measurements, one applies the stress (that is kept constant at each measurement) in small increasing increments. If the stress applied is below the yield stress, the system behaves as a viscoelastic solid. In this case, the strain shows a small increase at zero time and this strain remains virtually constant over the duration of the experiment (near zero shear rate). When the stress is removed, the strain returns to zero. This behaviour will be the same at increasing stress values, provided the applied stress is still below the yield stress. Any increase in stress will be accompanied by an increase in strain at zero time. However, when the stress exceeds the yield stress, the system behaves as a viscoelastic liquid. In this case, the strain rapidly increases at zero time, giving a rapid elastic response characterized by an instantaneous compliance J_0 (the compliance is simply the ratio between the strain and applied stress, Pa^{-1}). At times larger than zero, the strain shows a gradual and slow increase with time. This is the region of retarded response (bonds are broken and reformed at different rates). Ultimately, the system shows a steady state (with a constant shear rate), whereby the compliance increases linearly with increase of time. The slope of this linear portion gives the reciprocal viscosity at the applied shear stress (slope = J/t = Pa^{-1}/s = $1/Pa\,s$ = $1/\eta_\sigma$). After the steady state is reached, the stress is then removed and the system shows partial recovery, i.e. the strain changes sign and decreases with time reaching an equilibrium value. The creep curves are analyzed to obtain the residual (zero shear) viscosity, i.e. the plateau value at low stresses (below the yield stress) and the critical stress σ_{cr}, above which the viscosity shows a rapid decrease with further decrease in stress. This critical stress may be denoted as the "true yield value". In addition, by fitting the compliance-time curves to models, one can also obtain the relaxation time of the sample.

In dynamic (oscillatory) measurements, one applies a sinusoidal strain or stress (with amplitudes γ_0 or σ_0 and frequency ω in rad s^{-1}) and the stress or strain are measured simultaneously. For a viscoelastic system, the stress oscillates with the same

frequency as the strain, but out of phase. From the time shift of stress and strain, one can calculate the phase angle shift δ. This allows one to obtain the various viscoelastic parameters:

- G^* (the complex modulus),
- G' (the storage modulus, i.e. the elastic component of the complex modulus),
- G'' (the loss modulus or the viscous component of the complex modulus).

These viscoelastic parameters are measured as a function of strain amplitude (at constant frequency) to obtain the linear viscoelastic region whereby G^*, G' and G'' are independent of the applied strain until a critical strain γ_{cr} above which G^* and G' begin to decrease with further increase of strain, while G'' increases. Below γ_{cr}, the structure of the system is not broken down, whereas above γ_{cr} the structure begins to break. From G' and γ_{cr} one can obtain the cohesive energy density of the structure E_c. The viscoelastic parameters are then measured as a function of frequency at constant strain (that is kept within the linear viscoelastic region). For a viscoelastic liquid, G^* and G' increase with increase of frequency and ultimately both values reach a plateau that becomes independent of frequency. G'' increases with increase of frequency, reaching a maximum at a characteristic frequency ω^* and then it decreases with further increase of frequency, reaching almost zero at high frequencies (in the region of the plateau region of G'). From ω^*, one can calculate the relaxation time of the sample ($t_{relaxation} = 1/\omega^*$).

The above measurements are essential for relating rheology to sensory evaluation, e.g. mouthfeel, which will be discussed below.

22.3 Mouthfeel of foods: the role of rheology

Food products are generally designed with an optimum "consistency" for application in cutting, slicing, spreading or mixing [52]. During eating and mastication, the food loses its initial "consistency", at least partially. The mouthfeel of food products may be related to the loss of this initial "consistency". During the first stage of this mastication process, the food is comminuted by the action of the teeth into particles (few mm in size). At this stage, the food is close to its initial "consistency".

Thus, in the first stages of mastication, the mouthfeel may be related to its rheological characteristics. It is, therefore, possible to relate the mouthfeel during the first stages of mastication to rheological parameters such as "yield value", "creep compliance", "storage modulus", etc. After the initial stages of comminution, the food particles "soften" as a result of temperature rise and moisture uptake in the oral cavity. This results in a significant reduction in "consistency", which may reach values of stresses comparable to the levels encountered by the saliva flow in the oral cavity. When these stresses are reached, the food particles will be broken down into much smaller particles that are determined by the hydrodynamics of the "flowing" saliva.

The flow in the saliva is rather complex and calculation of shear stresses is not straightforward.

When the above stage is reached, the food product will form a "homogeneous" mix with the saliva and the mouthfeel will appear smooth. It is clear that if the "consistency" of the product does not decrease to a sufficient degree (such that the stresses are comparable to those encountered by the saliva flow), the masticated food will remain "thicker" and the mouthfeel will become unacceptable to the consumer (it will feel "grainy", "sticky" or "waxy"). Control of the "consistency" (rheological characteristics) of food products is essential for consumer acceptability and this may require sophisticated measurements and interpretation of the results obtained.

The reduction of the food products' size during mastication controls the flavour release. Assuming the particles produced are spherical, the time required for release is directly proportional to the square of the radius of the particles R (which is a measure of the surface area),

$$t \approx \frac{R^2}{D}, \tag{22.4}$$

where D is the diffusion coefficient of the flavour molecule that is inversely proportional to the viscosity of the medium (D is of the order of $10^{-9}\ m^2\ s^{-1}$ in dilute aqueous foods and can be as low as $10^{-11}\ m^2\ s^{-1}$ in fat foods).

To achieve adequate release of food flavours, R has to be reduced to $\approx 70\ \mu m$ for aqueous foods and much smaller sizes for fat continuous foods. The breakup of food products in the saliva is determined by the balance of two forces:

(i) hydrodynamic forces exerted by the saliva flow, which will deform the food produce;
(ii) interfacial forces and rheological properties of the food product that resists the deformation.

To investigate the breakup of food products during mastication one needs to know the following parameters:

(i) the stress exerted by the saliva flow;
(ii) the interfacial tension between the food material and saliva, relevant to both non-aqueous and fat continuous products
(iii) the rheological properties of the food products.

The relationship between the above forces and the droplet size of the product is known exactly for Newtonian liquids (e.g. oils). The breakup of Newtonian fluids in purely elongational flow is the most simple to analyze. Each element of volume is stretched without rotation of the direction of stretching. If the direction of stretching is not fixed, but it rotates, then in simple "shear flow" the rate of rotation of the axis of stretching and the rate of stretching are equal [52].

Using the above assumptions, it is possible to predict the droplet diameter of Newtonian oils during breakup by the flow in the saliva. In elongational flow, the stress σ_c acting on each drop is approximately equal to the stress in the continuous phase ($\eta_c\gamma$, where η_c is the fluid viscosity and γ is the shear rate),

$$\sigma_c = \eta_c\dot{\gamma}. \tag{22.5}$$

The interfacial tension γ resists deformation (i.e. it tries to keep spherical symmetry of the drops) and this effect can be accounted for by means of a "Young's modulus", E, equivalent to the Laplace pressure,

$$E = \frac{2\gamma}{R}. \tag{22.6}$$

The degree of deformation of the drop, ε_d, is the ratio between σ_c and E, i.e.,

$$\varepsilon_d = \frac{\sigma_c}{E} = \frac{\eta_c\dot{\gamma}R}{2\gamma}. \tag{22.7}$$

When drop elongation exceeds a certain value, the drop breaks up into smaller drops. ε_d is related to the capillary number Ω,

$$\Omega = \frac{\eta_c\dot{\gamma}d}{\gamma}, \tag{22.8}$$

where d is the droplet diameter. Note that $\Omega = 4\varepsilon_d$.

Using equations (22.7) and (22.8), one can obtain the droplet diameter from a knowledge of the stress acting on each drop (in elongational flow) and the interfacial tension between the oil/saliva interface. Alternatively, one can measure the droplet diameter of the oil drops produced in the saliva and, given knowledge of the viscosity of the saliva and the interfacial tension of the oil/saliva interface, one can estimate the stress in the flowing saliva. This is illustrated below.

22.3.1 Break-up of newtonaian liquids

The break-up of Newtonian liquids with various viscosities η_d can be investigated by mastication of small oil samples and measuring the resulting droplet size distribution, using a Coulter counter or a Mastersizer [52]. The samples are expectorated into a suitable surfactant solution, e.g. Tween (to prevent any coalescence during the measurements). η_d can be measured at 37 °C (body temperature) using a suitable rheometer (e.g. Haake-Rotovisco). The interfacial tension γ at the oil/saliva interface can be measured using the Wilhelmy plate method. A typical results for oil/saliva interface is $\approx 15\,\mathrm{mN\,m^{-1}}$. The interfacial tension between oil and saliva can be systematically reduced by dissolving various amounts of lecithin in the oil phase. To calculate the capillary number one needs to know σ_c; Initially, σ_c may be given an assumed value,

e.g. 1 Pa. The viscosity of saliva can be measured using the Haake and this is about 50 mPa s.

The experimental results using the above assumed value of σ_c are compared with the literature value for elongational flow. The measured d values were found to be ≈ 50 times lower than the literature value and this means that the actual saliva stress in the mastication process is ≈ 50 Pa. Under shear flow, there is a rapid increase in capillary number when $\eta_d/\eta_c > 1$.

22.3.2 Break-up of non-Newtonian liquids

Food products are usually non-Newtonian and they may be approximated by Bingham fluids,

$$\sigma = 2\sigma_\beta + \eta_b\dot{\gamma}, \tag{22.9}$$

where $2\sigma_\beta$ is the yield stress in elongation (assumed to twice the yield stress in shear flow) and η_{pl} is the Bingham plastic viscosity.

"Soft" foods, e.g. salad dressing and yoghurts, show a Bingham-like consistency at room temperature. More "solid" foods, e.g. fat spreads, cheese and puddings, become more liquid-like during mastication (melting and moisture uptake). The "yield stress" may decrease by several orders of magnitude during mastication. A "Bingham fluid" will only break-up when the stress exerted in the saliva (≈ 50 Pa) exceeds the yield stress of the food product. This means that the break-up of food products with a "yield stress" greater than ≈ 50 Pa is difficult in the oral cavity [52].

An example of a "model" food product with varying "yield stress" is W/O emulsions that can be prepared by emulsification of water in an oil such as ricinoleic acid or soya oil using an emulsifier with low HLB number such as polyglycerol ester. The yield stress of the resulting W/O emulsions can be systematically increased by increasing the water phase volume fraction, ϕ. The ratio of water to emulsifier should be kept constant in the above system. When $\phi = 0.6$, the emulsion is nearly Newtonian ($\sigma_\beta = 0$) and it becomes gradually more non-Newtonian as the water volume fraction increases, i.e. σ_β increases with increase in ϕ and may exceed 50 Pa when $\phi > 0.6$. During mastication, all emulsions show large drops, but the "Newtonian" emulsions with $\phi < 0.6$ showed a much larger number of small drops when compared with the non-Newtonian emulsions.

Using droplet size analysis and microscopy investigations. the above investigations can be used to study the effect of rheology on the "break-up" of non-Newtonian food products. They also allow one to study mouthfeel using panels and some correlations between rheology and mouthfeel may be obtained.

22.4 Complexity of flow in the oral cavity

The flow in the oral cavity is not a "steady" flow and hence the break-up process is not simple. Break-up in the oral cavity can only occur when this flow is maintained long enough, longer than the relaxation time of the drops. For most viscous oils ($\eta_d \approx 6$ Pa s) and $\eta \approx 15$ mN m^{-2}, the drop relaxation time is $\approx 5 \times 10^{-3}$ s giving an ultimate drop size of ≈ 20 µm. A range of 200–2,000 µm is initially produced with a relaxation time of 5×10^{-2}–5×10^{-1} s. Since these large drops break-up, the elongational flow remains steady over this period of time. When one considers how the jaws and the tongue drive the saliva flow, one must conclude that the flow cannot be kept steady for significantly longer times. The limited duration of elongational flow in the oral cavity is more important for food products showing viscoelastic behaviour at large degrees of deformation, e.g. for products containing thickeners such as hydrocolloids. Many food products contain hydrocolloids such as xanthan gum, which is added for reasons of physical stability and also to control the consistency of the product. In the presence of other food materials which increase the hydrodynamic stresses on the material of interest (e.g. bread), the drops produced could be much smaller [52].

22.5 Relationship between rheology and texture

During any flow process, whether during manufacture or during mastication of the food product, the flow stress affects the "structure" of the system, which in turn affects its rheological characteristics. The sensory perception and the mouthfeel depends to a large extent on the structure of the system (e.g. its "gel" behaviour) as well as its response to the stresses exerted by flowing saliva in the oral cavity. Using colloid and interfacial methods to study the "structure" and various rheological methods to assess the response of the food material to various shear regimes allows one to obtain a "texture"–rheology relationship [52].

A good example to consider is oil-in-water (O/W) emulsions, such as mayonnaise or sauces, which can be prepared using an industrial dispersion process. By controlling the energy input, one can control the droplet size of the emulsion. These emulsions are usually "structured" by the addition of emulsifier/"thickener" combinations such as proteins/polysaccharides. In laminar flow, the stresses acting in the gap of a dispersing process device are dominated by the viscous shear stress σ (viscosity × shear rate). For turbulent flow (which is the case for most dispersing devices) the so-called Reynolds stress σ_R is the dominant factor. A critical shear stress σ_{crit} has to be exceeded for droplet break-up, i.e.,

$$\sigma_{cr} = \frac{We\,\gamma}{d}, \tag{22.10}$$

where *We* is the critical Weber number that is a function of the ratio of the viscosity of the disperse phase and that of the continuous medium,

$$We = f\left(\frac{\eta_d}{\eta_c}\right), \tag{22.11}$$

where η_d is the viscosity of the disperse phase, η_c is the viscosity of the continuous medium, γ is the interfacial tension and d is the droplet diameter.

An O/W emulsion of mayonnaise (using for example sunflower oil) can be prepared at various oil weight fractions, e.g. 0.14, 0.65 and 0.85, using an emulsifier such as modified starch. The droplet size distribution of the resulting emulsions could be measured using a Coulter counter or Malvern Mastersizer (based on measurement of the light diffraction by the droplets). The texture of the mayonnaise could be assessed according to "spoonability" and mouthfeel (using panels). Various rheological methods may be applied as discussed above.

Using the above emulsion systems, it was shown that in many cases the mean droplet size decreased with increase in the volume energy input E_v (J m^{-3}). In some cases, the mean droplet size showed an increase after the initial increase, with increase in E_v. This could be due to emulsion droplet coalescence when E_v exceeded a critical value. Comparison of the various rheological results showed that the "structural" changes produced are determined by the value of the elastic modulus G'. G' was measured at low strains (in the linear viscoelastic region) and at a frequency of 1 Hz. G' is an elastic parameter and hence it reflects the interdroplet interaction as well as any interaction with the thickener. Since G' is measured at low deformation, it causes "minimum" change in the structure of the system during the measurement. An increase in G' reflects an increase in interaction. For example, for O/W emulsions without any thickener, decrease in droplet size increases the number of "contact" points between the emulsion droplets and this leads to an increase in G'. Any reduction in G' with increase in E_v (that leads to a decrease in droplet size) implies a reduction in the "networking" properties (produced for example by the emulsifier). In cases where G' increases with increase in E_v (particularly for high oil phase volume fraction) implies an increase in the "network" stability.

There seems to be a correlation between the sensorial texture parameter ("thickness" as measured by the spoon test) and the rheological parameters, G' (the storage modulus, the elastic component) and G'' (the loss modulus, the viscous component). One of the most useful parameters to measure is tan δ,

$$\tan\delta = \frac{G''}{G'}. \tag{22.12}$$

The reciprocal of tan δ is referred to as the dynamic Weissenberg number Wi',

$$Wi' = \frac{1}{\tan\delta} = \frac{G'}{G''}. \tag{22.13}$$

Wi' is a measure of the relative magnitudes of the elastic to the viscous moduli. Many food products such as yoghurt, egg products, etc. can be compared with the

microstructure of particulate gels. The structure is formed from a continuous colloidal network, which holds the product together and gives rise to its characteristic properties. A gel network structure can be formed from particles linked together forming strands, enveloping pores and/or droplets. During mastication, the gel structure breaks down and the new "structure" formed is perceived as "texture". An example of gel networks is protein gels formed for example from lactoglobulin. Several physical methods may be applied to characterize the gel produced. Image analysis and transmission electron microscopy could be applied to obtain the average pore size and particle size of the gel formed. Several rheological methods may be applied to study the properties of these gels:

(i) large deformation measurements, for example tensile tested by fracturing the sample using an Instron;
(ii) viscoelastic measurements (low deformation measurements) to obtain the storage and the loss modulus as well as the phase angle shift δ.

The low deformation measurements can be used to obtain quantitative information on the structure of the gel formed, for example the number of "cross links", the gel rigidity and its behaviour under low deformation.

The sensory tests which are carried out by panels (subjective tests) include manual texture measurement using light pressure with a fore finger, visual evaluation of the texture produced in a newly cut surface and oral texture (mouthfeel):

(i) manual texture, soft, resistance to light pressure by finger; springy, recovery of shape after light pressure;
(ii) visual texture, surface moisture water released from a newly cut surface; graininess of a newly cut surface;
(iii) oral texture, gritty during chewing; sticky, adherence to teeth after chewing; falling apart during chewing.

The perceived texture shows nonlinear dependence on the "microstructure". Gels formed at faster heating rates (12 °C/min) were more difficult to fracture when compared with gels formed at slower heating rates (1 °C/min). The gels formed at high heating rates have smaller pores and higher resistance to falling apart. The perception of "soft" and "springy" is related to the strand characteristics of the gel. Gels formed at slower heating rates (1 °C/min) have higher G' values when compared with those produced at higher heating rates (12 °C/min). Gels formed at 1 °C/min have stiff strands formed of many particles joined together (resulting in higher G'). Gels formed of flexible strands have lower G' values. The strand characteristics can explain the gel texture as assessed by viscoelastic measurements.

For analysis of the texture of gels one can perform two tests:

(i) destructive (Instron test) – this gives a measure of the overall network dimensions;
(ii) non-destructive (viscoelastic measurements).

The measured G' values are sensitive to the strand characteristics, which can be evaluated using microscopy. These measurements are carried out on gels produced under various conditions, such as heating rates in order to arrive at the desired properties.

It can be concluded from the above discussion that the combination of microscopy, sensory analysis and rheological properties (obtained under high and low deformation) using statistical evaluation methods can provide a correlation between sensory perception (as evaluated by expert panels) and the various characteristics of the gel [38]. The relationship between microstructure and texture is important in optimizing the properties of food products as well as in the development of new products with desirable properties. Modern techniques of microscopy (such as freeze fracture) can be applied to study the microstructure of gels. The viscoelastic properties of gels, which can be studied using oscillatory techniques (under various conditions of applied strain and frequency) can be correlated to the microstructure.

23 Practical applications of food colloids

Processed foods are often colloidal systems such as suspensions, emulsions and foams. Examples of food emulsions, which are the most commonly used products, are milk, cream, butter, ice cream, margarine, mayonnaise and salad dressings. Emulsions are also prepared as an intermediate step in many food processing, e.g. powdered toppings, coffee whiteners and cake mixes. These systems are dried emulsions that are re-formed into an emulsion state by the consumer.

Milk and cream are oil-in-water (O/W) emulsions consisting of fat droplets (triglycerides partially crystalline and liquid oils) typically in the size range 1–10 μm. The fat content of milk is 3–4 % by volume, and that of cream is 10–30 % by volume. The aqueous disperse medium contains milk proteins, salts and minerals. The fat droplets are stabilized by lipoprotein, phospholipids and adsorbed casein. This produces a very stable system against coalescence, as a result of steric stabilization and the presence of a viscoelastic film at the O/W interface. The only instability process in milk is creaming, since the gravity force exerted by the droplets exceed the Brownian diffusion. This problem of creaming is eliminated by homogenization of the milk using a high-pressure homogenizer. This reduces the droplet size to the submicron range and the gravity force becomes smaller than the Brownian diffusion.

Ice cream is an O/W emulsion that is aerated to form a foam. The disperse phase consists of butterfat (cream) or vegetable fat, partially crystallized fat. The volume fraction of air in the foam is approximately 50 %. The continuous phase consists of water and ice crystals, milk protein and carbohydrates, e.g. sucrose or corn syrup. Approximately 85 % of the water content is frozen at −20 °C. The foam structure is stabilized by agglomerated fat globules forming the surface of air cells in the foam. The added surfactants act as “destabilizers” controlling the agglomeration of the fat globules. The continuous phase is semi-solid and its structure is complex.

Both butter and margarine are W/O emulsions with the water droplets dispersed in a semi-solid fat phase containing fat crystals and liquid oil. With butter, the fat is partially crystallized triglycerides and liquid oil. Genuine milk fat globules are also present. The water droplets are distributed in a semi-solid plastic continuous fat phase. With margarine, the continuous phase consists of edible fats and oils, partially hydrogenated, of animal or vegetable origin. The dispersed water droplets are fixed in a semi-solid matrix of fat crystals. Surfactants are added to reduce the interfacial tension in order to promote emulsification during processing. The preparation of the W/O emulsion requires considerable energy to reduce the size of the dispersed phase droplets. Once the emulsion is produced, the whole system is chilled to enable the final emulsification and crystallization of the fat phase. The initial emulsion does not need to be very stable, since by cooling the water droplets become fixed in a semi-solid fat phase.

https://doi.org/10.1515/9783110588002-026

In the early development of margarine, egg yolk was first used as the emulsifier, since this contains lecithin and other phospholipids. Later, lipophilic emulsifiers such as mono-diglycerides of long chain fatty acids (C_{16}–C_{18}) were used in combination with soybean lecithin. The emulsifiers produce water droplets in the size range 2–4 μm. The consistency of margarine is strongly related to the amount of crystalline fat (solid fat content, SFC) which can be determined using dilatometry or low-resolution NMR spectroscopy. The solid fat content of margarine is in the range of 5–25 % at 20 °C. It is desirable to use fat blends that form small needle-shaped β′ crystals (about 1 μm long), which impart good plasticity. One should avoid transformation of these small needle shaped β′ crystals to large β crystals during storage. This results in an undesirable grainy consistency ("sandiness"). The crystal morphology may be controlled by using sorbitan esters and their ethoxylates, ethoxylated fatty alcohols, citric acid esters of monoglycerides, diacetyl tartaric acid esters of monoglycerides, sucrose monstearate, sodium stearoyl lactylate and polyglycerol esters of fatty acids. It was found that sorbitan monostearate and citric acid esters of monoglycerides were most effective in preventing the crystallization of tristearin from the α to the β form. However, when used in emulsions, the surfactants become adsorbed at the O/W interface and only lipophilic surfactants with high oil solubility can act as crystal growth inhibitors.

Low-calorie margarine contains at least 50 % water, 40 % fat and consists of protein milks, salts, flavour, vitamins and emulsifiers (mainly monoglycerides and soybean lecithin). Some products are based on milk fat and/or a combination of vegetable fats. With such high water content, a stable interfacial film is required. It has been shown that saturated monoglycerides are superior to unsaturated monoglycerides in terms of stabilizing water droplets. This is due to the formation of liquid crystalline films at the W/O interface.

An important class of O/W emulsions in the food industry is mayonnaise and salad dressings. Mayonnaise is a semisolid O/W emulsion made from minimum 65 % edible vegetable oil, acidifying ingredients, e.g. vinegar and egg yolk phosphatides as the emulsifying agent. The high-volume fraction of oil does not favour the formation of O/W emulsion and it is necessary to disperse the egg yolk in the water phase before addition of the oil phase. Colloid mills and other homogenizers must be used with care in order not to produce oil droplets that are too small (with high surface area), in which case the emulsifier content is not sufficient to cover the whole interface.

The main difference between mayonnaise and salad dressing is their oil contents, as salad dressings contain less oil. Thickening agents such as starch, cereal flour or hydrocolloids may be used. Egg yolk is the main emulsifying agent, but other food-grade surfactants may also be used, e.g polysorbates or esters of monoglycerides. The addition of salt can enhance the emulsion stability as a result of its effect on the protein conformation.

Several other food emulsions can be quoted such as coffee whiteners and cake emulsions. Coffee whiteners are O/W emulsions containing vegetable oils and fats

covering the size range 1–5 μm and an oil volume fraction of 10–15 %. The aqueous continuous phase contains proteins, e.g. sodium casinate, and carbohydrates, e.g. maltodextrin, salts and hydrocolloids. The emulsifying system consists of blends of nonionic and anionic surfactant with adsorbed protein.

Cake emulsions are very complex systems of fats or oil in an aqueous phase containing flour, sugar, eggs and micro ingredients. The mix is aerated during the mixing process and then further processed by baking. In many cake emulsions the air bubbles formed during mixing are located in the fat phase instead of the water phase. This is the case with high-ratio cakes that may contain 15–25 % plastic shortenings or margarine based on total batter weight. Fat-free cakes or high-ratio cakes made with liquid vegetable oils are aerated in the aqueous phase and the foam stability is provided by egg yolk and added surfactants. To obtain a satisfactory appearance, volume and texture, the shortening or margarine must have special properties with regard to the solid fat content and plasticity. Shortening containing fat crystals in the β′ form is ideal for entrapping and stabilizing the air cells. Unless egg yolk is present in the batter, the air cells in a fat particle tend to coalesce within the fat particles rather than be transferred as individual air cells in the aqueous phase. By heating during the baking process, the air cells are greatly enlarged by thermal expansion and by uptake of carbon dioxide from leavening agents and generated water vapour. At this point, the surface elasticity properties of the layers surrounding the air cells are very important. At the end of the baking process, the air cells become connected in an open network and the liquid fat droplets coalesce into a film which covers the inner surface of the air channels.

Surfactants play a major role in both fatless and fat-containing cakes. The types of surfactants commonly used are monoglycerides, polyglycerol esters, propylene glycol esters of fatty acids and polysorbates. These surfactants act as emulsifiers for the fat by reducing the interfacial tension thus aiding the dispersion of the fat phase. Plastic shortenings may contain 6–10 % lipophilic surfactants, such as monolglycerides or propylene glycol esters of fatty acids. These surfactants have no influence on the air/fat surface tension. The fat-based aeration is, therefore, highly dependent on the plasticity of the fat phase, which is controlled by the type of fats and surfactants used.

Surfactants such as monoglycerides may also interact with the starch fraction of the batter and form an insoluble amylose complex. This reduces gelatinization in the cakes, resulting in a better cake structure with improved tenderness. In fat-free cakes, special surfactant preparations in gel form or α-crystalline powder forms are often used as aerating agents. Monoglycerides of palmitic and stearic acids have been found to form liquid crystalline mesophases in cakes containing corn oil. These monoglycerides were found to encapsulate oil droplets at 94 °C by multilayer sheets. At higher temperatures, the transition of monoglycerides from lamellar to cubic phases enhances the viscosity and this plays an important role in stabilizing the sponge cake batter during baking.

References

[1] Krog NJ, Riisom TH. In: Becher P, editor. Encyclopedia of emulsion technology. Vol. 2. New York: Marcel Dekker; 1985. p. 321–365.
[2] Jaynes EN. In: Becher P, editor. Encyclopedia of emulsion technology. Vol. 2. New York: Marcel Dekker; 1985. p. 367–385.
[3] Friberg SE, Kayali I. In: El-Nokaly M, Cornell D, editors. Microemulsions and emulsions in food. American Chemical Society; 1991. p. 7. (ACS Symposium Series; vol. 448).
[4] Luzzati V. In: Chapman D, editor. Biological membranes. New York: Academic Press; 1968. p. 71.
[5] Krog N, Borup AP. J Sci Food Agric. 1973;24:691.
[6] Lindblom G, Larsson K, Johansson L, Fontell K, Forsen S. J Amer Chem Soc. 1979;101:5465.
[7] Larsson K, Fontell K, Krog N. Chem Phys Lipids. 1980;27:321.
[8] Pilman E, Tonberg E, Lartsson K. J Dispersion Sci Technol. 1982;3:335.
[9] Mierovitch H, Scheraga HA. Macromolecules. 1980;13:1406.
[10] Tanford C. Adv Protein Chem. 1970;24:1.
[11] Mobius D, Miller R, editors. Proteins at liquid interfaces. Amsterdam: Elsevier; 1998.
[12] de Gennes PG. Scaling concepts in polymer physics. Ithaca, New York: Cornell University Press; 1979.
[13] Darling DF, Birkett RJ. In: Dickinson E, editor. Food emulsions and foams. London: Royal Society of Chemistry Publication; 1987.
[14] Larsson K. J Dispersion Sci Technol. 1980;1:267.
[15] Dickinson E, Walstra P, editors. Food colloids and polymers: Stability and mechanical properties. Royal Society of Chemistry Publication; 1993.
[16] Goddard ED, Ananthapadmanqabhan KP, editors. Polymer-surfactant interaction. Boca Raton: CRC Press; 1992.
[17] Tadros T. Emulsions. Berlin: De Gruyter; 2016.
[18] Tadros T. Applied surfactants. Germany: Wiley-VCH; 2005.
[19] Friberg SE, Kayali I. In: El-Nokaly M, Cornell D, editors. Microemulsions and emulsions in food. American Chemical Society; 1991. p. 7. (ACS Symposium Series; vol. 448).
[20] Larsson K. J Dispersion Sci Technol. 1980;1:267.
[21] Friberg S, Jansson PO, Cederberg E. J Colloid Interface Sci. 1976;55:614.
[22] Jansson PO, Friberg S. Mol Cryst Liq Cryst. 1976;34:75.
[23] Criddle DW. The viscosity and viscoelasticity of interfaces. In: Eirich F, editor. Rheology. Vol. 3. New York: Academic Press; 1960. Chapter 11.
[24] Edwards DA, Brenner H, Wasan DT. Interfacial transport processes and rheology. London/ Boston: Butterworth-Heinemann; 1991.
[25] Prince A, Arcuri C, van den Tempel M. J Colloid and Interface Sci. 1967;24:81.
[26] Biswas B, Haydon DA. Proc Roy Soc. 1963;A271:296. 1963;A2:317. Kolloid Z. 1962;185:31. 1962;186:57.
[27] Einstein A. Ann Physik. 1906;19:289. 1911;34:591.
[28] Bachelor GK. J Fluid Mech. 1977;83:97.
[29] Krieger IM, Dougherty TJ. Trans Soc Rheol. 1959;3:137.
[30] Krieger IM. Advances Colloid and Interface Sci. 1972;3:111.
[31] van den Tempel M. Rheol Acta. 1958;1:115. J Colloid Sci. 1961;16:284.
[32] Papenhuizen JMP. Rheol Acta. 1972;11:73.
[33] D'Archy H. Les Fantaines Publique de la Vill de Dijon. Paris; 1961.
[34] Carmen PC. Trans Inst Chem Eng. 1937;15:150.

https://doi.org/10.1515/9783110588002-027

[35] Evans ID, Lipps A. In: Dickinson E, Walstra P, editors. Food colloids and polymers: Stability and mechanical properties. Cambridge: Royal Society of Chemistry; 1993. p. 214.
[36] Meakin P. Advances Colloid Interface Sci. 1988;28:249.
[37] Vreeker R, Hoekstra LL, den Boer DC, Agterof WG. In: Dickinson E, Walstra P, editors. Food colloids and polymers: Stability and mechanical properties. Cambridge: Royal Society of chemistry; 1993. p. 16.
[38] Tadros T. Formulation of disperse systems. Germany: Wiley-VCH; 2014.
[39] Lucassen J. In: Lucassen-Reynders EH, editor. Anionic surfactants. New York: Marcel Dekker; 1981. p. 217.
[40] Deryaguin BV, Churaev NV. Kolloid Zh. 1976;38:438.
[41] Deryaguin BV. Theory of stability of colloids and thin films. New York: Consultant Bureau; 1989.
[42] Deryaguin BV, Landua L. Acta Physicochimica USSR. 1941;14:633.
[43] Verwey EJ, Overbeek J. Theory of stability of lyophobic colloids. Amsterdam: Elsevier; 1948.
[44] de Vries AJ. Disc Faraday Soc. 1966;42:23.
[45] Vrij A, Overbeek J. J Amer Chem Soc. 1968;90:3074.
[46] Pugh RJ, Yoon RH. J Colloid Interface Sci. 1994;163:169.
[47] Claesson PM, Christensen HK. J Phys Chem. 1988;92:1650.
[48] Frieberg S. Mol Cryst Liq Cryst. 1977;40:49.
[49] Darling DF, Birkett RJ. Food colloids in practice. In: Dickinson E, editor. Food emulsions and foams. London: Royal Society of Chemistry Publication; 1987.
[50] Prins A. Theory and practice of formation and stability of food foams. In: Dickinson E, editor. Food emulsions and foams. London: Royal Society of Chemistry Publication; 1987.
[51] de Vries AJ. Rec Trav Chim. 155; 77:209.
[52] de Bruijne DW, Hendrickx H, Alderliesten L, de Looff J. In: Dickinson E, Walstra P, editors. Food colloids and polymers: Stability and mechanical properties. Cambridge: Royal Society of Chemistry; 1993. p. 204

Index